UNIVERSITY OF TASMANIA

LRP receptors in a novel mechanism of axon pathfinding and peripheral nerve regeneration

Menzies Research Institute Tasmania

By

Lila Landowski

B.MedRes (Hons).

Submitted in fulfilment of the requirement for the

Degree of Doctor of Philosophy (Medical Research)

University of Tasmania, April 2014.

DECLARATION OF ORIGINALITY

This thesis contains no material which has been accepted for a degree or diploma by the University of Tasmania or any other institution, except where acknowledged, and by way of background information and duly acknowledged in the thesis, and to the best of my knowledge and belief no material previously published or written by another person except where due acknowledgement is made in the text of the thesis, nor does the thesis contain any material that infringes copyright.

Some data points contributing to Figure 2.1, 2.1, 2.3 and 2.4 were included in my honours thesis, Landowski 2009, University of Tasmania

Lila Landowski

AUTHORITY OF ACCESS

This thesis may be made available for loan and limited copying and communication in accordance with the Copyright Act 1968.

Lila Landowski

STATEMENT OF ETHICAL CONDUCT

The research associated with this thesis abides by the international and Australian codes on human and animal experimentation, the guidelines by the Australian Government's Office of the Gene Technology Regulator and the rulings of the Safety, Ethics and Institutional Biosafety Committees of the University.

Lila Landowski

ACKNOWLEDGEMENTS

Dr. Lisa Foa – I have learnt an immense amount from you over the years. You have moulded me into a scientist, a better writer and a better presenter. I know I will continue to find things I have learnt from your supervision for many years to come.

Professor Adrian West – You have been an endless source of encouragement, support and ideas.

Professor Bruce Taylor - As a tour-de-force in epidemiology research and clinical neurology, you brought vital perspective and expert knowledge to my PhD. I have great respect for you.

Dr. Robert Gasperini – Thank you for all you taught me, and the times you saved me from technological disasters.

Professor David Small - Your scientific interrogation and advice taught me more than you will probably ever know.

Dr. Michelle Keske and Dr. Dino Premilovac – For all your technical advice and assistance with the diabetic models.

Dr. Bill Bennett – For all that you taught me, for the laughs, and your expert recommendations on chilli.

Justin "Giblet" Dittmann – My Lab bestie. Thanks for your technical advice, lab assistance, laughs, and for always "letting" me catch more fish than you.

Dr. Camilla Mitchell – My PhD sister; you were with me through through the thick, thin and everything in between.

Dr. Edgar Dawkins – The joy you brought me is exemplified by this quote:

Dr. Ben Hunn: "Did you make this card, Edgar?"

Dr. Edgar Dawkins: "Well I didn't actually make it; I expressed it in E. Coli."

Emily Ainslie – A funny, kind spirit that enriched my life during your time in the lab and beyond. It was a pleasure to teach and work with you. Favourite quote:

"You're so good at immuno, it should be called immuYES!

Dr Dave Klaver – You taught me my way around the lab. The following quote from you probably sums up your fatherly influence early in my PhD quite nicely: [in regards to nurturing me to get 1st class honours]

"Its the closest I've come to giving birth... its beautiful."

Emma Eaton – For your guidance, advice and for being an inspiration. Next on our list is finding a way to clone you. Forever Eaton-Bacon.

Dr. Kate Lewis – For always being willing to offer help and advice.

Dr. Kaylene Young – For your valuable insight.

To the rest of the Foa/Small/Young lab group, and the West/Chuah lab group, both past and present - Thank you for all the laughs, support and friendship, and for always pretending to be thankful for all the things I made for you out of laboratory product packaging.

Meg Good – Good by name, very good by nature. My kindred spirit. I drew so much strength from your friendship and support during the rocky roads through my PhD. You are a forever friend.

Dr. Dave Russell – Congratulations, you've passed the ultimate test!

ABSTRACT

Chemotactic axon guidance has an essential role in development and is important for re-innervation of target tissues after neuronal injury. The aim of the work described in this thesis was to determine whether the low density lipoprotein receptor-related protein 1 (LRP1) and LRP2 receptors mediate neurite chemoattraction, and to assess their therapeutic potential in a model of peripheral neuropathy. I found that LRP1 and LRP2 were expressed on growth cones at the leading edge and on filopodia, suggesting that they are part of the environment-sensing machinery. I used the growth cone turning assay to test whether a range of LRP ligands were chemotactic to growth cones *in vitro*. The ligands tested included metallothionein II (MTII), apolipoproteinE3, tissue plasminogen activator (tPA), alpha-2-macroglobulin (α2M), vitamin D and transthyretin. E16-18 embryonic rat sensory neuron growth cones grew towards a microgradient of MTII (+11.6°±2.1°, $p<0.0001$, *cf.* control -1.8°±1.1°), and turned away from a microgradient of MTIII (-13.8°±1.9, $P<0.0001$), α2M (-11.9°±3.4, $P<0.01$) and tPA (-11.1°±2.1 $P<0.001$). I used siRNA knock down and pharmacological inhibition to demonstrate that LRP1 and LRP2 were both required for growth cone responses to MTII and MTIII. Growth cone turning towards a gradient of MTII or MTIII was abolished by LRP-receptor inhibition with receptor associated protein and siRNA knockdown of LRP1 or LRP2. In addition, pharmacological inhibition of TrkA receptors significantly augmented the turning response. These data demonstrate that both LRP1 and LRP2 are necessary for MTII and MTIII-mediated chemotactic signal transduction, and potentially form part of a signalling hub, recruiting other co-receptors such as TrkA. MTII and MTIII-mediated chemotaxis was found to be dependent on calcium ion concentration: when neurons were depleted of extracellular calcium, the turning response underwent a complete switch in direction. Furthermore, pharmacological inhibition of

calcium/calmodulin-dependent kinase II suggested that LRP1 and LRP2 signal via established downstream effectors. I then asked whether LRP-mediated chemotaxis could be exploited to guide axon regeneration *in vivo*. I used a model of small-fibre neuropathy in rats. Ten age-matched rats had topical 8% capsaicin cream and placebo cream applied to contralateral areas on the lumbar dorsum. Treated areas were given 3x weekly intradermal injections of MTII or saline. Punch and epidermal roof biopsies were harvested weekly to monitor regeneration. At 14 days, regeneration was observed in saline treated capsaicin regions, compared to contralateral control skin, however MTII treated rats had complete regeneration by 7 days. LRP-mediated chemotaxis represents a novel, non-classical axon guidance signalling system. MTII has therapeutic potential as a disease-modifying agent for the injured nervous system.

TABLE OF CONTENTS

Declaration of originality ..... **i**

Authority of Access ..... **ii**

Statement of ethical conduct ..... **iii**

Acknowledgements ..... **iv**

Abstract ..... **vi**

Table of Contents ..... **viii**

Abbreviations **1**

Chapter 1: Introduction **8**

1.1 Neuronal networks **8**

1.1.1 The nervous system is interconnected 8

1.1.2 Axon pathfinding in development 9

1.1.3 Axon pathfinding is necessary for formation *and* regeneration of the central nervous system (CNS) and peripheral nervous system (PNS) 12

1.1.4 Axon pathfinding in regeneration 13

1.2 The mechanics of axon pathfinding **14**

1.2.1 Guidance cues and chemotactic factors 14

1.2.2 Intracellular signalling in growth cone navigation 15

1.2.3 The growth cone cytoskeleton 17

1.2.3 Receptors implicated in growth cone guidance 20

1.3 The multifunctional LDL receptor gene family **21**

1.4 LDL receptor family in neuronal function **23**

1.4.1 Overview of LDL receptor function in neurons 23

1.4.2 VLDL and ApoER2 receptors 24

1.4.3 LRP5 and LRP6 receptors 26

1.4.4 LR11 (SorLA) receptor 27

1.4.5 LRP1 receptor 28

1.4.6 LRP2 receptor 29

1.5 LRP1 and LRP2 extracellular ligands have important functions in neurons **31**

1.5.1 α2-macroglobulin (α2M) 32

1.5.2 Tissue-type plasminogen activator (tPA) 33

1.5.3 Apolipoprotein E (ApoE) 35
1.5.4 Transthyretin (TTR) 35
1.5.5 Vitamin D/vitamin D binding protein complex 36
1.5.6 Myelin-associated glycoprotein (MAG) 38
1.5.7 Metallothionein 39
1.6 LRP1 and LRP2 and their diverse cell signalling pathways in neurons 40
1.6.1 LRP1 intracellular signalling mechanisms 40
1.6.2 LRP2 intracellular signalling mechanisms 42
1.7 Nerve regeneration in peripheral neuropathy 45
1.8 Sensory nerves of the skin 46
1.9 Peripheral neuropathy 47
1.10 Diabetic neuropathy 48
1.10.1 Clinical presentation 48
1.10.2 Current therapeutics for diabetic neuropathy 49
1.10.3 Pathophysiology of diabetic neuropathy 50
1.10.4 Experimental models of diabetic neuropathy 52
1.10.5 Neurotrophic factors as experimental therapeutics in diabetic neuropathy 54
Justification for project 54
Chapter 2
Establishing the chemotactic responses of growth cones to LRP1 and LRP2 ligands *in vitro* 58
2.1 Introduction 58
2.2 Experimental Procedures & Materials 61
2.2.1 Disclosure 61
2.2.2 Primary DRG neuron culture 61
2.2.3 siRNA knockdown of LRP1 and LRP2 62
2.2.4 *In vitro* growth cone turning assay 62
2.2.5 Video acquisition in growth cone turning assay 64
2.2.6 Immunocytochemistry 64
2.2.7 Western Blot 65
2.2.8 Statistical analysis 66
2.3 Results 67
2.3.1 LRP1 and LRP2 are present in the chemical sensing region of the growth cone 67

2.3.2 Determine whether LRP1 or LRP2 ligands have chemotropic effects on neuronal growth cones 71

2.3.3 Determine whether LRP receptors are required in MTII or MTIII induced growth cone chemoattraction 77

2.3.4 Demonstrate reduced LRP1 and LRP2 expression in siRNA transfected DRG 78

2.3.5 Demonstration of LRP1 and LRP2 co-localisation in growth cones 86

2.4 Discussion 88

Chapter 3

The downstream signalling mechanisms that mediate LRP 1 and LRP2 signalling in sensory growth cone navigation 95

3.1 Introduction 95

3.2 Experimental Procedures & Materials 98

3.2.1 In vitro growth cone turning assay 98

3.2.2 Immunocytochemistry 99

3.2.3 Analysis of immunoreactivity, area and filopodia on growth cones 99

3.2.4 Analysis of FAK puncta 100

3.3 Results 101

3.3.1 Determine whether LRP-mediated growth cone guidance a calcium dependent process 101

3.3.2 Establish whether CaMKII is required for LRP-mediated growth cone turning 101

3.3.3 Determine whether TrkA is required for LRP-MT mediated chemotaxis 106

3.3.4 Establish whether MAPK pathways function in LRP-MT mediated chemotaxis 109

3.3.5 Determine whether reduced expression of LRP1 or LRP2 alters the morphology of growth cones 112

3.4 Discussion 115

3.5 Conclusion 124

Chapter 4

Site-directed delivery of MTII and synthetic MTII analogue, EmtinB, into the skin. 127

4.1 Introduction 127

4.2 Methods: 130

4.2 1. Disclosure 130

4.2.2 Biotinylation of MTII and EmtinB 130

4.2.3 Preparation of skin 131

4.2.4 Topical application 131

4.2.5 Topical application with carrier peptides 132
4.2.6 Iontophoresis 132
4.2.7 Intradermal injection..... 133
4.2.8 Tissue processing..... 133
4.2.9 Fluorescence immunohistochemistry 134
4.2.10 Fluorescence microscope image acquisition 134
4.2.11 Chromogenic immunohistochemistry..... 135
4.2.12 Light microscope image acquisition and analysis 135
Results: 137
4.3.1 Intradermal injection..... 137
4.3.3 Topical application with cell penetrating peptides (HR9 peptide) 156
4.3.4 Iontophoresis 164
4.3.5 Intradermal injection..... 167
4.4 Discussion 169
Chapter 5
Development and characterisation of in vivo nerve injury models:, Capsaicin-induced nerve retraction, Diabetic neuropathy and focal denervation via blister formation..... 174
5.1 Introduction 174
5.2 Methods 179
5.2.1 Disclosure 179
5.2.2 Diet 179
5.2.3 Synthesis of 8% w/w capsaicin cream and control cream 180
5.2.4 Induction of capsaicin-induced denervation 181
5.2.5 Treatment of capsaicin-denervated skin with MTII or saline..... 182
5.2.6 Biopsies for histological evaluation of capsaicin-denervation model 183
5.2.7 Punch biopsy..... 183
5.2.8 Induction of STZ/HFD diabetic model..... 184
5.2.9 Treatment of diabetic neuropathy hindlimb with MTII, EmtinB or saline 185
5.2.10 Blood glucose testing..... 187
5.2.11 Functional evaluation of sensory thresholds in the rat hindpaw in diabetic neuropathy model 187
5.2.12 Punch biopsy immunostaining..... 188
5.2.13 Image acquisition..... 188
5.2.14 Nerve density analysis 189

5.2.15 Induction of blisters 190
5.2.16 Blister injection 190
5.3 Results 195
5.3.1 Capsaicin-induced chemical denervation 195
5.3.2 Diabetic neuropathy 204
5.3.3 Blister-induced focal denervation 211
5.4 Discussion 214
Chapter 6: Conclusions and Future Directions 221
Appendix 1 230
7.1 Solution Protocols 230
7.1.1 DMEM-F12: 1L 230
7.1.2 Sensory neuron media (SNM): 50mL 230
7.1.3 Phosphate Buffered Saline (PBS): 1L 230
7.1.4 TBS 1:1: 1L 231
7.1.5 Hank's Balanced Salt Solution, Ca^{+2} free media: 30mL 231
7.1.6 0.4% Triton X: 100mL 231
7.1.7 4% Paraformaldehyde (PFA): 500mL 231
7.1.8 Zamboni's Fixative : 5L 232
7.1.9 Nuclear Fast Red solution: 100mL 232
7.1.10 Poly-L-ornithine 1mg/mL solution: To make 5ml 232
7.1.11 50mM TRIS: To make 10mL 232
7.1.12 50ug/mL Laminin: To make 1mL 232
7.1.13 150mM NaCl/50mM TRIS: To make 10mL 233
Bibliography 235

ABBREVIATIONS

α2M	alpha-2 macroglobulin
AGE	advanced glycation end-product
Akt	protein kinase B signalling pathway
ANKRA	ankyrin-repeat family A protein
ApoE	apolipoprotein E
ApoE2	apolipoprotein E2
ApoE3	apolipoprotein E3
ApoE4	apolipoprotein E4
ApoER2	apolipoprotein E receptor 2
APP	amyloid precursor protein
BACE1	beta-secretase 1
BDNF	brain-derived neurotrophic factor
BK	big potassium ion channel
BMP4	bone morphogenetic protein 4
°C	degrees Celsius
Ca^{2+}	calcium ion
CaMKII	Ca^{2+}/calmodulin-dependent kinase II
cAMP	cyclic adenosine monophosphate
CaN	calcineurin
cGMP	cyclic guanosine monophosphate
CICR	calcium-induced calcium release

CKII	casein kinase 2
CNS	central nervous system
CREB	cAMP response element-binding protein
CSF	cerebrospinal fluid
Dab-1	disabled 1
Dab-2	disabled 2
DBS	Donnai-Barrow syndrome
DCC	deleted in colorectal cancer
DNA	deoxyribonucleic acid
DRG	dorsal root ganglion
DMSO	dimethyl sulfoxide
ENF	epidermal nerve fibre
EPSP	excitatory postsynaptic potential
ERK	extracellular signal-related kinase, see MAPK
FAK	focal adhesion kinase
Fz	Frizzled receptor
GABA-A α4	gamma-aminobutyric acid (GABA) A receptor, alpha 4 subunit
GDNF	glial cell line-derived neurotrophic factor
GFR-alpha1	GDNF family receptor alpha 1
GFP	green fluorescent protein
GluR1	GluR1 alpha-amino-3-hydroxy-5-methyl-4-isoxazolepropionic acid (AMPA) receptor subunit
GSK3	glycogen synthase kinase 3

HBSS	Hank’s Balanced Salt Solution
HFD	high fat diet
HR9	histidine nona-arginine peptide
ICD	intracellular domain
IP3ICR	inositol 1,4,5-triphosphate (IP3)-induced calcium release
IP3R	inositol 1,4,5-triphosphate receptor
JIP-1	c-Jun N-terminal kinase interacting protein 1
JIP-2	c-Jun N-terminal kinase interacting protein 2
JNK	c-Jun N-terminal kinase
kDa	kilo Daltons; molecular weight
kg	kilograms
KO	knockout
LDL	low density lipoprotein
LDLR	low density lipoprotein receptor
LRP	low density lipoprotein receptor-related protein
LRP1	low density lipoprotein receptor-related protein 1
LRP1b	low density lipoprotein receptor-related protein 1b
LRP2	low density lipoprotein receptor-related protein 2; megalin
LRP5	low density lipoprotein receptor-related protein 5
LRP6	low density lipoprotein receptor-related protein 6
LRP8	low density lipoprotein receptor-related protein 8
LTD	long term depression
LTP	long term potentiation

MAG	myelin-associated glycoprotein
MAGI-1	membrane associated guanylate kinase
MAPK	mitogen-activated protein kinase
MAP2	microtubule-associated protein 2
mg	milligrams
mL	millilitre
mm	millimetre
MS	multiple sclerosis
MT	metallothionein
MTI	metallothionein 1
MTII	metallothionein 2
MTIII	metallothionein 3
MTIV	metallothionein 4
NeuN	neuronal nuclear marker
ND	normal diet
NGF	nerve growth factor
NGF-β	nerve growth factor beta
NT-3	neurotrophin-3
nM	nanomolar
NMDA	N-methyl-D-aspartate
NMDAR	N-methyl-D-aspartate receptor
NMHC-IIA	nonmuscle myosin heavy chain IIA
NT-2	neurotrophin 2

NT-3	neurotrophin 3
NT-4	neurotrophin 4
PBS	phosphate-buffered saline
PDGF	platelet-derived growth factor
PDGFR-β	platelet-derived growth factor receptor beta
PI3K	phosphatinositide 3-kinase
PKA	protein kinase A
PN	peripheral neuropathy
PNS	peripheral nervous system
PSD-95	postsynaptic density protein 95
p38	see MAPK
p75	low affinity nerve growth factor receptor
RAP	receptor-associated protein
RET	proto-oncogene receptor tyrosine kinase
Robo	roundabout protein
RyR	ryanodine receptor
SAD	seasonal affective disorder
SAPK	stress-activated protein kinase
SEM	standard error of the mean
SFK	Src family kinase
Shh	sonic hedgehog
siRNA	small interfering ribonucleic acid
sLRP1	low-density lipoprotein receptor-related protein, soluble extracellular domain

STZ	streptozotocin
SNM	sensory neuron media
TBS	tris-buffered saline
TGFβR-1	transforming growth factor beta receptor 1
tPA	tissue plasminogen activator
Trk	tyrosine kinase receptor
TrkA	tyrosine kinase A
TRP	transient receptor potential ion channel
TRPA	TRP ankyrin
TRPC	TRP canonical
TRPV1	TRP vanilloid receptor
TNF-α	Tissue necrosis factor-α
TTR	transthyretin
µm	micrometres
µM	micromolar
VDBP	vitamin D binding protein
VDCC	voltage-dependent calcium channel
VLDL	very low density lipoprotein
VLDLR	very low density lipoprotein receptor
25(OH)D3	Vitamin D3 (inactive)
1,25(OH)D3	Vitamin D3 (active metabolite)

CHAPTER 1

Introduction

CHAPTER 1: INTRODUCTION

1.1 NEURONAL NETWORKS

1.1.1 The nervous system is interconnected

As a staggeringly complex network of cell connections throughout the body, the nervous system governs virtually all body activity; from conscious movement and thought, to the completely unconscious action potential or ebb and flux of hormones and ions involved in homeostasis of the body's internal environment. There are trillions of synapses which allow for chemical and electrical continuity between neurons. Disruption or disconnection of these neuronal networks can occur commonly in trauma, neurodegenerative diseases, surgical procedures, systemic illnesses, and as a side effect of drug toxicity. Such damage may result in cognitive decline, in the loss of motor function and/or sensation, or the development of pain syndromes (Singer, 1986).

During development, neurons send out an axonal process which uses a range of guidance cues to navigate the embryonic environment, establishing the early framework of the neuronal circuitry. The existence of hundreds of billions of cells in the developing embryo means that finding the correct target with which to synapse is no small feat. Growth cones are exquisitely sensitive structures present at the distal end of axons that facilitate the growth of axon to target (Caudy and Bentley, 1986). The mechanism by which the direction of growth cones can be manipulated in development has been the topic of investigation for many decades, not only for an intrinsic understanding of development, but for its application in regenerative processes. This thesis focusses on growth cone pathfinding through novel

mechanisms in a developmental *in vitro* model, and its translation into an *in vivo* model of nerve injury, to promote regeneration. Specifically, the hypothesis that underpins this thesis is that members of the multifunctional low-density lipoprotein (LDL) receptor family posess novel roles in growth cone pathfinding. The first experimental chapters within this thesis investigate the chemotactic abilities of LDL receptor ligands on neuronal growth cones, and include an investigation into their mechanism of action. Elucidating these LDL receptor mediated growth cone guidance pathways is important for developing new mechanisms for promoting and enhancing neuronal regeneration after injury. Therefore, the later chapters describe the initial outcomes of the translation of this *in vitro* work into models of nerve injury.

This introductory chapter will review the process of growth cone guidance by chemotactic factors, and outline evidence relating to the potential involvement of the LDL receptor family in this activity. An examination of the application of chemotactic factors in neuropathy will follow, with specific emphasis on diabetic neuropathy, the most common form of neuropathy.

1.1.2 Axon pathfinding in development

Our understanding of axon pathfinding has blossomed since Ramón y Cajal first described growth cones as "battering rams" that are "endowed with amoeboid movements" which force their way between cells to direct these axons to their targets (Cajal, 1952, Landmesser, 1986). Structure and function studies have since demonstrated the exquisite complexity of growth cones and their role in sensing and responding to the internal environment, in axon turning, extension and in initiating bifurcation (Sato et al., 1994, Hollyday and Morgan-Carr, 1995). The growth cone mediates axonal pathfinding: a complex process that is essential for the

development of the nervous system and for its maintenance following neuronal injury or turnover. In early development, neuronal growth cones respond to soluble and substrate-bound chemotactic guidance cues spatially and temporally, to allow the axon to navigate the internal milieu and make appropriate connections (Sperry, 1963). There is consensus that a similar process is involved in the adaptive capacity of mature neurons: that is, in synaptic plasticity and regeneration of the nervous system (Kolodkin, 1996).

During axon pathfinding in development, neurons extend an axonal process ending in a growth cone, which navigates through the extracellular matrix, extending to meet the target cell with which it synapses (Caudy and Bentley, 1986). A growth cone comprises a membranous, receptor-rich, fan-shaped structure (lamellipodia) which extends between long finger-like projections (filopodia) (Fig 1.1). Its cytoskeleton, comprised of filamentous actin (F-actin), closely interacts with the axonal microtubule core (Lewis and Bridgman, 1992, Bentley and O'Connor, 1994, Suter and Forscher, 2000) (Fig 1.1). F-actin forms bundles in filopodia, and an irregular cross-linked arrangement along the leading edge, which also gives structure to the lamellipodia (Lewis and Bridgman, 1992, Korey and Van Vactor, 2000, Suter and Forscher, 2000) (Fig 1.1). Microtubules are arranged as parallel bundles along the neurite and splay outwards within the growth cone (Bridgman and Dailey, 1989). Microtubules interact and cooperate with F-actin in order to adhere to the matrix, sense and respond to growth cues in the extracellular milieu, and allow extension to the target (or repulsion from an inhibitory cue). These principles are the basis for the development of "the growth cone turning assay" developed by M.M. Poo that detects the response of growth cones to stimuli (Lohof et al., 1992). Thus, the growth cone provides a powerful model for studying the interaction of neurons with their extracellular environment, and also for the receptor

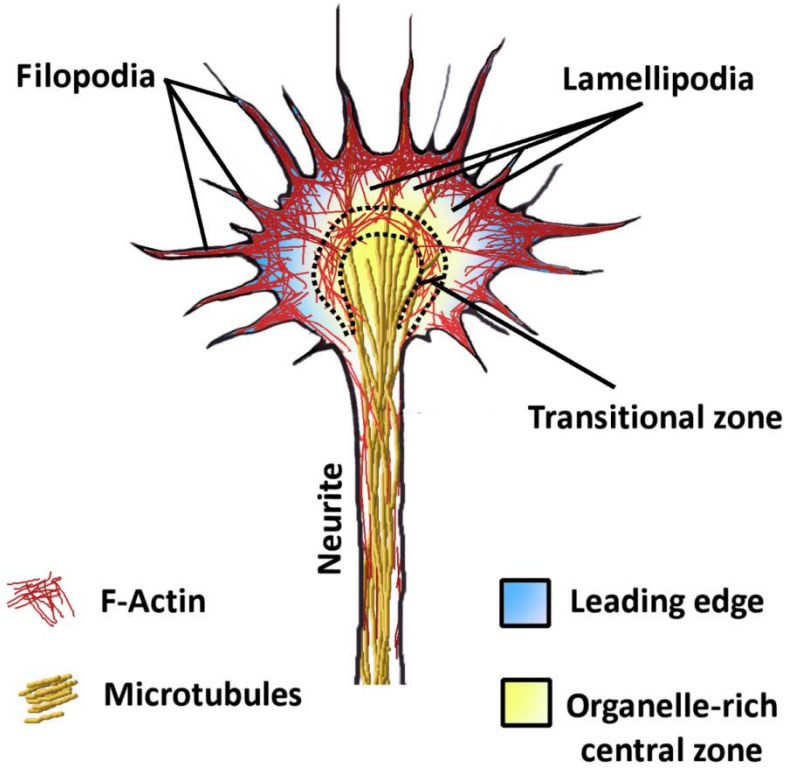

Figure 1.1 Structure of the neuronal growth cone

A growth cone comprises a membranous, receptor-rich, fan-shaped structure (lamellipodia) which extends between long finger-like projections (filopodia). Its cytoskeleton, comprised of filamentous actin (F-actin), and microtubules, closely interact (Lewis and Bridgman, 1992, Bentley and O'Connor, 1994, Suter and Forscher, 2000).

signalling pathways which transduce this information into directional changes in axonal growth. Such signalling pathways could be critically important for promoting regeneration after neuronal damage.

1.1.3 Axon pathfinding is necessary for formation *and* regeneration of the central nervous system (CNS) and peripheral nervous system (PNS)

Subtle errors in axon pathfinding during development contribute to a range of disorders of the nervous system such as schizophrenia, epilepsy, and mental retardation (Marco et al., 1997, Mason et al., 2001). The failure of regeneration in the adult CNS can be evidenced by several pathologies of the nervous system, including neurodegenerative diseases such as Alzheimer's disease, Parkinson's disease and amyotrophic lateral sclerosis, which involve the loss of neurons and their synaptic connections (Van Uden et al., 1999, Mason et al., 2001, Puttaparthi et al., 2002, Hoglund and Salter, 2013). In addition, failure of regeneration may result in neuropathies, developed as sequelae of systemic diseases such as diabetes, as a consequence of chemotherapeutic drug use, or during traumatic injury, where sensation and/or movement may be permanently lost distal to the injury (Mar et al., 2014). Although axon guidance is primarily involved in development of the nervous system, it also has an essential role in peripheral nerve regeneration and re-innervation of target tissues after neuronal injury. The processes encompassing neuronal re-sprouting after injury closely recapitulate those that occur during axon pathfinding in development, making the study of developmental processes particularly relevant in the context of neuronal injury (Hoffman and Cleveland, 1988).

Neuronal injury activates a series of pathological processes, including inflammation, scar formation, necrosis and apoptosis (Fitch and Silver, 2008, Huebner and Strittmatter, 2009). Damage to neural tissue in the adult CNS is virtually always irreparable, due to a combination of inhibitory factors and glial scar formation, the incapacity to re-express developmental molecules associated with guidance and growth, and inherent inability of the neuron to form functional regenerative sprouts (Buffo et al., 2009). In the peripheral nervous system (PNS), however, nerves are sometimes able to regenerate and re-innervate post injury, although this process is very slow and often inaccurate, and may result in aberrant function and pain syndromes (Aguayo et al., 1981). Hence, there is a need for therapeutic intervention to improve the outcome in neuronal injury of the CNS and PNS.

1.1.4 Axon pathfinding in regeneration

The development of an approach to enhance axonal regrowth after injury or neuropathy has been a goal for researchers for many centuries. In 1830, Theodor Schwann reported the phenomena of nerve regeneration in rabbits. Almost a century later, Santiago Ramon y Cajal first postulated that nerve regeneration required chemotactic signals; however this was not demonstrated until 1963 by Sperry (Sperry, 1963). The discovery of the first of many neuronal chemotactic factors arose from the identification of a substance in a mouse sarcoma which was found to enhance nerve growth. The substance Rita Levi-Montalcini and collaborators identified was nerve growth factor (Cohen et al., 1954). The use of chemotactic factors in animal models of nerve damage has had great success and promise (Levi-Montalcini and Angeletti, 1963, Varon et al., 1979). However, in humans, most trials using chemotactic factors to promote regeneration have had poor functional outcomes (Calcutt et al., 2008). Poor outcomes have been largely resultant of differences in therapeutic dose, and

low tolerance resulting from inappropriate (often systemic) administration of trophic factors whose expression is usually spatially restricted (Apfel, 2002).

1.2 THE MECHANICS OF AXON PATHFINDING

1.2.1 Guidance cues and chemotactic factors

In the process of axon pathfinding, growth cones must respond to a multitude of diffusible and substrate-bound chemotactic factors and guidance cues in the extracellular environment, and integrate this information into a directional response (Tessier-Lavigne and Goodman, 1996). Growth cones are fitted with an elaborate suite of receptors that allow for the simultaneous integration of a multitude of chemotactic cues (Tessier-Lavigne and Goodman, 1996). The presence of chemotactic factors is detected by their specific receptors located on the growth cone membrane, inducing an intracellular signalling cascade. This cascade manipulates the cytoskeletal elements, and dictates whether the response of the growth cone culminates in turning, extension, stasis or retraction, collapse or bifurcation (Suter and Forscher, 2000). This diverse range of responses produces a highly specific set of movements and allows the axon to be directed to an individual target. By necessity, studies in growth cone guidance and axon pathfinding have looked at the relative involvement of individual chemotactic cues; although in the human body, microenvironments may contain numerous chemotactic cues and their simultaneous integration is not only necessary for directional responses, but also the adaptation to changing cues in different intermediate targets (Tessier-Lavigne et al., 1988, Shirasaki et al., 1998, Tojima, 2012). Whilst growth cues generally produce a characteristic growth cone turning response (eg. inducing attraction); this response can be altered or switched depending on the developmental stage of the neuron, the type of

neuron, the extracellular environment, the status of intracellular second messengers, or differential receptor expression (Song and Poo, 1999, Gallo and Letourneau, 2002, Dontchev and Letourneau, 2003). Therefore, the targeting of a growth cone to its correct cellular target is the product of multiple signalling events, both intracellular and extracellular.

1.2.2 Intracellular signalling in growth cone navigation

The intracellular signalling pathways that mediate growth cone chemotaxis are varied and yet to be fully elucidated. It is well established that calcium ions (Ca^{2+}) are an early second messenger of most chemotactic signalling cascades that influence the direction of the developing neuron (Song and Poo, 1999). Ca^{2+} is able to mediate both attractive and repulsive responses in growth cones (Song and Poo, 1999). The ability for Ca^{2+} to mediate repulsion or attraction is principally modulated by to two factors: 1) the spatial and temporal localisation of the Ca^{2+} signal, and; 2) the activation of differentially sensitive calcium-dependent signalling molecules (Song and Poo, 1999, Wen et al., 2004, Tojima et al., 2009). The source of Ca^{2+} is important in mediating a directive signal: attraction towards a chemotactic cue results when there is a large change in intracellular Ca^{2+} levels, whereas repulsion occurs when the influx is modest (Berridge et al., 2000). A large change in intracellular Ca^{2+} can be achieved by an influx of extracellular Ca^{2+}, combined with release from intracellular stores within the endoplasmic reticulum, in a process called calcium-induced calcium-release (CICR) or inositol 1,4,5 trisphosphate-induced calcium-release (IP3ICR) (Ooashi et al., 2005). When an influx of Ca^{2+} occurs in the absence of CICR or IP3ICR, (ie. solely from the extracellular milieu, through Ca^{2+} channels), the resulting change in Ca^{2+} is modest and repulsion occurs (Ooashi et al., 2005). In light of this finding, it has recently been proposed that changes in calcium-dependent regulation of neurite outgrowth

tends to follow the IP3ICR pathway early in development, but the voltage dependent calcium channel (VDCC) or ryanodine receptor (RyR) pathways in later stages of development (Arie et al., 2009). Secondary to the Ca^{2+} signal are the downstream effectors of growth cone turning – with the role of differentially sensitive calcium-dependent signalling molecules having major importance. Calcineurin phosphatase (CaN) is highly sensitive to Ca^{2+} and mediates growth cone repulsion. If the influx of Ca^{2+} in response to a trophic cue is modest, CaN is preferentially activated, and the growth cone will be repelled (Wen et al., 2004). Calmodulin dependent kinase II (CaMKII), which is abundant in growth cones, has a lower affinity for Ca^{2+}, and therefore larger influxes of Ca^{2+} are required to activate CaMKII (Wen et al., 2004). A higher abundance of activated CaMKII over CaN in the growth cone will therefore initiate growth cone attraction (Fig 1.2). Regardless of whether the cue is attractive or repulsive, relatively higher concentrations of Ca^{2+} are observed on the side of the growth cone where the concentration of soluble chemotactic cue is highest, in turn facilitating an asymmetric rearrangement of cytoskeletal elements and growth cone turning (Tojima, 2012).

Cyclic nucleotides (cAMP and cGMP) are also important downstream effectors of growth cone turning, with crosstalk occurring between cyclic nucleotides and local Ca^{2+} levels (Nishiyama et al., 2003, Forbes et al., 2012). Cyclic nucleotide signalling operates within an optimal concentration range, and levels are dependent on the rate of conversion of adenosine triphosphate and guanosine triphosphate to cAMP and cGMP, respectively (Song et al., 1998, Song and Poo, 1999, Nishiyama et al., 2003). Importantly, Nishiyama and colleagues (2003) determined that when a guidance cue induces a high ratio of cAMP:cGMP, the directional response of growth cones is modulated, such that neurons are attracted; however when the ratio is low, growth cones can instead be repulsed (Nishiyama et al., 2003). One of the ways

that cAMP is able to promote attraction of growth cones is by inhibition of CaN, the Ca^{2+} dependent effector of growth cone repulsion, shifting the balance towards attraction (Wen et al., 2004). Taken together, the magnitude of Ca^{2+} influx, in conjunction with its temporal and spatial localisation, together are able to elicit both attractive and repulsive responses in growth cones.

1.2.3 The growth cone cytoskeleton

As a growth cone advances, actin filaments are continuously transported away from the peripheral domain to the transitional zone by a myosin-motor driven process known as retrograde F-actin flow (Bentley and O'Connor, 1994). When the growth cone is subjected to a gradient of the guidance cue, the side of the growth cone facing the higher concentration will have a larger influx of Ca^{2+} ions, allowing a directional response to be propagated. Microtubules and F-actin polymerise on the side of the growth cone where the concentration of Ca^{2+} is highest, meanwhile they will be destabilised on the side with the lower concentration, facilitating a directional response (Fan and Raper, 1995, Gallo et al., 2002). In response to a chemorepulsive cue, the change in i[Ca^{2+}] is moderate, leading to the activation of CaN, which culminates in the re-assembly of cytoskeletal elements, and ultimately, to neurite repulsion. Repulsive cues activate actin destabilising proteins, and promote F-actin retrograde flow. Microtubules and actin are destabilised on the side of the growth cone where the concentration of the repulsive cue is highest, meanwhile stabilisation instead is favoured on the opposite side of the growth cone, allowing the growth cone to turn away

Figure 1.2 The cytoskeletal events that underlie growth cone navigation

Inside the growth cone, the initiation of turning is usually elicited by a change in i[Ca^{2+}] (shown by graded colour bar). As a growth cone advances, actin filaments are continuously transported away from the peripheral domain to the transitional zone (Bentley and O'Connor, 1994). When the growth cone is subjected to a gradient of chemoattractant, the side of the growth cone facing the higher concentration will have a larger influx of Ca^{2+} ions, resulting in stabilisation and polymerisation of microtubules and F-actin. Microtubules and F-actin are destabilised on the side with the lower concentration of attractive cue (Gallo et al., 2002). In response to a chemorepulsive cue, the change in i[Ca^{2+}] is moderate, leading to the activation of CaN, and microtubules and F-actin are destabilisation and disassembly. Stabilisation instead is favoured on the opposite side of the growth cone, allowing the growth cone to turn away from the gradient (Gallo and Letourneau, 2002). Original figure.

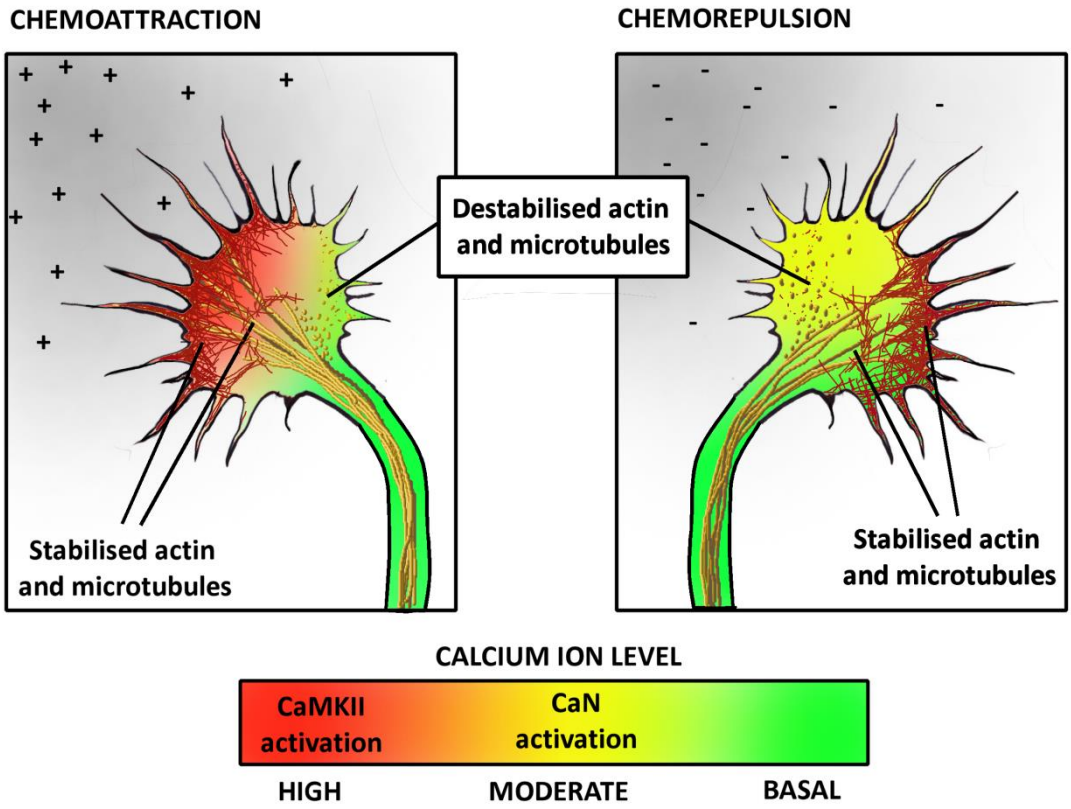
CHEMOATTRACTION
CHEMOREPULSION
Destabilised actin and microtubules
Stabilised actin and microtubules
Stabilised actin and microtubules
CALCIUM ION LEVEL
CaMKII activation
CaN activation
HIGH
MODERATE
BASAL

from the gradient (Gallo and Letourneau, 2002). If, however, the cue is chemoattractive, CICR or IP3ICR is activated, the resultant change in i[Ca^{2+}] is high, CaMKII is activated, which also inhibits CaN. Attractive cues inhibit F-actin retrograde flow, and activate actin stabilising proteins and promote the anterograde assembly of actin at the peripheral domain (Bhide and Frost, 1991, Dontchev and Letourneau, 2003). Microtubule monomers are destabilised and disassembled on the side with the lowest concentration of chemoattractant; the monomers are subsequently targeted to the side with the highest concentration of chemoattractive cue by stabilising proteins (Gallo and Letourneau, 2002). Coupling of actin and microtubule assembly is imperative for growth cone motility. The exact mechanism by which Ca^{2+} regulates the cytoskeleton remains elusive. These data are summarised in Fig 1.2.

1.2.3 Receptors implicated in growth cone guidance

Signal transduction mechanisms initiated during growth cone guidance are necessarily highly complex, in order to navigate through many different tissues within the body. Many receptors will function in concert to produce a distinct turning response of a growth cone in the body and deliver it to its target. Well defined receptors for chemotactic signals include the family of tyrosine related kinase (Trk) receptors, the low-affinity p75 neurotrophin receptor, the receptor tyrosine kinase RET, Nogo-66 receptor, neuropilin, ephrins, roundabout (Robo) and deleted in colorectal cancer (DCC) (Dickson, 2002). Recent studies allude to the potential role of another receptor family: low-density lipoprotein (LDL) receptors. All LDL receptors are expressed in the nervous system and knockout studies suggest an indispensable role in neurodevelopment of higher-order organisms (Beffert et al., 2004). The hypothesis that underpins this thesis is that receptors of the LDL family are

involved in growth cone guidance. Hence, this review will now focus on the LDL receptor family and their known roles in the nervous system, and the evidence pertaining to a possible role in growth cone guidance.

1.3 THE MULTIFUNCTIONAL LDL RECEPTOR GENE FAMILY

The LDL receptor family comprises a large group of multi-ligand receptors with a diverse range of functions. The family includes core members: LDL receptor, the LDL receptor-related protein (LRP1, also known as CD91 and α-2-macroglobulin receptor) (Herz et al., 1988), LRP1b (Liu et al., 2000a), LRP2 (LRP2, also known as GP330 or megalin) (Raychowdhury et al., 1989), the VLDL receptor (VLDLR) (Takahashi et al., 1992), Apolipoprotein receptor-2 (ApoER2, also known as LRP8) (Kim et al., 1996), LRP5 (Hey et al., 1998), LRP6 (Brown et al., 1998), and sorLA-1 (also known as LR11) (Yamazaki et al., 1996) (See Fig 1.3). Owing to their ability to interact with other cell-surface receptors, ion channels and adhesion molecules, the LDL receptor family is able to initiate a diverse range of physiological processes. The LDL receptor family is characterised by its ability to endocytose ligands and nutrients, carrying them to acidic endosomes where release of the ligand can occur, while the receptor is cycled back to the cell surface (Brown et al., 1997). The LDL receptor family is traditionally described for its endocytic roles in lipid metabolism, cellular entry of viruses and toxins and vitamin uptake; cell signalling; and activation of various proteases and enzymes (Li et al., 2001a).

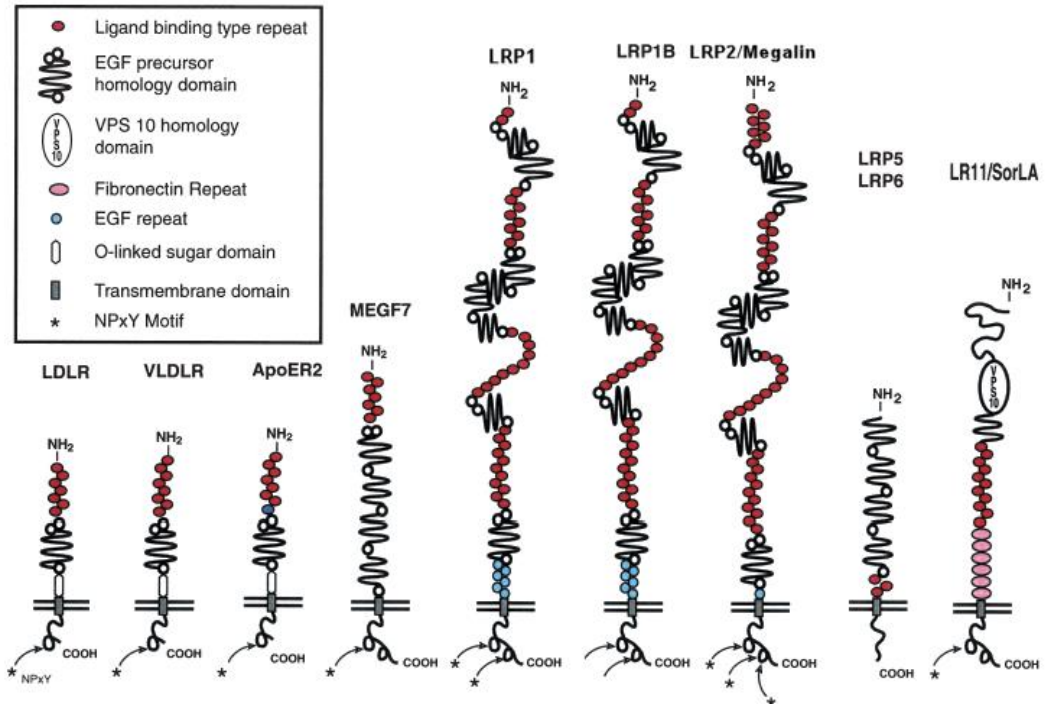

Figure 1.3 The core members of the LDL receptor family.

The common structural motifs are highlighted, demonstrating similarity between the family members. (Adapted from May *et al.* 2004)

1.4 LDL RECEPTOR FAMILY IN NEURONAL FUNCTION

1.4.1 Overview of LDL receptor function in neurons

The LDL receptor family have been implicated in numerous functions of the nervous system. These processes include neuronal outgrowth (Handelmann et al., 1992), synaptogenesis (Mauch et al., 2001, Pfrieger, 2003b, Mulder et al., 2004), synaptic transmission (May et al., 2004, Martin et al., 2008), neuromuscular junction formation (Weatherbee et al., 2006), long-term potentiation (Weeber et al., 2002), neuronal migration and neuronal patterning (Trommsdorff et al., 1999, Spoelgen et al., 2005). The LDL receptor family has an integral role in cholesterol metabolism. Cholesterol is a principal component of cell membranes and myelin sheaths, and stabilises membrane lipid rafts (Pfrieger, 2003a). Therefore, LDL receptors have a pivotal role in the developing nervous system, and in maintenance of the adult brain. Cholesterol uptake is regulated by receptor mediated endocytosis of ApoE-flagged chylomicron, with ApoE a ligand of most LDL family receptors. *In vitro*, the addition of cholesterol to neurons enhances the number and efficacy of synapses (Mauch et al., 2001).

Some of the most pertinent evidence of LDL receptor function in neurons can be ascertained from receptor knockout studies. LDLR deficient mice have deficits in learning and memory, likely due to reduced synaptic density (Mulder et al., 2004). LRP5 and LRP6 form morphogenic signalling domains with the canonical Wnt/Frz complex involved in development; not surprising is the finding that either LRP5 or LRP6 knockout mice have gross malformations in neuronal patterning. LRP5 and LRP6 double knockout mice are embryonic lethal (Tamai et al., 2000, Kato et al., 2002, Kelly et al., 2004). ApoER2 and VLDL double knockout mice have abnormalities in the layering of the brain, including

ectopic placement of neurons (Trommsdorff et al., 1999, Weeber et al., 2002). LRP1 and LRP2 are the largest and most promiscuous members of the receptor family. Individual knockout studies involving LRP1 of LRP2 in mice have shown that these knockouts are both almost exclusively embryonic lethal and associated with malformations of the brain (Willnow et al., 1996a, Lillis et al., 2008). All LDL family receptors are expressed in the central nervous system and the knockout studies mentioned above suggest an indispensable role in neurodevelopment. Some of the roles of LDL receptors in neurodevelopment have been the subject of intense investigation and are described in detail below.

1.4.2 VLDL and ApoER2 receptors

Knockout mice lacking both VLDL and ApoER2 exhibit migration defects resulting in malformations of the cortex, cerebellum and spinal cord, as well as failed retino-geniculate connectivity (Trommsdorff et al., 1999, Su et al., 2013). These defects are phenotypically identical to the very distinct and unique disordered lamination displayed in knockout mice lacking extracellular signalling ligand Reelin or its downstream intracellular adapter molecule disabled-1 (Dab-1) (Trommsdorff et al., 1999). In subsets of neurons, Reelin stimulates dendrite outgrowth and polarisation, as well as adhesion and stabilisation of these dendritic processes, culminating in migration of neurons (Niu et al., 2004, Nichols and Olson, 2010, Sekine et al., 2012). This led to the discovery that ApoER2 and VLDL are high affinity receptors of Reelin (D'Arcangelo et al., 1999, Hiesberger et al., 1999). ApoER2/VLDL are also necessary for migration of neuroblasts in the forebrain, in a process independent of Reelin (Andrade et al., 2007). Single ApoER2 or VLDL knockout mice have a milder phenotype, in part due to redundancy in function of the two receptors. More recently, it has been demonstrated that there are temporal differences in the expression of these receptors

during critical stages of development which may also lead to differences in phenotype observed between single ApoEr2 or VLDL knockout mice (Cheng et al., 2011). Humans with mutations of the VLDL receptor gene are at increased risk of schizophrenia, which is thought to be due to subtle migration defects of neurons within the brain (Deutsch et al., 2010).

The Reelin-ApoER2/VLDLR signalling system is also implicated in dendritic spine development and synaptic transmission and plasticity in the hippocampus (Weeber et al., 2002, Beffert et al., 2005, D'Arcangelo, 2005, Niu et al., 2008). Modulation of synaptic transmission occurs through controlling Ca^{2+} entry through NMDA receptors. ApoER2 is able to phosphorylate NMDA receptors by tyrosine phosphorylation of its cytoplasmic tail, and VLDL is able to interact with NMDA receptors physically, although the exact molecular mechanisms underpinning this interaction are yet to be fully elucidated (Chen et al., 2005, Herz, 2009). Hippocampal plasticity, in the form of long-term potentiation (LTP) or long term depression (LTD) is essential for learning and memory, as well as general cognition (Grover and Teyler, 1990, Norris et al., 1996, Norris et al., 1998). Plasticity occurs when tetanic stimulation of the dendrite increases (LTP) or decreases (LTD) excitatory postsynaptic potentials (EPSPs). Perfusing hippocampal slices with Reelin increases miniature EPSPs (Qiu et al., 2006). Supporting these observations, infusion of Reelin into the ventricles of wild type mouse brains increased dendritic spine density, hippocampal LTP, and improved performance in various associative and spatial learning and memory tasks (Rogers and Weeber, 2008), thereby demonstrating the involvement of Reelin/VLDL/ApoER2 signalling in cognitive processes.

1.4.3 LRP5 and LRP6 receptors

LRP5 and LRP6 are closely related to each other in structure and amino acid sequences, and are widely co-expressed in neurons (Houston and Wylie, 2002). Together LRP5 and LRP6 (LRP5/6) are implicated in neuronal migration by virtue of their involvement in Wnt signalling pathways (Pinson et al., 2000, Wehrli et al., 2000, Houston and Wylie, 2002). Wnt proteins are extracellular signalling molecules with important signalling functions during development of the central nervous system, particularly in establishing cell polarity, cell type, axon guidance and synapse formation (Wodarz and Nusse, 1998, Strutt, 2003). LRP5/6 knockout mice have gross developmental malformations of the nervous system which result from disruptions in Wnt signalling (Pinson et al., 2000, Kelly et al., 2004). LRP5 and LRP6 form a signalling complex Frizzled (Fz) receptors, and through this complex interact with Wnt-1, Wnt-3a, Wnt-3 or Wnt-7a (Yang-Snyder et al., 1996, Pinson et al., 2000, Tamai et al., 2000). When Wnts are bound to the LRP5/6/ Fz complex, the Wnt-β-catenin canonical pathway, is activated causing an accumulation of β-catenin in the cytoplasm and its eventual translocation into the nucleus, where it is able to regulate gene transcription pathways essential for neuronal development (Pinson et al., 2000, Wehrli et al., 2000, He et al., 2004, Tamai et al., 2004). Furthermore, Wnts have a direct role in axon guidance through their function as chemotactic factors, and have pivotal roles in anterior-posterior axon guidance, particularly for commissural axons in mice (Lyuksyutova et al., 2003, Domanitskaya et al., 2010). Taken together, LRP5/6 and Wnts have crucial roles in axon pathfinding and development of the nervous system.

1.4.4 LR11 (SorLA) receptor

SorLA is a receptor that is highly conserved, and robustly expressed in the brain, having features of both LDL receptors and the sortilin family of receptors, which are known for sorting proteins through secretory and endocytic pathways (Jacobsen et al., 2001). SorLA is involved in the control of neurotrophic activity through regulating the secretion and cellular uptake of glial cell line-derived neurotrophic factor (GDNF) (Saarma and Sariola, 1999, Geng et al., 2011). SorLA and GDNF knockout mice exhibit the same phenotype, which includes severe disruption of nigrostriatal connectivity in the CNS (Glerup et al., 2013). GDNF plays a critical role in neuronal survival, differentiation and function (particularly for dopaminergic neurons in the CNS, and various subsets of sympathetic, parasympathetic, sensory and enteric neurons of the PNS), as well as modulating cell migration, neurite outgrowth and synapse formation (Saarma and Sariola, 1999, Ibanez, 2010, Bespalov et al., 2011). In addition, recycling of the GDNF co-receptor, GFR-α1, is mediated by SorLA (Glerup et al., 2013). SorLA is a negative regulator of amyloid precursor protein (APP), thus indirectly modulates the neuritogenic effects of soluble APP, and as such SorLA is a major risk factor of Alzheimer's disease (Andersen 2005, Rohe 2008). SorLA has been demonstrated to interact with the highly multifunctional family member LRP1 (Gliemann et al., 2004, Spoelgen et al., 2009). Head activator peptide, a ligand of the SorLA orthologue found in hydra, is responsible for regeneration of the organism's head (Hampe et al., 1999). This intriguing role in regeneration may be of relevance to humans, but has not been investigated in detail.

1.4.5 LRP1 receptor

LRP1 is a 600kDa cell surface receptor with established roles in the kidney and the brain. LRP1 is highly expressed in neurons, particularly in the entorhinal cortex, hippocampus and cerebellum, and is also present in Schwann cells, activated astrocytes and microglia (Wolf et al., 1992, Bu et al., 1994, Rebeck, 2009, Marzolo and Farfan, 2011). Within neurons, LRP1 is predominantly localised to the postsynaptic region where it interacts with NMDA receptors via intracellular scaffold postsynaptic density protein 95 (PSD-95) (Trommsdorff et al., 1998, Gotthardt et al., 2000). LRP1 is able to influence the activity of NMDA receptors and regulate their distribution and internalisation (May et al., 2004, Maier et al., 2013, Nakajima et al., 2013). LRP1 is also able to modulate the NMDA-induced internalisation of AMPA receptor subunit GluR1 (Nakajima et al., 2013). The very nature of this LRP1/NMDA receptor relationship suggests LRP1 plays an integral role in neurotransmitter-induced calcium signalling, particularly in synaptic plasticity and thus learning and memory (Maier et al., 2013, Nakajima et al., 2013). This relationship has been demonstrated by neuron-specific cre-lox deletion of LRP1 in mice. These mice exhibit severe tremor and dystonia, behavioural abnormalities, hyperactivity, age-dependent dendritic spine degeneration, synapse loss, neuroinflammation, memory loss, eventual neurodegeneration and premature death (May et al., 2004, Liu et al., 2010), clearly demonstrating that LRP1 is crucial to neuronal function.

LRP1 contains multiple signalling domains. During post-translational modification, LRP1 is cleaved into two subunits by furin, which subsequently re-join in a non-covalent manner (Willnow et al., 1996b). LRP1 comprises a 515kD subunit and an 85kD transmembrane subunit (Willnow et al., 1996b). The soluble extracellular domain of LRP1 (sLRP1) can be cleaved by enzymes including BACE1 (von Arnim et al., 2005) and metalloproteinase

(Selvais et al., 2011), and can be detected in the blood and CSF (Liu et al., 2009, Zlokovic, 2011). sLRP1 contains the α-chain and a 55kDa fragment of the β-chain (Quinn et al., 1999). The physiological function of sLRP1 is poorly understood, but as it can bind most LRP1 ligands, one function may be as a mechanism to terminate cell signalling events, and quench excess ligands (Gaultier et al., 2008). sLRP1 administered prior to sciatic nerve constriction injury in mice was found to decrease expression of proinflammatory mediators Tissue necrosis factor-α (TNF-α) and IL-1α local to the contusion site (Gaultier et al., 2008). Furthermore, sLRP1 also inhibited p38 MAPK activation (Gaultier et al., 2008) which is induced during cellular stress, such as during apoptosis and inflammation (Chang and Karin, 2001). sLRP1 administration significantly decreased measures of neuropathic pain, concomitant with a decrease in inflammatory cytokine expression in the spinal dorsal horn, where neuropathic pain processing occurs (Gaultier et al., 2008).

1.4.6 LRP2 receptor

LRP2 (also known as megalin) is a 600kDa endocytic receptor with key roles in protein reabsorption in the kidney (Nykjaer et al., 1999). In the CNS, LRP2 is highly expressed in the forebrain, optic stalk and optic vesicle. It is also present early in development on the apical surface of the neural tube. In adult mice, expression of LRP2 in the nervous system is predominantly in the choroid plexus (Chun et al., 1999), ependymal cells (Gajera et al., 2010) and spinal cord (Wicher et al., 2005). LRP2 KO mice (on a 129SvEv x C57BL/6 hybrid background) have a series of midline defects that include cleft palate, arhinencephaly (lack of olfactory bulb formation) and holoprosencephaly (a syndrome in which the forebrain hemispheres are fused and only one ventricle forms), and most die perinatally (Willnow et al., 1996a). Holoprosencephaly results from altered activation of LRP2 ligand, bone

morphogenetic protein 4 (BMP4), and the decreased expression of LRP2 ligand sonic hedgehog (Shh) (McCarthy et al., 2002, Spoelgen et al., 2005, Christ et al., 2012). BMP4 and Shh have competing effects on neuronal stem cell proliferation (Spoelgen et al., 2005, Balordi and Fishell, 2007). LRP2 promotes neurogenesis in the adult mammalian brain by down-regulating BMP4-mediated anti-proliferative signals (Gajera et al., 2010). However, this function of LRP2 in the morphogen signalling pathways of neuronal development must be an evolutionarily recent adaptation in higher order vertebrates, as loss of LRP2 in zebrafish does not alter forebrain development (Kur et al., 2011). LRP2 also promotes neuronal migration through Shh-signalling pathways by sequestering Shh so that it can bind its other receptor, Patched-1 (Christ et al., 2012). The few mice that survive LRP2 KO have severe Vitamin D3 deficiency, as Vitamin D and its carrier protein Vitamin D binding protein (VDBP), normally reabsorbed by LRP2 in the kidney proximal tubule, are instead excreted in the urine (Willnow et al., 1996a, Nykjaer et al., 1999). Vitamin D has been implicated in cognition and depressive symptoms (Wilkins et al., 2006, Przybelski and Binkley, 2007, Shaffer et al., 2014), suggesting a further role in neuronal function which remains to be fully elucidated. LRP2 mutation in humans results in Donnai-Barrow syndrome (DBS), or facio-oculo-acoustico-renal syndrome. DBS is an autosomal recessive disorder that in its presentation includes disrupted brain formation, including agenesis of the corpus callosum, and is associated with developmental delay (Kantarci et al., 2007).

1.5 LRP1 AND LRP2 EXTRACELLULAR LIGANDS HAVE IMPORTANT FUNCTIONS IN NEURONS

LRP1 and LRP2 serve uniquely important functions roles as suggested by their expression throughout development and adulthood, and conservation among eukaryotes (Nimpf et al., 1994, Christensen and Birn, 2002). LRP1 and LRP2 share structural similarities, overlapping ligands and a remarkable array of functions (Spuch et al., 2012), setting them apart from the rest of the LRP receptors, and as such will form the focus of this thesis.

Recently, the role of LRP1 and LRP2 receptors in mediating regenerative growth of injured neurons has been a topic of investigation (Fitzgerald et al., 2007, Ambjorn et al., 2008, Chung et al., 2008, Fleming et al., 2009a, Leung et al., 2012). Following binding by the ligand metallothionein, an endogenous protein released by astrocytes following injury, LRP1 and LRP2 receptors have been shown to promote post-injury neurite sprouting in the CNS (Chung et al., 2008). LRP1 and LRP2 also promote regenerative axonal growth of peripheral DRG neurons (Leung et al., 2012). Each receptor also binds other ligands that are known to have important functions in neurons. LRP1 binds a number of distinct ligands, such as apolipoprotein E (ApoE) (Herz and Bock, 2002), tissue-type plasminogen activator (tPA) (Bu et al., 1993, Grobmyer et al., 1993), transthyretin (TTR) (Sousa et al., 2000), α-macroglobulin (α2M) (Hanover et al., 1983, Marynen et al., 1984), ß amyloid (Krieger and Herz, 1994), neuronal prion protein (Lauren et al., 2009) and metallothionein (Klassen et al., 2004). LRP2 binds some overlapping ligands including ApoE (Herz and Bock, 2002) and metallothionein (Klassen et al., 2004), as well as other proteins with putative roles in neuronal function, such as Vitamin D/VDBP complexes (Nykjaer et al., 1999).

Owing to their numerous ligand-binding complement-type repeat domains, LRP1 and LRP2 are able to bind more ligands than any other LDLR family member. LRP1 and LRP2 are able to bind at least 40 different ligands extracellularly, many of which are structurally unrelated (Spuch et al., 2012). As such, LRP1 and 2 are able to be involved in diverse biological processes, including synaptic function, neurite outgrowth, neuronal protection, cell migration and cell growth. The ligands discussed herein have pertinent roles in nervous system function, and as candidates for involvement in axon guidance, many will form the basis of the investigation of LRP1 and LRP2 function in growth cone guidance within this thesis.

1.5.1 α2-macroglobulin (α2M)

Activated human α2M is a 720KDa glycoprotein that is a ligand of LRP1 and ApoER2 (Sottrup-Jensen et al., 1985, Ashcom et al., 1990, Strickland et al., 1990, Stockinger et al., 1998), though most of the described effects in neurons are mediated through LRP1 signalling. α2M is a serum pan-proteinase inhibitor, structurally related to complement proteins, that is able to direct proteinase clearance when endocytosed by LRP1 (Sottrup-Jensen et al., 1985, Sottrup-Jensen, 1989). α2M is synthesised by numerous cell types, including neurons, where it is able to modulate migration, neuroprotection and neurite outgrowth (Mori et al., 1990, Moestrup et al., 1992, Higuchi et al., 1994, Narita et al., 1997, Du et al., 1998, Yamamoto et al., 1998). Because of the ability of α2M to bind a large number of neurotrophins, cytokines and growth factors, it has been ascribed roles in innate immunity, regulation of inflammation, and cell signalling, particularly in response to neuronal injury (Crookston et al., 1994, Gonias et al., 1994, Skornicka et al., 2002). When activated in PNS injury, α2M binds a number of inflammation-associated cytokines including interleukins (IL-6 and IL-8) and TNF-α. Consistent with an immunomodulatory role, α2M is structurally related to complement

components C4 and C3 (Armstrong and Quigley, 1999, Samonte et al., 2002). The ability of α2M to bind brain-derived neurotrophic factor (BDNF), neurotrophin-3 (NT-3), neurotrophin-4 (NT-4) and nerve growth factor-β is thought to regulate their neurotrophic activity (Wolf 1994). Intracranial infusion of α2M decreases dopamine production *in vivo* (Hu et al., 1994), and as such, deregulation of α2M may have roles in neurodegenerative disorders such as Parkinson's disease. Activated α2M is able to modulate Ca^{2+} influx through NMDA receptors in an LRP1-dependent mechanism (Bacskai et al., 2000, Qiu et al., 2002a). Accordingly, exposure of hippocampal neurons to α2M reduces the basal Ca^{2+} levels within the neuron *in vitro,* and was found to inhibit long-term-potentiation in hippocampal slices (Cavus et al., 1996, Qiu et al., 2002a). NMDA channels are essential in development, synaptic plasticity and in generation of long term potentiation, and the disruption of these channels can lead to numerous neurological disorders (Qiu et al., 2002b).

1.5.2 Tissue-type plasminogen activator (tPA)

LRP1 ligand tissue-type plasminogen activator is a serine protease that has a pivotal role in fibrin clot degradation and haemostasis via the well-established tPA/plasminogen cascade and blood-brain barrier permeability (Medcalf, 2007). The expression of tPA is very high in neurons and microglia in regions of the brain associated with learning and memory (hippocampus), motor learning (cerebellum), fear and anxiety (amygdala), and autonomic and endocrine functions (hypothalamus) (Qian et al., 1993, Seeds et al., 1995, Seeds et al., 1999, Salles and Strickland, 2002, Pawlak et al., 2003, Seeds et al., 2003, Teesalu et al., 2004). Activity-dependent glutamatergic transmission through N-methyl-D-aspartate (NMDA) receptors is modulated by tPA. tPA increases the permeability of NMDA to Ca^{2+} (Nicole et al., 2001, Samson et al., 2008). Depolarisation of dendritic spines and axon

terminals in the hippocampus (particularly in response to LTP) induces release of tPA, and through its proteolytic activity plays a role in modifying the extracellular matrix, allowing synaptic changes to occur during learning and memory (Qian et al., 1993, Lochner et al., 2006). A similar role for tPA is found in synaptic remodelling associated with emotional learning and fear conditioning. tPA is upregulated in the amygdala in response to restraint stress in mice, preceding anxiety-like behavioural changes (Pawlak et al., 2003). In addition, mice lacking tPA do not develop anxiety behaviour in response to restraint stress (Pawlak et al., 2003). Although tPA knockout mice do not have any macroscopic phenotype (Carmeliet et al., 1995) they do exhibit marked impairment in the rate and extent of motor learning (Seeds et al., 2003). The ability for tPA to modify the extracellular environment by proteolysis also has implications for axon pathfinding and cell migration. tPA is secreted from the tip of growth cones, thus modulating the extracellular environment and facilitating axon pathfinding (Krystosek and Seeds, 1981, 1984, 1986). Mice lacking tPA exhibit retarded neuronal migration in the cerebellum, which is postulated to be due to the loss of tPA secretion (Seeds et al., 1999). The role of tPA is has also been investigated in morphine and alcohol addiction pathways. Upregulation of tPA occurs in the nucleus accumbens and limbic system during morphine and ethanol addiction, respectively. In tPA knockout mice, however, in the absence of tPA the reward effect of alcohol and morphine is diminished (Nagai et al., 2004). Taken together, these studies demonstrate the importance of tPA in both development of the nervous system and synaptic modulation.

1.5.3 Apolipoprotein E (ApoE)

ApoE is a 34-kDa secreted glycoprotein that associates with LDL receptors and primarily functions in plasma to promote the endocytosis of cholesterol-rich chylomicron (Herz et al., 2000). There are three isoforms of ApoE resulting from single-nucleotide polymorphisms, most commonly ApoE3, followed by ApoE4 and ApoE2. ApoE has been implicated in development, synapse formation and neuronal plasticity (Masliah et al., 1995, Fagan et al., 1996, Mauch et al., 2001, Ji et al., 2003, Hoe and Rebeck, 2005). Mice deficient in ApoE develop normally, but have an age-dependent decrease in spine density and arborisation in the hippocampus and frontal cortex, as well as dysregulation of microtubules in dendrites (Masliah et al., 1995). By 6 months of age, mice lacking ApoE demonstrated significant deterioration in working memory (Gordon et al., 1995). Consistent with a role in learning and memory formation, application of recombinant ApoE to hippocampal slices revealed that compared to controls, apoE4 exposure increased LTP, while apoE2 decreased LTP. ApoE3 application had no effect on LTP (Korwek et al., 2009). ApoE3 is able to promote neurite extension *in vitro,* suggesting a role in trophic support to neurons (Holtzman et al., 1995, Hayashi et al., 2007), highlighting the importance of ApoE in maintenance of the nervous system.

1.5.4 Transthyretin (TTR)

LRP2 ligand, Transthyretin (TTR), is a plasma and cerebrospinal fluid protein chiefly known for its role in retinol and thyroxine transport (Sousa et al., 2000). Mutations of TTR are associated with increased aggregation and deposition in the PNS, triggering development of the peripheral neurodegenerative amyloidopathy known as familial amyloid polyneuropathy

(Saraiva, 2003). TTR knockout mice do not have any macroscopic phenotypes, however they have impaired performance in sensorimotor and cognitive tests (Sousa et al., 2004, Fleming et al., 2007, Sousa et al., 2007). TTR knockout mice are also associated with decreased signs of depressive behaviour and anxiety, demonstrated by increased exploratory behaviour (Sousa et al., 2004). The mechanism by which this occurs has not been fully elucidated, but evidence suggests involvement of noradrenergic neurons of the limbic region (Sousa et al., 2004). TTR has been demonstrated to have roles in neuronal maintenance and regeneration, enhancing neurite outgrowth *in vitro* and promoting nerve regeneration following injury *in vivo* (Fleming et al., 2007, Fleming et al., 2009a).

1.5.5 Vitamin D/vitamin D binding protein complex

Neurons obtain Vitamin D when the vitamin D/vitamin D binding protein complex is internalised by neurons via LRP2 (Nykjaer et al., 1999). Vitamin D is able to elicit roles within cells by binding the vitamin D receptor in the nucleus, where it acts as a transcription factor principally upregulating expression of proteins involved in Ca^{2+} absorption (Chatterjee, 2001). However, the classic non-genomic function of vitamin D is through its metabolised form calcitriol, in regulation of serum calcium levels (Haussler et al., 2013). Vitamin D is reported to have a number of protective roles in various neurological disorders in humans, with much of our understanding of vitamin D amassing from investigations into one of its inactive precursors, 25(OH)D3 (vitamin D3), which is metabolised into its active form, 1,25(OH)D3. Vitamin D3 has been observed to increase expression of neurotrophins nerve growth factor (NGF), neurotrophin-3 (NT-3), GDNF *in vitro* (Neveu et al., 1994, Naveilhan et al., 1996, Cornet et al., 1998) as well as *in vivo* (Wang et al., 2000). Therefore, perhaps not surprising was the finding that vitamin D3 supplementation improves myelination and

functional recovery after rat peroneal nerve transection (Chabas et al., 2013), and is neuroprotective in response to various toxic insults to the nervous system (Garcion et al., 2002). Vitamin D3 deficiency is commonly reported in patients with multiple sclerosis (MS), and is associated with a poorer disease prognosis (van der Mei et al., 2007). The immunomodulatory action of vitamin D3 likely plays an important role in the pathogenesis of MS (Hewer et al., 2013). A number of clinical trials using vitamin D3 supplementation in MS support the notion that vitamin D3 may improve the clinical outcome (Aivo et al., 2012, Stewart et al., 2012). A similar observation has been made relating to low vitamin D3 and the risk of epilepsy (Harms et al., 2011). A recent study reporting that vitamin D3 supplementation was found to reduce the incidence of seizures in epilepsy by 40% (Hollo et al., 2012). Although the study was limited by a small sample size, the results did highlight the importance of vitamin D in normal brain function.

Severe vitamin D3 deficiency has been linked to cognitive deficits, but the exact process by which vitamin D3 is involved remains enigmatic. Seasonal affective disorder (SAD) is a common depressive disorder that has long has been associated with low vitamin D levels (Stumpf and Privette, 1989). Maternal vitamin D3 deficiency during pregnancy results in altered neurodevelopment in rat offspring (Eyles et al., 2003). Enlarged ventricles, thinner cortices and enhanced cell proliferation were observed, with concomitant reductions in NGF, GDNF, and p75 neurotrophin receptor (Brown et al., 2003, Eyles et al., 2003, Cui et al., 2007, Eyles et al., 2009). Even after these offspring were maintained on a normal diet, persistent changes in the adult brain were still observed (Feron et al., 2005). These included enlarged ventricles and reduced NGF expression, as well as reduced expression of neurofilament, MAP-2 and GABA-A (α4), which are important for neuronal structure and

transmission, respectively (Feron et al., 2005). Vitamin D3 levels during pregnancy are also inversely correlated with autism (Cannell and Grant, 2013) and schizophrenia (McGrath et al., 2010) risk in offspring. Given the varied etiology of schizophrenia and autism-spectrum disorders, the mechanisms by which vitamin D3 may be implicated are likely diverse. Numerous mechanisms for this association have been proposed. For example, the ability for the active metabolite of vitamin D3 to upregulate DNA repair genes (Chatterjee, 2001) may promote repair of the *de novo* mutations contributing to the risk of autism (Sanders et al., 2012) and schizophrenia (Xu et al., 2011). Vitamin D has numerous immunomodulatory and anti-autoimmune actions; both schizophrenia and autism have also been linked to autoimmune dysfunction, with various brain-specific autoantibodies (Cabanlit et al., 2007, Ezeoke et al., 2013) appearing to influence the disease severity in a dose-dependent manner (Mostafa and Al-Ayadhi, 2011). Taken together, vitamin D/VDBP have roles in many aspects of neuronal function, both in the developing and adult nervous system.

1.5.6 Myelin-associated glycoprotein (MAG)

The strongest evidence to date, linking LRP1 to axon pathfinding, is the recent identification of LRP1 as a novel receptor for myelin-associated glycoprotein (MAG). MAG is a sialic-acid binding Ig-family lectin cell-membrane glycoprotein implicated in neurite outgrowth inhibition, growth cone collapse, and has important and well established roles in development and maintenance of the nervous system (Henley et al., 2004, Hines et al., 2010). MAG is able to bind LRP1 directly, independently of its lectin activity (Stiles et al., 2013), to form a complex with p75 neurotrophin receptor, activating RhoA (Mantuano et al., 2013). RhoA is localised to developing axons and growth cones, where it is established as a potent mediator of growth cone collapse and neurite retraction (Wu et al., 2005). Inhibition of growth is

equally as important as promotion of growth in nervous system development, as the balance between these two processes allows for target discrimination in axon pathfinding.

1.5.7 Metallothionein

Metallothioneins (MTs) are highly conserved, small (6-7 kDa), inducible heavy metal binding proteins. By virtue of a high cysteine content (30% of amino acid sequence), MTs are also avid scavengers of reactive oxygen species (Thornalley and Vasak, 1985). There are four isoforms of MT: MTI and MTII, which are widely expressed in the nervous system and body; MTIII, which is primarily a brain-specific isoform, and MTIV, which is found in some stratified squamous epithelia and has not been identified in nervous tissue (Kobayashi et al., 1993, Quaife et al., 1994, reviewed in Coyle et al., 2002). MTI and MTII only differ by a few amino acids, and to the best of our current understanding, are identical in function (Hidalgo et al., 2001), therefore are often referred to in the literature as MTI/II. MTI/II and III encompass a surprisingly diverse range of functions, which importantly includes neuronal protection, cognition, neuronal outgrowth and regeneration (West et al., 2008). MTI/II are ligands of LRP1 and LRP2 (Klassen et al., 2004, Ambjorn et al., 2008), although whether LRP1 and LRP2 are receptors for MTIII is yet to be determined. MTI/II are constitutively expressed, and are upregulated in response to neuronal injury, protecting neurons from apoptosis as well as promoting regrowth and repair *in vivo* (Giralt et al., 2002a, Chung et al., 2003). MTI/II knockout mice exhibit impaired cognition, are associated with a poorer outcome in response to CNS injury, and are more susceptible to toxicants and oxidative stressors (Lazo et al., 1995, Carrasco et al., 2000, Giralt et al., 2002b, Trendelenburg et al., 2002, Levin et al., 2006). The association of MT I/II with LRP1 and LRP2 receptors transiently activates Akt and ERK, which belong to the mitogen activated protein kinase

(MAPK) and the phosphoinositide-3 kinase/Akt (PI3K/Akt) intracellular signalling pathways (Asmussen et al., 2009a), which have established roles in neuronal differentiation and survival respectively (Brunet et al., 2001, Chang and Karin, 2001). The sustained response of neurite outgrowth seen is due to MT initiated activation of the transcription factor, CREB, which alters gene transcription of proteins that are conducive to sustaining neuroprotection and neurite outgrowth (Ambjorn et al., 2008).

1.6 LRP1 AND LRP2 AND THEIR DIVERSE CELL SIGNALLING PATHWAYS IN NEURONS

Although LRP1 and LRP2 are able to endocytose many ligands and target them for lysosomal degradation, it has become increasingly evident that this describes only one of many functions (Herz et al., 2000). LRP1 and LRP2 have a complex extracellular domain and an intracellular domain that together allow for the propagation of diverse signalling pathways (Spuch et al., 2012). The intracellular domains of both LRP1 and LRP2 have been shown to interact with numerous signalling and scaffold proteins in a phosphorylation-dependent manner, allowing for the formation of signalling hubs through the binding of co-receptors (Spuch et al., 2012).

1.6.1 LRP1 INTRACELLULAR SIGNALLING MECHANISMS

The intracellular domain (ICD) of LRP1 contains several motifs that regulate receptor endocytosis, cell signalling and binding to co-receptors. There are a number of co-receptors of LRP1 that have been identified, including platelet-derived growth factor receptor beta (PDGFR-β) (Boucher et al., 2002, Loukinova et al., 2002), tyrosine kinase receptor A (TrkA)

(Shi et al., 2009), TGFβR-I (Huang et al., 2003), Frizzled-1 (Pinson et al., 2000, Tamai et al., 2000), amyloid precursor protein (APP) (Knauer et al., 1996) and insulin-like growth factor 1 receptor (Woldt et al., 2011). These associations compound the number of intracellular pathways by which distinct LRP1 ligands may elicit their effects in neurons. LRP1 can be cleaved by ɣ-secretase to release the ICD allowing it to translocate to the nucleus, where it has been demonstrated to act as a transcription factor (Zurhove et al., 2008). The role of the LRP1 ICD as a transcription factor highlights the diverse ways in which LRP1 can signal intracellularly.

LRP1 ICD contains two di-leucine motifs, one YXXL motif and two NPXY motifs, which together are able to bind many cytosolic ligands in a phosphorylation dependent manner (Li *et al.* 2001). LRP1 can activate various processes via signalling through adaptor proteins. For example, as a result of binding scaffold Dab1(Trommsdorff et al., 1998), LRP1 is able to activate tyrosine kinases involved in cytoskeletal remodelling and cell motility (Hiesberger et al., 1999). LRP1 is able to bind PSD-95 (Gotthardt et al., 2000) which is a scaffold that regulates the dynamic synaptic environment. LRP1 is also able to bind JIP-1/JIP-2, (Gotthardt et al., 2000) which are involved in inhibition of the pro-apoptotic stress-activated protein kinase/c-Jun N-terminal kinase JNK/SAPK signalling pathway (Kyriakis et al., 1994). LRP1 can be phosphorylated by cAMP-dependent protein kinase A (PKA) (Li et al., 2001b). Src family kinases (SFKs) can mediate tyrosine phosphorylation of the second NPxY motif in the LRP1 ICD, which allows Shc to bind, allowing for the propagation of MAPK pathways (Barnes et al., 2001). MAPK pathways are important for neurite outgrowth, and cell survival signalling (Chang and Karin, 2001). In response to PDGFR-β receptor activation, or to α2M or tPA binding to LRP1, SFKs phosphorylate LRP1 (Boucher et al., 2002, Loukinova et al.,

2002, Shi et al., 2009). LRP1 phosphorylation activates the downstream MAPK pathway (Boucher et al., 2002, Loukinova et al., 2002), and transactivates TrkA, which in turn activates downstream target Akt (Boucher et al., 2002, Loukinova et al., 2002, Shi et al., 2009)Shi et al., 2009). The many intracellular binding proteins of LRP1 highlight the diverse array of pathways that can be elicited in response to LRP1 receptor binding.

1.6.2 LRP2 INTRACELLULAR SIGNALLING MECHANISMS

Like LRP1, LRP2 can be proteolytically cleaved by ɣ-secretase to release an ICD that is able to regulate gene expression (Zou et al., 2004, Li et al., 2008). There are a number of motifs that are present in the LRP2 ICD that are likely involved in intracellular signalling processes, and they include: one dileucine motif, three NXPY motifs, two proline-rich sequences, one PDZ terminal motif, a Src-homology 3 binding motif, a Src-homology 2 binding motif, several putative protein kinase C and casein kinase II phosphorylation motifs as well as one PKA phosphorylation motif (Hjalm et al., 1996). However, the roles of many of these motifs, particularly in neurons, are not as well defined for LRP2 as they are for LRP1. Given the paucity of information about LRP2 intracellular signalling pathways, some evidence comes from the interaction of intracellular adapter molecules and their known roles in neuronal signalling. Some possible signalling pathways in neurons, relevant to development, are discussed below.

An adaptor site for casein kinase II (CKII) is present on the LRP2 ICD (Hjalm et al., 1996) CKII is able to regulate NMDA activity (Hu et al., 2014), and thus may be a link between LRP2 and Ca^{2+}signalling. NMDA Ca^{2+}signalling is important for synaptic function, and this relationship is cemented by the finding that LRP2 binds PSD-95 (Larsson et al., 2003). PSD-

95 has well established roles in the postsynaptic density as a scaffold for glutamatergic receptors, and regulating their function and trafficking (Xu, 2011). Ankyrin-repeat family A protein (ANKRA) interacts with the PXXPXXP within the proline rich region. ANKRA binds the large-conductance Ca^{2+} activated K^{+} (BK) channel and positively regulates its activity (Lim and Park, 2005). The BK channel regulates excitability of neurons and neurotransmitter release in the CNS (Pedarzani et al., 2000) and neuropathic pain in the PNS (Chen et al., 2009). Intriguingly, TRPV1, a cation channel also involved in nociception, has been found to cross talk and bind BK channels (Wu et al., 2013) raising the possibility that LRP2 can modulate complex Ca^{2+} signalling events in the CNS and PNS.

An additional intracellular adapter that can bind the ICD of LRP2 is membrane-associated guanylate kinase with inverted orientation-1 (MAGI-1) (Patrie et al., 2001). Little is known about the function of MAGI-1 but it is thought to act as a scaffold in cell adhesion. MAGI-1 has been identified in growth cones (Ito et al., 2012) and has been shown to bind p75 neurotrophin receptor (p75NTR) (Ito et al., 2013a), and as such, LRP2, via MAGI-1, may be involved in the regulation of neurite outgrowth or guidance of peripheral neurons.

The third NXPY motif of LRP2 binds cytosolic scaffold protein disabled protein-2 (Dab2) (Oleinikov et al., 2000, Gallagher et al., 2004). As a scaffold protein, Dab2 has diverse roles within the cell and is implicated in cell proliferation and differentiation (Hocevar et al., 2003). One function of Dab2 is as a negative regulator of canonical Wnt signaling (which involves LRP5/6, discussed at 1.4.3) by stabilising the β-catenin destruction complex, thereby promoting degradation of β-catenin and terminating Wnt signalling (Hocevar et al., 2003). Dab2 is able to modulate RhoA, which as outlined earlier, is important for growth cone navigation (Huang et al., 2007). Dab2 is also able to bind nonmuscle myosin heavy chain

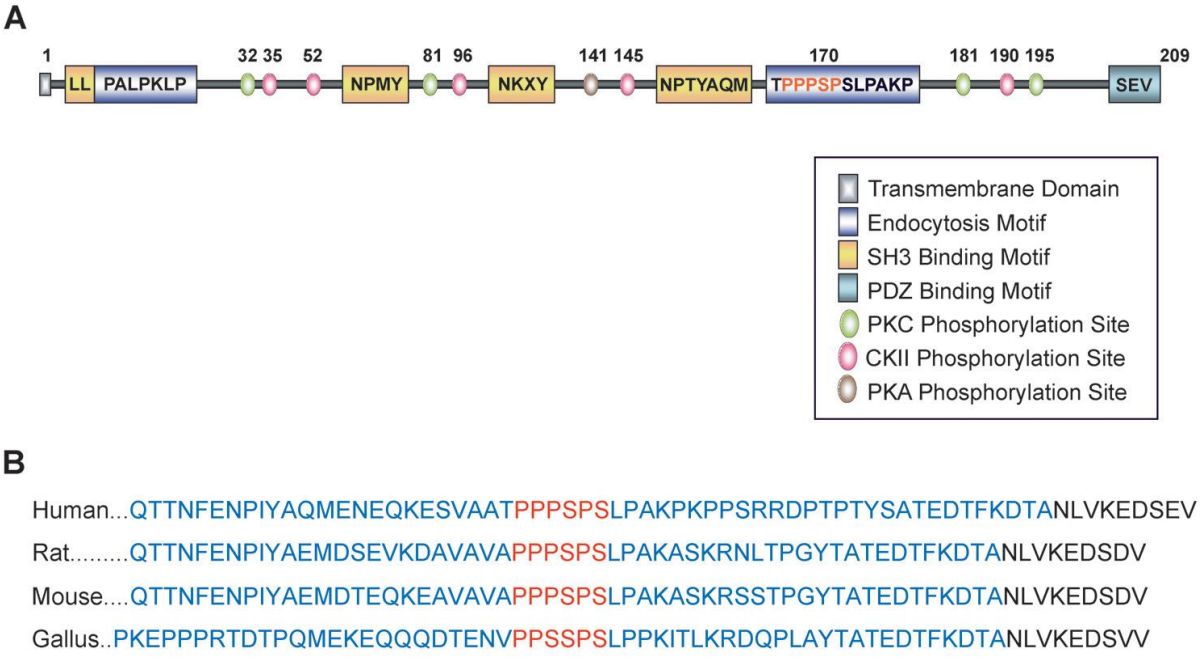

Figure 1.4. Intracellular domain of LRP2

Schematic of LRP2 structure. The PDZ domain facilitates binding to PSD-95 and MAGI-1. PXXPXXP binds ANKRA. The highly conserved PPPSP (red) motif is responsible for the interaction allowing LRP2 to be constitutively phosphorylated by GSK3 which has a role in negative-regulation of LRP2 recycling to endosomes (Yuseff et al., 2007). Figure from (Marzolo and Farfan, 2011).

IIA (NMHC-IIA); indeed LRP2, Dab2 and NMHC-IIA were able to be isolated as a functional complex in kidney cells along with beta actin (Hosaka et al., 2009). Class II myosins such as NMHC-IIA are thought to be important for cytoskeleton organization, which is important for cell motility (Sellers, 2000). These associations support a potential role of LRP2 in neuronal growth and axon guidance.

1.7 NERVE REGENERATION IN PERIPHERAL NEUROPATHY

To date I have described a number of LRP1 and LRP2 ligands that have protective effects on neurons, and may be candidates for promoting axon pathfinding; as such, the properties of these ligands will be investigated within the experimental chapters to follow. The overarching aim within this thesis is to identify a candidate chemotactic molecule that can be used therapeutically in peripheral neuropathy or denervation, to guide the regenerative growth of neurons *in vivo* and promote functional regeneration. As such, a discussion into chemotactic factors and peripheral neuropathy follows.

Peripheral neuropathies are diseases of the nerves of varied etiology and complexity (Brannagan, 2012). In the past two decades, the potential of growth factors as a means of directing neuronal repair and preventing apoptosis of damaged neurons in neuropathy has become increasingly apparent (Terenghi, 1999). There is evidence that the expression of growth factors (particularly neurotrophins) and/or their receptors is altered in various forms of peripheral neuropathy (Leinninger et al., 2004). Given that neurotrophins promote survival and maintenance of neurons, it has led to the therapeutic application of neurotrophins, both *in vitro* and *in vivo,* to promote neuronal regeneration in models of diabetic neuropathy (Leinninger et al., 2004).

1.8 SENSORY NERVES OF THE SKIN

The principal neurons affected in peripheral neuropathies are sensory neurons (Lauria et al., 2005). Sensory neurons are a heterogenous group that convey different kinds of information, and are classified broadly by diameter of the cell body: small (20um, called C-fibres), medium (21-40um, called A-δ) and large (>40um, called A-α and A-β) (Baron, 2006). Epidermal nerve fibres (ENFs) are the nerves that exist in the outermost layer of the skin, the epidermis. ENFs comprise of C-fibres and A-δ fibres (Baron, 2006). Peripheral nerve terminals relay normal and abnormal sensory input, such as thermal, mechanical or chemical information, as electrical action potentials of varied intensity into the CNS (Julius and Basbaum, 2001). Although research demonstrates there is increasing overlap between characteristics of the crudely delineated subtypes, there is some general consensus: C-fibres are unmyelinated and involved in nociception and heat; A-δ are lightly myelinated mechanoreceptive fibres; A-α and A-β are the heavily myelinated, fast conducting proprioceptive fibres (Julius and Basbaum, 2001). Heavily myelinated processes tend to enter the spinal cord medially, and terminate in deeper laminae of the dorsal horn, whereas smaller unmyelinated fibres enter laterally and terminate in superficial lamina, such as lamina I and II of the dorsal horn (Light et al., 1979). Although individual ENFs are initially myelinated, once they reach the basement membrane, they lose their Schwann cell ensheathment (Kennedy and Wendelschafer-Crabb, 1993). Peripheral neuropathies are characterised based on the trigger and on the subtype of neuron affected.

1.9 PERIPHERAL NEUROPATHY

Peripheral neuropathies (PN) are an indication of many diseases, specifically affecting peripheral nerves (Martyn and Hughes, 1997), and are associated with a significantly decreased quality of life. PN occurs through disparate etiologies, including: as a symptom of systemic illness such as diabetes, vitamin deficiency (such as vitamin B12), renal failure and as a side effect of medications such as some chemotherapeutic drugs (Martyn and Hughes, 1997).

Epidemiological studies tend to underestimate the prevalence of these conditions in the general population, due to neuropathy being present in some individuals without overt symptoms (and therefore requiring sensitive equipment for its detection), and in some cases a lack of consensus of the diagnostic criteria. Although there is a scarcity of epidemiological studies of PN, the data that exists from early studies suggests a prevalence of between 2.4 and 7% in the general population (Bharucha et al., 1991, Martyn and Hughes, 1997, Philip-Ephraim et al., 2013, Remiche et al., 2013). However, a systematic meta-analysis of studies examining neuropathic pain (as symptom of some, but not all PNs) suggest that neuropathic pain has a prevalence of 6.9 to 10% in the general population (van Hecke et al., 2014), which would indicate that the earlier epidemiological studies on PN incidence are at best, an inadequate representation. Assessing the incidence of peripheral neuropathies as a whole allows us to emphasise the impact of disability and socioeconomic burden of PN related disease in the community, and requires further investigation.

1.10 DIABETIC NEUROPATHY

1.10.1 Clinical presentation

In the western world, diabetic neuropathy is the most prevalent form of peripheral neuropathy, with mild to severe forms of the disease affecting between 20-60% of people with diabetes (Ziegler et al., 1992, Dyck et al., 1993, Won et al., 2014). Diabetic neuropathy is the most common complication of diabetes mellitus (Candrilli et al., 2007). Diabetes mellitus is a group of diseases of heterogenous etiology, that are characterised by high blood sugar (Zimmet et al., 2001). The pathophysiology of diabetic neuropathies can be just as diverse as the etiology of the underlying disease. The neuropathy may affect sensory, motor and autonomic nerve fibres, and is associated with axonal atrophy, demyelination, attenuated regenerative potential, inflammation and progressive loss of peripheral nerve fibres (Sinnreich et al., 2005). The disease often affects the longest nerves first, such that nerves in the feet are initially affected, followed by the hands, progressing from distal to proximal sites, forming a characteristic stocking/glove distribution (Sinnreich et al., 2005). The clinical manifestation of the most common form of the disease (diabetic peripheral neuropathy) includes symptoms such as development of mechanical allodynia (pain that results in response to stimulus that would not normally cause pain), hyperalgesia (increased sensitivity to painful stimuli), muscle weakness and sensory loss (Sinnreich et al., 2005). Sensory loss (loss of light touch and pain) predisposes individuals to lesions on the feet and ulcerations, which when untreated and unrecognised, can result in limb amputation secondary to gangrene (Sorensen et al., 2006b). Neuropathic pain is a common and poorly tolerated symptom that is resistant to most therapeutic interventions (Zimmermann 2001). Frequently, the neuropathy will decrease the quality of life more than the underlying disease itself and as such poses a

significant socioeconomic burden (Ziegler and Luft, 2002). Underlying these symptoms is the pathology of the neuropathy itself, which not only includes loss and degeneration of neurons, but the associated Schwann cells as well (Dey et al., 2013).

In diabetic peripheral neuropathy, there is withdrawal of nerve fibres from the epidermis, and their improper termination instead occurs in the dermis (Fig 1.5). The improper termination of these fibres contribute to pain syndromes. Loss of ENFs can occur early in diabetes even before the onset of overt symptoms or slowed nerve conduction, although is more severe in patients experiencing neuropathic pain (Sorensen et al., 2006a, Loseth et al., 2008). Furthermore, there is increasing evidence that neuropathy can develop during impaired glucose tolerance, prior to the onset of diabetes (Novella et al., 2001, Singleton et al., 2001, Sumner et al., 2003). C-fibres are among the most commonly affected in diabetic neuropathy (Polydefkis et al., 2003). The extent of ENF loss is a function of the duration of diabetes (Shun et al., 2004, Lauria, 2007).

1.10.2 Current therapeutics for diabetic neuropathy

There is currently no curative treatment for diabetic neuropathy, other than restoration and maintenance of normoglycaemia, although complete reversal of severe neuropathy is unlikely in humans. The use of insulin to restore normoglycaemia in some animal models of diabetic neuropathy reversed the neuropathic phenotype (conduction slowing and restored sensory axon calibre) however such favourable results are rarely seen in humans (Zochodne et al., 2004). Existing therapies only address the underlying disease (diabetes mellitus) or the symptom of pain, (although for many this is inadequate or poorly tolerated), and do not treat the nerve fibre dysfunction itself or promote nerve regeneration.

1.10.3 Pathophysiology of diabetic neuropathy

Understanding the pathologic basis of diabetic neuropathy is important for devising effective therapeutics. Despite intense investigations over the decades, the definitive pathogenesis of diabetic neuropathy has remained controversial and for the most part unclear (Vincent et al., 2011). The pathophysiological triggers for DN can be diverse, as is evidenced by the many types of nerve fibre affected (Sinnreich et al., 2005). Furthermore, the course of disease may be influenced by a number of modalities, for example, the type of diabetes (Vincent et al., 2011). The development of diabetic neuropathy is propelled by hyperglycemia and is also affected by insulin deficiency and dyslipidemia (Vincent et al., 2011). Mechanisms implicated in the disease include microangiopathy with ischemia, deficiency in neurotrophic factors and/or their receptors, excessive formation of advanced-glycation end-products, oxidative stress, mitochondrial dysfunction, genetic susceptibility and polyol flux (Vincent et al., 2011). Polyol accumulation in diabetic neuropathy leads to a number of downstream deregulations within the cell. Polyol accumulation occurs in cells that do not require insulin to take up glucose (such as neurons), and as such are subject to the large fluctuations in blood glucose (Greene and Lattimer, 1985). In a hyperglycaemic state, aldose reductase becomes flooded with glucose and metabolises some to sorbitol (Clements, 1986). Sorbitol (the polyol implicated in this pathway) cannot cross cell membranes and thus accumulates, causing an osmotic imbalance, disrupting ion channels, impairing transport of cytoskeletal proteins, and culminating in slowed conduction speeds (Naziroglu et al., 2012). In advanced diabetes where vascular insufficiencies exist and exacerbate the course of neuropathy, one argument may be that the vascular insufficiency is due to a loss in growth factors. Nerves and blood vessels arborise in an orderly pattern throughout the body, often together, and recent studies

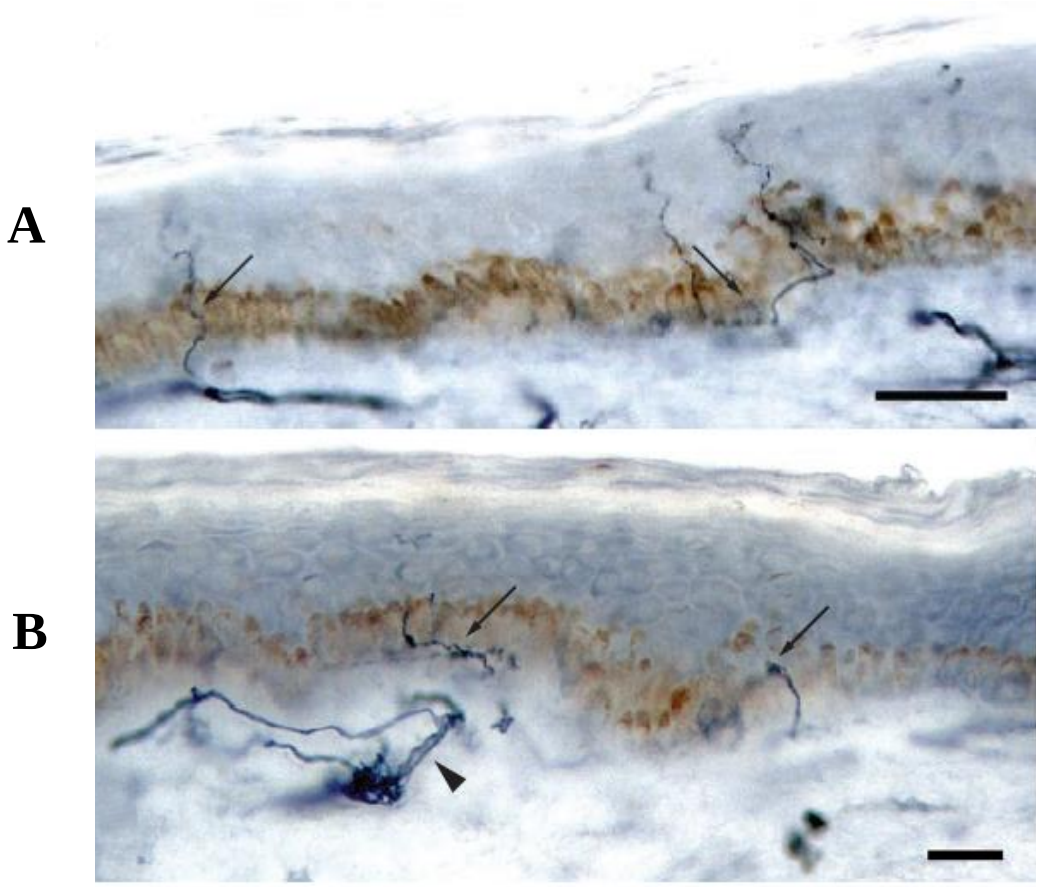

Figure 1.5 Innervation of the epidermis in the distal leg of humans

Sensory neurons stained in black. Arrows indicate ENFs within **(A)** Normal skin. Fibres have a straight course and slight varicosities. **(B)** Diabetic skin. Fibres terminate improperly and ENFs are short and tortuous. Scale bar 50µm. (Lauria, 2007)

have revealed that guidance cues involved in the development of the nervous system also help blood vessels navigate to their targets (Carmeliet and Tessier-Lavigne, 2005). Neurons in diabetic neuropathy demonstrate a diminished regenerative potential (Bisby, 1980, Ekstrom and Tomlinson, 1989, Kennedy and Zochodne, 2005, Zochodne et al., 2007). In diabetic peripheral neuropathy, there is a significant decrease in the neurotrophins NGF, BDNF, NT-3 and GDNF (Anand, 2004). These neurotrophins have well established roles in sensory neuron survival (Maisonpierre et al., 1990, Davies, 1994). The nerves affected in diabetic neuropathy are in a diseased state, and may be particularly vulnerable to further insult. A decrease in survival signals from neurotrophic factors thus likely contributes to the course of disease. Regardless of the underlying pathogenesis of diabetic neuropathy, two things remain clear: in order to treat diabetic neuropathy, firstly nerve degeneration must be prevented, and secondly, nerve regeneration must be promoted.

1.10.4 Experimental models of diabetic neuropathy

Experimental models are a means by which therapeutics for diabetic neuropathies can be developed. While mouse models of diabetic neuropathy have been widely used, there remains a lack of consensus of the most appropriate animal models for diabetic neuropathy, due to the differences in disease markers, and inconsistencies between symptoms measured in human disease pathogenesis and that of the murine model (Bierhaus and Nawroth, 2012). Rat models are less widely used despite their closer symptomatic profile to humans, and possession of very similar skin architecture (Islam, 2013). This discrepancy between use of rat and mouse models is likely due to housing requirements and cost factors. Obese Zucker rats, which have a deletion in the leptin receptor, are a very popular model of type II diabetes

(Islam, 2013). However, the emergent role of leptin as an important neuroprotective factor deems this model inappropriate for the study of diabetic neuropathy (Folch et al., 2012).

Although many models of diabetes are raised through genetic manipulation, diabetes can also be induced artificially through use of the drug streptozotocin, which has specific toxicity for insulin producing β-cells in the pancreas (Like et al., 1978). Extensive review of the literature suggests that the best rodent model of diabetic neuropathy is the high-fat diet low-streptozotocin-treated rat, first described in 2000 by Reed and colleagues (Reed et al., 2000). This model of type 2 diabetes has been used for preclinical screening of drugs, however, like most diabetic models, neural function has been insufficiently categorised and profiled. The accepted best-practice protocol for high-fat low-streptozotocin induced diabetes involves introduction of a high-fat diet (22% fat by weight) at least two weeks prior to injection of streptozotocin (30-50mg/kg) (Reed et al., 2000, Srinivasan et al., 2005). Although rats solely fed a high fat diet do not become hyperglycemic, streptozotocin damages insulin producing β-cells such that hyperglycaemia develops (Reed et al., 2000). Rats treated with streptozotocin combined with a high fat diet results in the development of mechanical allodynia, and exhibit a substantial loss of ENF secondary to characteristic insulin resistance, hyperglycemia and dislipidemia (Reed et al., 2000). In humans, type 2 diabetes develops when hyperglycaemia occurs secondary to a decrease in insulin production and insulin resistance, and is usually associated with a nutritionally poor high fat diet; indicating that the high-fat low-streptozotocin model is representative of the disease.

1.10.5 Neurotrophic factors as experimental therapeutics in diabetic neuropathy

In the past two decades the potential of neurotrophic factors and growth factors as candidate therapeutics in neuropathy has become evident, because they are able to direct neuronal regrowth, promote sprouting, survival and phenotypic maintenance, and protect neurons from mechanical, oxidative or ischemic damage (Siegel and Chauhan, 2000). Indeed, several neurotrophins have been tested in rodent models of diabetic neuropathy, with encouraging results (Akkina et al., 2001, Pradat et al., 2001, Schmidt et al., 2001, Christianson et al., 2007). However, many experimental therapies have had poor translation into human therapeutics (Apfel, 1999). Further understanding in the area of diabetic neuropathies continues to suggest a beneficial role of neurotrophins. More rigorous considerations of the dosage and delivery system are needed for future success of neurotrophins as a therapeutic in neuropathy (Apfel, 2002). Understanding the mechanisms by which these factors elicit these effects on cells offers an opportunity into the development of unique therapeutics.

JUSTIFICATION FOR PROJECT

The loss of neuronal connections as a result of disease contributes to the pathogenesis of neuropathies such as diabetic neuropathy. The 'connection' of neurons is the product of individual growth cones responding to a myriad of chemotrophic growth cues. There would be great therapeutic benefit if it was possible to harness the properties of chemotactic cues and use them to guide and accelerate neuronal repair after connections have been damaged or lost, thereby having implications in the treatment of some neurological diseases, or in re-innervating tissues that have lost their neuronal connections as a result of disease or traumatic injury. The primary challenge encountered when promoting regeneration of nerves is the

ability to reintegrate into neural circuitry and form functional connections. It is therefore important to understand the mechanisms by which chemotactic factors function, to provide additional avenues for enhancing directed neurite regrowth and connectivity in neuropathy. Although some surgical strategies exist for enhancing regeneration in gross nerve lesions of the PNS, the intricate network of nerves in the skin region is not amenable to surgical repair. Conceptually, a repair strategy could be based on the topical application of chemotactic factors, which attracts the regrowth of ENFs back to their correct locations into the epidermis (Fig 1.6).

It is well established that LRP receptors are capable of forming complex signalling domains by recruiting co-receptors. Given the emerging role of LRP1 and LRP2 in modulation of neuronal growth, especially during injury, I ask whether ligands of LRP1 or LRP2 could guide neuronal growth, and promote regeneration in animal models of neuropathy. Such a system would represent a novel, non-classical axon guidance system. Furthermore, understanding the mechanisms by which these factors elicit these effects on neurons presents an opportunity into the development of unique therapeutic analogues.

To address this hypothesis, this thesis explores two overarching aims:

1. To examine the ability of LRP1 and LRP2 ligands (with known roles in neuronal function), to promote growth cone guidance *in vitro* and determine the mechanism of action
2. To examine the effect of candidate LRP1 and LRP2 ligand/s to guide regenerative growth and promote reinnervation after peripheral nerve damage *in vivo.*

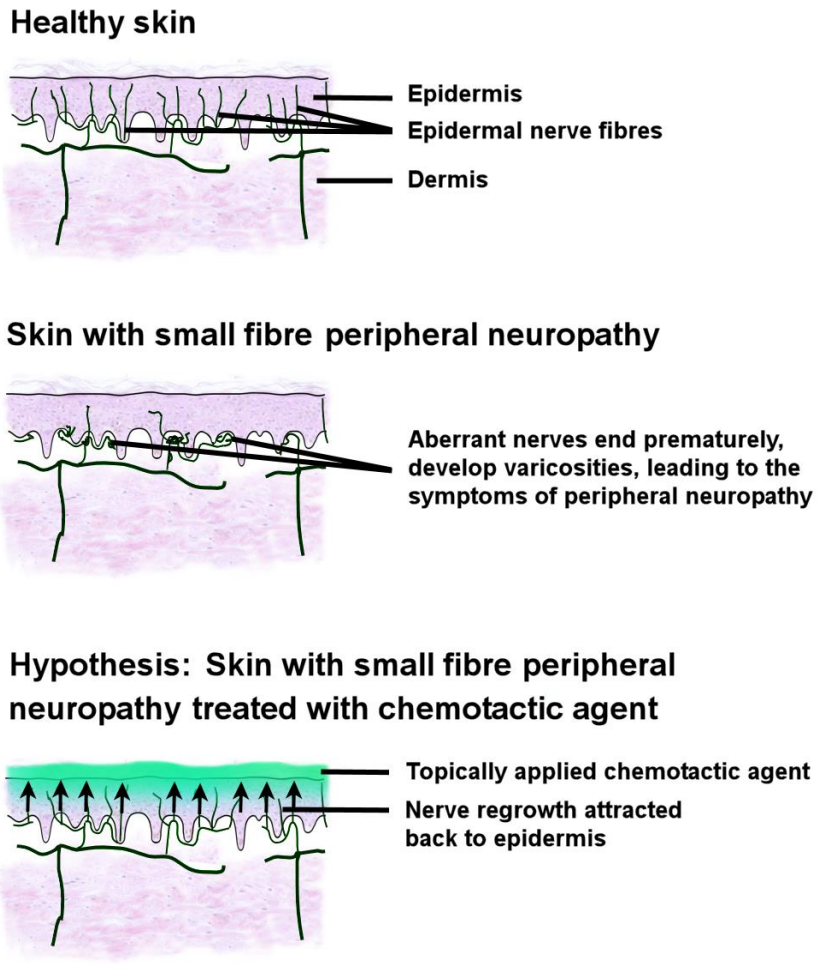

Fig 1.6. Visual representation underlying the hypothesis of a topical repair strategy utilising chemotactic factors as a therapeutic for diabetic neuropathy

In the instance of diabetic neuropathy, where specific regrowth of nerves back into the epidermis is the goal, the concentration gradient of a chemoattractive factor would necessarily be highest in the epidermis and gradually diffuse downwards into the underlying dermis in order to deliver a directional signal. It was hypothesised that a topical application would most likely produce such a gradient. Original figure.

CHAPTER 2

Establishing the chemotactic responses of growth cones to LRP1 and LRP2 ligands *in vitro*

CHAPTER 2

ESTABLISHING THE CHEMOTACTIC RESPONSES OF GROWTH CONES TO LRP1 AND LRP2 LIGANDS *IN VITRO*

2.1 INTRODUCTION

During axon pathfinding, neuronal growth cones respond to substrate-bound and soluble chemotactic guidance cues both spatially and temporally, to allow the axon to navigate the internal milieu and make appropriate connections (Tessier-Lavigne and Goodman, 1996). The poor ability of neurons to recover from insult has led researchers to hunt for chemotactic factors that may enhance axonal regrowth and restore connections lost after injury or neuropathy (Gordon, 2009).

The low-density lipoprotein (LDL) receptor family has more recently been implicated in neuronal regeneration and correct wiring of the nervous system (Willnow et al., 1996a, Herz and Bock, 2002, May et al., 2004). LRP1 and LRP2 are the largest and most complex members of the LDL receptor family which have been ascribed a number of functions in the nervous system (Herz and Bock, 2002, Lillis et al., 2008, Spuch et al., 2012). Global gene knockout models of both LRP1 and LRP2 reveal a critical, but largely undefined role in development and neuronal migration (Herz et al., 1992, Lillis et al., 2008, Christ et al., 2012). Given the emerging role of LRPs in modulation of neuronal growth, especially during injury (Yoon et al., 2013), this chapter addresses whether LRP1 or LRP2 were able to regulate neuronal growth cone motility. To the best of our knowledge, there has been no investigation into ligands of LRP1 and LRP2 and their ability to promote growth cone guidance. Such a system would represent a novel, non-classical axon guidance system.

While there are many LRP1 and 2 ligands, I focused on a selection from those implicated in neuronal function: namely, Apolipoprotein E (ApoE), α-2 macroglobulin (α2M), transthyretin (TTR), vitamin D/vitamin D binding protein complex (vitamin D/VDBP), tissue plasminogen activator (tPA), metallothionein II (MTII) and LRP receptor associated protein, RAP. ApoE, a promiscuous ligand of both LRP1 and LRP2, has been implicated in neuronal development and cognition, and is known to promote neurite extension in sensory neurons *in vitro* (Postuma et al., 1998). MTII, a ligand of both LRP1 and LRP2, is a metal binding protein that has roles in neuroprotection, neurite outgrowth and nerve regeneration *in vivo* (West et al., 2008). Vitamin D/VDBP is an LRP2 ligand, and has been linked to cognitive function (Dean et al., 2011). Vitamin D promotes neurite outgrowth in hippocampal neurons *in vitro* (Brown et al., 2003). α2M is a ligand of LRP1 and has been implicated in neuronal signal transduction, and has been shown to both enhance and repress neurite outgrowth and migration (Mori et al., 1990, Cavus et al., 1996, Yamauchi et al., 2013). Transthyretin mediates neuroprotection and neurite extension via LRP2 (Fleming et al., 2009b). tPA is an LRP1 ligand that is involved in axon pathfinding and neuronal migration, and through regulation of NMDA receptor activity has roles in learning and memory (Krystosek and Seeds, 1981, Hu et al., 2006). RAP is a chaperone of the LRP-receptor family, and is an established pan-LRP receptor inhibitor (Strickland et al., 1990, Williams et al., 1992, Medved et al., 1999).

The specific focus of the present chapter was to screen LRP1 and LRP2 receptor ligands for the ability to regulate growth cone chemotaxis. Sensory neurons from the dorsal root ganglion (DRG) of E16-18 rat embryos were used in the growth cone turning assay (Lohof et al., 1992, Gasperini et al., 2009), to determine whether LRP1 and LRP2 ligands function in

axon guidance. The turning assay is a well-characterised *in vitro* assay that can be used to screen for novel axon guidance cues and deduce their signalling pathways (Lohof et al., 1992, Gasperini et al., 2009). I also determined whether the chemotactic effects of LRP ligands required signalling via LRP1 or LRP2, using the pan-LRP inhibitor RAP and siRNA.

2.2 EXPERIMENTAL PROCEDURES & MATERIALS

2.2.1 Disclosure

All animal experimentation was performed in accordance with the guidelines and protocols of the Animal Ethics Committee, University of Tasmania (Ethics number A0012322), and are compliant with the Australian NHMRC Code of Practice for the Care and Use of Animals for Scientific Purposes.

2.2.2 Primary DRG neuron culture

Primary culture of embryonic day 16-18 dorsal root ganglia (DRG) from Sprague Dawley rats was performed as described previously (Gasperini et al., 2009). Briefly, thoracolumbar DRGs were dissected and placed in sensory neuron media (SNM). SNM comprises: Dulbecco's Modified Eagle's F-12 Medium (Gibco Biosciences, CA, USA), 1:1 Penicillin G (100U/mL) and streptomycin (100µg/mL; Gibco Biosciences, CA, USA), nerve growth factor (50ng/mL; Sigma-Aldrich, MO, USA), foetal calf serum (5% v/v; Bovogen Biologicals, VIC, Australia) and N2 neural medium supplement (1x; Gibco Biosciences, CA, USA). The DRGs were mechanically dissociated by trituration. The cell suspension was then plated at low density, onto laminin (50µg/mL; Invitrogen, CA, USA) and poly-L-ornithine (1mg/ml; Sigma-Aldrich, MO, USA) coated coverslips, embedded in 35mm petri dishes (Iwaki, Tokyo, Japan). Unless otherwise stated, cultures were allowed to grow for a minimum of 2 hours prior to imaging, at 37°C, 5% CO_2.

2.2.3 siRNA knockdown of LRP1 and LRP2

We used siRNA to reduce LRP protein in DRG neurons, using a previously published technique (Gasperini et al., 2011). Four LRP1 siRNA were trialled: GGGCAUUUGUGCUGGACGA, GGACAGACGUGACGACCCA, UCAAUAAGCAGACGGGAGA and UGGACAAGAUCGAACGUAU. Four LRP2 siRNA were trialled: CCUCAGUUGACGACGAAUA, GAGGGAAAUCAGCGUGUUA, GGAACAUCUUCAAACGAAA and GGAUGGUAGCAAUCGGAA. There was no cross reactivity between LRP1 and LRP2 sequences. All specific and negative control siRNA were obtained from Thermo Fisher Scientific, MA, USA. Individual siRNA (50µM) were loaded into neurons by trituration with the DRGs, prior to plating, as per section 2.2.2. Cultures were allowed to grow for a minimum of 6 hours prior to imaging. Reduction of LRP1 and LRP2 protein expression was quantified by immunofluorescence and western blot. LRP1 expression with LRP2 siRNA and vice versa was evaluated quantitatively by immunofluorescence and no crossreactivity was noted (Pavez, 2013).

2.2.4 *In vitro* growth cone turning assay

The growth cone turning assay was performed as described previously (Lohof et al., 1992, Gasperini et al., 2009). A molecular microgradient was generated by the pulsatile ejection of various guidance cues or LRP ligands via a micropipette pulled from glass into a live cell imaging dish. Primary DRG neuron culture was performed as per section 2.2.2. DRG cultures were placed on an inverted microscope (Eclipse TiE, Nikon Instruments) and images were captured using a EMCCD digital camera (Evolve, Photometrics) and using a 40x Fluor-S oil-immersion objective (Nikon). Isolated growth cones were positioned at a 45° angle and 90µM from the micropipette, such that the concentration of guidance cues and ligands at the

growth cone were 10^{-3} less than that within the pipette (Lohof et al., 1992, Gasperini et al., 2009).

Reagents used to generate the microgradient were: LRP ligands [MTII (HPLC purified human MTIIA, 300µg/mL, Zn_7 form, Bestenbalt LCC, Tallinn, Estonia), apolipoprotein E3 (ApoE, 1.8mg/mL R+D systems, Minneapolis, MN, USA), LRP receptor-associated protein RAP (1mg/mL, in Tris-buffered saline; a kind gift from David Small, Tasmania, Australia), alpha-2-macroglobulin (α2m, from human plasma, 2.25mg/mL, Sigma, MO, USA), wild-type transthyretin (8mg/mL, a gift from David Small, Tasmania, Australia), vitamin D (100umol/L, Sigma, MO, USA) combined with 1:1 molecular ratio of vitamin D binding protein (Abcam, Cambridge, UK), tissue-type plasminogen activator (tPA, 3.3mg/mL, Abcam, Cambridge, UK), EmtinA (1mg/mL, Schafer N, Copenhagen, Denmark,), EmtinB (1mg/mL, Schafer N, Copenhagen, Denmark)]; putative LRP ligand MTIII (1mg/mL, Zn_7 form, Bestenbalt LCC, Tallin, Estonia); control solutions [Netrin-1 (5µg/mL, R&D Systems, MN, USA), BDNF (10µg/mL, R&D Systems, MN, USA), zinc sulphate (50mM; Sigma, MO, USA)]; saline to assess for any effects of mechanical disturbance attributed to the pulsatile ejection technique (Phosphate buffered saline, pH 7.4, comprising 10mM Na_2HPO_4, 1.8mM KH_2PO_4, 137mM NaCl and 2.7mM KCl, all from Sigma, MO, USA. *see Appendix 1, Solution protocols*). Bath applied pharmacological agents added to the culture media were: RAP (25µg/mL) and Tris-buffered saline control (25µl/mL; comprising 50mM Tris and 150mM NaCl, both from Sigma, MO, USA). These were added to the culture media 20 minutes prior to imaging.

2.2.5 Video acquisition in growth cone turning assay

Time lapse images of growth cones in the growth cone turning assay (section 2.2.4) were acquired by Matlab & Stimulink V7.1.0.124 (The Mathworks, MA, USA). Images were captured every 7 seconds for 30 minutes. After 30 minutes of imaging, axonal trajectories were measured using ImageJ (NIH, MD, USA). Axons that extended less than 10µm were excluded from analysis. Statistical analysis was conducted in GraphPad Prism V4.03 (Software Mackiev, CA, USA). Attraction and repulsion was defined as a positive or negative turning angle, respectively, that was significantly different from the PBS control. All significance values are the product of a Mann-Whitney t-test (Lohof et al., 1992).

2.2.6 Immunocytochemistry

DRG cultures, grown on cover slips for 2-8 hours, were fixed *in situ* in 4% paraformaldehyde (Sigma-Aldrich, MO, USA) in PBS pH 7.4 at 4°C overnight, followed by blocking in 5% goat serum (Sigma-Aldrich, MO, USA), 0.04% Triton X-100 (Sigma-Aldrich, MO, USA) in PBS for 30 minutes.

Antibodies used: Anti LRP1 antibody (L2170, 1:1000; Sigma, MO, USA) was raised in rabbits against a synthetic peptide corresponding to amino acids in the intracellular C-terminus of human LRP1. Anti-LRP2 primary antibody used was raised in rabbits against the intracellular C-terminal fragment of human LRP2 (sc-H245, 1:1000; Santa Cruz Biotechnology, CA, USA). Fixed cells were incubated overnight at 4°C with the primary antibody, diluted in PBS with 5% goat serum. Controls for immunolabelling were performed by omitting the primary antibody (zero primary control). After washing, the cells were incubated with the secondary antibody, fluorescent goat anti rabbit Alexa 594-conjugated

(1:1000, Molecular probes, OR, USA), in the dark, overnight at 4°C, or at room temperature for 4 hours. The actin component of the cytoskeleton was labeled with phalliodin-Alexa 488 (5U/mL, 20 mins; Molecular Probes, OR, USA). Cultures were mounted with DPX fluorescent mounting media (Koch-Light Laboratories, England, UK).

Images were acquired using an Olympus BX50 microscope, equipped with a UP-lanSApo 60x-1.35 water immersion lens (Olympus, Tokyo, Japan), and captured with MagnaFire V2.1c (Optronics, CA, USA), with a cooled CCD camera (Optronics, CA, USA). During image capture the exposure time was set so that cells would not be over exposed and the pixels not saturated. Exposure was kept constant throughout the imaging session. Images were processed using Image J (NIH, MD, USA), JASC Paint Shop Pro V 9.0 (JASC Software Inc., MN, USA).

2.2.7 Western Blot

To determine LRP1 and LRP2 knockdown with siRNA, protein levels were quantified using western blot and analysis of pixel intensity, as previously described (Gasperini et al., 2011). Briefly, DRG neurons were loaded with either no siRNA, control siRNA or one of four LRP1 or LRP2 siRNAs, in an identical protocol as per section 2.2.3. Cells were grown with siRNA for 6 hours, then cells were harvested from the culture dish by scraping down into a small volume of RIPA buffer (50 mM Tris pH 7.4, 150 mM NaCl, 1 mM phenylmethylsulphonyl fluoride, 1 mM EDTA, 5 ug/ml aprotinin, 5 ug/ml leupeptin, 1% Triton X-100, 1% Na deoxycholate, 0.1% SDS, all from Sigma, MO, USA), and immediately frozen. Sample protein concentration was measured using the Bio-Rad DC protein assay kit (Bio-Rad Laboratories Pty. Ltd., Gladesville, Australia) with bovine serum albumin as standard.

Samples with total protein of 15ug were separated on 8% SDS-PAGE and electroblotted onto 0.2um PVDF membrane. Membranes were blocked in 5% skim milk powder for 30 minutes. Membranes were incubated with antibodies for LRP1 (1:1000; Sigma-Aldrich, St Louis, MA USA), LRP2 (1:1000; Santa Cruz, CA USA), or β-actin (1:40,000; Sigma-Aldrich, St Louis, MO, USA) at room temperature for 2-4 hours, then rinsed thoroughly. Membranes were then incubated with goat anti-rabbit HRP secondary antibody (Dako, Glostrup, Denmark) for 2 hours at room temperature, and rinsed thoroughly. Blots were processed using ECL chemiluminescence reagent (Pierce, Rockford, IL, USA) and detected using a Chemi-Smart 5000 gel documentation system (Viber Lourmat, Torcy, France). Images were captured, and signal intensity was quantified using Image J software (RSB; NIH, http://rsbweb.nih.gov/ij/index.html). The ratio of immunoreactivity for each protein relative to the respective β-actin loading control was calculated.

2.2.8 Statistical analysis

Means and standard error of the mean were calculated for each group using GraphPad Prism 6.0. Mann Whitney *t*-test was used to calculate the statistical significance for growth cone turning assays. Students *t*-test was used for comparisons between control and knockdown protein levels in western blot. Western blots were repeated at least three times.

2.3 RESULTS

2.3.1 LRP1 and LRP2 are present in the chemical sensing region of the growth cone

In order to test the hypothesis that LRP1 and LRP2 are able to modulate growth cone turning, I first determined whether LRP1 and LRP2 were present in DRG sensory neurons *in situ*, and specifically within the highly specialized and motile growth cone *in vitro*. Immunoreactivity for LRP1 (Figure 2.1.A-B) and LRP2 (Figure 2.1.C-D) were identified within the neuronal cell bodies and surrounding glial cells of thoracolumbar E17 DRG, and was consistent with the work of others (Postuma et al., 1998, Fleming et al., 2009b, Yamauchi et al., 2013). In order to detect LRP2 and LRP1 expression within growth cones cultures were stained (Representative images shown in Figure 2.1 E-M). Whilst it has been previously reported that LRP1 and LRP2 are present in DRG (Postuma et al., 1998, Fleming et al., 2009b, Yamauchi et al., 2013), their subcellular location has not been examined in detail. For the first time we show the distribution of LRP1 and LRP2 immunoreactivity in DRG growth cones. LRP1 staining was diffuse, and extended throughout the lamellipodia of the leading edge (Figure 2.1.J) and filopodia. LRP2 positive immunoreactivity was identified on the leading edge and filopodia (Figure 2.1. M;). The leading edge and filipodia are the regions of the growth cone actively involved in chemical sensing of the environment; suggesting that LRP1 and LRP2 are distributed in regions involved in growth cone navigation. LRP receptors, as endocytic receptors, are known to be recycled through endosomal compartments following endocytosis that occurs after the receptor binds a ligand. Therefore, it is plausible that the large immunoreactive puncta located in the central zone are endocytic vesicles or endosomes with LRP inclusions. However, it is important to mention

Figure 2.1 LRP1 and LRP2, are present in rat DRG in situ, and rat DRG growth cones in vitro.

(A) LRP1 positive staining (red) and neuronal nuclear marker, NeuN (green) in E17 rat embryo DRG *in situ*. **(B)** Magnification of LRP1 and NeuN staining in DRG from panel A. **(C)** LRP2 positive staining (red) and neuronal nuclear marker, NeuN (green) in E17 rat embryo DRG *in situ*. **(D)** Magnification of LRP2 and NeuN staining in DRG from panel A. **(E-K)** Representative images of thoracolumbar DRG growth cones from E16-18 rat embryos cultured *in vitro.* Growth cone morphology is highlighted with filamentous actin labelling (green). **(E-G)** Zero primary control demonstrates the specificity of secondary antibody. **(H-J)** LRP1 immunopositive puncta combined with diffuse immunoreactivity are located throughout the growth cone, including the leading edge and filopodia. **(K-L)** Immunoreactivity of a growth cone for an antibody specific to LRP2 receptor (red). Large LRP2 immunopositive puncta are distributed throughout the growth cone, including the leading edge, in a similar manner to LRP1. A and C conform to the same scale bar. E-K conform to the same scale bar. *Images K-M in Figure 2.1 were assessed as part of my honours thesis, Landowski 2009.*

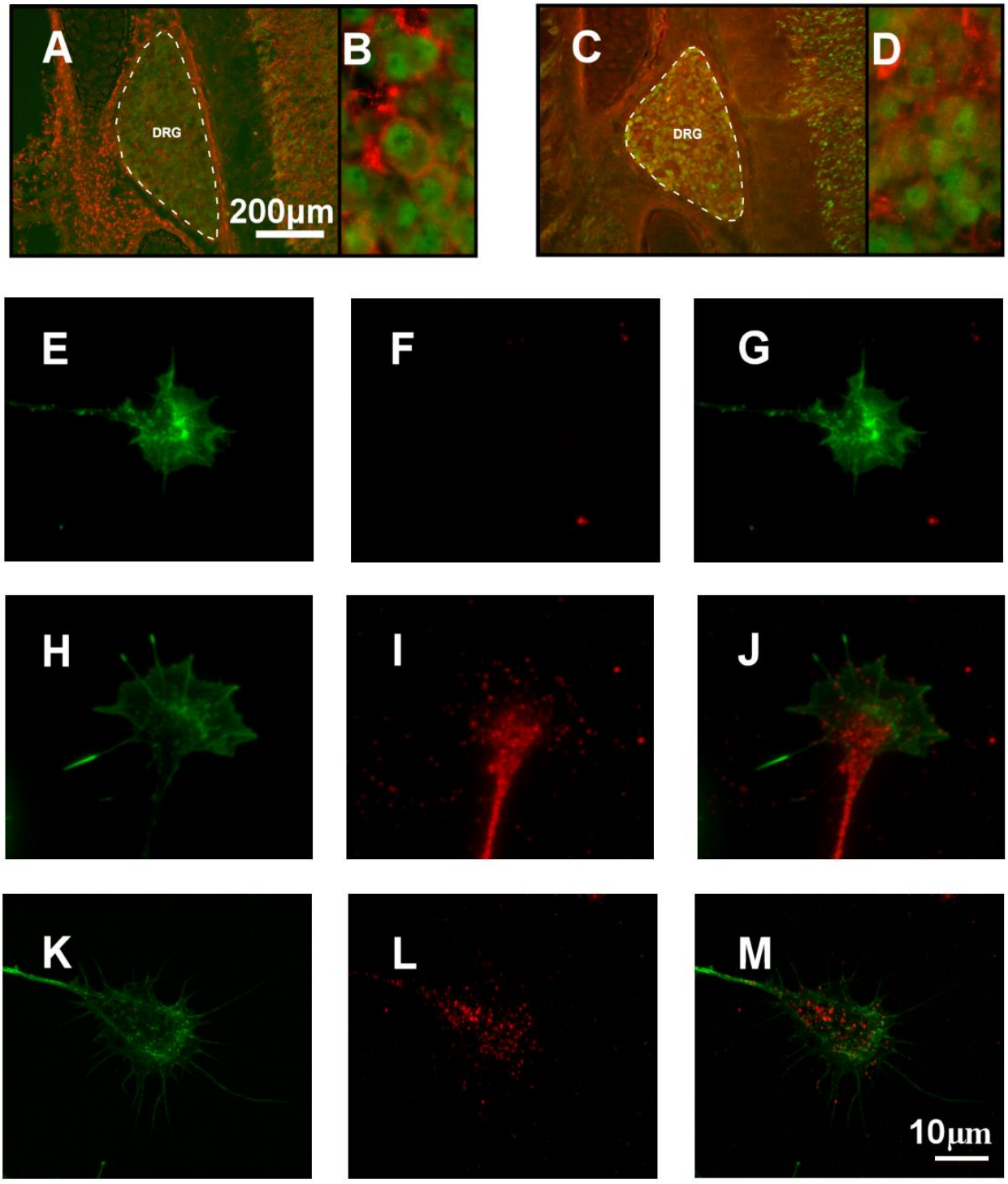
A
DRG
200µm
B
C
DRG
D
E
F
G
H
I
J
K
L
M
10µm

that the cultures shown were not given additional permeabilisation as maintaining membrane integrity is important for LRP staining. As such, the immunoreactivity shown mostly reflects expression on the cell membrane.

2.3.2 Determine whether LRP1 or LRP2 ligands have chemotropic effects on neuronal growth cones

Given that LRP1 and LRP2 are present in growth cones, we sought to determine whether any of the well characterised ligands of these receptors had chemotactic effects on growth cones. To ascertain whether LRP1 and LRP2 were involved in growth cone chemotaxis, we used selected LRP ligands, and control solutions, in the well described growth cone turning assay (Lohof et al., 1992). The vehicle control was phosphate buffered saline (PBS), a balanced salt solution, which caused random growth (-1.8° ± 1.1,) with no net attraction or repulsion. A concentration gradient of ApoE3, TTR, VD/VDBP and RAP (applied as a concentration gradient, not as an inhibitor in the culture bath), all resulted in random growth and not significantly different from the control (Fig 2.2). α2M and tPA induced growth cone repulsion, compared to the control (-11.9° ± 3.4, $p<0.01$ and -11.1° ± 2.1 $p<0.001$, respectively; Fig 2.2). The repulsion induced by gradients of α2M and tPA was found to be more robust than the repulsion in response to Semaphorin3a (-8.2° ± 1.9, $p<0.02$; Fig 2.2), an established chemorepulsive cue. A gradient of MTII induced significant chemoattraction of growth cones towards its concentration gradient (11.6° ± 2.1, $p<0.001$), which was comparable to growth cone turning in response to the classic chemoattractant, BDNF (14.87° ± 1.8 $p<0.0001$; Fig 2.2). Axon extension was also measured during the 30 minutes of imaging, to ensure that growth cones were healthy, were not involved in external interactions, and to assess whether additional effects were observed, for example growth cone collapse.

Figure 2.2 The LRP ligands, tPA, α2M and MTII induce chemotaxis in DRG growth cones.

A chemical microgradient of LRP ligands and controls were applied to isolated growth cones *in vitro.* **(A)** Quantification for average turning angles of neurites in response to vehicle control (1:1 phosphate buffered saline, pH 7.4), standard attractive cue, BDNF; standard repulsive cue, Sema3a; apoE3, transthyretin, tPa, α2M, vitamin D bound to Vitamin D binding protein, MTII and RAP. **(B)** Axon extension for the same growth cones were analysed, and with the exception of RAP did not differ significantly after 30 minutes of imaging. Error bars represent standard error of the mean. ***$p<0.0001$, **$p<0.002$. Asterisks (*) directly above error bars indicate significance when compared to control. Numbers within parentheses indicate the number of growth cones that were analysed per treatment group and apply to both **(A)** & **(B)**. *Note that some of the growth cone turning data points included within the results for PBS, Sema3a, BDNF, MTII, and RAP in Figure 2.2 were assessed as part of my honours thesis, Landowski 2009. The remaining data is a result of PhD work. The control and MTII data points are used in Chapters 2 and 3.*

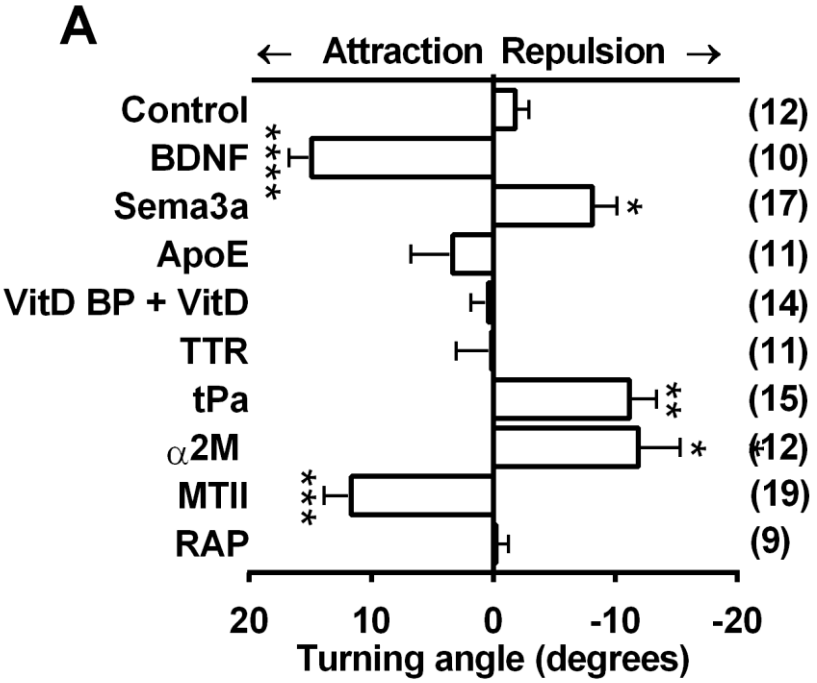
A
← Attraction Repulsion →
Control
BDNF
Sema3a
ApoE
VitD BP + VitD
TTR
tPa
α2M
MTII
RAP
(12)
(10)
(17)
(11)
(14)
(11)
(15)
(12)
(19)
(9)
20
10
0
-10
-20
Turning angle (degrees)

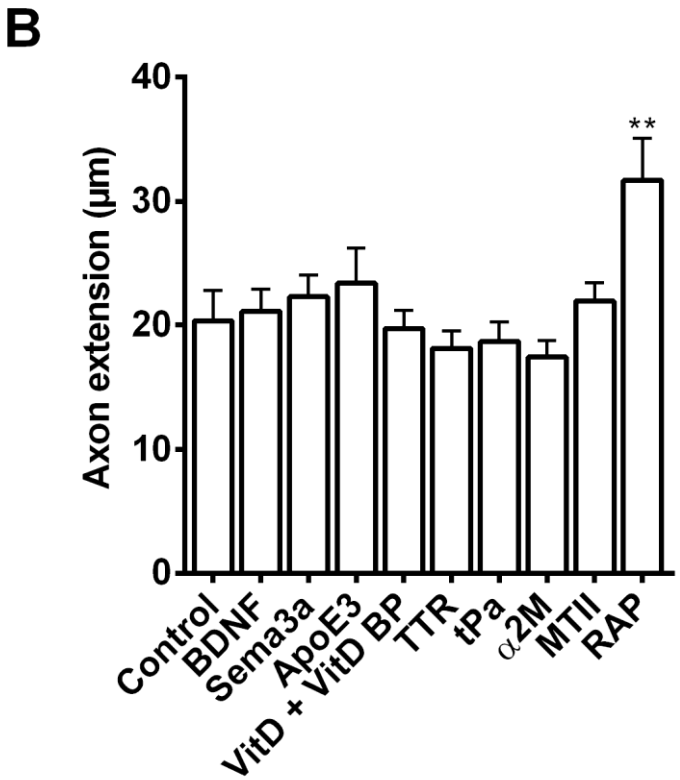
B
Axon extension (µm)
40
30
20
10
0
Control
BDNF
Sema3a
ApoE3
VitD + VitD BP
TTR
tPa
α2M
MTII
RAP

Extension was uniform across all treatment groups except for RAP, which mitigated a significant enhancement of neurite outgrowth ($p<0.03$), which is in agreement with previous observations (Postuma et al., 1998).

The observation of a turning effect of growth cones towards MTII was followed up with an investigation into the importance of protein structure for eliciting this effect (Figure 2.3). Structurally similar family members, MTIII and MTIV, were examined for chemotactic ability, as well as the truncated synthetic analogues of MTII, EmtinA and EmtinBn. Surprisingly, MTIII had a significant and opposing effect to MTII (-13.2 ± 1.9 $p<0.0001$). Furthermore, MTIII was significantly more repulsive than established repulsive guidance cue, Sema3a ($p<0.04$). MTIV, EmtinA and EmtinBn had no significant chemotactic effect. Additionally, as MTs are metal-binding proteins used in their zinc bound form, it was important to assess whether a zinc solution (zinc sulphate, 50mM) alone exerted any directional influence. It is known that zinc is able to transactivate neurotrophin receptor TrkB (Huang et al., 2008). However, zinc solution did not have any chemotactic effect. Axon extension, which is also measured during the 30 minutes of imaging, was significantly enhanced in the EmtinA and zinc treatment group; these findings are consistent with previous studies that demonstrate enhanced neurite outgrowth (Nusetti et al., 2005, Asmussen et al., 2009a).

Figure 2.3 MTs can be chemoattractive or chemorepulsive

(A) A chemical gradient of MTII, MTIII, MTIV and synthetic metallothionein-mimetic peptides, EmtinA and EmtinB, were used in the growth cone turning assay. Only MTII and MTIII elicited a significant turning angle. **(B)** EmtinA, EmtinB and Zinc significantly increased axon outgrowth after 30 minutes of imaging. ****$p<0.0001$. **$p<0.007$. Error bars represent SEM. Asterisks (*) directly above error bars indicate significance when compared to control. Numbers within parentheses indicate the number of growth cones that were analysed per treatment group and apply to both **(A)** & **(B)**. *Note that some of the growth cone turning data points included within the results for MTIII in Figure 2.3 was assessed as part of my honours thesis, Landowski 2009. The remaining data is a result of PhD work. The MTIII data points are used in Chapters 2 and 3.*

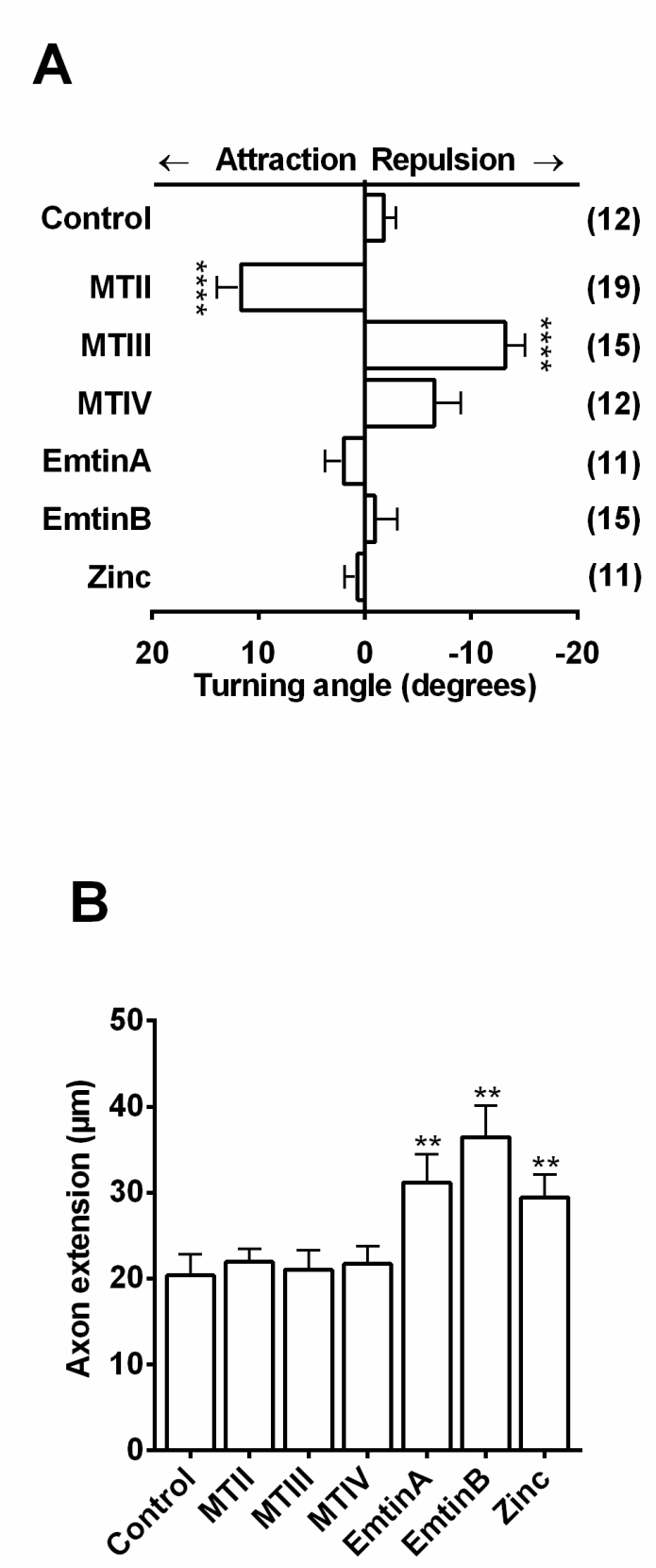
A
← Attraction Repulsion →
Control
MTII
MTIII
MTIV
EmtinA
EmtinB
Zinc
(12)
(19)
(15)
(12)
(11)
(15)
(11)
****
****
20
10
0
-10
-20
Turning angle (degrees)
B
Axon extension (µm)
50
40
30
20
10
0
**
**
**
Control
MTII
MTIII
MTIV
EmtinA
EmtinB
Zinc

2.3.3 Determine whether LRP receptors are required in MTII or MTIII induced growth cone chemoattraction

In order to determine whether chemoattractive signalling is elicited by MTII interacting with LRP receptors, the chemotactic response of MTII was measured in the presence of an LRP receptor inhibitor. Receptor associated protein (RAP) is a 39kDa chaperone protein residing in the endoplasmic reticulum involved in the correct folding of LDL family receptors (Bu et al., 1995). When applied exogenously, RAP can act as a competitive inhibitor of all LDL family receptors and this has been demonstrated both *in vitro* and *in vivo* (Willnow et al., 1992). RAP binds LDL-receptors LRP1 and LRP2 with high affinity and LDLR, VLDLR and apoER2 to a lesser degree (Herz et al., 1991). On the premise that LRP1 and LRP2 ligands elicit chemotaxis by signalling solely through receptors of the LRP family, we would expect that the addition of RAP or small interfering RNA (siRNA) would abolish the chemotactic response. Pan-inhibitor of the LRP-family, receptor-associated protein (RAP), was added to the culture media 30 minutes prior to imaging, and growth cones were subsequently exposed to a concentration gradient of MTII or MTIII. The addition of RAP significantly abrogated the turning effect elicited by MTII and MTIII to control levels (-0.6°± 1.2, p=0.0015 and 0.9°± 1.2, p=0.0002, respectively; control, -1.8°± 1.1; Fig 2.4A). Axon extension was not affected (data not shown). These findings suggest that LRP receptors are capable of mediating chemoattraction in response to MTII and MTIII, but it does not discern which of the MTII or MTIII receptors, LRP1 or LRP2, are implicitly involved.

2.3.4 Demonstrate reduced LRP1 and LRP2 expression in siRNA transfected DRG

In order to determine which specific LRP receptor/s are responsible for mediating the growth cone chemoattractive response, I used siRNA to reduce endogenous expression of LRP1 and LRP2, the known receptors of MTII. The level of protein expression in DRG cultures were assayed with western blot and quantified relative to actin loading controls (Fig 2.4B-E). For both LRP1 and LRP2, all 4 siRNAs yielded equally significant knock down of protein expression after 6 hours. Compared to levels of LRP1 and LRP2 in control siRNA treated tissue, LRP1 siRNAs gave an average of 50% ± 3 reduction in LRP1 ($p<0.03$) and LRP2 siRNAs gave an average of 71% ± 4 reduction, ($p<0.0001$) (Fig 2.4C and Fig 2.4E).

Figure 2.4 Perturbation of MT-mediated growth cone turning with Pan-inhibition of LRPs suggests that reduced expression of specific LRP receptors is required

(A) Quantification of growth cone trajectories demonstrate that the addition of competitive inhibitor of LRP receptors, RAP, to the imaging media, prior to growth cone exposure to a concentration gradient of MTII and MTIII. Error bars represent standard error of the mean. Numbers within parentheses indicate the number of growth cones that were analysed per treatment group. **(B)** Western blot and analysis of lysate from DRG culture treated with control siRNA or one of the four specific LRP1 siRNA demonstrates reduced LRP1 expression after 6 hours of siRNA treatment. **(C)** Quantification of western blot shows an average of 50% decrease in immunoreactivity compared to the control, with all specific siRNA being equally effective (n=3). **(D)** Western blot and analysis of lysate from DRG culture treated with control siRNA or one of the four specific LRP2 siRNA demonstrates LRP2 knockdown after 6 hours of siRNA treatment. **(E)** Quantification of western blot shows an average of 71% decrease in immunoreactivity when compared to the control, with all specific siRNA being equally effective (n=3). Values are expressed as a percentage of the control and are obtained over 3 experiments. Error bars represent SEM. *$p<0.05$, *** $p<0.0001$. Unpaired t-test. *Note that some of the growth cone turning data points included within the results for Figure 2.4A were assessed as part of my honours thesis, Landowski 2009.*

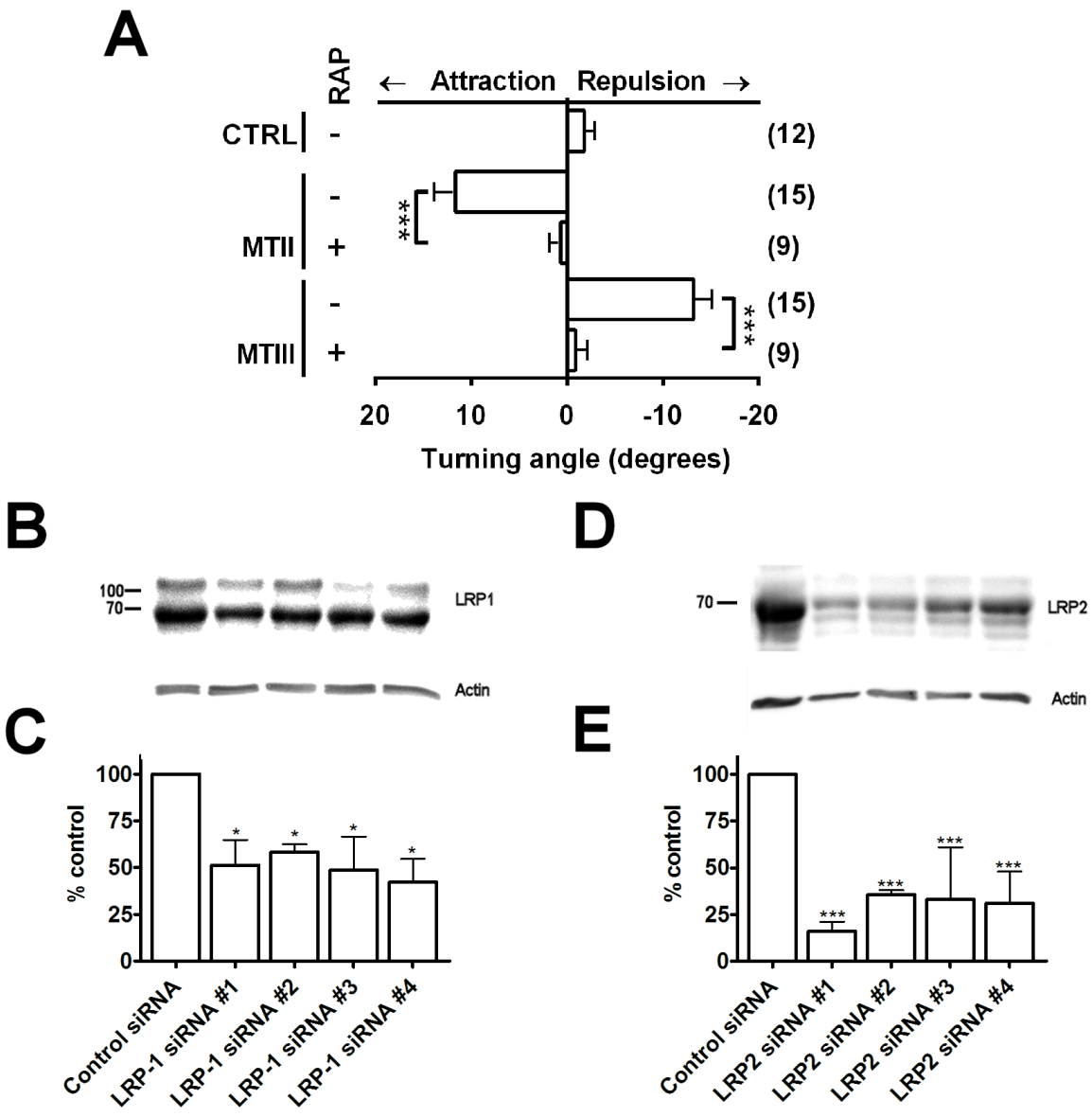
A
RAP
← Attraction Repulsion →
CTRL
MTII
MTIII
-
+
(12)
(15)
(9)
(15)
(9)
***
***
20
10
0
-10
-20
Turning angle (degrees)
B
100
70
LRP1
Actin
C
% control
100
75
50
25
0
Control siRNA
LRP-1 siRNA #1
LRP-1 siRNA #2
LRP-1 siRNA #3
LRP-1 siRNA #4
D
70
LRP2
Actin
E
% control
100
75
50
25
0
***
Control siRNA
LRP2 siRNA #1
LRP2 siRNA #2
LRP2 siRNA #3
LRP2 siRNA #4

2.3.5 MTII and MTIII-mediated growth cone chemotaxis is LRP1 and LRP2 dependent

The turning response of growth cones to MTII and MTIII were used in growth cones transfected with siRNA to knock down expression of LRP1 or LRP2 individually, or LRP1 + LRP2 simultaneously. Knockdown of LRP1 or LRP2 abolished growth cone turning in response to MTII (3.5° ± 1.9, p=0.003 and 3.6° ± 2.6, p=0.03 respectively, compared to the turning response of growth cones to MTII in control siRNA culture, (12.9° ± 2.7; Figure 2.5). Furthermore, dual LRP1/LRP2 receptor knockdown also abolished the growth cone turning response to MTII (0.6° ± 1.5, p=0.002; Figure 2.5).

To ensure that reduced LRP expression did not interfere with the turning machinery of growth cones, or abolished the turning response to guidance cues in a non-specific manner, I examined growth cone turning in response to netrin, a well-established chemoattractive guidance cue, after dual reduction of LRP1 and LRP2. Netrin induces chemoattraction via DCC receptors (Ming et al., 1999). There was no difference in growth cone turning in response to netrin after dual reduction of LRP1 and LRP2 compared to cultures transfected with control siRNA (Fig 2.5).

It is yet to be determined whether LRP1 and LRP2 are receptors for MTIII. Surprisingly, reduced expression of LRP1 or LRP2 appeared to switch the turning effect in response to MTIII (5.8° ± 2.6, p=0.0005 and 10.0° ± 2.8, p<0.0001 respectively, compared to the turning response of MTIII in control siRNA culture, -13.9° ± 4.0; Fig 2.6). Furthermore, while reduced expression of LRP1 and LRP2 abolished the growth cone turning response to MTII (0.6° ± 1.5, p=0.002; Fig 2.6), MTIII reverted back to a repulsive response, albeit weakened, (-7.1° ± 2.8; Fig 2.6) suggesting complex receptor interplay.

Figure 2.5 Targeted LRP1 and LRP2 receptor knockdown with siRNA perturbed MTII-induced growth cone chemoattraction

(A) A chemical gradient of MTII, in the presence of various LRP modulators, were used in the growth cone turning assay. Quantification of average turning angles demonstrates that the incorporation of siRNA against LRP1, or LRP2, into DRG neurites abolishes the response of neurites to MTII. Similarly, dual reduction of LRP1/LRP2 abolishes MTII-mediated attraction. Netrin, a chemotactic guidance cue which does not signal through LRP receptors, is not significantly affected by the simultaneous addition of both LRP1 and LRP2 siRNA, compared to control siRNA. **(B)** Axon extension did not differ significantly after 30 minutes of imaging. Error bars represent standard error of the mean. Numbers within parentheses indicate the number of growth cones that were analysed per treatment group and apply to both **(A)** & **(B)**. *$p<0.02$, **$p<0.002$ and ***$p<0.001$

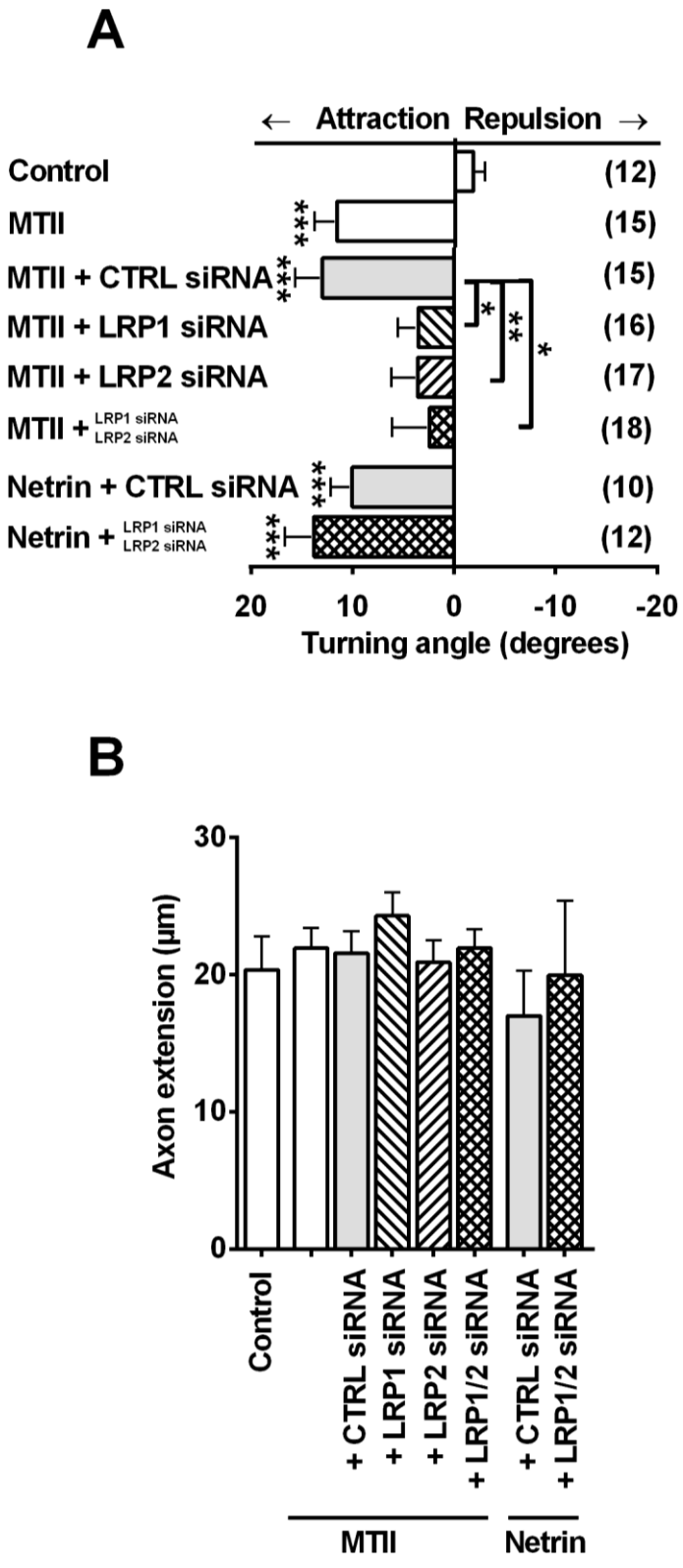
A
← Attraction Repulsion →
Control
MTII
MTII + CTRL siRNA
MTII + LRP1 siRNA
MTII + LRP2 siRNA
MTII + LRP1 siRNA LRP2 siRNA
Netrin + CTRL siRNA
Netrin + LRP1 siRNA LRP2 siRNA
(12)
(15)
(15)
(16)
(17)
(18)
(10)
(12)
***
***
***
*
**
*
20
10
0
-10
-20
Turning angle (degrees)
B
Axon extension (µm)
30
20
10
0
Control
+ CTRL siRNA
+ LRP1 siRNA
+ LRP2 siRNA
+ LRP1/2 siRNA
+ CTRL siRNA
+ LRP1/2 siRNA
MTII
Netrin

Figure 2.6 Targeted LRP1 and LRP2 receptor knockdown with siRNA perturbed MTIII-induced growth cone chemorepulsion

(A) A chemical gradient of MTIII, in the presence of various LRP modulators, were used in the growth cone turning assay. LRP1 or LRP2 knockdown reversed the turning angle in response to MTIII. However, dual reduction of LRP1/LRP2 expression attenuated the turning response of growth cones to MTIII; the response was neither significantly different from the control nor to the normal response of growth cones to MTIII. **(B)** Axons did not differ significantly after 30 minutes of imaging. Error bars represent standard error of the mean. Numbers within parentheses indicate the number of growth cones that were analysed per treatment group and apply to both **(A)** & **(B)**. *P<0.05 and ***P<0.0001.

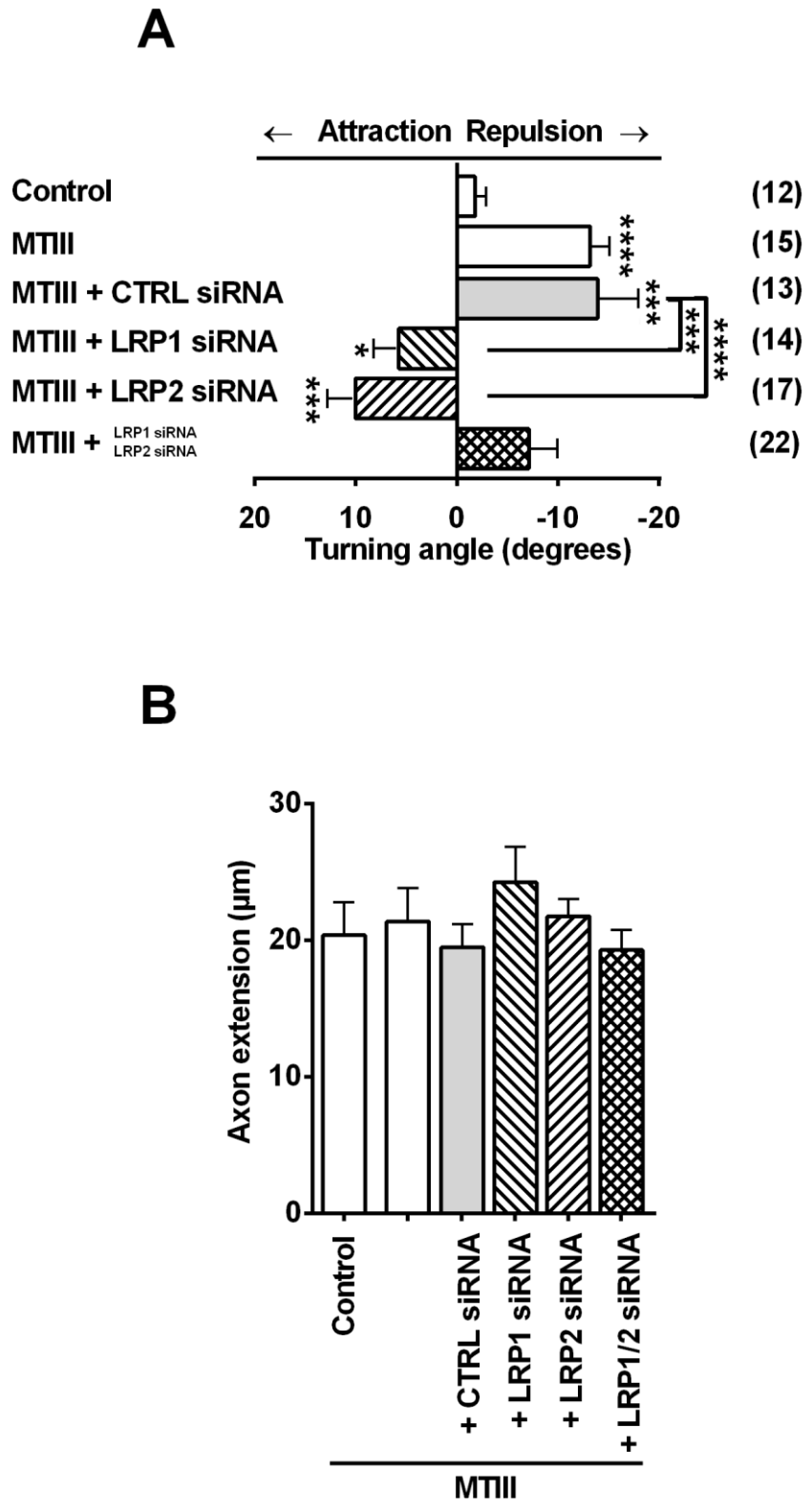
A
← Attraction Repulsion →
Control
MTIII
MTIII + CTRL siRNA
MTIII + LRP1 siRNA
MTIII + LRP2 siRNA
MTIII + LRP1 siRNA LRP2 siRNA
(12)
(15)
(13)
(14)
(17)
(22)
****
***
***
*
***
*****
20 10 0 -10 -20
Turning angle (degrees)
B
Axon extension (µm)
30
20
10
0
Control
+ CTRL siRNA
+ LRP1 siRNA
+ LRP2 siRNA
+ LRP1/2 siRNA
MTIII

2.3.5 Demonstration of LRP1 and LRP2 co-localisation in growth cones

The finding that LRP1 and LRP2 both appear to be necessary for the chemoattractive effect of MTII raised the question whether these receptors may be signalling together in close proximity. Dual staining for LRP1 and LRP2 in growth cones undergoing random growth revealed significant colocalisation throughout the lamellipodia and filopodia in a punctate distribution (Fig 2.7, arrows), supporting the notion that LRP1 and LRP2 are signalling together, potentially in a complex signalling hub.

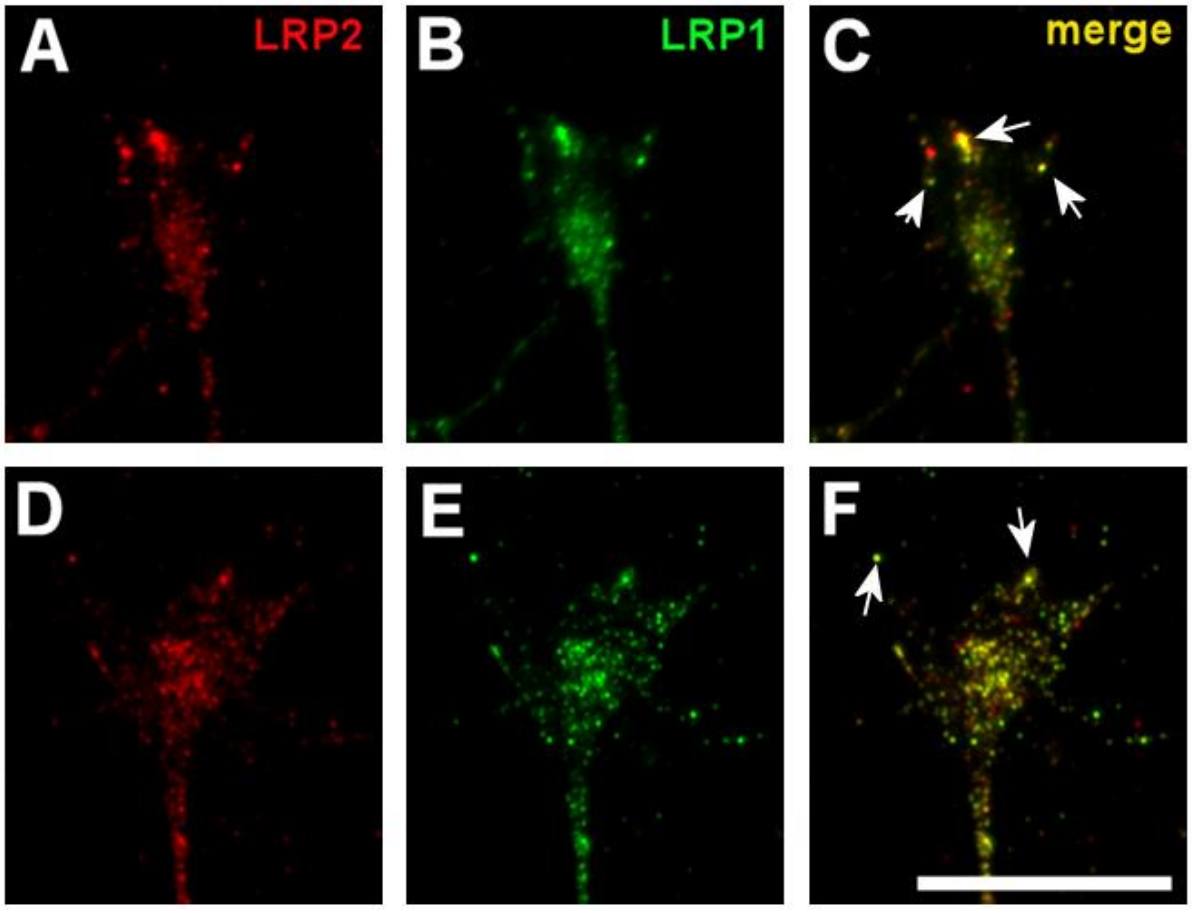

Figure 2.7 LRP1 and LRP2 colocalise in growth cones in vitro

Representative images of immunoreactivity of growth cones with an antibody specific to LRP1 (green) and LRP2 (red). Significant areas of colocalised immunopositive puncta are present, as demonstrated by yellow staining in the merged images (arrows). Colocalisation is located throughout the growth cone, including the leading edge. Scale bar is 10µm and applies to all images.

2.4 DISCUSSION

A new neuron specific role for LRP1 and LRP2 was identified in mediating growth cone chemotaxis. LRP ligand MTII induced neurite chemoattraction, while α2M, tPA and MTIII were found to have chemorepulsive effects. I demonstrated that LRP1 and LRP2 signalling could mediate chemoattraction and chemorepulsion. The remaining LRP ligands tested had no discernible chemotactic effect. LRP1 and LRP2 were present in growth cones in chemical sensing regions (leading edge and filopodia), and colocalisation of these receptors was also observed *in vitro.* These data demonstrate that LRP receptors are able to direct axon guidance *in vitro.*

The chemoattractive effects of MTII are not unique to neuronal growth cones, and have been described in other cell types, promoting keratinocyte and astrocyte migration *in vitro* after scratch injury (Carrasco et al., 2003, Morellini et al., 2008). The MT genes are in close proximity to other chemokine genes, located on chromosome 16q13, and MT proteins share some amino acid motifs characteristic of cytokines (Yin et al., 2005). Again, as with many cytokines it was found that leucocytes migrate towards a gradient of MTI/II, and this activity increased F-actin content, as occurs in growth cones (Yin et al., 2005). Metallothionein I/II knockout mice exhibit subtle neurocognitive deficits; although the underlying mechanism involved is currently unknown, these data support the notion that the LRP-MTII system has roles in neuronal function (Yoshida et al., 2005, Levin et al., 2006).

α2M is expressed in the spinal cord and brain during development while axon pathfinding is occurring (Kodelja et al., 1986), and is important for trophoblast invasion during implantation (Esadeg et al., 2003). Whether α2M is directly involved in axon pathfinding processes

remains unknown. α2M has been shown to promote migration of many cell types, including Schwann cells, Müller glial cells and neutrophils (Hakansson and Venge, 1983, Mantuano et al., 2010, Barcelona et al., 2013). α2M affects cell migration both directly and indirectly through modulating activity and expression of other proteinases and cytokines, or by binding other proteins; for example, α2M indirectly promotes macrophage migration by binding type I collagen (Larin et al., 2002). Given that most chemotactic cues to growth cones require Ca^{2+} as a second messenger to initiate turning, it is interesting to note that microapplication of α2M results in a transient calcium influx in mouse cortical neurons via NMDA receptors (from 88 ± 29nM to 396 ± 22nM) (Bacskai et al., 2000). NMDA receptors are involved in growth cone migration in Xenopus spinal neurons (Zheng et al., 1996) and are present and functional on mammalian and hippocampal neurons (Wang et al., 2011). Although NMDA receptors are not established mediators of growth cone guidance in mammalian DRG neurons, they have well characterised functional roles in this cell type (Liu et al., 1997, Coggeshall and Carlton, 1998, Kung et al., 2013). As such, NMDA receptor activity may relate to a novel mechanism of LRP-mediated growth cone repulsion.

tPA has well established roles in axon pathfinding, via secretion at the growth cone tip and thus modulating the extracellular environment and facilitating advancement of the growth cone (Krystosek and Seeds, 1981, 1984, 1986). The observation that microapplication of tPA directly resulted in growth cone repulsion therefore was surprising. It is known that tPA is able to proteolytically cleave many proteins, including laminin immobilised on a substrate base (Salonen et al., 1984). The growth cone turning assay requires laminin as the primary cell adhesion substrate for growth cones. Therefore, the observation that growth cones were repulsed from a gradient of tPA, may in fact be secondary to tPA cleaving the laminin

substrate, and as such, making the substrate closest to the micropipette inhibitory to growth cones, culminating in growth cone repulsion.

Previous studies using surface plasmon resonance have demonstrated that MTII associates with LRP1 and LRP2 in neurons (Ambjorn et al., 2008), hence it was perhaps not surprising that both these receptors proved necessary for growth cone responses to MTII. Reduction of LRP1 or LRP2 expression abolished the turning response to MTII; these data suggest that LRP1 and LRP2 are part of a heterogenous signalling hub. Indeed, immunocytochemical staining corroborated these results, demonstrating that LRP1 and LRP2 were co-localised in growth cones, indicative of a close physical association. It is pertinent to mention our laboratory has established that LRP1 knockdown does not affect LRP2 expression, and vice versa (Pavez, 2013). Although it is well established that LRP receptors are capable of forming complex signalling domains by recruiting co-receptors, it is currently unknown whether LRP1 and LRP2 may recruit each other. The only suggestion in the literature that LRP1 and LRP2 may signal in a complex is from Vaillant and colleagues who reported that protease nexin 1, which is endocytosed by LRP1, modulated sonic hedgehog (Shh) signalling (Vaillant et al., 2007). Shh is a morphogen with important roles in neuronal development, and binds LRP2 with high affinity, sequestering it in a complex with co-receptor, patched 1 (Christ et al., 2012). Vaillant and colleagues did not discuss the unusual result of an LRP1 ligand modulating an LRP2-dependent process; however their findings support the notion of LRP1/LRP2 receptor crosstalk. Taken together, these results, along with the data within this chapter, support a putative role of LRP1 and LRP2 in axon guidance.

MTIII shares significant structural homology with MTII however it was found to have contrasting chemorepulsive effects on growth cones. It has not been previously determined

whether LRP1 or LRP2 are receptors for MTIII. TrkA, a neurotrophin receptor, has been identified as a receptor necessary for MTIII to mitigate its anti-apoptotic effects in neurons (Kim et al., 2009). Reduced expression of LRP1 or LRP2 in growth cones exposed to a microgradient of MTIII resulted in a switch from repulsion to attraction. Furthermore, simultaneous reduction of both LRP1 and LRP2 expression reverted the growth cone turning response back to repulsion, albeit, attenuated. Although this suggests involvement of LRP1 and LRP2, the mechanism appears to be much more complex than MTII and likely involves other co-receptors such as TrkA. From the data in this thesis, it is evident that growth cone turning in response to LRP ligands occurs through highly complex signalling pathways. This phenomenon will be investigated in more detail in Chapter 3.

Not surprisingly, although many of these ligands have been described to promote neurite outgrowth *in vitro,* not many ligands were observed to promote neurite outgrowth in this acute model of ligand exposure. Given that growth cones are only measured for 30 minutes, it is highly unlikely that typical transcriptional events leading to enhanced neurite outgrowth (such as CREB activation) are engaged (Nakajima et al., 2013). Instead one might postulate involvement of local mediators of cytoskeletal assembly, such as enhanced activation of phosphatases involved in microtubule stabilisation (Bentley and O'Connor, 1994) and assembly and hence neurite outgrowth.

Whether these chemotactic effects on growth cones in response to MTII, MTIII, tPA, or α2M have physiological significance *in vivo* remains to be determined. It is likely that the molecules that are able to promote growth cone turning include many more in addition to the classical chemotactic guidance cues with established roles in development, such as BDNF and Semaphorin3a. Furthermore, chemotactic guidance cues are conceivably specific for

different contexts: for example, the extracellular environment associated with growth cones in the developing nervous system is likely to be very different to that found in the mature brain, in neuropathy, or in the vicinity of regenerating neurons following physical injury. This raises the question whether other receptor-ligand systems outside those established in developmental axon pathfinding, such as the LRP-MTII system, may be involved in, for example, regenerative processes. Recently, the role of MTs in mediating regenerative growth of injured neurons has been a topic of investigation (Giralt et al., 2002b, Carrasco et al., 2003, Chung et al., 2003, Fitzgerald et al., 2007, Asmussen et al., 2009a, Leung et al., 2012), so it is possible that the LRP-MT signalling system may function *in vivo* in neuronal regeneration.

The finding that MTII is chemoattractive to growth cones raises particular interest from a therapeutic context. Neurite chemotaxis is a functionally important component of neuronal regeneration, as regrowth must be directed to the lesion site, so that appropriate sprouting can occur and ultimately connections can be re-formed (Alto et al., 2009). MTII has been implicated in nerve regeneration *in vivo*, and given the ability of MTII to induce neurite chemoattraction, we propose MTII as a possible therapeutic in neuropathies and neuronal injury. The finding that MTII can induce attraction of neurites *in vitro* is novel, but whether MTs in the extracellular environment support tropic regrowth and regeneration of neurons into the site of injury *in vivo* remains unknown and will be the subject of further investigation in chapter 5 of this thesis. Since the processes that are involved in neurite regeneration closely recapitulate those that occur during neurite outgrowth in development (Dyson et al., 1988), the chemotactic effects of MTs observed here in developing sensory neurons *in vitro* may also be applicable to neurites that have re-sprouted during post-injury regeneration *in vitro* or *in vivo.*

Understanding the mechanisms by which MTs elicit these responses in neuronal growth cones has important implications for future therapeutic developments of MTs in neuropathies and neuronal injury. Hence, the following chapter will examine the underlying mechanism of MT-mediated growth cone turning.

CHAPTER 3

The downstream signalling mechanisms that mediate LRP1 and LRP2 signalling in sensory growth cone navigation

CHAPTER 3

THE DOWNSTREAM SIGNALLING MECHANISMS THAT MEDIATE LRP 1 AND LRP2 SIGNALLING IN SENSORY GROWTH CONE NAVIGATION

3.1 INTRODUCTION

The findings in Chapter 2 suggest that LRP ligand, MTII, is a candidate disease-modifying agent for the injured peripheral nervous system. The finding that MTII has a chemoattractive effect on peripheral sensory neurites alludes to therapeutic potential in regenerating nerves damaged after local insult or toxicity. As LRP-MTII signalling represents a novel, non-classical axon guidance system, investigating the mechanism of action at the intracellular level is pertinent to developing MTII as a therapeutic. The finding that MTIII, a protein structurally similar to MTII (Shi et al., 2002), had opposing effects was an intriguing result, and therefore was also investigated. To the best of our knowledge, there is no evidence of a known mechanism by which LRP1 and LRP2 could promote growth cone turning and axon guidance, despite the known involvement of LRP1 and LRP2 in cell migration (Lillis et al., 2005).

The signalling pathways that underlie growth cone navigation are not completely understood. Growth cone guidance cues are often described as Ca^{2+} dependent and Ca^{2+} independent (Song and Poo, 1999). Given that LRPs coordinate Ca^{2+} as part of their secondary structure (Simonovic et al., 2001, Andersen et al., 2003), it is likely that MTII and MTIII growth cone chemotaxis is Ca^{2+} dependent. The involvement of Ca^{2+} in LRP1 and LRP2 ligand mediated neurite chemotaxis was examined, as was the downstream calcium dependent signalling protein, Ca^{2+}/calmodulin-dependent kinase II (CaMKII).

While Ca^{2+} signalling pathways represent traditional growth cone signalling pathways, LRPs are known to interact with a variety of other intracellular signalling molecules. By virtue of their long intracellular domains, LRP1 and LRP2 are capable of forming complex signalling domains by recruiting co-receptors and eliciting a wide array of effects within the cell (Beffert et al., 2004). LRP activity in growth cone navigation likely involves interactions with other co-receptors and intracellular binding partners. One such binding partner is TrkA, the nerve growth factor neurotrophin receptor which has established roles in growth cone guidance (Gundersen and Barrett, 1980, Gallo et al., 1997). Kim and associates (2009) recently identified TrkA, as a putative MTIII receptor. Furthermore, it has been shown that TrkA receptors can be transactivated by LRP1 (Shi et al., 2009). In light of this work, the interaction of TrkA with LRP-MT signalling was investigated in both MTII and MTIII mediated chemotaxis.

Clues into the mechanisms of LRP signalling in growth cones may come from studies looking at the signalling pathway of MTI/II in the context of neuronal protection. The association of MT I/II with LRP1 and LRP2 receptors promotes neurite outgrowth and transiently activates Akt and ERK, which belong to the mitogen activated protein kinase (MAPK) and the phosphoinositide-3 kinase/Akt (PI3K/Akt) intracellular signalling pathways, and are required in neuronal differentiation and survival respectively (Brunet et al., 2001, Chang and Karin, 2001, Ambjorn et al., 2008). These pathways culminate in the activation of the transcription factor, CREB, which alters gene transcription of proteins that are conducive to sustaining neuroprotection and neurite outgrowth (Chang and Karin, 2001, Ambjorn et al., 2008). MAPK pathways have been implicated in growth cone turning (Doherty et al., 2000),

and in light of this, MAPK involvement in MT-mediated growth cone turning was also investigated.

Anchoring points between the cell and its surrounding environment (focal adhesions) are important for growth cone motility (Conklin et al., 2005). An investigation of the turning response of growth cones from LRP1 and LRP2 knockdown cultures yielded unexpected observations. Anomalies in the morphology of these knockdown cultures were observed. As LRPs are intimately associated with focal adhesions (Orr et al., 2003), this chapter will also address the question whether LRP1 or LRP2 receptor knockdown results in morphological changes to the growth cone. The data in this chapter demonstrates that LRP-MT signalling is Ca^{2+} dependent and functions through complex receptor interactions.

3.2 EXPERIMENTAL PROCEDURES & MATERIALS

3.2.1 In vitro growth cone turning assay

Primary DRG neuron culture was performed as per section 2.2.2

The growth cone turning assay was performed as per section 2.2.4, however additional pharmacological agents were used. Bath applied pharmacological agents added to the culture media were: KN93 (5µM, Calbiochem, CA, USA), KN92 (5µM, Calbiochem, CA, USA), SKF953659636 HCl (TOCRIS, Bristol, UK) and K525a (100nM, Calbiochem, CA, USA). Pharmacological inhibitors were added to the culture media 20 minutes prior to imaging.

All growth cone assays were conducted in cultures grown in SNM, except for 'Low extracellular calcium' media turning assays. In the instance of a 'Low $[Ca^{2+}]_{EC}$' media turning assay, the SNM was removed immediately prior to imaging, and replaced with Ca^{2+} free Hank's Balanced Salt Solution (HBSS), or modified 1mM Ca^{2+} Ringers solution. There was no statistical difference in turning angles between the two groups and thus results were pooled. HBSS comprises of Hank's Balanced Salt Solution Ca^{2+} and Mg^{2+} free media (Gibco Biosciences, CA, USA), Penicillin G (100U/mL) and streptomycin (100µg/mL) (Gibco Biosciences, CA, USA), nerve growth factor (50ng/mL; Sigma-Aldrich, MO, USA), and N2 neural medium supplement (Gibco Biosciences, CA, USA). 1mM Ca^{2+} modified Ringer's solution (Ming et al., 1999) comprises 140 mM NaCl, 1 mM $MgCl_2$, 0.9 mM CaCl2, 5mM KCl, 4 mM EGTA, and 10 mM HEPES (pH 7.4). siRNA knockdown of LRP-1 and LRP-2 was performed as per section 2.2.3.

Statistical analysis was performed as per section 2.2.8.

Table 3.1 Pharmacological agents used to probe LRP-MT mediated growth cone navigation

Low $[Ca^{+2}]_{EC}$	Recapitulates the effect of a low extracellular **Ca^{2+} environment**
KN93	Inhibitor of CaMKII
KN92	Inactive analogue and control for KN93
K252a	Inhibitor of TrkA tyrosine phosphorylation
SKF95365	Inhibitor of most TRP Ca^{2+} channels and some voltage gated Ca^{2+} channels
PD98059	Inhibitor of MAPK Kinase

3.2.2 Immunocytochemistry

Immunocytochemistry was performed as per section 2.2.4. Anti-FAK antibody (clone 4.47, Merck Millipore, Darmstadt, Germany) was used in addition to the listed primary antibodies.

3.2.3 Analysis of immunoreactivity, area and filopodia on growth cones

DRG cultures were treated with control or specific LRP1 and LRP2 morpholino oligonucleotides using protocols described in section 2.2.3. Immunocytochemistry was performed as per section 2.2.4. Images of LRP1 and LRP2 immunoreactivity were acquired across all treatment groups were acquired using a cooled CCD 16-bit camera (Optronics, CA, USA) on an Olympus BX-50 microscope and 60x water immersion objective using identical acquisition settings (1sec). Images of F-actin distribution were acquired in parallel. Growth

cone area was calculated from f-actin images, and the number of filopodia per growth cone were counted. From overlaid F-actin images, the LRP1 and LRP2 average immunoreactivity were calculated and expressed as a function of area. Unpaired *t*-test was used to compare average immunoreactivity between groups.

3.2.4 Analysis of FAK puncta

Focal adhesion kinase (FAK) analysis of rat DRG growth cones was performed using ImageJ (NIH, MD, USA). Briefly, DRG cultures were treated with control or specific LRP1 and LRP2 morpholino oligonucleotides using protocols described in section 2.2.3. Localisation of FAK puncta was performed using standard immunocytochemical protocols. Images of FAK immunoreactivity across all treatment groups were acquired using a cooled CCD 16-bit camera (Optronics, CA, USA) on an Olympus BX-50 microscope and 60x water immersion objective using identical acquisition settings (1sec). Images of F-actin distribution were acquired in parallel to FAK immunoreactivity.

The following image analysis were performed by Dr. Robert Gasperini: FAK images were first background corrected using a 5-pixel rolling ball radius, followed by binary thresholding. Particle analysis was subsequently used to quantitate numbers of FAK puncta (9-50 pixel^2 and circularity 0.3-1.0). Growth cone area was calculated from an overlaid f-actin image allowing the calculation of FAK density (puncta/μm^2) in DRG growth cones. FAK density across treatment groups was compared using a Mann-Whitney *U* test (IgorPro, Wavemetrics, OR, USA)

3.3 RESULTS

3.3.1 Determine whether LRP-mediated growth cone guidance a calcium dependent process

It is well established that Ca^{2+} is an early second messenger in growth cone navigation (Song and Poo, 1999, Bootman et al., 2001). Determining whether the LRP-mediated turning response was dependent on extracellular Ca^{2+} may provide important clues about the underlying intracellular signalling pathways. In low extracellular Ca^{2+} media, the LRP-mediated turning response was switched: For MTIII, growth cones switched from an average turning angle of -13.2°±2.0 to +12.4°±3.6, $P<0.0001$; conversely for MTII, growth cones switched from an average turning angle of +11.6°±2.2, to -8.1° ± 3.8; $P<0.0001$ (Fig 3.1A and 3.2A). This switch in the turning angle is reminiscent of the molecular switch formed by the alternate activation of the repulsion-inducing Ca^{2+}-binding protein, calcineurin (CaN) and attraction-evoking Ca^{2+}/calmodulin-dependent kinase II (CaMKII) (Wen et al., 2004). As such, the requirement of CaMKII in response to LRP-MT signalling was assessed.

3.3.2 Establish whether CaMKII is required for LRP-mediated growth cone turning

CaMKII activation is required for growth cone attraction towards a guidance cue gradient (Wen et al., 2004, Tojima et al., 2011). To confirm whether CaMKII is required for LRP-mediated turning response, cultures were incubated with CaMKII inhibitor, KN93. Inhibition of CaMKII resulted in a switch in the chemotactic response to MTII (+11.6°±2.2 to -10.4° ±

Figure 3.1. LRP-MTII mediated growth cone turning is Ca^{2+} dependent

Growth cone turning was measured in response to a chemical gradient of MTII. All experiments were performed in normal sensory media with normal calcium concentration, except for Low Ca^{2+} EC medium. **(A)** Reduction of extracellular Ca^{2+} with Low Ca^{2+} EC medium abolished growth cone turning towards MTII. Inhibition of calcium-calmodulin dependent kinase, CaMKII, with KN93, induced growth cone repulsion to MTII. In the presence of KN92, an inactive analogue of KN93, the turning response was unperturbed. The general non-selective Ca^{2+} channel inhibitor SKF95365, did not abrogate the turning response to MTII. **(B)** Axon extension for the same growth cones were analysed and did not differ significantly after 30 minutes of imaging. ****P<0.0001. Error bars represent SEM. Numbers within parentheses indicate the number of growth cones that were analysed per treatment group and apply to both **(A)** & **(B)**.

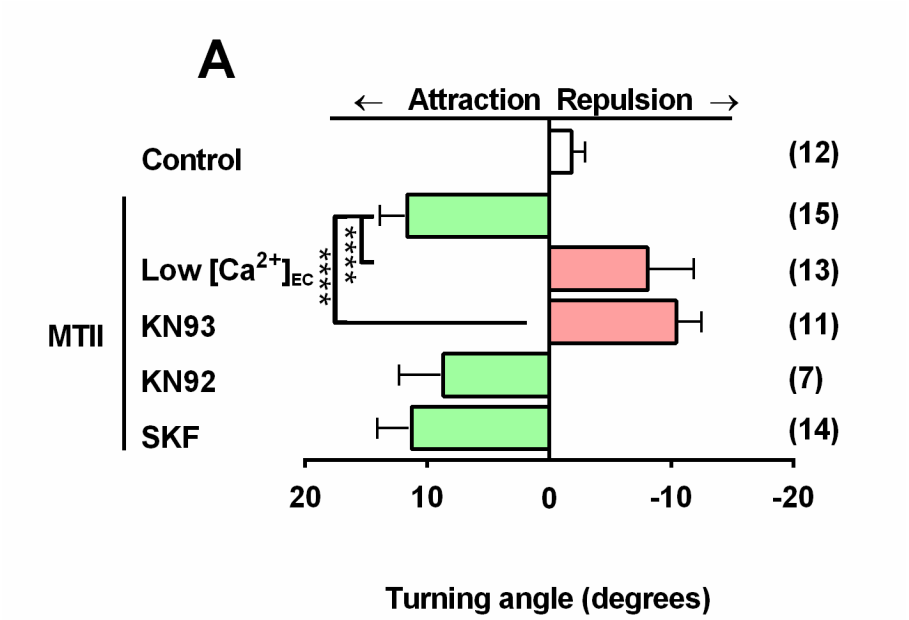
A
← Attraction Repulsion →
Control
Low [Ca2+]EC
KN93
KN92
SKF
MTII
****
****
(12)
(15)
(13)
(11)
(7)
(14)
20
10
0
-10
-20
Turning angle (degrees)

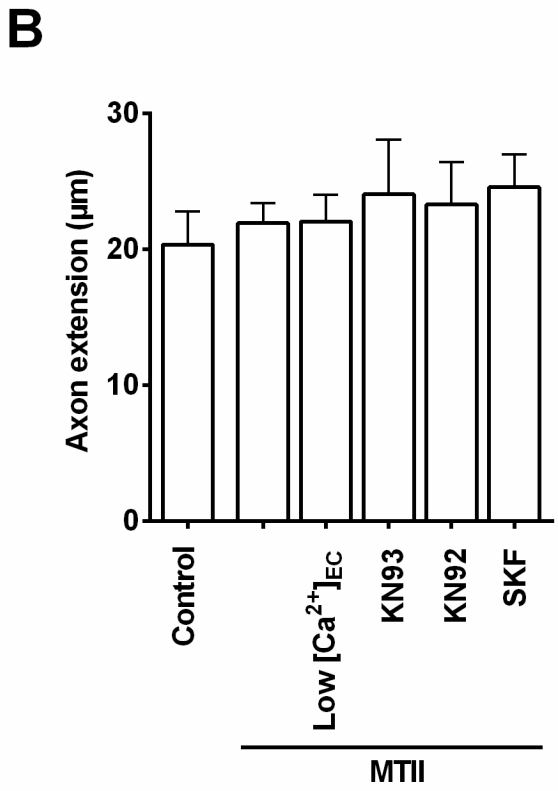
B
Axon extension (µm)
30
20
10
0
Control
Low [Ca2+]EC
KN93
KN92
SKF
MTII

Figure 3.2. LRP-MTIII mediated growth cone turning is Ca^{2+} dependent

Growth cone turning was measured in response to a chemical gradient of MTIII. All experiments were performed in normal sensory media with normal calcium concentration, except for [Low $Ca^{2+}]_{EC}$ medium. **(A)** Reduction of extracellular Ca^{2+} with [Low $Ca^{2+}]_{EC}$ medium reversed the growth cone turning response to MTIII. Inhibition of calcium-calmodulin dependent kinase, CaMKII, with KN93, reversed the growth cone turning response to MTIII. In the presence of KN92, an inactive analogue of KN93, the turning response was unperturbed. **(B)** Axon extension for the same growth cones were analysed and did not differ significantly after 30 minutes of imaging with the exception of KN93 treatment. Error bars represent SEM. ****P<0.0001. Numbers within parentheses indicate the number of growth cones that were analysed per treatment group and apply to both **(A)** & **(B)**. Inhibitors are summarised in Table 3.1.

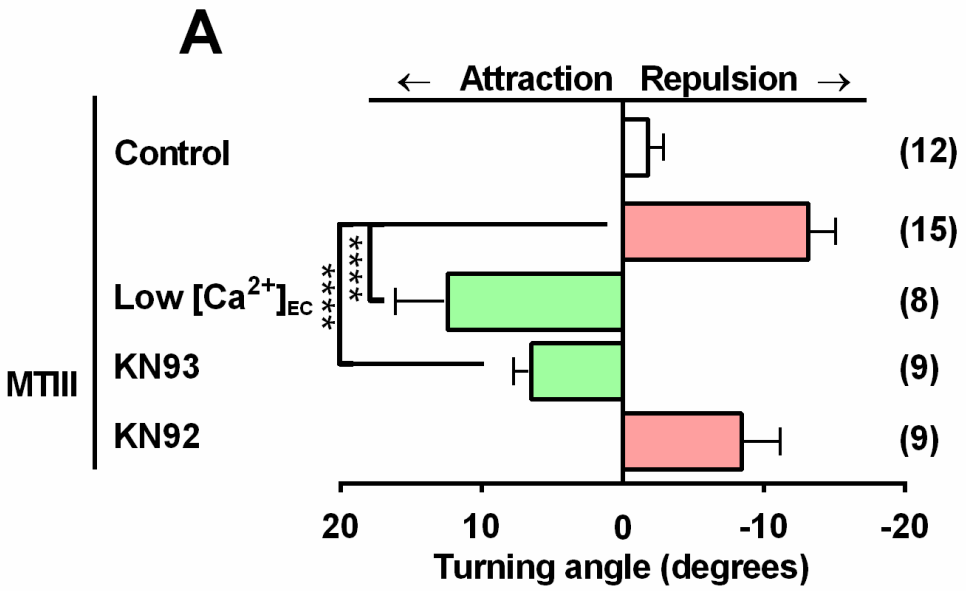
A
← Attraction Repulsion →
Control
Low [Ca2+]EC
KN93
KN92
MTIII
****
(12)
(15)
(8)
(9)
(9)
20
10
0
-10
-20
Turning angle (degrees)

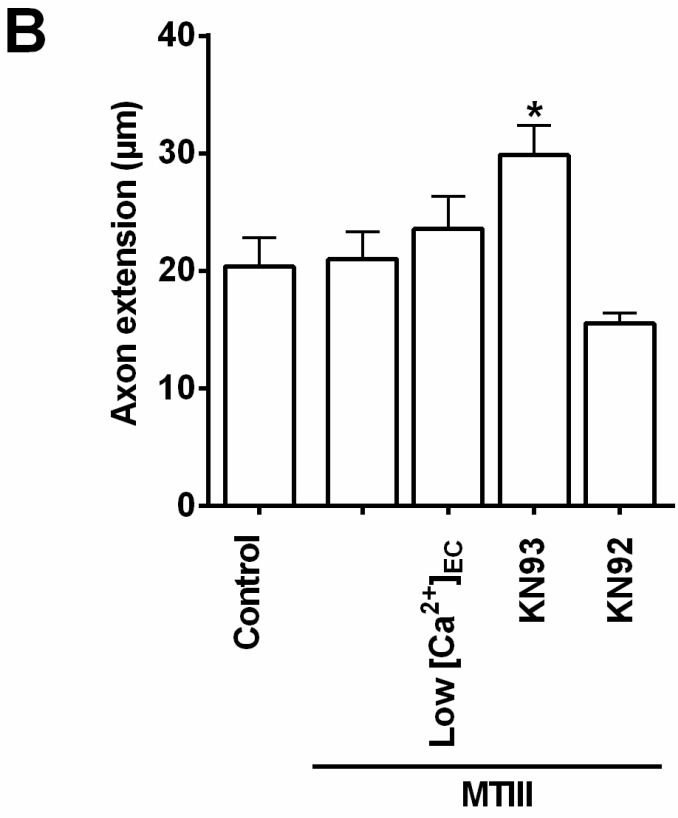
B
Axon extension (µm)
40
30
20
10
0
*
Control
Low [Ca2+]EC
KN93
KN92
MTIII

2.0, P<0.0001) and MTIII (-13.2°±1.9 to + 6.4° ± 1.2, P<0.0001) (Fig 3.1A and 3.2A). KN92, the inactive analogue of KN93, was used as a control, and had no significant effect on the turning response of either MTII or MTIII. This result further supports the hypothesis that LRP signalling is Ca^{2+} and CaMKII dependent, requiring the activation of classical Ca^{2+} signalling pathways. Furthermore, axon extension did not differ (Fig 3.1B), demonstrating the effect was specific to growth cone motility.

Given that LRP-MT signalling requires influx of extracellular $Ca^{2+}$to activate intracellular Ca^{2+} binding proteins, I next asked whether TRP Ca^{2+} channel activation was required. The requirement Ca^{2+} channels was investigated using SKF95365, which is a non-selective inhibitor of several Ca^{2+} channels, including TRP channels, which are implicated in growth cone turning (Singh et al., 2010). Addition of SKF95365, however, did not alter the turning response of growth cones to MTII (Fig 3.1A), suggesting that Ca^{2+} influx is via other Ca^{2+} channels.

3.3.3 Determine whether TrkA is required for LRP-MT mediated chemotaxis

TrkA is a well-established neurotrophin receptor, and putative receptor for MTIII (Kim et al., 2009). There is also evidence that LRP-1 receptors crosstalk with TrkA receptors (Shi et al., 2009). Given the structural similarity of both MTII and MTIII and possible overlap in signalling processes, the involvement of TrkA in both MTII and MTIII-mediated growth cone turning was examined. K252a, an inhibitor of tyrosine phosphorylation, blocks TrkA signal transduction but is known to also have more general actions, such as inhibiting protein kinases such as PKA (Zong et al., 1994). K252a was used to determine whether TrkA was

Figure 3.3 Inhibition of TrkA perturbed growth cone turning in response to LRP-MT

Growth cone turning was measured in response to a chemical gradient of MTII and MTIII. **(A)** Average turning angles of growth cones in response to MTII and MTIII in the presence of bath-applied TrkA inhibitor, K252a, with or without reduced LRP1/2 expression. In the presence of K252a, growth cones exposed to a concentration gradient of MTII trended towards growth cone repulsion. Reduced LRP1/2 expression combined with bath-applied K252a abolished turning towards MTII. Reduced LRP1/2 expression combined with bath-applied K252a abolished turning towards MTIII. **(B)** Axon extension for the same growth cones were analysed and did not differ significantly after 30 minutes of imaging. ****P<0.0001, ***P<0.0005, **P<0.002. Error bars represent SEM. Numbers within parentheses indicate the number of growth cones that were analysed per treatment group and apply to both **(A)** & **(B)**.

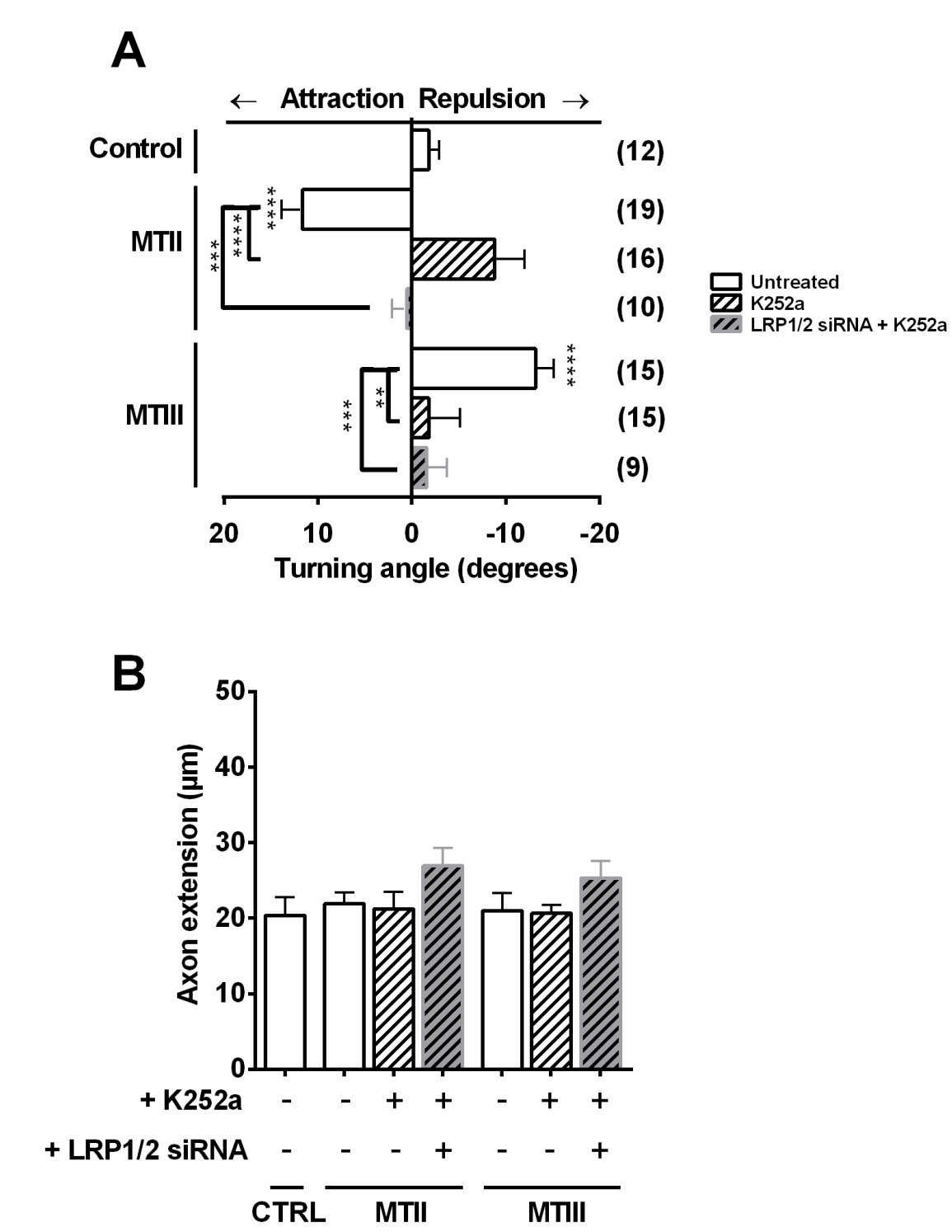
A
← Attraction Repulsion →
Control
MTII
MTIII
(12)
(19)
(16)
(10)
(15)
(15)
(9)
Untreated
K252a
LRP1/2 siRNA + K252a
20
10
0
-10
-20
Turning angle (degrees)
B
Axon extension (µm)
50
40
30
20
10
0
+ K252a
+ LRP1/2 siRNA
CTRL
MTII
MTIII

important for LRP-MT-mediated chemoattraction (Fig 3.3.A). The addition of K252a to the culture medium resulted in an apparent switch in the turning angle of growth cones in response to MTII (from 11.6°±2.2 to -8.8°±3.1, P<0.0001, Fig 3.3). Bath-applied K252a abolished the turning effect of growth cones exposed to a concentration gradient of MTIII (from -13.2°±1.9 to -1.8°±3.3, P<0.002, Fig 3.3). Furthermore, reduced expression of both LRP1 and LRP2 in growth cones, in conjunction with bath applied K252a, abolished the turning effect of MTII, as was predicted (Fig 3.3A). Taken together, these results suggest complex receptor interplay between LRP1, LRP2, TrkA, and other as yet unknown receptors.

3.3.4 Establish whether MAPK pathways function in LRP-MT mediated chemotaxis

MAPK pathways have been implicated in growth cone turning, and have been demonstrated as downstream effectors of MTII in neurite extension and neuroprotection (Leung et al., 2012). Inhibition of the p38/p42 MAPK pathway with PD98059 had no significant effect on the response of growth cones turning towards MTII, although there was a non-significant trend towards decreasing the turning response (11.6°±2.2 to 5.1°±2.2, P<0.054, Fig 3.4). However, Inhibition of MAPK growth caused a switch in the turning effect in response to MTIII (-13.2°±1.9 to +13.1°±3.7, P<0.0001, Fig 3.4). This observation implicates very different signalling processes for MTII and MTIII. The requirement of MAPK in response to MTIII and not MTII suggests that the binding of MTII and MTIII results in the recruitment of different co-receptors or phosphorylation events, thereby activating separate or additional downstream signalling pathways.

Figure 3.4 Inhibition of MAPK perturbed growth cone turning in response to LRP-MT

Growth cone turning was measured in response to a chemical gradient of MTII and MTIII. **(A)** Average turning angles of growth cones in response to MTII and MTIII in the presence of MAPK inhibitor PD98059 demonstrate that the response of growth cones to MTII is unperturbed (although a reduced trend is appreciated), while MAPK inhibition reversed turning in response to MTIII. **(B)** Axon extension for the same growth cones were analysed and did not differ significantly after 30 minutes of imaging. ****P<0.0001. Error bars represent SEM. Numbers within parentheses indicate the number of growth cones that were analysed per treatment group and apply to both **(A)** & **(B)**.

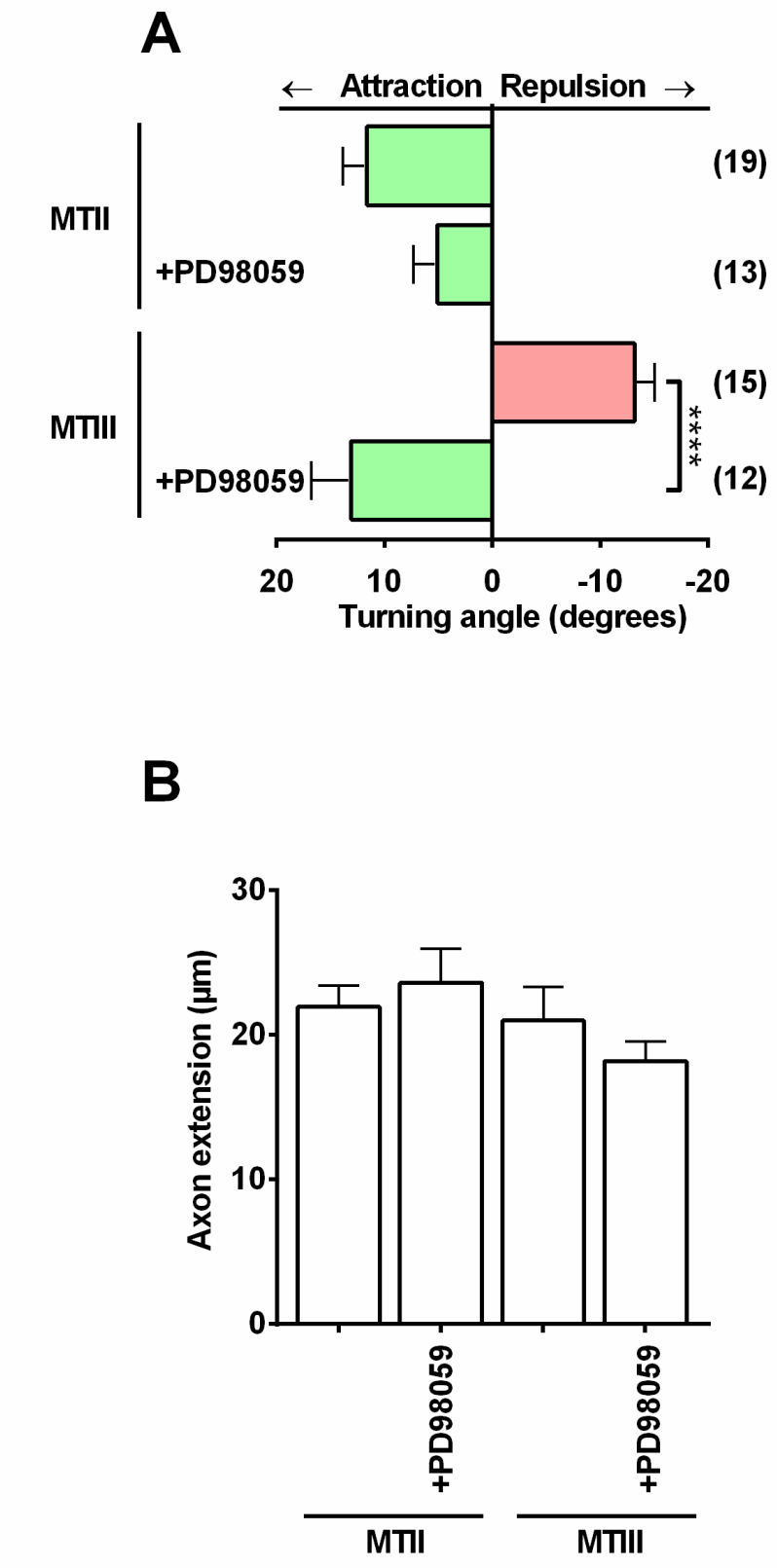
A
← Attraction Repulsion →
MTII
+PD98059
MTIII
+PD98059
(19)
(13)
(15)
(12)
****
20
10
0
-10
-20
Turning angle (degrees)
B
Axon extension (µm)
30
20
10
0
+PD98059
+PD98059
MTII
MTIII

3.3.5 Determine whether reduced expression of LRP1 or LRP2 alters the morphology of growth cones

Reducing the expression of LRP1 or LRP2 in growth cones cultures yielded unexpected observations: anomalies in the morphology of growth cones. Fig 3.5 demonstrates the change in morphology after 6 hours of receptor knockdown. After 6 hours, growth cone immunoreactivity for LRP1 and LRP2 was reduced by 75 and 73%, respectively, in conjunction with a significant concomitant decrease in growth cone area and filopodia number (Figure 3.5 A-C). These findings suggested LRP1 and LRP2 mitigate a change in cytoskeletal or substrate interactions. Due to the intimate relationship ascribed between LRP1 and focal adhesions (Orr et al., 2003), focal adhesion kinase (FAK) immunoreactivity was examined in control cultures and cultures with reduced LRP1 or LRP2 expression. FAK immunoreactivity was reduced in growth cones with reduced LRP1 expression, but not reduced LRP2 expression. Furthermore, a significant decrease in puncta size was observed in LRP1 KD growth cones ($p<0.005$) (*puncta size analysis by R. Gasperini*), suggesting that LRP1 signalling is important for assembly of FAK-immunopositive puncta in navigating growth cones. Furthermore, the observation that reduced LRP2 expression was associated with reduced area and filopodia number suggest a possible undocumented direct interaction with focal adhesions, or modulation of focal adhesions indirectly through LRP1.

Figure 3.5. Reducing LRP1 or LRP2 expression changed morphology of growth cones.

(A-D) Quantification of growth cones with reduced LRP1 and LRP2, compared to growth cones with control siRNA. **(A)** Significant decrease in LRP1 and LRP2 immunoreactivity in growth cones with reduced LRP1 and LRP2 expression **(B)** Reduction of LRP1 or LRP2 results in a significant decrease in growth cone size. **(C)** Reduction of LRP1 or LRP2 results in a significant decrease in the number of filopodia per growth cone. (n = 5 cultures, 15-30 growth cones). **(D)** Significant decrease in the average number of FAK positive puncta per μm^2 per growth cone in growth cones with reduced LRP1 expression. **(E-G)** Representative images of growth cones 6 hours after siRNA transfection. **(E)** FAK immunopositive puncta in control growth cones. **(F)** Reduced FAK immunopositive puncta per μm^2 in growth cones with reduced LRP1. **(G)** FAK immunopositive puncta in growth cones with reduced LRP2.

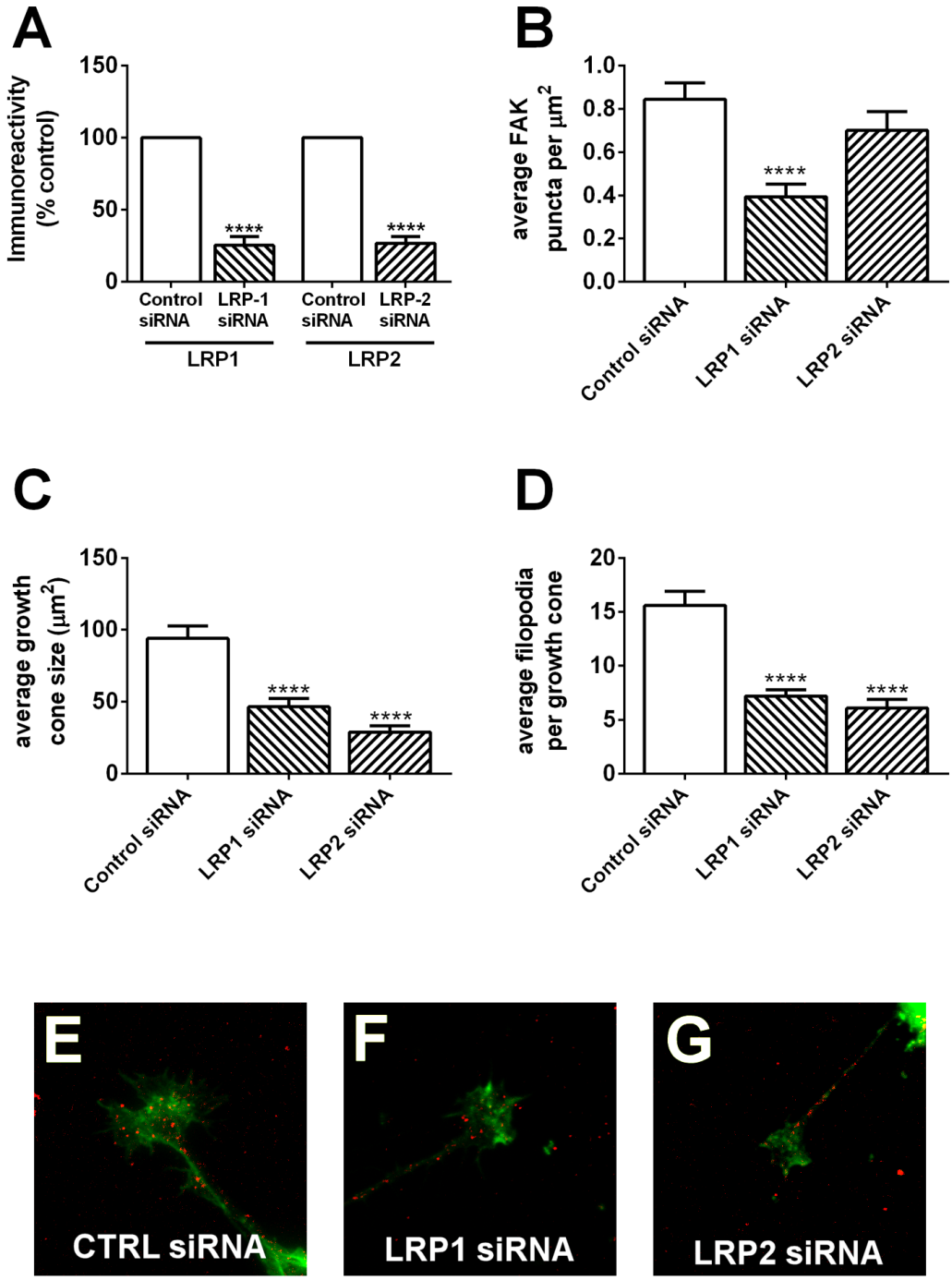
A
Immunoreactivity (% control)
150
100
50
0
****
****
Control siRNA
LRP-1 siRNA
Control siRNA
LRP-2 siRNA
LRP1
LRP2
B
average FAK puncta per µm2
1.0
0.8
0.6
0.4
0.2
0.0
****
Control siRNA
LRP1 siRNA
LRP2 siRNA
C
average growth cone size (µm2)
150
100
50
0
****
****
Control siRNA
LRP1 siRNA
LRP2 siRNA
D
average filopodia per growth cone
20
15
10
5
0
****
****
Control siRNA
LRP1 siRNA
LRP2 siRNA
E
CTRL siRNA
F
LRP1 siRNA
G
LRP2 siRNA

3.4 DISCUSSION

In Chapter 2, it was identified that LRP-MTII induced growth cone attraction, whereas LRP-MTIII induced potent growth cone repulsion. Consistent with the contrasting effects of MTII and MTIII, in Chapter 3, a divergence in their downstream signalling pathways was established. While both MTII and MTIII signalled in a Ca^{2+}-dependent manner, MTII signalling occurred through established Ca^{2+} signalling pathways, MTIII chemorepulsion was dependent on kinase activity.

In growth cone chemotaxis, receptor activation results in the initiation of a downstream intracellular cascade, culminating in cytoskeletal reorganisation and orientation of the growth cone towards or away from the trophic molecule. In the majority of instances, calcium ions (Ca^{2+}) are an important intracellular mediator of this process (Tojima, 2012). LRP ligands such as tPa and α2m have been shown to induce calcium influxes in neurons (Bacskai et al., 2000, Samson et al., 2008). Spatial and temporal fluxes of intracellular Ca^{2+} concentration ($[Ca^{2+}]_i$) in the growth cone are able to trigger both attraction to and repulsion from chemotactic agents (Zheng, 2000). This is in part due to the activation of differentially sensitive calcium-dependent binding proteins, such as CaN and CaMKII (Wen et al., 2004, Gomez and Zheng, 2006). Both MTII and MTIII were dependent on an influx of extracellular Ca^{2+} ions for initiation of chemotactic effects on growth cones. When Ca^{2+} ions were reduced, a directional switch was observed in response to MTII and MTIII. MTII, which was inherently attractive, caused growth cone repulsion in the presence of low extracellular calcium. This phenomenon was consistent with the CaN/CaMKII switch reported by Wen and associates (2004). CaN is highly sensitive to Ca^{2+} and mediates growth

cone repulsion; where the influx of $[Ca^{2+}]_i$ in response to a chemotrophic cue is modest, the growth cone will be repelled. Conversely, if the influx is large, CaMKII tends to be activated preferentially, resulting in attraction. As global intracellular calcium levels had been reduced by the use of low-Ca^{2+} media, and the extracellular concentration of Ca^{2+} was low, it is likely that the change in $[Ca^{2+}]_I$ was only small, hence the CaN pathway was activated preferentially.

To confirm involvement of the CaN/CaMKII switch, inhibitor of CaMKII, KN93, was added to the media, and the effect on MTII-mediated growth cone turning was assessed. Inhibition of CaMKII reversed MTII-mediated chemotaxis. This may indicate that in the absence of CaMKII activation the repulsive CaN-mediated pathway was initiated. This data is in part supported by the finding that CaMKII is activated in response to MTII application, and CaMKII inhibition blocks MT-II mediated neuroprotection and neurite outgrowth (Asmussen et al., 2009b).

Given the established role of CaMKII in attractive growth cone turning, inhibition of CaMKII was not predicted to have an effect on repulsive LRP-MTIII signalling. However, CaMKII is known to bind LRP-1, although the functional significance of this relationship is unknown (Guttman et al., 2010). A direct interaction of LRP1 and CaMKII may explain why inhibition of CaMKII reversed turning in response to MTIII. For example, in LRP-MTIII signalling, CaMKII may be recruited to the receptor complex, where it facilitates phosphorylation of other co-receptors. The ability of CaMKII to activate the cytoskeletal processes that direct growth cone turning may represent a direct link between LRP1 and growth cone motility.

The requirement of Ca^{2+} channels in MTII-mediated growth cone attraction was also investigated. SKF95365 is a non-selective inhibitor of Ca^{2+} entry via most TRP channels, and some voltage gated Ca^{2+} channels (Merritt et al., 1990, Kiselyov et al., 1998, Singh et al., 2010). TRP channels comprise 6 subfamilies, including TRP canonical (TRPC), TRP vanilloid (TRPV), TRP melastatin (TRPM) and TRP ankyrin (TRPA). TRP channels have been implicated in growth cone turning in response to several guidance cues: for example, BDNF, a chemoattractive guidance cue that signals through TrkB, has been demonstrated to require TRPC to elicit this effect in growth cones (Li et al., 2005). However, addition of SKF95365 did not affect the turning response of growth cones to MTII, suggesting involvement of other calcium channels. It is possible that the Ca^{2+} influx required for MTII-mediated growth cone attraction may involve, for example, TRPA or NMDA channels. A recent study has suggested that MTIII is able to activate TRPA directly (Ghasemlou et al., 2012); furthermore SKF95365 has not been shown to inhibit TRPA, revealing this as a promising candidate. Furthermore, there is ample evidence demonstrating the involvement of LRP1 in Ca^{2+} influx via NMDA receptors (Qiu et al., 2002a, Martin et al., 2008, Maier et al., 2013, Mantuano et al., 2013, Nakajima et al., 2013). Although NMDA receptors are not established mediators of growth cone guidance in mammalian DRG neurons, they have been shown to mediate growth cone guidance in Xenopus spinal neurons (Zheng et al., 1996). NMDA receptors are present and functional in DRG (Liu et al., 1997, Coggeshall and Carlton, 1998, Kung et al., 2013), and as such this adds weight to a possible novel mechanism involving NMDA receptors in mammalian growth cone navigation.

MTIII-mediated chemorepulsion was switched from repulsion to attraction in Ca^{2+} depleted media. Although it is unlikely that the classical CaN/CaMKII molecular switch accounts for

this response, cyclic nucleotides (cAMP and cGMP) can be modulated by Ca^{2+} levels and have also been determined as downstream effectors of growth cone turning (Nishiyama et al., 2003). Together, Ca^{2+} and cyclic nucleotides are crucial for growth cone turning (Togashi et al., 2008, Akiyama et al., 2009). Differences in cAMP:cGMP can dictate the turning response of a growth cone, such that when the local ratio of cGMP to cAMP is high, neurites are repulsed, but when the ratio is low, neurites are attracted (Wen et al., 2004). It is known that Ca^{2+} signalling is able to interact with cyclic nucleotide ratios by controlling adenylate cyclase and guanylyl cyclases, which generate cAMP and cGMP, respectively (Lolley and Racz, 1982, Koch and Stryer, 1988, Xia and Storm, 1997). Activation of cAMP or cGMP pathways results in reciprocal inhibition, such that elevated cAMP reduces cGMP levels and vice versa, by phosphodiesterase activity (Shelly et al., 2010). The switching phenomenon in LRP-MTIII signalling is potentially due to spatial and temporal shifts in the ratio of cyclic nucleotides in the growth cone, which is perturbed when using various Ca^{2+} channel and binding protein inhibitors.

The involvement of TrkA in the trophic responses elicited by MTs was examined. It has been established that TrkA can be transactivated by LRP-1 (Shi et al., 2009). Given that inhibition of TrkA with K252a alters the response of growth cones to MTII or MTIII, we propose that LRP-mediated chemoattraction occurs via a TrkA-dependent mechanism. LRP-MTII mediated growth cone turning was switched after TrkA inhibition, suggesting that TrkA activation occurs downstream of LRP1/2 signalling. However, inhibition of TrkA abolished the turning response of growth cones to MTIII, which may suggest that TrkA has a primary role in MTIII signalling, with crosstalk occurring between TrkA, LRP1 and LRP2. It has been previously demonstrated that MTIII interacts directly with TrkA (Kim et al., 2009), and

these findings support these observations. Furthermore, LRP2 has been shown to sequester ligands such as sonic hedgehog to facilitate binding of sonic hedgehog to its co-receptor (Christ et al., 2012). It is possible that a similar mechanism is involved in LRP2/TrkA/LRP1 signalling. It is pertinent to mention that k252a, which is used as an inhibitor of TrkA, can also inhibit tyrosine kinase phosphorylation and inhibits PKA and CaMKII at the concentration used. It is therefore possible that the results observed are due to manipulation of the LRP-MTII downstream signalling pathways, rather than purely a blockade of TrkA signalling. Future work would require the use of more specific inhibitors. The potential LRP signalling pathways are summarised in Fig 3.6 and 3.7.

Unexpectedly, LRP1 and LRP2 deficient growth cones were found to be significantly smaller and less dense in filopodia (all $P<0.0001$), suggesting an undefined role for LRPs in growth cone morphology. Given that growth cones with reduced expression of both LRP1 and LRP2 behaved normally in response to non-LRP dependent guidance cue Netrin, (see Fig 2.5), the change in morphology likely did not have functional consequences in growth cone motility in response to soluble guidance cues. A decrease in lamellipodia has been reported after LRP1 knockdown in smooth muscle cells, although an increase has been reported in Schwann cells, so the effect on lamellipodia is likely cell-type specific (Mantuano et al., 2010, Revuelta-Lopez et al., 2013). LRP1 and LRP2 have important roles in lipid and cholesterol metabolism in the body (May et al., 2005). Forebrain specific knockout of LRP1 is enough to disrupt the entire lipid balance in the brain and contribute to severe effects within neuronal function (Liu et al., 2010). Therefore, the observation of small growth cones in LRP1 and LRP2 knock down neurons maybe due to disruption of membrane synthesis and composition. However, as cholesterol-rich lipid rafts are important for chemotropic guidance of neuronal growth cones,

if this was the case we would expect to see perturbed signalling to netrin as well (Guirland et al., 2004). Furthermore, LRP1 has been shown to act as a survival signal in cells (Yamauchi et al., 2013), and as such, its knockdown may reduce cell viability, reflected as a decrease in growth cone size. Alternatively, the change in morphology may result from disruption of focal adhesions. LRP1 associates with calreticulin, and through this interaction regulates the assembly of focal adhesions (Orr et al., 2003). Focal adhesions are contact points between the cytoskeleton and the receptors binding the extracellular substrate and are well known to be vital for growth cone motility (Chang et al., 1995, Navarro and Rico, 2014). LRP1, but not LRP2 knockdown growth cones, had a significant decrease in focal adhesion kinase puncta. Fewer adhesions would help account for the decrease in growth cone size and filopodia. The decrease in area and filopodia number in growth cones with reduced LRP2 suggests a possible undocumented direct interaction between LRP2 and focal adhesions, or modulation of focal adhesions indirectly as a result of LRP1/LRP2 receptor crosstalk.

The switch phenomenon is a recurrent theme with MTIII-mediated growth cone turning in the presence of all inhibitors and receptor knockdown methods used in this thesis (Fig 2.6, 3.2, 3.3, 3.4). The requirement of CaMKII and MAPK highlights the importance of phosphorylation events in this signalling cascade. These findings suggest that the effect elicited by MTIII on 'normal' cells is likely a threshold dependent process, whereby a full strength signal is required to initiate chemorepulsion, whereas a partial signal activates a default attractive response. This may have implications for physical or chemical neuronal injury, where the normal homeostatic balance of intracellular messengers and receptors becomes disrupted, allowing an individual protein to have a multifaceted response depending on the demands of the both the intra- and extracellular environment.

To the best of our knowledge, there is no prior evidence of a mechanism by which LRP1 and LRP2 promote growth cone motility. Based on evidence within this chapter, I have proposed the concept of LRP1 and LRP2 receptor crosstalk, and suggest their formation of a heterogeneous signalling hub with other co-receptors, including (but not necessarily limited to) TrkA. Consistent with the contrasting effects of MTII and MTIII, this chapter reveals a disparity in their downstream signalling pathways. For the first time, I provide evidence that MTIII-LRP signalling requires kinase activity, suggesting that phosphorylation is a key mediator of the downstream pathway. MTII- and MTIII-LRP signalling requires Ca^{2+} and Ca^{2+} binding proteins, suggesting signalling via classical and non-classical signalling pathways.

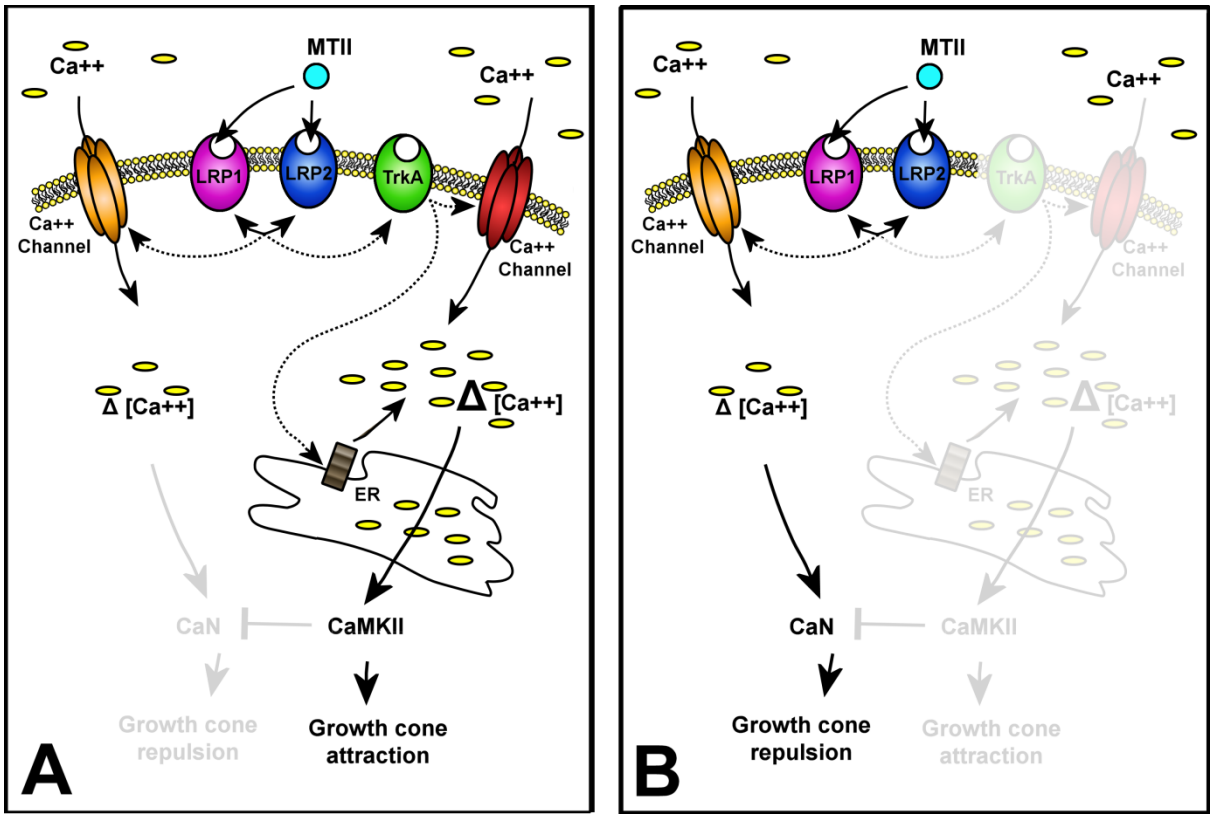
MTII
Ca++
Ca++
LRP1
LRP2
TrkA
Ca++ Channel
Ca++ Channel
Δ [Ca++]
Δ [Ca++]
ER
CaN
CaMKII
Growth cone repulsion
Growth cone attraction
A
MTII
Ca++
Ca++
LRP1
LRP2
TrkA
Ca++ Channel
Ca++ Channel
Δ [Ca++]
Δ [Ca++]
ER
CaN
CaMKII
Growth cone repulsion
Growth cone attraction
B

Figure 3.6 Putative signalling pathway for MTII-LRP chemotaxis

(A) MTII binds LRP1 and LRP2, which engage in receptor crosstalk, recruiting TrkA. This pathway likely activates Ca^{2+} channels and release of Ca^{2+} from internal stores such as the endoplasmic reticulum (ER) resulting in a large change in intracellular Ca^{2+} levels. This would activate CaMKII and culminate in growth cone attraction. **(B)** In the event of a loss of LRP1 or LRP2, the receptor crosstalk cannot occur and thus there is no growth cone turning. If TrkA is inhibited, it is likely that a small influx of Ca^{2+} occurs through a TrkA-independent

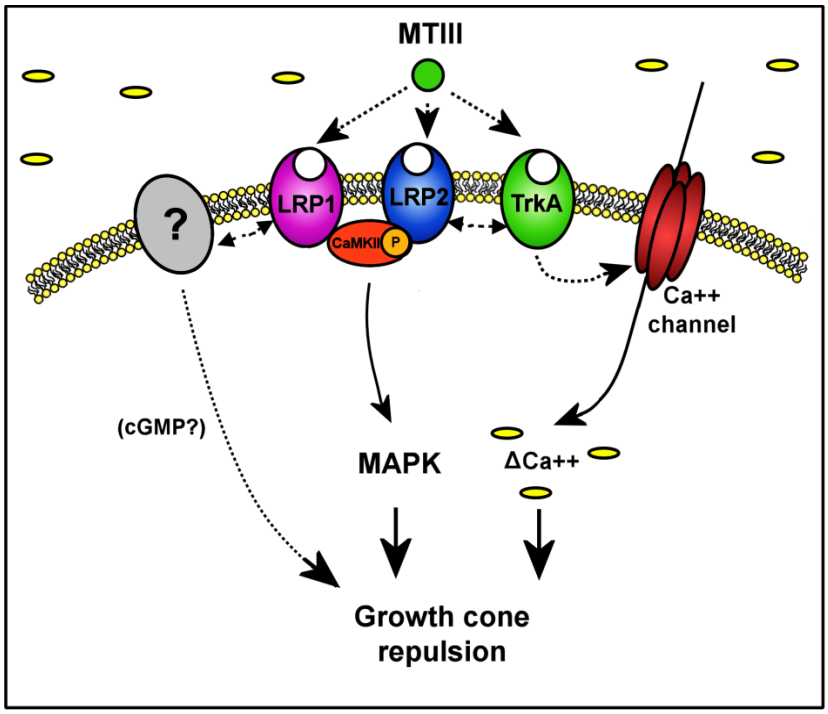

LRP1/2 dependent process, activating CaN and the repulsive pathway.

Figure 3.7 Putative signalling pathway for MTIII-LRP chemotaxis

MTIII likely initially interacts with TrkA, recruiting LRP1 and LRP2 or facilitating binding to LRP1 and LRP2. LRP1, LRP2 and TrkA engage in receptor crosstalk and likely recruit additional co-receptor/s. This pathway likely activates Ca^{2+} channels and results in a modest change in intracellular Ca^{2+} levels. This would activate CaN and the repulsive pathway. Phosphorylation of co-receptors or downstream signaling targets may be mediated by kinases including CaMKII and MAPK. Furthermore, cGMP could contribute to this signalling pathway if produced by a co-receptor, creating a high cGMP:cAMP and propagating the repulsive pathway. In the event that TrkA is lost, the receptor crosstalk cannot occur and there is no LRP-MTIII signalling. LRP1 or LRP2 receptors are lost, the receptor crosstalk that would facilitate binding of an additional binding partner (which, for example, generated cGMP) is lost. The pathway at present is difficult to consolidate and requires further investigation.

3.5 CONCLUSION

In the present study, for the first time, I have described the novel involvement of LRP1 and LRP2 in growth cone turning. Furthermore, I propose that LRP1 and LRP2 engage in receptor crosstalk. Finally, I have identified a novel chemoattractive protein, MTII, which has therapeutic potential. Growth cone chemotaxis is a functionally important component of neuronal regeneration, as regrowth must be directed to the lesion site, so that appropriate sprouting and ultimately new connections can be re-formed. Developing a method to regenerate and guide neurons after injury has been pursued by neuroscientists for decades. Damage to neural tissue in the CNS is virtually irreparable, and even in the PNS, the ability

to repair and recover from damage is often limited. Therefore, therapeutic intervention to enhance repair of these tissues would have great implications in some neuropathies or in re-innervating tissues after traumatic injury. The involvement of MTs in recovery after CNS injury has been explored; for example, it is known that MTI/II are required for optimal recovery post-CNS injury (Giralt et al., 2002b). Since the processes that are involved in neurite regeneration closely recapitulate those that occur during neurite outgrowth in development (Hoffmann, 1988), I hypothesise that the chemotactic effects of MTII may be applied to both developing peripheral neurons and peripheral axons that have re-sprouted during post-injury regeneration. Whether MTII in the extracellular environment may support the regeneration of neurons into the site of injury *in vivo* remains unknown, and forms the basis of the following chapters within this thesis. Understanding the mechanisms by which MTII elicits this response in the neuronal growth cone offers the opportunity to not only use MTII itself, but also other agents that manipulate the same signal transduction pathways, as therapeutics for a wide range of peripheral nerve diseases and insults.

CHAPTER 4

Site directed delivery of MTII and synthetic MTII analogue, EmtinB, into the skin

CHAPTER 4

SITE-DIRECTED DELIVERY OF MTII AND SYNTHETIC MTII ANALOGUE, EMTINB, INTO THE SKIN.

4.1 INTRODUCTION

The overarching aim of the translational side of my project was to establish whether MTII and its synthetic analogue, EmtinB, could act as disease-modifying small molecules for small fibre peripheral neuropathies *in vivo*. In order to test this hypothesis, I first must expose epidermal nerve fibre termini to MTII or EmtinB, and most preferably, do so in a fashion that produces a microgradient, in order to create an *in vivo* paradigm similar to conditions under which MTII stimulates chemoattraction of sensory neurites *in vitro* (Chapters 2-3).

Small fibre peripheral neuropathies such as diabetic neuropathy are characterised histologically by the presence of aberrant nerve fibres which terminate prematurely beneath their correct anatomical location in the epidermis (as shown in Chapter 1, Fig 1.5), leading to the pain syndromes associated with the disease (Polydefkis et al., 2004, Shun et al., 2004). Diseases affecting the skin, including small fibre peripheral neuropathies, lend themselves to topical drug delivery approaches. My hypothesis is that chemoattractive property of MTII observed *in vitro* (as shown in Chapter 2, Fig 2.2) may be present *in vivo,* thereby attracting regenerative growth of nerve fibres back into the correct anatomical location in the epidermis, ameliorating the pathology (Figure 4.1). Furthermore, as previous work on MTII in sensory neurons and other neuronal types indicate a role of MTII in promoting axon extension (Fitzgerald et al., 2007, Ambjorn et al., 2008, Chung et al., 2008, Leung et al., 2012), I

hypothesise that an outcome of administration of MTII would include stimulation of axon outgrowth. The finding that MTII is chemoattractive along a concentration gradient *in vitro* (Chapter 2, Fig 2.2) has implications for its mode of administration and delivery *in vivo*. The aim was to dispense the MTII in a fashion that would result in a local concentration gradient being formed inwards from the outermost layer of the skin, and therefore represent the ideal system with which the chemotactic effect can be harnessed (as shown in Chapter 1, Fig 1.6). In order to establish whether MTII exerts chemotactic effects *in vivo*, it is first necessary to establish a means of delivery across the skin barrier into the epidermis in a manner that produces a concentration gradient.

EmtinB is a synthetic analogue of MTII which retains neuroprotective and growth promoting properties (Ambjorn et al., 2008), but lacks chemotactic effects on the neuronal growth cone (Chapter 2, Fig 2.3). The lack of chemotactic ability of EmtinB would allow a distinction between the effects of regeneration due to chemotactic guidance, versus growth promotion (exhibited by both EmtinB and MTII), to be elucidated *in vivo*, and therefore is included in this chapter.

The most simple and obvious method would be to apply MTII topically. A major function of skin is that of a protective barrier, with a lipid-rich, keratinised layer that is impervious to most molecules. Transdermal delivery of proteins has always been particularly challenging due to their physicochemical properties (Prausnitz and Langer 2008). In order to successfully deliver MTII to the region of interest affected in small fibre peripheral neuropathies (epidermis and underlying dermis), a system is required to effectively transport small molecules across this barrier. The aim within this chapter is to establish a method for delivering MTII and EmtinB into the superficial layers of the skin in a manner that produced

a concentration gradient. Several approaches were taken. Initially, topical preparations using established carrier vehicles such as oleic acid and DMSO, which are known to enhance the penetration of many molecules topically (Benson, 2005), were trialled. A specialised carrier peptide, which was recently demonstrated to effectively transport green fluorescent protein into human cells (Liu et al., 2011, Liu et al., 2012), was also tested. Iontophoresis was trialled as a non-invasive approach to deliver charged molecules (including proteins) into the skin using a low-intensity electric current (Prausnitz and Langer, 2008). Finally, intradermal injection bypasses the stratum corneum, and was used as a robust technique for delivering MTII and EmtinB directly into the skin.

4.2 METHODS:

4.2 1. Disclosure

All rat procedures were conducted with the approval of the University of Tasmania Animal Ethics Committee (approval numbers #A13109 and #A11302), and are compliant with the Australian NHMRC Code of Practise for the Care and Use of Animals for Scientific Purposes. Rats were supplied water, food *ad libitum* and had a 12 h light/dark cycle.

4.2.2 Biotinylation of MTII and EmtinB

This procedure was carried out using the ImmunoProbe Biotinylation Kit (Sigma-Aldrich, MO, USA) according to the supplier's manual *(all procedures and the respective results are shown in Appendix 2)*. Briefly, 10.8mg of EmtinB dimer was dissolved in 400µL of sterile PBS, and 5mg MTII was dissolved in 2mL basic PBS, pH9 (1 drop 1M NaOH, Sigma-Aldrich, MO, USA). Both EmtinB and MTII were prepared separately as follows. 5mg of biotinamidohexanoic acid 3-sulfo-N-hydroxysuccinimide ester were dissolved in 30µL of dimethyl sulfoxide (DMSO; Sigma-Aldrich, MO, USA) and 470µL of PBS (pH 7.4; comprising 10mM Na_2HPO_4, 1.8mM KH_2PO_4, 137mM NaCl and 2.7mM KCl, all from Sigma-Aldrich, MO, USA). The ester was then gently combined with MTII or EmtinB and incubated on a horizontal shaker in ice for 2 hours. To isolate the labelled protein, a sephadex-G25M column (Sigma-Aldrich, MO, USA) was equilibrated in 6 x 5mL of PBS (30mL total) and the reaction mixture was applied. The column was then eluted with 10x 1mL PBS and collected in 1mL fractions. Protein content in the fractions was measured

using a BCA protein assay, read on a microplate reader (TECAN GENios) at an absorbance of 562nm, and pooled. Biotinylation was confirmed according to manufacturer's instructions.

4.2.3 Preparation of skin

Rats were anaesthetised under isofluorane (Piramal Healthcare limited, Mumbai, India), placed in the prone position on a heated pad (37°), and maintained under (2-3.5%) isofluorane inhalation. Breathing and responsiveness was monitored closely through the duration of the experiment and the percentage of isofluorane adjusted accordingly. The dorsal region of the skin was shaved and depilatory cream applied for 5 minutes (or until depilation was complete when tested). The depilatory cream was thoroughly removed with tissues moistened with water. The final step of skin preparation involved consecutively applying and removing sticky tape (Scotch Tape, 3M, St. Paul, MN) applied to the surface of skin, twice in the same area.

4.2.4 Topical application

Skin was prepared as per section 4.2.3; however, depilatory cream was omitted from the procedure. $1cm^2$ regions of skin were demarcated and treated with 50µL of various topical preparations, for 20, 40 or 60 minutes. Topical preparations were: (either combined with or without 1mg/mL MTII); water; 0.9% saline; 100% ethanol; 30% acetone/70% olive oil; lipid carrier Intralipid® 20%; 8% oleic acid/5%DMSO; or 5% DMSO in saline (all supplied by Sigma-Aldrich, MO, USA). Furthermore, Intralipid® 20%; 8% oleic acid and 5% DMSO preparations were also trialled with 1mg/mL biotinylated MTII. At the end of treatment (20, 40 or 60 minutes), excess topical preparation was blotted. The animal was immediately

euthanised by CO_2 inhalation, with the skin harvested and placed in 4% paraformaldehyde as rapidly as possible.

4.2.5 Topical application with carrier peptides

Skin was prepared as per section 4.2.3; however, depilatory cream was omitted from the procedure. A cell penetrating peptide, HR9, (Genscript, NJ, USA) with the peptide sequence CHHHHHRRRRRRRRRHHHHHC, was combined with 1mg/mL Biotinylated MTII or 1mg/mL biotinylated EmtinB in PBS, in either a 1:3 or 1:6 molecular ratio of Protein:HR9, and placed on a rotator at room temperature for 1h. This preparation was then used immediately, as per the topical application protocol described above. Briefly, $1cm^2$ regions of skin were demarcated and treated with 50µL of biotinylated MTII:HR9 1:3, Biotinylated MTII:HR9 1:6, biotinylated EmtinB:HR9 1:3, or biotinylated EmtinB:HR9 1:6, for 20, 40 or 60 minutes. At the end of treatment, excess topical preparation was blotted. The animal was immediately euthanised by CO_2 inhalation, with the skin harvested and placed in 4% paraformaldehyde as rapidly as possible.

4.2.6 Iontophoresis

Skin was prepared as per section 4.2.3. Skin from the thoracolumbar dorsal region of rats was shaved and hair removal cream applied for 5 minutes or until depilation was complete. The hair removal cream was then removed and the area cleaned with tissues saturated with warm water, followed by a final wipe with sterile ethanol sheets. Skin was allowed to dry before proceeding. Iontophoresis experiments were performed *in vivo* using iontophoresis rig MIC2™ (Moor Instruments, Devon, UK). An electrode (connected to either the positive or negative pole) was placed approximately 5 cm from the iontophoresis chambers (connected

to the negative or positive pole, respectively). Both the electrode and the iontophoresis chambers were placed on the same side of the animal, to avoid the conducted charge crossing the heart. Iontophoresis was performed using 1mg/ml MTII in either MQ water, NaCl 0.9% or NaCl 0.9%/5%DMSO solution. Iontophoresis was performed with a current intensity set at 100µA, at a rate of one 20second pulse per minute (and either 10 or 20 pulses).

4.2.7 Intradermal injection

Skin was prepared as per section 4.2.3; however, depilatory cream was omitted from the procedure. A 31G needle filled with 1mg/mL biotinylated-MTII was placed bevel side down and inserted into the skin at a shallow angle (approximately 5° to the skin surface). As the epidermis and underlying dermis is only 1-2mm thick, as soon as resistance from the skin was felt, the needle had penetrated the skin sufficiently. At this point, the depth was appropriate to successfully inject intradermally, with 25ul deposited at each injection site.

4.2.8 Tissue processing

Skin sheets were harvested and fixed in 4% PFA (Sigma-Aldrich, MO, USA) in PBS (pH 7.4; comprising 10mM Na_2HPO_4, 1.8mM KH_2PO_4, 137mM NaCl and 2.7mM KCl, all from Sigma, MO, USA) at 4°C for 2 hours. Post fixation, tissue was washed several times in PBS. Samples were then cryoprotected with 30% sucrose in PBS pH7.4 until samples sank into the liquid. Tissue was then embedded in optimal cutting temperature compound (ThermoFisher Scientific, MA, USA) at -25°C. 50-µm cryosections were obtained in a Leica CM1850UV sliding microtome (Wetzlar, Germany). To ensure adequate sampling, each slide contained several sections, each with profiles from different regions of the same sample. Prepared

slides were dried overnight at 37°C. Excess OCT was removed with PBS prior to immunolabelling.

4.2.9 Fluorescence immunohistochemistry

Samples were permeabilised in 0.4% Triton-X (Sigma-Aldrich, MO, USA) in PBS for 4 hours, before being transferred to 5% goat serum in PBS blocking agent for 30 minutes. Samples were then incubated overnight at 4°C with either mouse anti-Metallothionein antibody (1:200, Dako, Glostrup, Denmark) diluted in PBS with 5% goat serum (Invitrogen, ThermoFisher Scientific, MA, USA) or Alexa 488 conjugated-streptavidin (1:1000, Molecular probes, OR, USA), depending on whether the sample used MTII or biotinylated MTII, respectively. Controls for immunolabelling were performed by using untreated tissue. After washing in 0.5 M Tris buffer (pH 7.4; 50mM Tris and 150mM NaCl, both from Sigma, MO, USA), the cells treated with anti-metallothionein antibody were incubated with the secondary antibody, fluorescent Alexa 488-conjugated goat anti mouse (1:1000, Molecular Probes, OR, USA), in the dark, overnight at 4°C, or at room temperature for 4 hours. Tissue sections were washed in Tris pH 7.4 and allowed to dry, then mounted with DPX fluorescent mounting media (Koch-Light Laboratories, England, UK).

4.2.10 Fluorescence microscope image acquisition

Fluorescence images were acquired using an Olympus BX50 microscope, equipped with a UP-lanSApo 40x-1.35 lens (Olympus, Tokyo, Japan), and captured with MagnaFire V2.1c (Optronics, CA, USA), with a cooled CCD camera (Optronics, CA, USA). During image capture the exposure time was set so that cells would not be over exposed and the pixels not saturated, to produce the most natural depiction of the area of interest. All images were

captured with the same exposure. Images were processed using Image J (NIH, MD, USA) and JASC Paint Shop Pro V 9.0 (JASC Software Inc., MN, USA).

4.2.11 Chromogenic immunohistochemistry

Samples were permeabilised in 0.4% Triton-X (Sigma-Aldrich, MO, USA) in PBS for 4 hours, before being transferred to 5% goat serum in PBS blocking agent for 30 minutes. Samples were then incubated overnight at 4°C with either mouse anti-Metallothionein antibody (1:200, Dako, Glostrup, Denmark) diluted in PBS with 5% goat serum (Invitrogen, ThermoFisher Scientific, MA, USA) or HRP-streptavidin (1:1000, Molecular probes, OR, USA), depending on whether the sample used MTII or biotinylated MTII, respectively. Controls for immunolabelling were performed by using untreated tissue. After washing in Tris buffer, the cells treated with anti-metallothionein antibody were incubated with the secondary antibody, or HRP-streptavidin (1:1000, Molecular probes, OR, USA), overnight at 4°C, or at room temperature for 4 hours. Tissue sections were washed in Tris buffer, then exposed to DAB substrate (Vector Laboratories, CA, USA), and counterstained with haematoxylin or nuclear fast red. Tissue sections were washed in Tris buffer and allowed to dry, then mounted with Pertex mounting media (ThermoFisher Scientific, MA, USA).

4.2.12 Light microscope image acquisition and analysis

Fluorescence images were acquired using a Leica DM2500 microscope (Leica Microsystems, Wetzlar, Germany), equipped with a Leica HC-PL FLUOTAR 40x lens, and captured with Leica ApplicationSuite software with a Leica DFC495 camera. During image capture the exposure time was set so that cells would not be over exposed and the pixels not saturated, to produce the most natural depiction of the area of interest. All images were

captured with the same exposure. Images were processed using Image J (NIH, MD, USA) and JASC Paint Shop Pro V 9.0 (JASC Software Inc., MN, USA).

RESULTS:

4.3.1 Intradermal injection

Intradermal delivery was used as a positive control for the direct administration of MTII and EmtinB to the epidermis and dermis. Rat skin was injected with MTII, biotinylated MTII or biotinylated EmtinB. The presence of biotin was detected using both chromogenic and fluorescent staining (Fig 4.1). Strong positive staining for MTII, biotinylated MTII and biotinylated EmtinB was detected within the epidermis, dermis, and diffused into the underlying subcutaneous tissues. Biotinylated protein was used as it allowed the differentiation of endogenous and injected MTII; EmtinB was biotinylated to facilitate detection as there is no antibody for EmtinB. Negative control tissue was injected with saline only and demonstrated almost negligible levels of endogenous MT (primarily localised to hair follicle) and undetectable levels of endogenous biotin. Autofluorescence was detected in the stratum corneum (the outer layer of the skin) of all sections viewed under green fluorescence. These data demonstrate that intradermal injection is a robust delivery method for MTII and EmtinB.

Figure 4.1. Rat skin with 25ul intradermal injection of biotinylated MTII and MTII

Dorsal skin **(A)** injected with saline; brown DAB staining endogenous MTII, indicating background levels of staining. **(B)** Injected with saline; green fluorescent staining indicating background levels of MTII and autofluorescence. **(C)** Injected with 25uL bolus of 1mg/mL biotinylated MTII. Brown DAB staining indicating presence of MTII **(D)** Injected with biotinylated MTII bolus. Green fluorescent staining indicating presence of exogenous and endogenous MTII. **(E-G)** Injected with 25uL bolus of 1mg/mL MTII. Brown DAB staining indicating presence of excess MTII. A gradient of MTII expression into the surrounding tissue is observed. All panels represent distribution 20 minutes after injection. Scale bars are 300µm. Scale bar in D applies to A-D, scale bar in F applies to E-F.

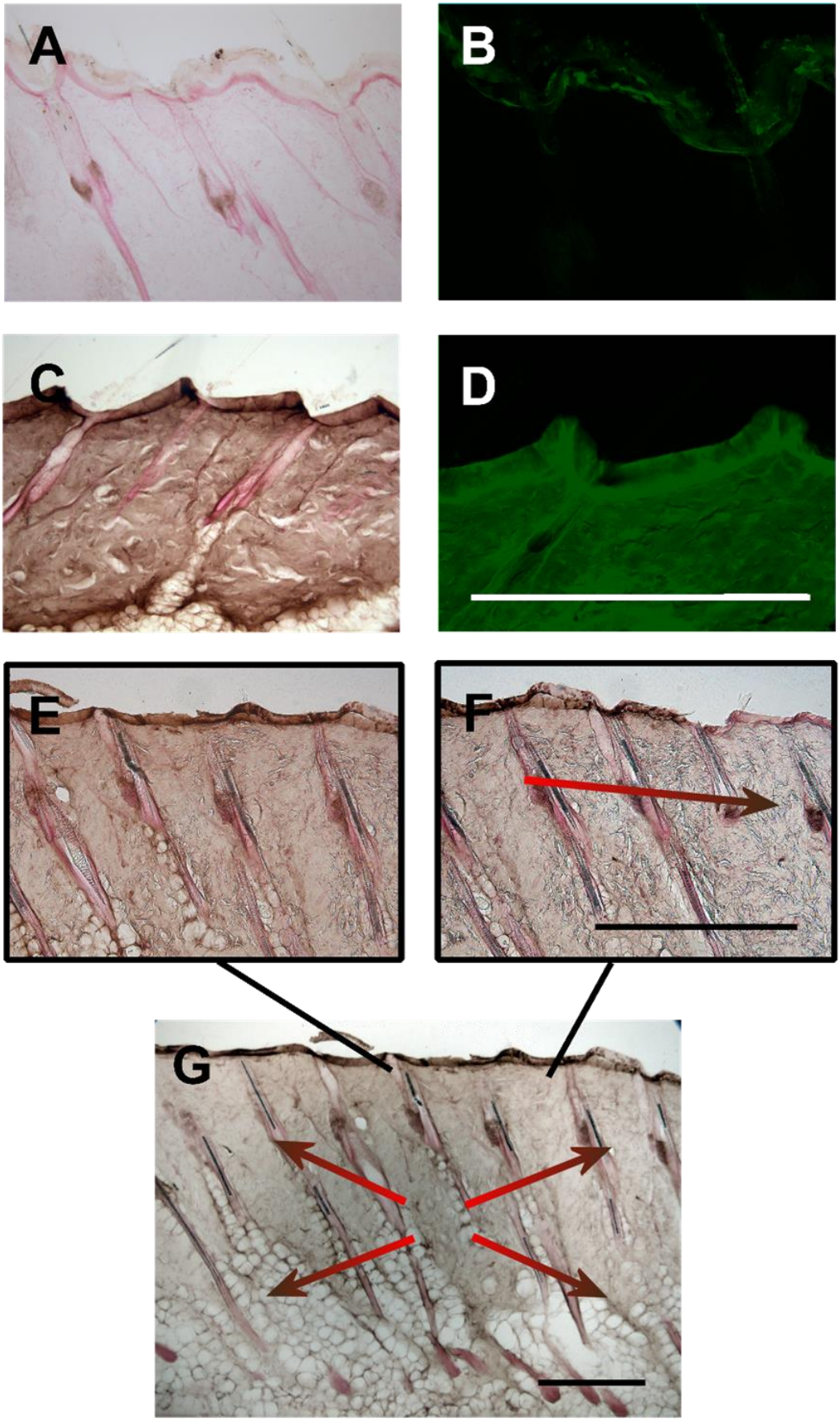
A
B
C
D
E
F
G

4.3.2 Topical application

To investigate whether biotinylated MTII and biotinylated EmtinB could be delivered into the skin topically, formulations of MTII and EmtinB proteins were prepared. Preparations of MTII and EmtinB were formulated with agents known to enhance passage of proteins and peptides through the corneum stratum into deeper skin layers.

Preparations of varying complexity were developed, initially using basic vehicles and carriers (water, ethanol and 30% acetone/70% olive oil) to deliver MTII into the skin. Ethanol may enhance transdermal delivery by decreasing surface tension, allowing the solution to spread and absorb better. Acetone/olive oil preparations deliver hydrophilic protein into the lipid phase – with lipid preparations being optimal for topical drug delivery. However, after one hour of application, MTII was not detected in the deep epidermis or underlying dermis. Exogenous MTII was visualised as a crust on the stratum corneum, indicating failure to penetrate. The findings demonstrated that these approaches were unable to deliver MTII into the skin (Fig 4.2).

In an effort to improve MTII topical delivery, preparations were seeded with well-established chemical penetration enhancers, 5% dimethylsulphoxide (DMSO), Intralipid emulsion, and 8% oleic acid. Intralipid and oleic acid preparations were also combined with 5% DMSO, as this was required to make the preparation miscible with the hydrophilic MTII and EmtinB proteins. However, after one hour of application of 5% DMSO (only) preparations, exogenous EmtinB and MTII were observed within the stratum corneum and into the hair follicle shaft. No EmtinB or MTII were detected in the deep epidermis or underlying dermis after 1 hour of application. EmtinB and MTII were detected within the epidermis and hair

follicle shaft only, suggesting that these approaches were unable to deliver EmtinB or MTII into the skin (Fig 4.3-4.4).

Lipid preparations are much more likely to combine with endogenous lipids in the skin to facilitate transdermal delivery into the underlying tissue. Lipid emulsions have the ability to enhance permeation of MTII into the skin through two mechanisms: by carrying hydrophilic proteins (such as MTII) in a lipid shell, and through solubilisation of the lipid rich stratum corneum via surfactants inherently present in all emulsions. Both oleic acid and Intralipid® appeared unable to deliver MTII into the underlying dermis (Fig 4.5-4.8), again, leaving a detectable crust of MTII and EmtinB on the skin surface. As a result, different approaches for getting MTII and EmtinB into the skin were trialled (summarised in Table 4.1).

Table 4.1. Summary of topical vehicles used and outcomes

Vehicle/carrier	**MTII**	**EmtinB**
H_20	No increase in skin permeability	
Ethanol	No increase in skin permeability	
30%Acetone/70%Ethanol	No increase in skin permeability	
5% DMSO	No increase in skin permeability	No increase in skin permeability
8% Oleic acid/5% DMSO	No increase in skin permeability	No increase in skin permeability
66% Intralipid/5% DMSO	No increase in skin permeability	No increase in skin permeability

Figure 4.2 Water, ethanol and acetone/ethanol preparations are not suitable carriers for MTII.

Representative images of dorsal skin **(A)** with no treatment. Brown DAB staining indicating presence of endogenous MTII. **(B)** Injected with MTII. Brown DAB staining indicating presence of excess exogenous MTII. **(C)** MTII applied topically in water vehicle. MTII is visualised above the stratum corneum. **(D)** MTII applied topically in ethanol vehicle. MTII is visualised above the stratum corneum. **(E)** MTII applied topically in a 30% acetone/70% olive oil emulsion. All panels represent distribution 60 minutes after application. Counter stain is haematoxylin. Scale bar is 200um.

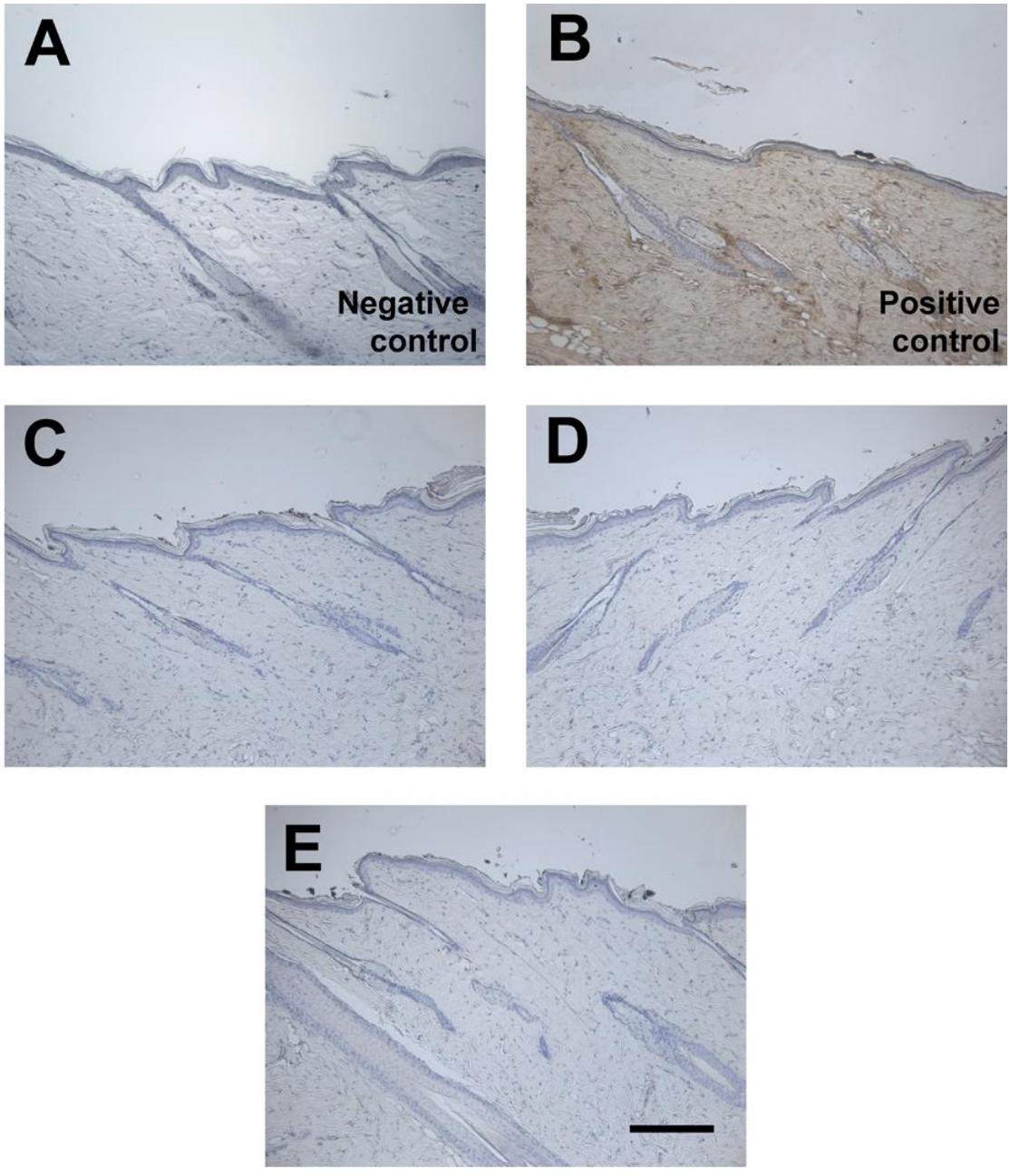
A
Negative control
B
Positive control
C
D
E

Figure 4.3. 5% w/w DMSO is not an effective topical carrier for MTII after 1 hour of treatment

Representative images of dorsal skin **(A)** Injected with saline. Brown DAB indicating background levels of staining from endogenous biotins. **(B)** Injected with saline. Green fluorescence indicating background staining and autofluorescence of the stratum corneum. **(C)** Injected with 25uL bolus of 1mg/mL biotinylated MTII. Brown DAB staining indicating presence of excess exogenous MTII. **(D)** Injected with 25uL bolus of 1mg/mL biotinylated MTII. Green fluorescent staining indicating background staining. **(E-J)** Biotinylated MTII applied topically in 5% DMSO vehicle for **(E-F)** 20 minutes **(G-H)** 40 minutes and **(I-J)** 60 minutes. Crust of biotinylated MTII visualised on stratum corneum. Counter stain is Fast Red. Scale bar is 200um and applies to all images.

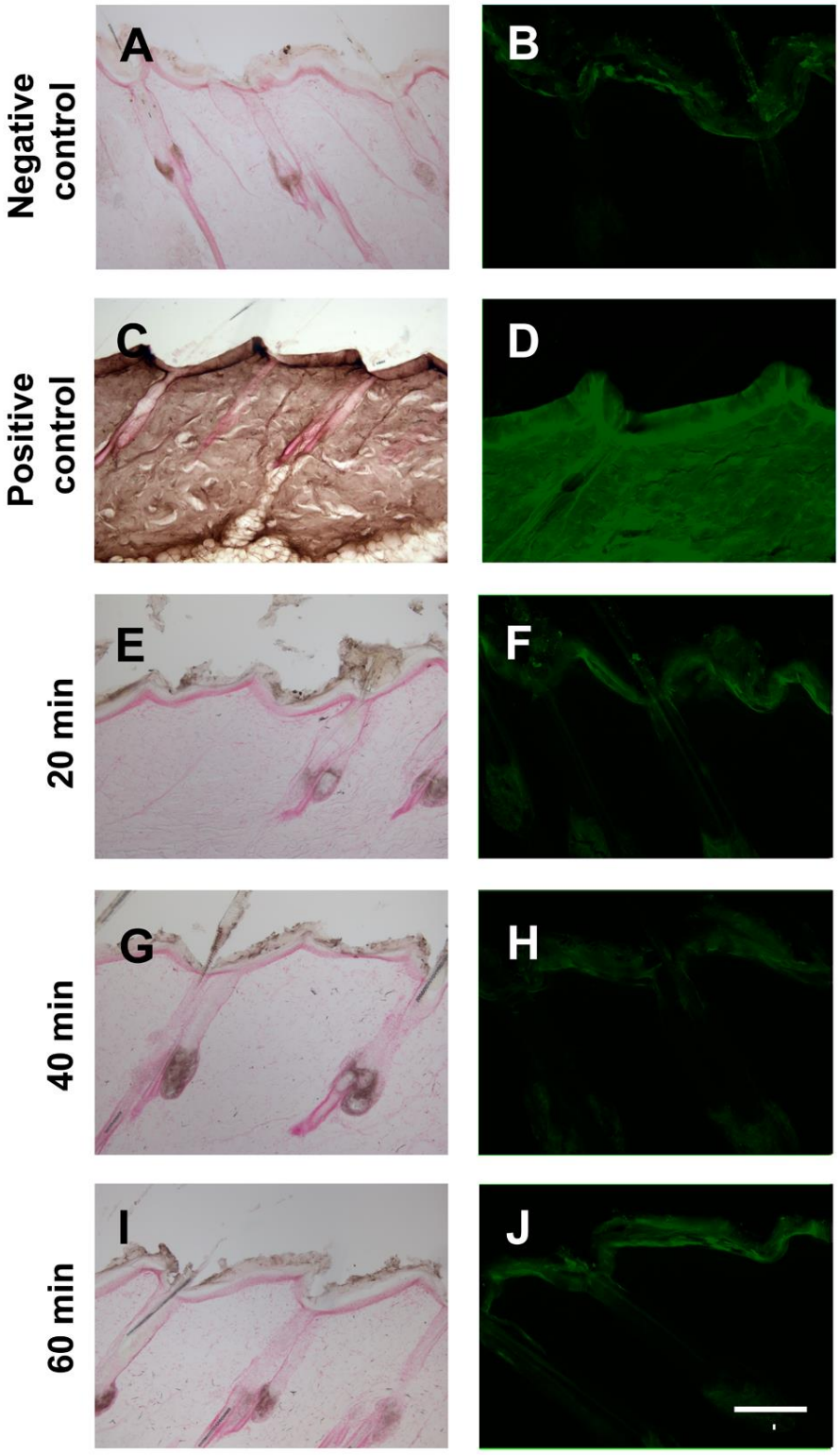
Negative control
A
B
Positive control
C
D
20 min
E
F
40 min
G
H
60 min
I
J

Figure 4.4. 5% w/w DMSO is not an effective topical carrier for EmtinB after 1 hour of treatment

Representative images of dorsal skin **(A)** Injected with saline. Brown DAB indicating background levels of staining from endogenous biotins. **(B)** Injected with saline. Green fluorescence indicating background staining and autofluorescence of the stratum corneum. **(C)** Injected with 25uL bolus of 1mg/mL biotinylated EmtinB. Brown DAB indicating presence of excess exogenous biotinylated EmtinB. **(D)** Injected with 25uL bolus of 1mg/mL biotinylated EmtinB. Green fluorescent staining indicating background staining. **(E-J)** Biotinylated EmtinB applied topically in 5% DMSO vehicle for **(E-F)** 20 minutes **(G-H)** 40 minutes and **(I-J)** 60 minutes. Crust of biotinylated EmtinB visualised on stratum corneum. Counter stain is Fast Red. Scale bar is 200um and applies to all images.

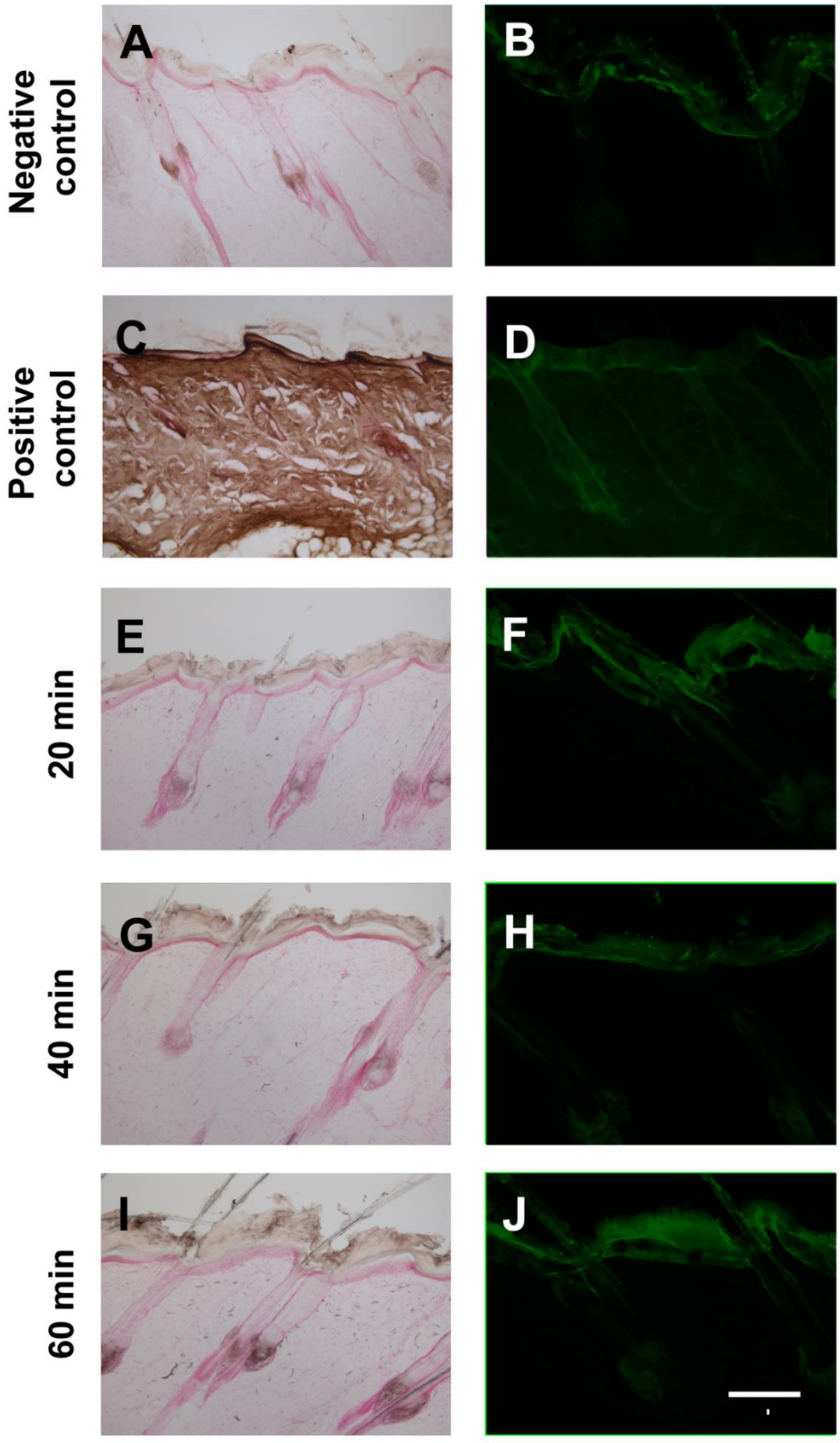
Negative control
Positive control
20 min
40 min
60 min
A
B
C
D
E
F
G
H
I
J

Figure 4.5. 8% w/w Oleic acid/5%DMSO is not an effective topical carrier for MTII after 1 hour of treatment

Representative images of dorsal skin **(A)** Injected with saline. Brown DAB indicating background levels of staining from endogenous biotins. **(B)** Injected with saline. Green fluorescence indicating background staining and autofluorescence of the stratum corneum. **(C)** Injected with 25uL bolus of 1mg/mL biotinylated MTII. Brown DAB indicating presence of excess exogenous biotinylated MTII. **(D)** Injected with 25uL bolus of 1mg/mL biotinylated MTII. Green fluorescent staining indicating background staining. **(E-J)** Biotinylated MTII applied topically in 8% oleic acid/5% DMSO vehicle for **(E-F)** 20 minutes **(G-H)** 40 minutes and **(I-J)** 60 minutes. Crust of biotinylated MTII visualised on stratum corneum. Counter stain is Fast Red. Scale bar is 200um and applies to all images.

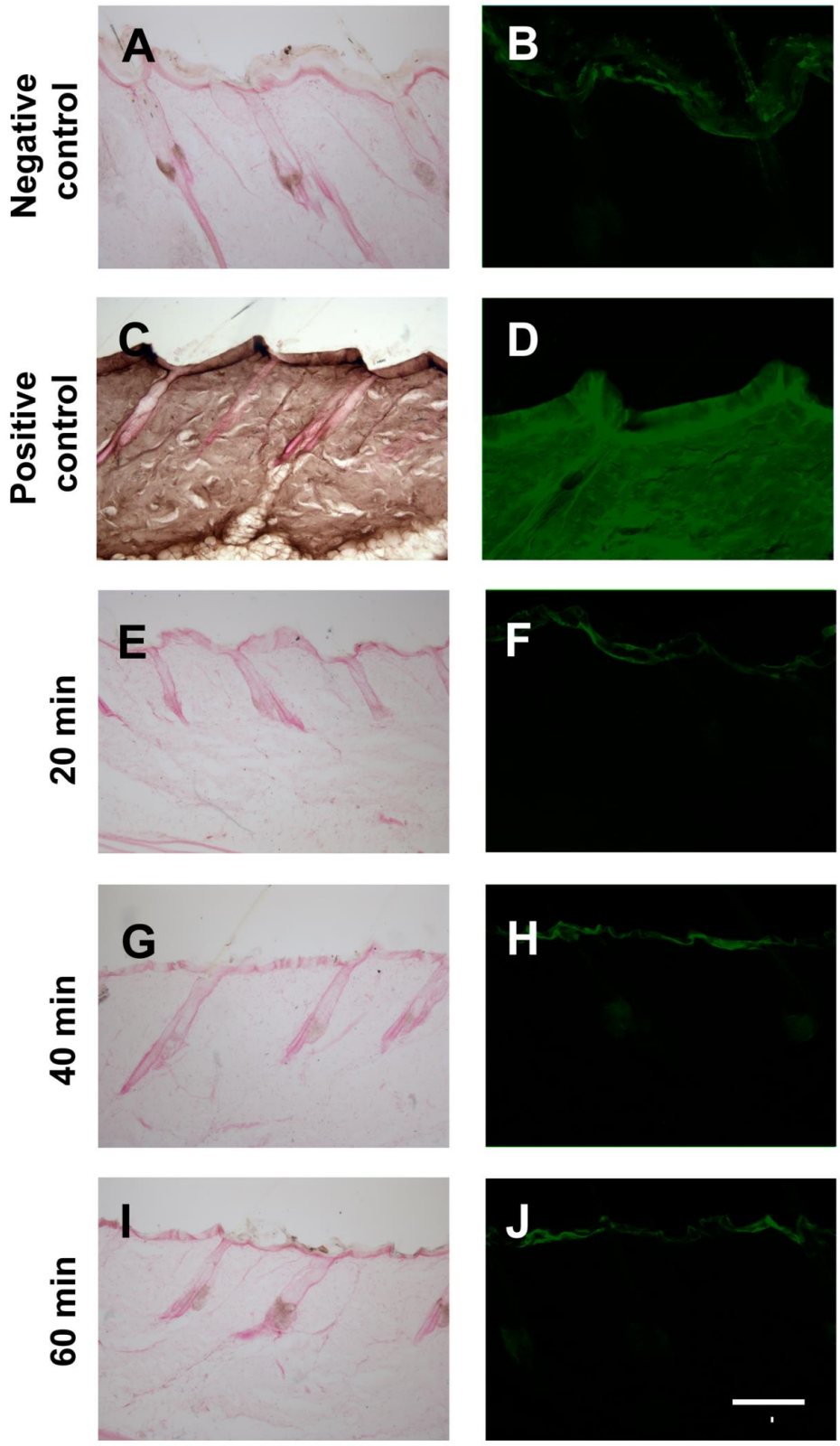
Negative control
A
B
Positive control
C
D
20 min
E
F
40 min
G
H
60 min
I
J

Figure 4.6. 8% w/w Oleic acid/5%DMSO is not an effective topical carrier for EmtinB after 1 hour of treatment

Representative images of dorsal skin **(A)** Injected with saline. Brown DAB indicating background levels of staining from endogenous biotins. **(B)** Injected with saline. Green fluorescence indicating background staining and autofluorescence of the stratum corneum. **(C)** Injected with 25uL bolus of 1mg/mL biotinylated EmtinB. Brown DAB indicating presence of excess exogenous biotinylated EmtinB. **(D)** Injected with 25uL bolus of 1mg/mL biotinylated EmtinB. Green fluorescent staining indicating background staining. **(E-J)** Biotinylated EmtinB applied topically in 8% oleic acid/5% DMSO vehicle for **(E-F)** 20 minutes **(G-H)** 40 minutes and **(I-J)** 60 minutes. Although there appeared to be an increase in EmtinB positive staining in image **(I)**, this was not corroborated with the respective fluorescence image **(J)**. Crust of biotinylated EmtinB visualised on stratum corneum. Counter stain is Fast Red. Scale bar is 200um and applies to all images.

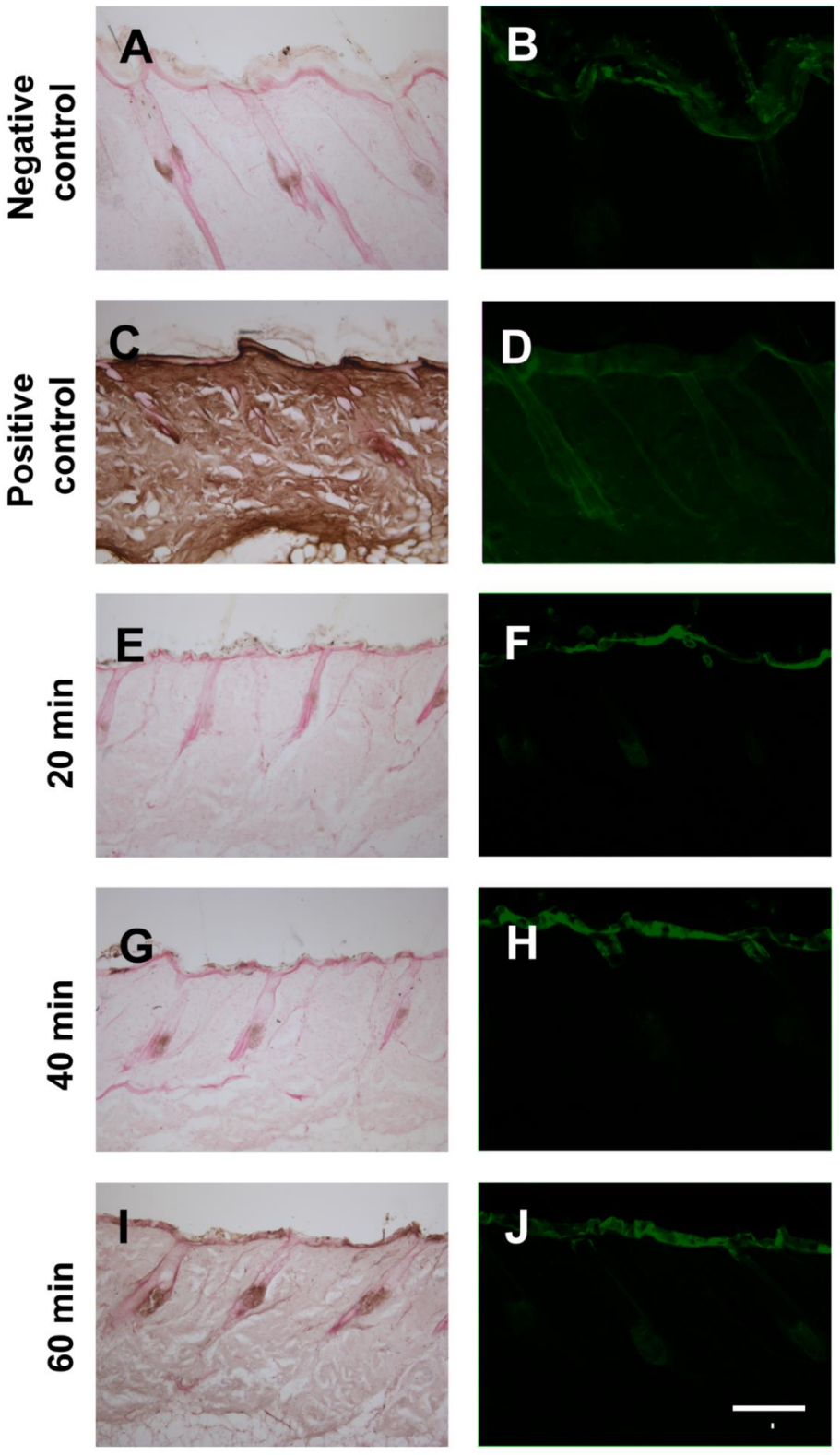
Negative control
Positive control
20 min
40 min
60 min
A
B
C
D
E
F
G
H
I
J

Figure 4.7. Intralipid is not an effective topical carrier for MTII after 1 hour of treatment

Representative images of dorsal skin **(A)** Injected with saline. Brown DAB indicating background levels of staining from endogenous biotins. **(B)** Injected with saline. Green fluorescence indicating background staining and autofluorescence of the stratum corneum. **(C)** Injected with 25uL bolus of 1mg/mL biotinylated MTII. Brown DAB indicating presence of excess exogenous biotinylated MTII. **(D)** Injected with 25uL bolus of 1mg/mL biotinylated MTII. Green fluorescent staining indicating background staining. **(E-J)** Biotinylated MTII applied topically in 66% Intralipid/5% DMSO vehicle for **(E-F)** 20 minutes **(G-H)** 40 minutes and **(I-J)** 60 minutes. Crust of biotinylated MTII visualised on stratum corneum. Counter stain is Fast Red. Scale bar is 200um and applies to all images.

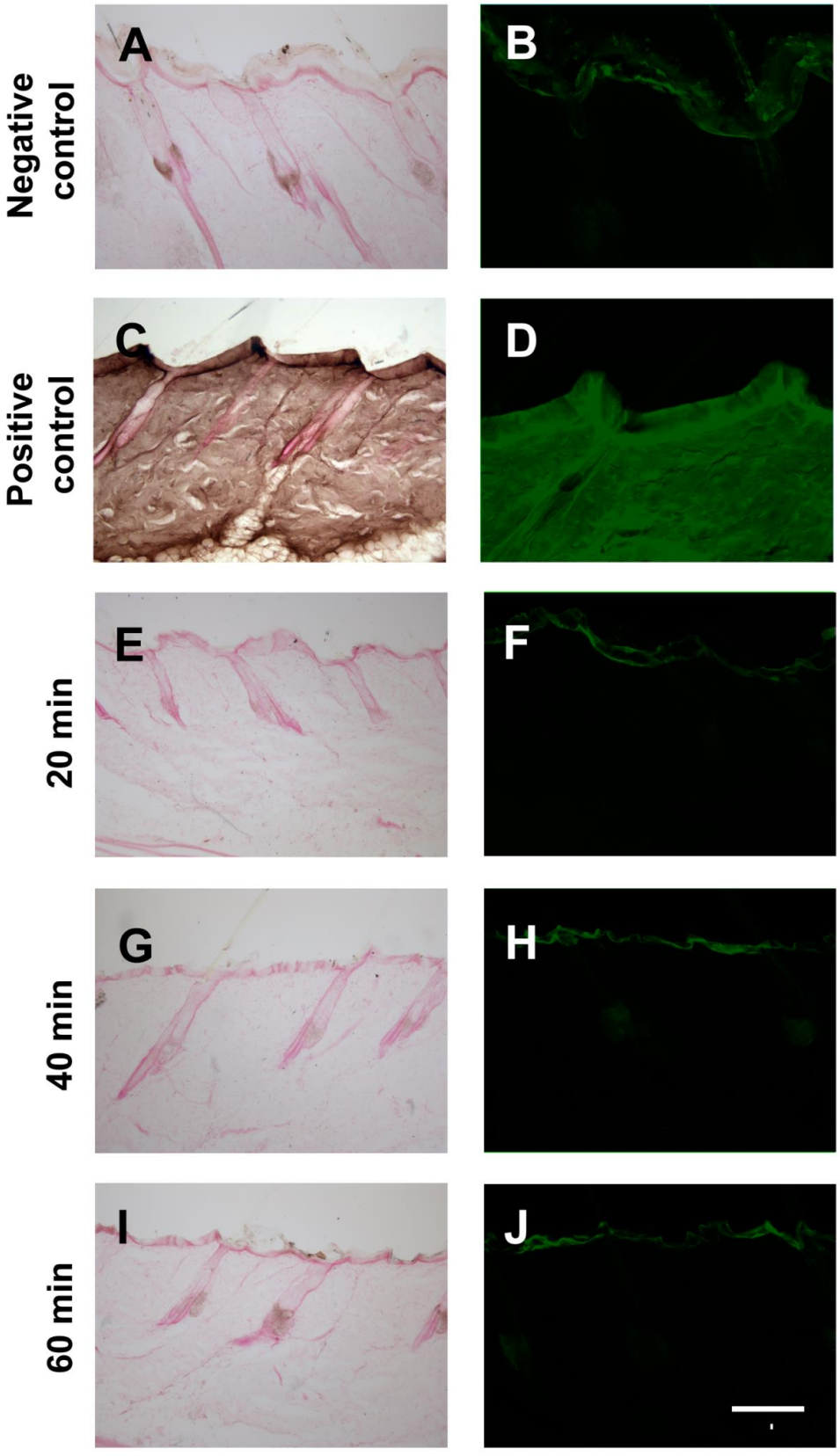
Negative control
Positive control
20 min
40 min
60 min
A
B
C
D
E
F
G
H
I
J

Figure 4.8. Intralipid is not an effective topical carrier for EmtinB after 1 hour of treatment

Representative images of dorsal skin **(A)** Injected with saline. Brown DAB indicating background levels of staining from endogenous biotins. **(B)** Injected with saline. Green fluorescence indicating background staining and autofluorescence of the stratum corneum. **(C)** Injected with 25uL bolus of 1mg/mL biotinylated EmtinB. Brown DAB indicating presence of excess exogenous biotinylated MTII. **(D)** Injected with 25uL bolus of 1mg/mL biotinylated EmtinB. Green fluorescent staining indicating background staining. **(E-J)** Biotinylated EmtinB applied topically in 66% Intralipid/5% DMSO vehicle for **(E-F)** 20 minutes **(G-H)** 40 minutes and **(I-J)** 60 minutes. Crust of biotinylated EmtinB visualised on stratum corneum. Counter stain is Fast Red. Scale bar is 200um and applies to all images.

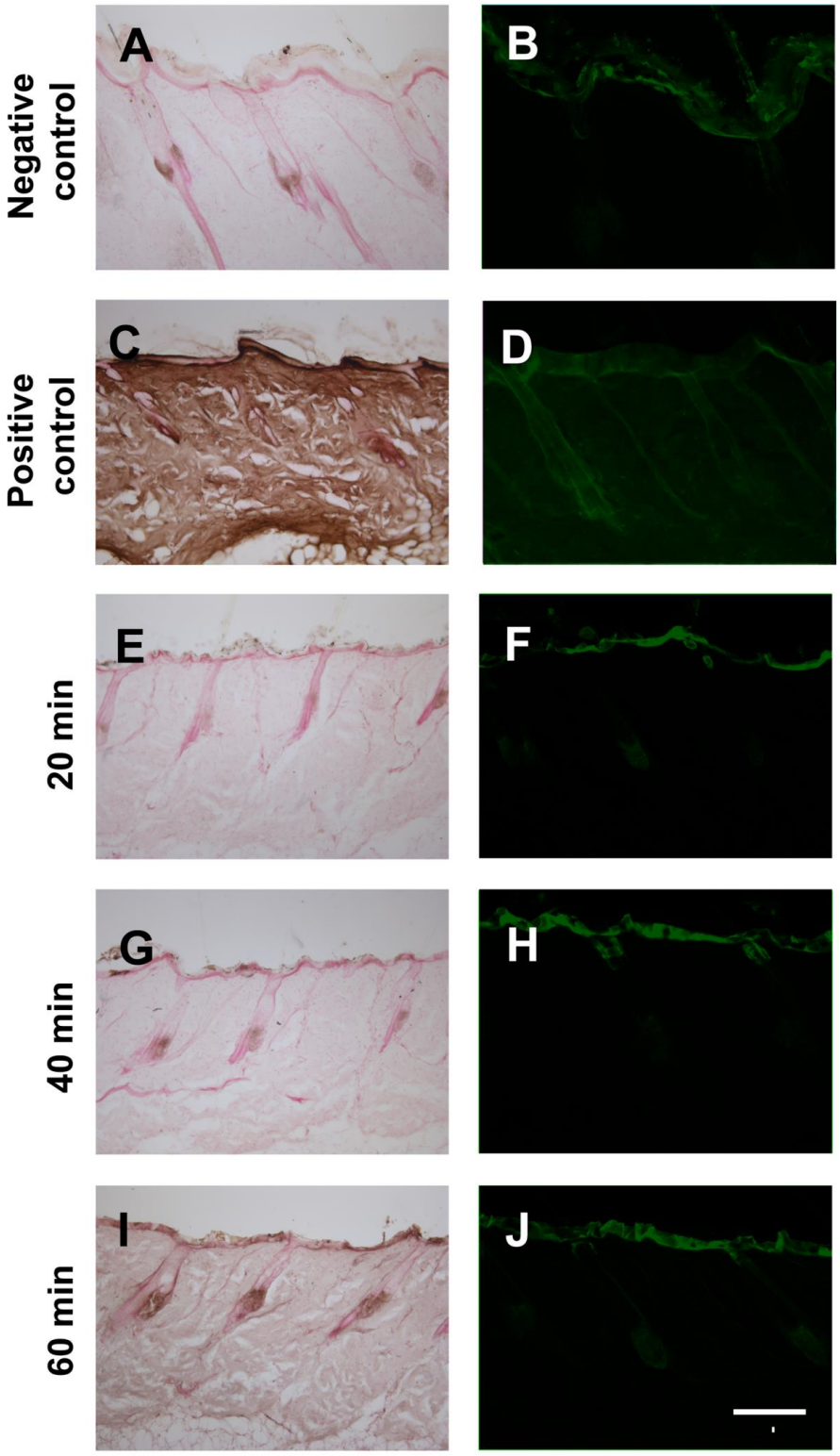
Negative control
A
B
Positive control
C
D
20 min
E
F
40 min
G
H
60 min
I
J

4.3.3 Topical application with cell penetrating peptides (HR9 peptide)

Cell penetrating peptides (also known as protein transduction domains), have been demonstrated to effectively deliver molecules into the skin through an as yet undetermined mechanism (Vasconcelos et al., 2013). To determine whether cell penetrating peptides could serve as carriers for MTII and EmtinB topically, the ability of the HR9 peptide to facilitate transport of MTII and EmtinB across rat skin was tested. HR9 peptide was chosen in favour of the well described cell penetrating peptide, TAT, for several reasons. MT-TAT fusion proteins have limited ability to cross lipid bilayers (Lim et al., 2010, Park et al., 2011). Furthermore, Liu and colleagues have reported that TAT-mediated uptake of HIV-1 virus via LRP1 inhibits binding, uptake and degradation of physiological ligands for LRP, including α2M, and thus may have off target effects (Liu et al., 2000b). The dorsal region of rats were treated with $1cm^2$ regions of biotinylated EmtinB or biotinylated MTII with either 1:3 (Fig 4.0-4.10) or 1:6 ratio (Fig 4.11-4.12) of protein:HR9, for 20, 40 or 60 minutes. Tissue was examined by light and fluorescent microscopy. Although this preparation was rapidly absorbed into the skin (15 minutes), the skin treated with all formulations resulted in fluorescence in the stratum corneum only. These results demonstrated that the HR9 protein carrier was unable to deliver EmtinB or MTII to the skin when combined non-covalently and applied for at least 60 minutes. Further work may be required trialling these protein carrier mixtures combined with penetration enhancers such as oleic acid.

Figure 4.9. MTII:HR9 (1:3) is not an effective after 1 hour of treatment

Representative images of dorsal skin **(A)** Injected with saline. Brown DAB indicating background levels of staining from endogenous biotins. **(B)** Injected with saline. Green fluorescence indicating background staining and autofluorescence of the stratum corneum. **(C)** Injected with 25uL bolus of 1mg/mL biotinylated EmtinB. Brown DAB indicating presence of excess exogenous biotinylated MTII. **(D)** Injected with 25uL bolus of 1mg/mL biotinylated EmtinB. Green fluorescent staining indicating background staining. **(E-J)** Biotinylated MTII:HR9 (1:3) applied topically in for **(E-F)** 20 minutes **(G-H)** 40 minutes and **(I-J)** 60 minutes. Crust of biotinylated EmtinB visualised on stratum corneum. Counter stain is Fast Red. Scale bar is 200um and applies to all images.

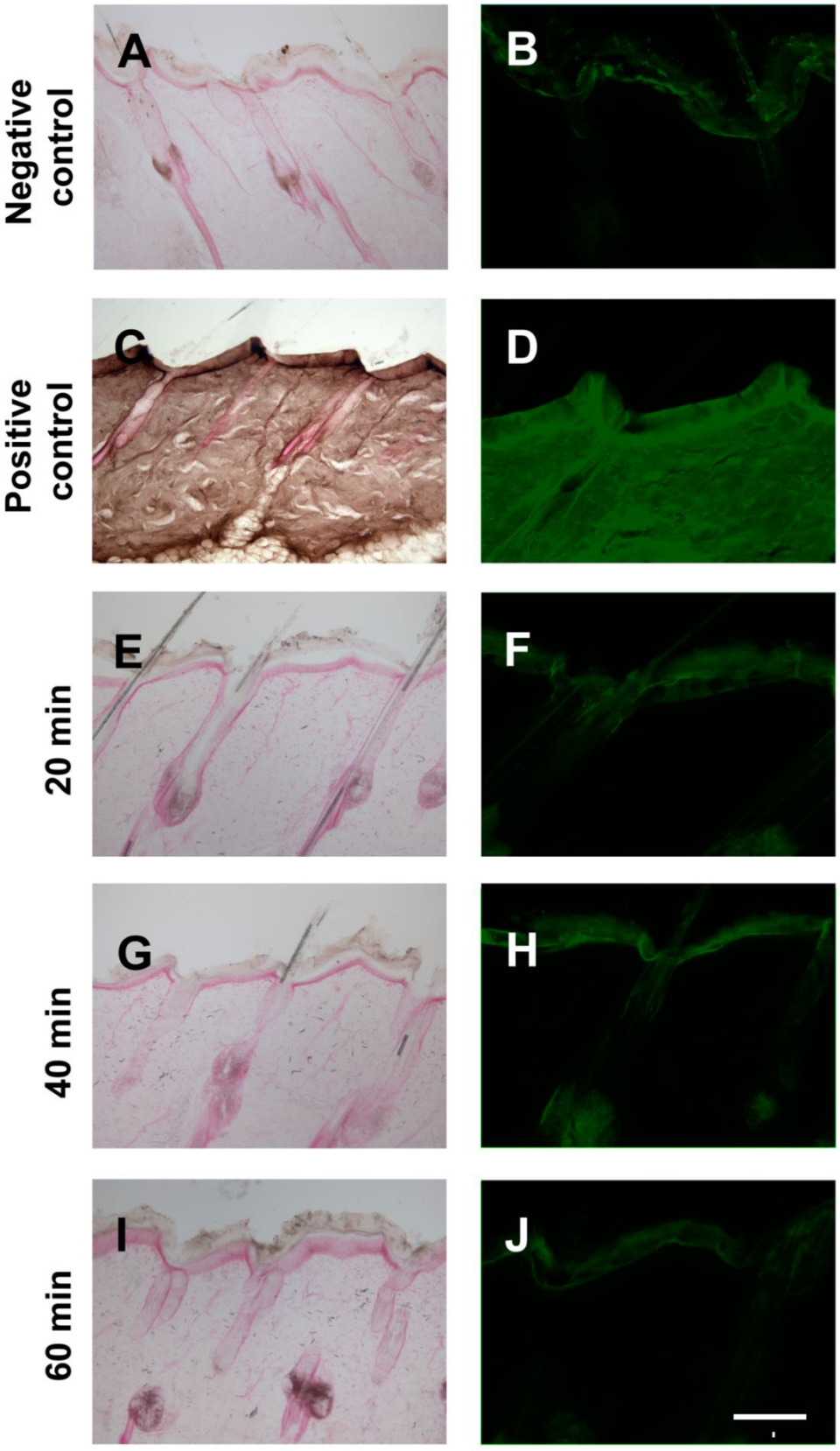
Negative control
A
B
Positive control
C
D
20 min
E
F
40 min
G
H
60 min
I
J

Figure 4.10. EmtinB:HR9 (1:3) is not an effective after 1 hour of treatment

Representative images of dorsal skin **(A)** Injected with saline. Brown DAB indicating background levels of staining from endogenous biotins. **(B)** Injected with saline. Green fluorescence indicating background staining and autofluorescence of the stratum corneum. **(C)** Injected with 25uL bolus of 1mg/mL biotinylated EmtinB. Brown DAB indicating presence of excess exogenous biotinylated MTII. **(D)** Injected with 25uL bolus of 1mg/mL biotinylated EmtinB. Green fluorescent staining indicating background staining. **(E-J)** Biotinylated EmtinB:HR9 (1:3) applied topically in for **(E-F)** 20 minutes **(G-H)** 40 minutes and **(I-J)** 60 minutes. Crust of biotinylated EmtinB visualised on stratum corneum. Counter stain is Fast Red. Scale bar is 200um and applies to all images.

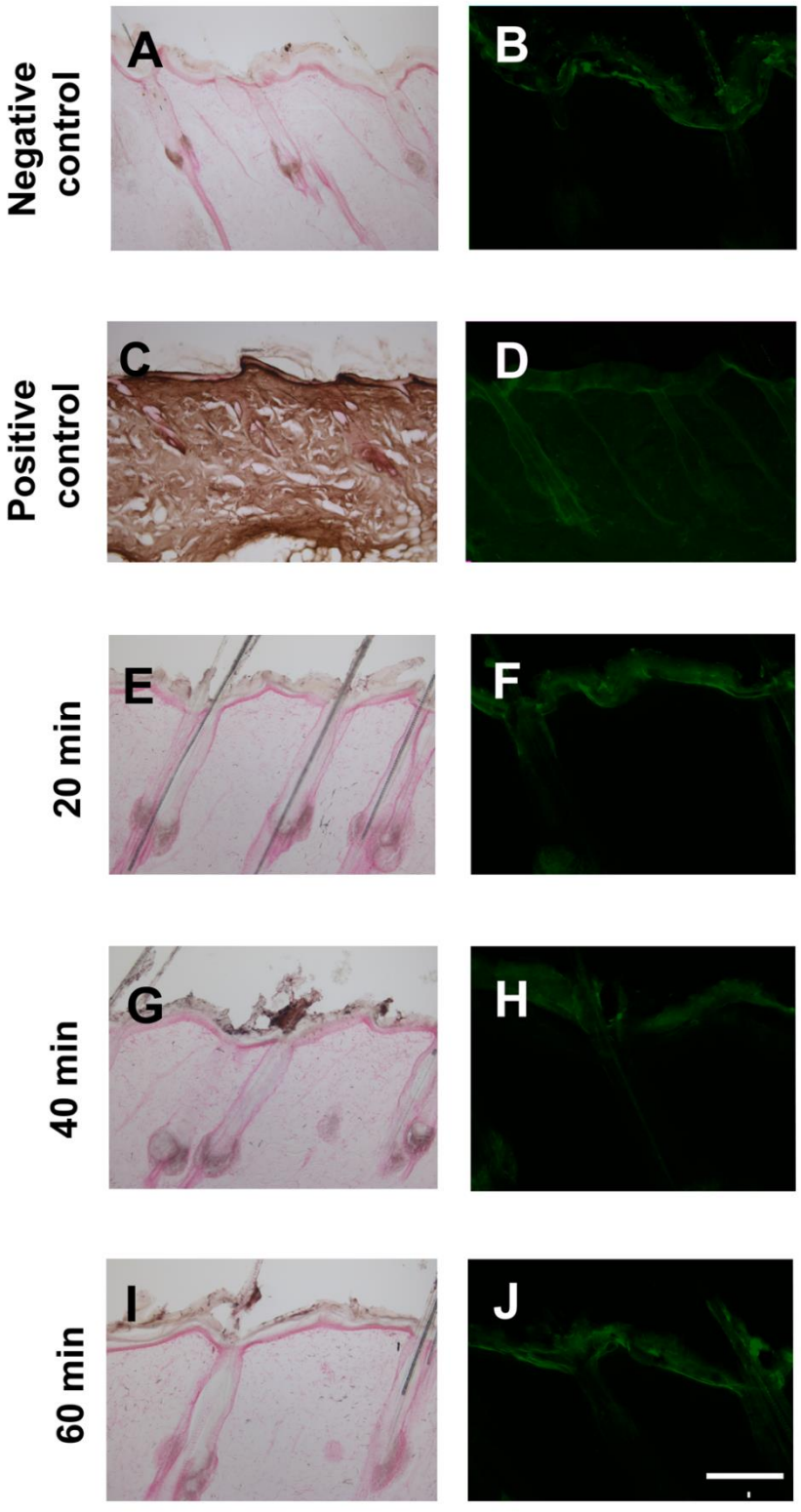
Negative control
A
B
Positive control
C
D
20 min
E
F
40 min
G
H
60 min
I
J

Figure 4.11. MTII:HR9 (1:6) is not an effective after 1 hour of treatment

Representative images of dorsal skin **(A)** Injected with saline. Brown DAB indicating background levels of staining from endogenous biotins. **(B)** Injected with saline. Green fluorescence indicating background staining and autofluorescence of the stratum corneum. **(C)** Injected with 25uL bolus of 1mg/mL biotinylated EmtinB. Brown DAB indicating presence of excess exogenous biotinylated MTII. **(D)** Injected with 25uL bolus of 1mg/mL biotinylated EmtinB. Green fluorescent staining indicating background staining. **(E-J)** Biotinylated MTII:HR9 (1:6) applied topically in for **(E-F)** 20 minutes **(G-H)** 40 minutes and **(I-J)** 60 minutes. Crust of biotinylated EmtinB visualised on stratum corneum. Counter stain is Fast Red. Scale bar is 200um and applies to all images.

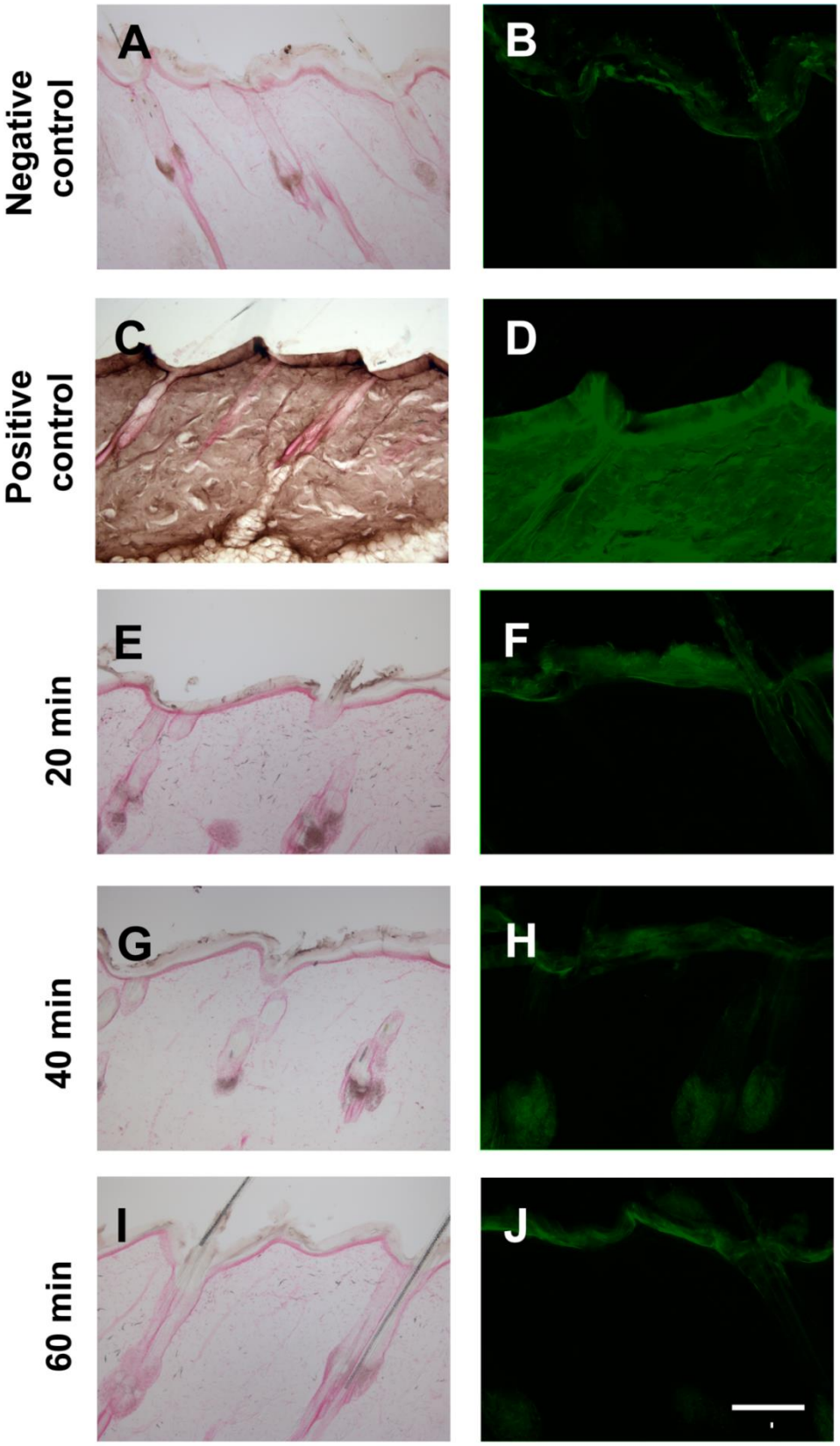
Negative control
Positive control
20 min
40 min
60 min
A
B
C
D
E
F
G
H
I
J

Figure 4.12. EmtinB:HR9 (1:6) is not an effective after 1 hour of treatment

Representative images of dorsal skin **(A)** Injected with saline. Brown DAB indicating background levels of staining from endogenous biotins. **(B)** Injected with saline. Green fluorescence indicating background staining and autofluorescence of the stratum corneum. **(C)** Injected with 25uL bolus of 1mg/mL biotinylated EmtinB. Brown DAB indicating presence of excess exogenous biotinylated MTII. **(D)** Injected with 25uL bolus of 1mg/mL biotinylated EmtinB. Green fluorescent staining indicating background staining. **(E-J)** Biotinylated EmtinB:HR9 (1:6) applied topically in for **(E-F)** 20 minutes **(G-H)** 40 minutes and **(I-J)** 60 minutes. Crust of biotinylated EmtinB visualised on stratum corneum. Counter stain is Fast Red. Scale bar is 200um and applies to all images.

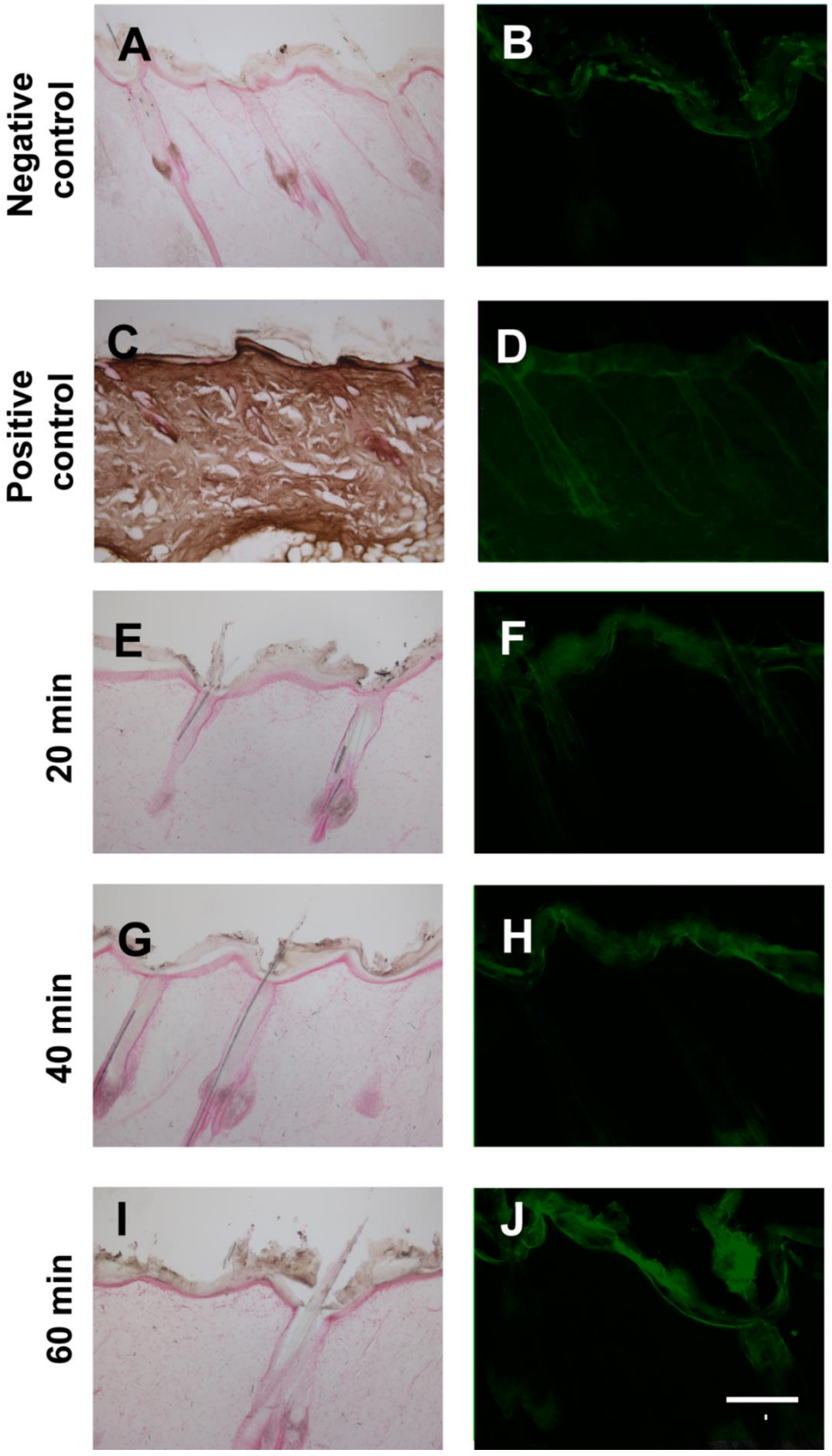
Negative control
A
B
Positive control
C
D
20 min
E
F
40 min
G
H
60 min
I
J

4.3.4 Iontophoresis

Iontophoresis provides an electrical force for transport of charged molecules through the stratum corneum into the underlying epidermis and dermis, and is used experimentally and clinically to treat a number of indications. For example, in 1995 iontophoresis of Lidocaine/epinephrine (Iontocaine®) for local dermal analgesia was patented (Prausnitz and Langer, 2008). The objective of this experiment was to determine the efficacy of iontophoretic transfer of biotinylated MTII into rat skin.

Iontophoresis of the rat dorsum was well tolerated, with no sign of irritation or erythema observed after applying the iontophoretic well. Anodal and cathodal iontophoresis was applied for 10 or 20 minutes, with 1x20 second 100mV pulse per minute (Fig 4.14). Given that MTII has 8 positively charged amino acid residues (Arg + Lys), and contains 4 negatively charged residues (Asp + Glu) within the core of the proteins secondary structure, the overall charge of MTII is positive. However, MTII has a net negative charge when bound to zinc ions, due to ionisation of cysteine residues. Given that net charge of MTII can vary according to metallation status and pH, both anodic and cathodic iontophoresis was examined. No clear evidence of biotinylated MTII delivery into in the skin was observed, with positive staining for biotinylated MT both absent from the dermis and lower epidermis, and only observed as a film on the surface of the stratum corneum.

Figure 4.13. Iontophoresis is unable to deliver biotinylated MTII into the skin at the parameters tested.

Representative images of dorsal skin treated with iontophoretic delivery of biotinylated MTII in 0.9% saline. **(A)** Cathodic delivery of MTII, performed with 10x 100V pulses, each of 20 second duration, over 10 minutes. **(B)** Cathodic delivery of MTII, performed with 20x 100V pulses, each of 20 second duration, over 10 minutes. **(C)** Anode delivery of MTII, performed with 10x 100V pulses, each of 20 second duration, over 10 minutes **(D)** Anodic delivery of MTII, performed with 20x 100V pulses, each of 20 second duration, over 10 minutes. Counter stain is Fast Red. Scale bar is 200µm and applies to all images.

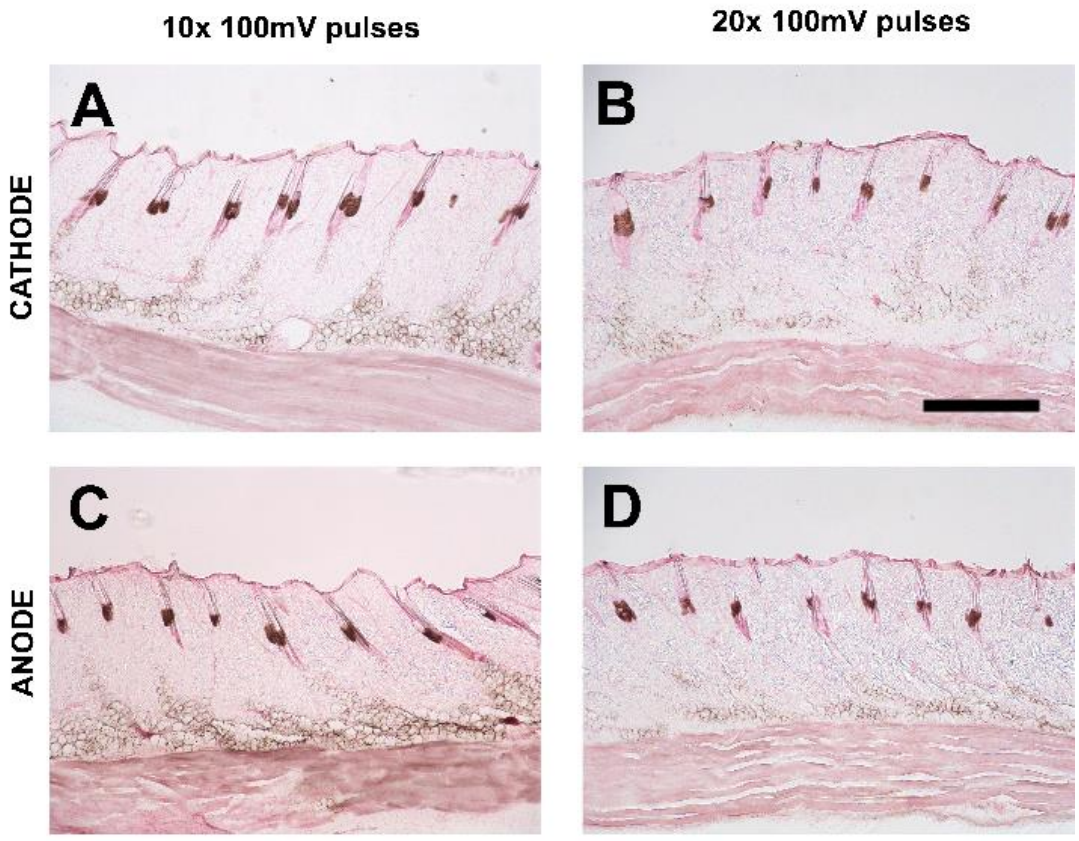
10x 100mV pulses
20x 100mV pulses
A
B
C
D
CATHODE
ANODE

4.3.5 Intradermal injection

Given the failure or unsuitability of the other approaches trialled, intradermal injection was investigated in more detail. India ink was injected intradermally to visualise the spread of an injection bolus. All injections raised a small lump, but this lump appeared to be absorbed into the surrounding tissue within 40 minutes. India ink was clearly observed macroscopically and measured with a ruler. A 25µl injection of india ink formed an initial bolus of 3 mm diameter. 30 min later, the bolus spread 5 mm. A 50µl injection had an initial bolus of 5mm, which spread to a diameter of ~8mm 30 minutes later. However, this diameter was irregular. 75µl bolus created a large amount of tissue distortion, raising a large, hard greyish lump that was likely impeding vascular flow to the area, and was therefore deemed unsuitable and not investigated any further. Given the greater predictability of spread for a 25µl bolus, and the likelihood of this volume causing the least tissue disruption, this volume was used for further investigations (summarised in Table 4.2).

Table 4.2. Visualised spread of india ink intradermal injection

Bolus volume	Initial diameter when injected intradermally (mm)	Diameter 30 minutes after injection (mm)
25µl	3	5
50µl	5	7-9 (irregular)
75µl	9 Bolus created large, hard lump	

4.4 DISCUSSION

The primary objective of this chapter was to develop a reproducible method of topical MTII and EmtinB delivery into the epidermis and underlying dermis of experimental animals, such that a concentration gradient forms from the outer to the deeper layers of the skin. Methods examined included topical administration, including the use of penetration enhancers such as carrier peptides; Iontophoresis; and finally, direct intradermal injection. The latter method provided the only robust and reproducible technique for administering MTII and EmtinB, although the potential exists for further optimisation of the other techniques.

The results demonstrate that all the topical approaches trialled were ineffective at transdermal delivery of MTII and EmtinB into the epidermis and underlying dermis, at the timepoints and concentrations tested. Lipophilic molecules have significantly higher success through transdermal drug delivery approaches, due to the nature of skin itself being lipid rich and having hydrophobic properties (Benson, 2005). The grand average of hydropathicity (GRAVY) index indicates solubility of a protein, where a positive index indicates that the protein is hydrophilic, and a negative indicating hydrophobicity (or lipophilic nature) (Gasteiger et al., 2005). MTII has a GRAVY index of 0.131, meaning it is hydrophilic and therefore less amenable to transdermal delivery approaches (Gasteiger et al., 2005). The physicochemical properties of EmtinB have not been fully investigated, and therefore elude further comment.

Multiple preparations with and without chemical enhancers were used in an attempt to deliver MTII into the skin. Carrier peptides have been previously established to deliver proteins into the skin rapidly (within minutes). The archetypal cell penetrating peptide, TAT, derived from HIV-1 virus, is widely exploited experimentally for its cell penetrating properties, but as it is known to reduce binding of LRP1 ligands it was not an appropriate candidate for MTII (Liu et al., 2000b). Unexpectedly, the use of carrier peptides did not prove effective at delivering MTII or EmtinB transdermally, despite brisk absorption of the bulk of the preparation into the skin. It has been previously demonstrated that the carrier peptide used in this study, histidine-rich nona-arginine (HR9), was able to deliver green fluorescent protein (GFP) into human cells with high efficacy *in vitro* (Liu et al., 2011, Liu et al., 2012), with similar peptides of even lesser efficacy tested in this *in vitro* approach (serine-rich nona-arginine) being able to deliver GFP into mouse skin *in vivo* (Hou et al., 2007). Given that MTII is a quarter of the size of GFP (Yang et al., 1996), one might have predicted a much higher success rate at transdermal delivery using this technique. However, it must be noted that GFP is hydrophobic (Yang et al., 1996), whereas, MTII is hydrophilic: this may be sufficient to cause the discrepancy between transdermal delivery successes.

Iontophoresis is a non-invasive approach with the particular advantage of allowing the delivery of hydrophilic and charged drugs into the skin to be adjusted in real time. Although the charge of MTII can vary depending on pH and metallation state, it is likely that MTII has a negative charge overall. Negatively charged MTII may be repelled into the skin under the direct influence of the electric field of the cathode, or alternatively may be carried in solution with positively charged molecules at the anode, in a process called electro-osmosis. The

hydrophilic nature of MTII was likely sufficient in preventing the anode from effective transdermal delivery of MTII during Iontophoresis. Iontophoresis may be affected by many factors, including the pH of the solution, skin temperature, physicochemical properties of the compound delivered (and its formulation), and the current strength (Dixit et al., 2007). Only two sets of parameters were tested in this study and perhaps other permutations of voltage and time may have been successful at delivering MT or EmtinB into the epidermis.

An important consideration regarding all transdermal drug delivery assessment is that the clearance of some molecules from the dermis may be rapid (Roustit et al., 2009), whereas others may remain for several days (Siddoju et al., 2011), and the speed at which clearance occurs is likely a function of blood flow and activity. Therefore, it is possible that small amounts of MT or EmtinB entered the skin using the aforementioned approaches, but were cleared quickly (however the strong presence of MTII in the skin 60 minutes after intradermal injection, as seen in Fig 4.1 may suggest otherwise). Alternatively, immunohistochemical techniques used in this chapter may have insufficient sensitivity to detect very low concentrations of MTII or EmtinB.

The results demonstrate that all the non-invasive topical approaches trialled were ineffective at transdermal delivery of MTII and EmtinB into the epidermis and underlying dermis. However, intradermal injections were a reliable and robust approach, as they directly bypass the impervious stratum corneum and deliver a calculable set volume/concentration at the injection site. However, as this method mechanically perforates skin, it may cause pain and localised trauma, and may result in the formation of scar tissue. Of the approaches trialled,

intradermal injection is the most efficacious method for delivery of MTII and EmtinB into the superficial layers of the skin. Given the kinetics of diffusion of india ink from the injection site, it is likely that 25ul injections of MTII or EmtinB 1cm apart will result in blanket coverage of the area treated. Therefore, this will be the administration regime trialled in the investigations in the chapters to follow.

CHAPTER 5

Development and characterisation of *in vivo* nerve injury models: Capsaicin-induced nerve retraction, diabetic neuropathy and focal denervation via blister formation

CHAPTER 5:

DEVELOPMENT AND CHARACTERISATION OF IN VIVO NERVE INJURY MODELS:, CAPSAICIN-INDUCED NERVE RETRACTION, DIABETIC NEUROPATHY AND FOCAL DENERVATION VIA BLISTER FORMATION.

5.1 INTRODUCTION

Injuries to peripheral nerves (neuropathy) may result in the loss of motor, sensory and autonomic functions, or development of debilitating neuropathic pain distal to the injury site (Woolf and Salter, 2000). These symptoms persist, as nerve regeneration after injury is often poor, absent, or aberrant (Flores et al., 2000). Accurate nerve regeneration relies on directed guidance of regrowing axons to restore these connections (Alto et al., 2009). In chapter 2 and 3, I demonstrated that the MTII-LRP signalling system is able to induce peripheral sensory neurite chemoattraction *in vitro.* In this chapter, I propose to extend this work and demonstrate that MTII is a therapeutic candidate to guide regenerating neurons and repair nerves in peripheral neuropathy and traumatic denervation *in vivo.*

The ultimate goal of this study is to establish the therapeutic value of MTII in diabetic peripheral neuropathy. Diabetic peripheral neuropathy is developed as sequelae of diabetes mellitus and currently has no cure. Resolution of the underlying disease (for example, by pancreatic islet transplant) has limited ability to reverse neuropathy in humans (Lee et al., 2005), despite promising results in streptozotocin (STZ) induced diabetic rat models (Remuzzi et al., 2009, Figliuzzi et al., 2013). Although the exact pathogenesis of diabetic neuropathy is yet to reach scientific consensus, oxidative stress, excessive formation of

advanced-glycation end-products (AGEs), and deregulation of trophic factors are well established co-contributors. Furthermore, zinc dysregulation and deficiency is strongly implicated in diabetes and diabetic complications (Miao et al., 2013). It has been proposed that targeting each of these individual pathogenic processes independently, is necessary to treat the disease (Farmer et al., 2012). The indications for MTII as a candidate therapeutic in diabetic neuropathy are multifaceted; the work described earlier in this thesis demonstrates the ability of MTII to guide neuronal growth, and in addition, MTII is known to be a powerful antioxidant, to have protective roles against the effects of AGEs, to be neuroprotective, promotes neurite outgrowth and has essential roles in intracellular trafficking of zinc *in vivo* (Lim et al., 2008, West et al., 2008). It has been reported that zinc has protective effects against the development of diabetic peripheral neuropathy in STZ-diabetic rats via upregulation of MT (Liu et al., 2014). Furthermore, MT and superoxide dismutase, when combined with cell penetrating peptides and delivered by intraperitoneal injection, delayed the development of diabetic neuropathy in Otsuka Long-Evans Tokushima fatty rats, a model of type 2 diabetes (Min et al., 2012). The current body of knowledge thus strongly supports the therapeutic value of MTII in neuropathy; in particular, diabetic neuropathy.

Normal skin is innervated by both unmyelinated and myelinated axons terminating in thermoreceptors, mechanoreceptors and nociceptors (Birder and Perl, 1994). Epidermal nerve fibres (ENFs) are primarily TRPV1+, unmyelinated C-fibres involved in thermal nociception, although lightly myelinated Aδ fibres are also present (Nolano et al., 1999, Malmberg et al., 2004). The cell bodies of these ENFs lie in the dorsal root ganglion. TRPV1 cation channel positive neurons are particularly susceptible to stress-induced damage in diabetes (Hong and

Wiley, 2005), therefore it is not surprising that in diabetic neuropathy, a histological hallmark is significant loss of ENFs (Facer et al., 2007). Damage to C-fibres is associated with the development of hyperalgesia, generalised pain and aberrant perception of temperature, whereas development of paresthesias (such as stabbing, burning or tingling sensations) and mechanical allodynia are largely associated with Aδ fibres (Tavee and Zhou, 2009). One approach to ameliorating these symptoms is to restore ENF density, which may be possible if a chemotactic substance is applied topically, causing a directed regeneration of nerve fibres back into the epidermis. However, this restoration of ENF density necessarily must be a tightly regulated process, as excess sprouting may result in hyperalgesia and/or allodynia (Taylor and Ribeiro-da-Silva, 2011).

In this chapter, the aim was to examine the efficacy of MTII as a therapeutic agent in neuropathy and denervation in three different models, with changes in ENF density measured as the primary outcome. The first model of nerve damage used chemically-induced denervation of the skin. Capsaicin is an agonist of TRPV1 cation channels, which are key mediators of pain in the C-fibre neurons which predominate within the epidermis (Caterina et al., 1997). Topical capsaicin treatment has been shown to cause a reversible retraction of TRPV1+ epidermal nerve fibres, which in humans regenerate after 50-100 days (Polydefkis et al., 2004, Anand and Bley, 2011). Capsaicin is used clinically to ablate nerves in an excitotoxic fashion, thus reducing symptomatic pain in conditions such as post-herpetic neuralgia (Wallace and Pappagallo, 2011). Topical capsaicin is also a validated experimental model of denervation (Rajan et al., 2003, Polydefkis et al., 2004, Ebenezer et al., 2011), that is highly reproducible and experimentally convenient model for screening the therapeutic effects of small molecules such as MTII.

The second model of nerve damage, diabetic neuropathy, is clinically relevant. Low-dose STZ-induced high-fat diet fed (HFD) rats are an experimental model of type 2 diabetes routinely used for testing anti diabetic agents (Reed, et al. 2000; Zhu, et al. 2010; Wang, et al. 2009; Zhang, et al. 2008; Gaikwad, et al. 2007; Ding, et al. 2005). STZ/HFD rats are ideal models because they develop complex pathophysiological sequelae that closely resemble symptoms of human disease, and include the common dietary confounder (a high fat diet). There is variability in the literature regarding the dose of STZ ("low dose" ranges between 20-50mg/kg), the percentage of calories from fat in the diet (40-50%), as well as the age and species of the rat to best induce this model of diabetes (Reed et al., 2000, Islam and Choi, 2007). Experience from collaborators at our institute suggests that in Sprague-Dawley rats, a dual injection of 50mg/kg STZ, combined with a 23% fat diet (44% of calories from fat), produces a reproducible model of type II diabetes (Zhang et al., 2008). The STZ/HFD model develops mechanical allodynia and has a substantial loss of ENF secondary to characteristic insulin resistance, hyperglycemia and dyslipidemia (Reed et al., 2000).

The final model is a novel technique that focally denervates the epidermis, by the formation of small blisters on the skin's surface. Blisters separate the epidermis from the dermis directly along the basement membrane, dividing the two regions (Nanchahal and Riches, 1982). Within this void between dermis and epidermis lie the severed end terminals of ENFs which initially retract and form regenerative growth cones. Theoretically, it would be plausible to inject MTII into the void and thus directly to the site of interest, thereby creating a concentration gradient that could direct growth cone navigation. Although the blister approach is not intended to be a viable drug delivery method in humans, it could serve as an

excellent “proof of concept” model for assessing the ability of MTII to direct the growth of growth cones on regenerating neurons *in vivo* (Fig 5.4)

The efficacy of MTII in ameliorating denervation was measured by histological characterisation of skin biopsies, a method commonly used to evaluate nerve pathology and regeneration in both the experimental and clinical setting. Punch biopsies allow for the evaluation of nerve branching, morphology, and density, as well as general skin architecture (Polydefkis et al., 2001). Blister biopsies are a relatively new technique that is used to visualise the length of ENFs, and can be used to evaluate ENF density with greater accuracy (Kennedy et al., 1999, Panoutsopoulou et al., 2009). This study focused on the distribution of neurons (stained by pan-neuronal marker, βIII-tubulin) in the rat PNS, and changes in peripheral nerve fibres in rats with diabetic neuropathy, or after capsaicin treatment. In the diabetic neuropathy model, a means of functional assessment was also established. Given that STZ/HFD model develops a widespread neuropathy, functional effects could be measured using well-validated plantar mechanical threshold tests. Von Frey monofilaments can be used to measure the “paw withdrawal threshold,” which is a measure of sensitivity to mechanical touch. This behavioural test is widely used as a physiological measure of nerve sensation (Weinstein, 1993, Boric et al., 2013), and was used to assess whether there are changes in nerve sensation, such as development of mechanical allodynia, or as a result of nerve regeneration. The data in this chapter provide support for the hypothesis that the MTII-LRP chemotactic signalling system has therapeutic benefit in neuropathies *in vivo.*

5.2 METHODS

5.2.1 Disclosure

All rat procedures were conducted with the approval of the University of Tasmania Animal Ethics Committee (approval numbers #A13109 and #A11302), and are compliant with the Australian NHMRC Code of Practise for the Care and Use of Animals for Scientific Purposes. Rats were supplied water, food *ad libitum*, were in a temperature controlled environment (22°) and had a 12 h light/dark cycle.

5.2.2 Diet

Male Sprague Dawley rats (6 weeks of age) were obtained from the Monash University Animal Services, Victoria. On arrival, the rats were allowed to acclimatise for a week, and were maintained on either a normal diet (ND; 4.8% fat wt./wt., 12% calories from fat; Gibsons, Hobart, TAS, Australia) or, where specified, switched to a high fat diet (HFD; 23% fat wt./wt., 44% calories from fat, SF01-025; Specialty Feeds, Glen Forrest, WA, Australia) for the duration of the study.

Table 5.1 Macronutrient composition of the Normal diet (ND) and high fat diet (HFD) as wt./wt

	Normal diet (ND)	**High fat diet (HFD)**
Total Fat (%)	4.80	22.30
Protein (%)	20.00	19.40
Crude Fibre (%)	4.80	5.30
Digestible Energy (MJ / Kg)	14	18.5
Total calculated digestible energy from lipids (%)	12.00	44.00

5.2.3 Synthesis of 8% w/w capsaicin cream and control cream

Capsaicin was formulated as an 8% cream. Capsaicin powder (Sigma-Aldrich, MO, USA) was weighed and dissolved in a nominal volume of ethanol (0.1%w/w). Emulsifying ointment B.P. (BiotechPharm QLD, AUS) was gently warmed to a temperature of ~35 degrees until liquid consistency was reached. Liquid emulsion was added drop by drop to the capsaicin solution until the correct final weight was reached. The emulsion was carefully agitated until fully combined. Due to quick solidification of the emulsion, continued heating during this process is required. Control cream was produced the same way; however capsaicin was omitted and only 0.1%w/w ethanol added. The cream was stored at room temperature.

5.2.4 Induction of capsaicin-induced denervation

Rats were anaesthetised and skin was prepared as outlined in chapter 4 section 4.2.3.

1 x 6cm rectangles, separated by 1.5cm were demarcated either side along the rat lumbo-sacral dorsum using a permanent marker, overlaid by ordinary marker. Capsaicin cream was applied with a cotton swab to the left hand side, liberally, within the demarcated area, taking care to apply cream right to the boundaries. Control cream was applied in the same manner to the right hand side. After 60 minutes, the creams were gently scraped off using cartridge paper, scraping in towards the centre of the demarcated area so as not to spread the cream. Owing to the use of an ordinary marker overlay which coloured the lipophilic emulsion at the boundaries, the extent of feathering/spread of the cream could be seen and accounted for (this was nominal, less than 1mm). The lipophilic cream was then progressively removed using several fresh alcohol wipes. This removal process was done with great care to ensure no residual capsaicin remained on the skin which the rat may otherwise ingest during routine grooming. The demarcated area was re-drawn with permanent marker, and rats were withdrawn from anaesthesia and allowed to recover.

Figure 5.1 An overview of the procedures for the capsaicin-induced denervation model

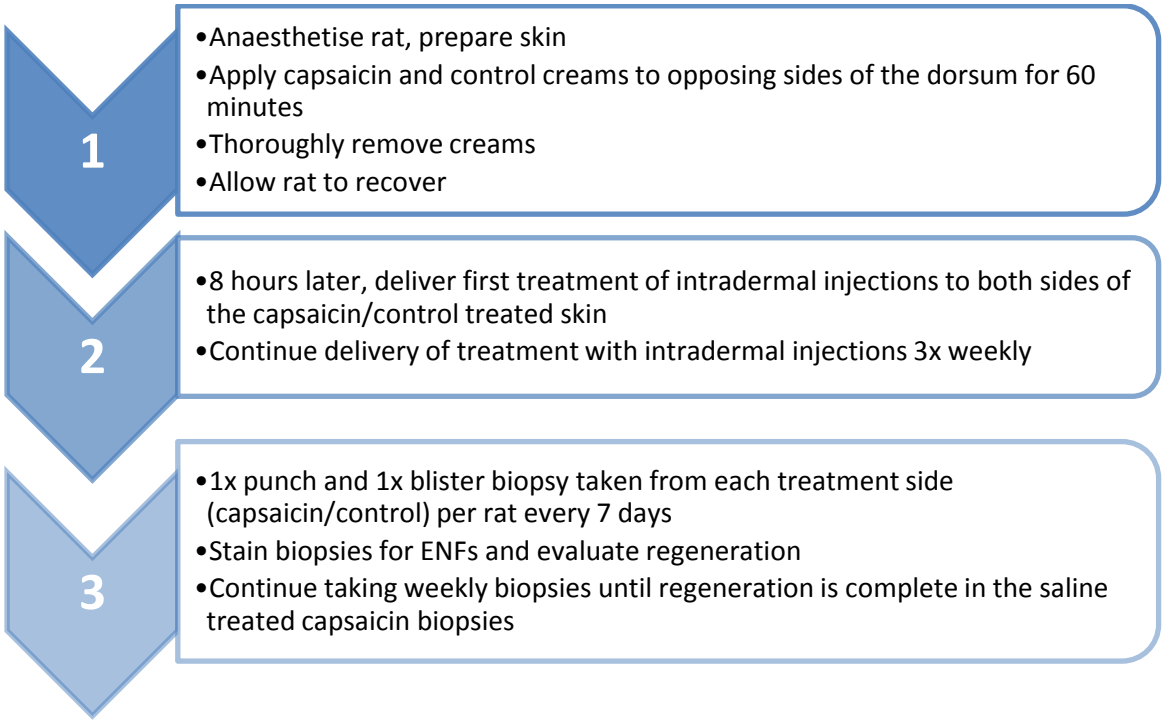

5.2.5 Treatment of capsaicin-denervated skin with MTII or saline

A cohort of 12 8-week old rats (approximately 500g) were divided into two groups, with 6 being allocated to the saline treatment group, and 6 to the MTII treatment group. Rats were anaesthetised, placed in the prone position on a heated pad (37°C), and maintained under (2-3.5%) isofluorane inhalation, and shaved to expose the demarcated area (if required). Skin was cleansed with an isopropanol wipe. Rats were injected with a total of 500µL 0.3mg/mL MTII (Zn_7 form, Bestenbalt LCC, Tallinn, Estonia), or 0.9% normal saline on *both* the control cream and capsaicin treated regions of the dorsum (i.e. 250µL per side). For an overview of treatment, see Fig 5.1. Injections sites were transiently visible, allowing 12 equally spaced intradermal injections (approximate volume 20uL) to be given on each side to

each rat (Figure 5.3; Injections were performed three times weekly, for four weeks. The first injections were given 8 hours after capsaicin treatment.

Figure 5.2 Example of treated skin immediately after intradermal injections

5.2.6 Biopsies for histological evaluation of capsaicin-denervation model

Biopsies were taken from both sides from each rat every 7 days for a total of 28 days or until regeneration is complete. Both a blister biopsy and a punch biopsy were taken from either side. Punch biopsies were taken as per section 5.2.7. Blister biopsies were also taken, but not evaluated due to time constraints.

5.2.7 Punch biopsy

Rats were anaesthetised and skin was prepared as outlined in chapter 4 section 4.2.3. Punch biopsies were taken by applying a sterile 3mm biopsy punch to the skin surface and rotating until the resistance of the skin was lost (indicating the punch had reached the hypodermis). The punch biopsy was then removed with forceps, gently severing the connective tissue, and

placed into Zambonis fixative immediately for a minimum of 2 hours and maximum of 5 hours. Biopsies were washed in a fume hood using PBS, until the solution ran clear. Biopsies were then placed in 30% sucrose until processed.

5.2.8 Induction of STZ/HFD diabetic model

20 Sprague Dawley rats, (6-weeks old, approximately 250g), were randomly divided into four groups: 1) Control/saline group (CTRL/SAL; No STZ/HFD, saline injections), 2) Diabetic/saline group (DB/SAL; STZ/HFD, saline injections), 3) Diabetic/MTII group (DB/MTII; STZ/HFD, MTII injections), and 4) Diabetic/EmtinB group (DB/EmB; STZ/HFD, EmtinB injections). The control group was fed with ND, and the other four groups were given HFD. After two weeks, STZ or control injections were given. Following a 6 hour fast, rats were individually weighed, then induced under isofluorane anaesthesia, and placed in the prone position. Tail vein blood was extracted using a 1mL syringe and 18-gauge needle, with blood glucose measured immediately using Accu-chek Performa blood glucose strips and testing device (Roche, NSW, Australia). The remaining blood was refrigerated. Rats in DB/SAL, DB/MTII, DB/EmB groups were injected intraperitoneally with 50mg/kg STZ (Sigma-Aldrich, MO, USA) in citrate buffer (0.9mg/mL saline, buffered with citric acid to pH 4.5, all from Sigma-Aldrich, MO, USA). Rats in CTRL/SAL group were injected with citrate buffer only. Rats were allowed to recover. Blood samples were then spun in a centrifuge for 5 minutes at 15,000rpm, and the serum separated and stored at -80°C for insulin assays. A second STZ or control injection was given 3 days later using the same protocol. Top-up doses of STZ were given in the event that blood glucose levels returned to the normal range for two consecutive tests. The protocol for this model is outlined in Figure 5.3.

5.2.9 Treatment of diabetic neuropathy hindlimb with MTII, EmtinB or saline

Rats were anaesthetised, placed in the supine position on a heated pad (37°), and maintained under (2-3.5%) isofluorane inhalation. Breathing and responsiveness was monitored closely through the duration of the experiment and the percentage of isofluorane adjusted accordingly. The hindlimb (anatomical left) was shaved and intradermal injections were given. Rats were injected with a total of 500μL 0.3mg/mL MTII (DB/MTII group) or 0.9% normal saline (CTRL/SAL group or DB/SAL group) or 1mg/mL EmtinB (DB/EmB group Emtin B from Schafer N, Copenhagen, Denmark).

Figure 5.3 An overview of the procedures for the STZ/HFD diabetic model

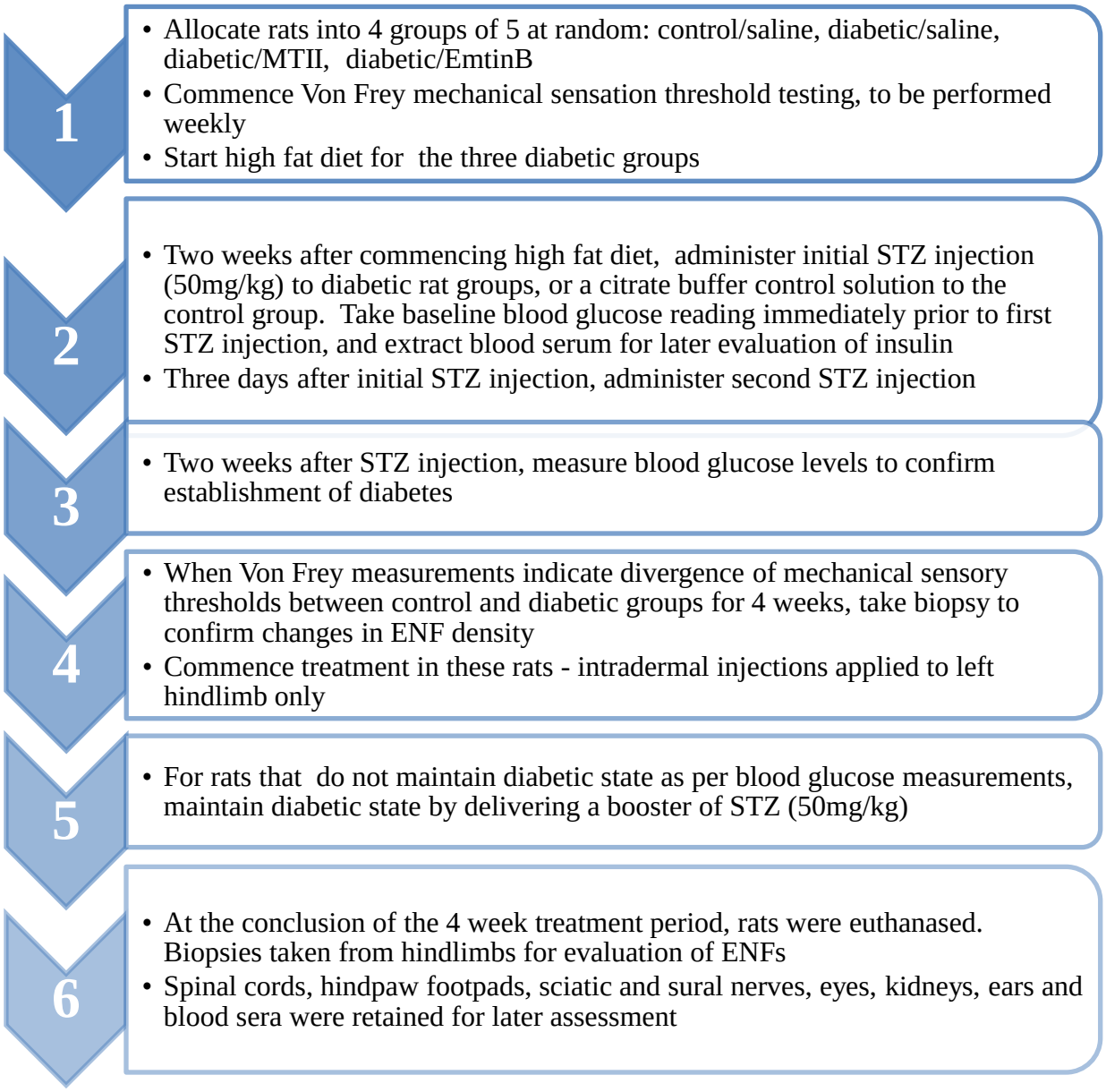

5.2.10 Blood glucose testing

Rats were subject to weekly blood glucose tests (performed concurrently with intradermal injections). Rats were tested prior to 10am in the morning to ensure they were not inadvertently in a fasting state. Rats were tested immediately after isofluorane induction so as not to allow anaesthesia to augment blood glucose. Tail vein blood was extracted by producing a shallow 5mm horizontal incision across the lower third of the tail, and then coaxed by applying pressure immediately proximal to the incision, until a droplet formed. Blood glucose measured immediately using Accu-chek Performa blood glucose strips and testing device (Roche, NSW, Australia).

5.2.11 Functional evaluation of sensory thresholds in the rat hindpaw in diabetic neuropathy model

Nerve sensory function (specifically, nociception) was assessed by analysing mechanical allodynia at weekly intervals, commencing prior to the first streptozotocin treatment (or the equal timepoint in control rats), and every week thereafter. The paw withdrawal threshold method was used, which is a non-noxious measure of sensitivity to touch, and can be used as a non-invasive measure of nerve sensibility (Weinstein, 1993). The tactile sensory response to mechanical stimuli was evaluated by stimulation of both hind paw plantar surfaces with a calibrated set of von Frey filaments (Stoelting Co., Wood Dale, IL). Briefly, animals were placed in individual perspex chambers with a wire mesh floor (JD Built Custom Scientific, TAS, AUS) for at least 15 minutes to acclimatise. Filaments were then applied to the bending point for 3 s, and brisk paw withdrawal was considered as a positive response. The response threshold was determined as the lowest force that provoked a minimum of 50% positive

retractions from a total of 20 stimulations per paw. To reduce variability, two training sessions were performed to acclimatise the animals to the procedure.

5.2.12 Punch biopsy immunostaining

Punch biopsies were processed and sectioned as outlined in chapter 4 section 4.2.19. Samples were permeabilised in 0.4% Triton-X in PBS for 4 hours, before being transferred to 5% goat serum in PBS blocking agent for 30 minutes. Samples were then incubated overnight at 4°C with primary antisera. Primary antisera included βIII-tubulin (mouse, 1:1000, Promega, WI, USA), CGRP (rabbit, 1:2000, Sigma), TRPV1 (goat, 1:5000, Santa Cruz Biotechnology, CA, USA). Controls for immunolabelling were performed by using untreated tissue, or by using the respective IgG control sera in place of the primary antibody. After washing three times in 0.5 M Tris buffer pH7.4 over 12 hours, the tissue were incubated with 4,6-diamidino-2-phenylindole (DAPI; 1:1000, Sigma-Aldrich, MO, USA) and the secondary antibody, fluorescent Alexa 594-conjugated goat anti mouse (1:1000, Molecular probes, OR, USA), in the dark, overnight at 4°C. Tissue sections were washed in Tris over 12 hours and allowed to dry, then mounted with DPX fluorescent mounting media (Koch-Light Laboratories, England, UK).

5.2.13 Image acquisition

Fluorescence images were acquired using Volocity software (Perkin Elmer, MA, USA) with a Nikon Eclipse T.I confocal microscope (Nikon, Tokyo, Japan), equipped with a x40 Plan Apo lens (Nikon, Tokyo, Japan). All images were captured with the same exposure and laser intensity at 40x magnification. Images were processed using Image J (NIH, MD, USA) and JASC Paint Shop Pro V 9.0 (JASC Software Inc., MN, USA).

Double immunostaining was used to localise the dermal/epidermal junction and ENFs in the same preparation. Two digital images were captured for each section, one corresponding to nuclear marker DAPI, and the other corresponding to nerves stained by pan-neuronal marker βIII-tubulin. DAPI staining was used to identify the epidermal/dermal junction due to a clear differentiation of cellular density.

5.2.14 Nerve density analysis

Quantification of nerve density of punch biopsy samples was performed using ImageJ (NIH, MD, USA). Biopsies were harvested as described previously (5.2.7) and sectioned at 50um. βIII-tubulin staining was performed as described in section 5.2.11. Blinded images of βIII-tubulin immunoreactivity across all treatment groups were acquired using a Nikon Eclipse T.I confocal microscope (Nikon, Tokyo, Japan), equipped with a 40x Plan Apo (Nikon, Tokyo, Japan) objective using identical acquisition settings (1sec). Images were not taken near hair follicles. Images of DAPI staining were acquired in parallel to βIII-tubulin immunoreactivity. All samples were evaluated blind. βIII-tubulin images were first background corrected using a 5-pixel rolling ball radius. In the DAPI image, a line was drawn 7um above the basement membrane of the epidermis, and then the image was changed to the βIII-tubulin channel. A plot profile of signal intensity along the line was acquired and transferred to an Excel spreadsheet. A threshold point was evaluated based on examination of several images, and was set as a pixel intensity of 30. Any signal intensity above the threshold indicated presence of a traversing immunoreactive nerve fibre. Given that width of immunoreactive nerve fibres were variable, positive threshold scores that occurred next to each other were measured as 1 immunopositive crossover (and thus one fibre) and were calculated per μm (immunoreactive crossovers/μm). If nerves overlapped each other and as

such were visualised as one immunoreactive point, these were adjusted for manually. A minimum of 5 fields of each sample, corresponding to 4 sections at various locations within the biopsy, were processed for quantification. Values were decoded by an independent evaluator and density of ENFs were compared between groups using the two-tailed Student's t test in GraphPad Prism (Lauria et al., 2005).

5.2.15 Induction of blisters

Rats were anaesthetised and skin was prepared as outlined in chapter 4 section 4.2.3. Blisters were produced by placing a 5mm suction cupule (JD Built Custom Scientific, TAS, AUS) on pre-prepared skin; the cupule was attached to a vacuum providing negative pressure of approximately 300 mmHg. After 40 minutes, a partially fluid-filled blister formed. This blister was injected via an indirect approach, inserting a 31G needle through adjacent skin and entering the blister void through the dermis underneath.

5.2.16 Blister injection

Blisters were raised as per section 5.2.15. 1mg/mL biotinylated-MTII was slowly injected into the void by inserting the needle in adjacent intact skin and delivering the needle tip into the blister. Due to the skin being glaborous, hair follicles anchored the blister roof to the underlying dermis; however these anchor points were lifted and formed open pores as the blister was injected and filled, and therefore needed to be sealed with surgical glue during the injection process to prevent the solution leaking out.

Figure 5.4. Proposed method for blister induced focal denervation experiment

A blister was raised on the skin's surface using a gentle vacuum to separate the tissue along the papillary junction between the dermis and epidermis, severing nerves and causing a fluid filled void to form (Nanchahal and Riches, 1982). Nerve endings should initially retract into the dermis. Growth cones are predicted to form at the nerve ends, and direct regenerative growth. By injecting a chemoattractant such as MTII into the blister void, it was hypothesised that regeneration would be directed towards the source of chemoattractant. Schematic shows approach required for injection, to prevent complete rupture of the delicate epidermal layer. Original figure.

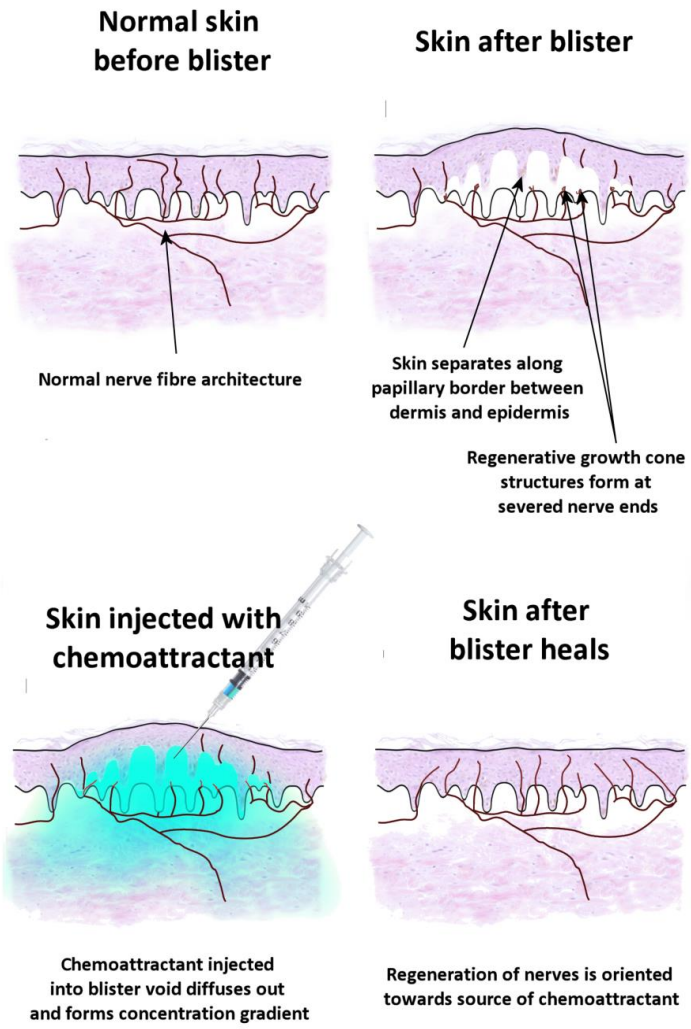

Injection method

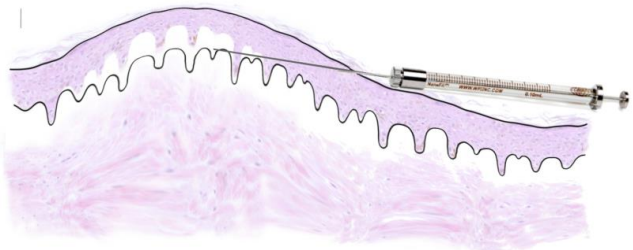

A 31 gauge needle was inserted into adjacent tissue and fluid was delivered from underneath the blister. Tissue was gently squeezed to deform the surface and allow for straight injection.

Figure 5.5 An overview of experimental procedures for focal denervation via blister formation

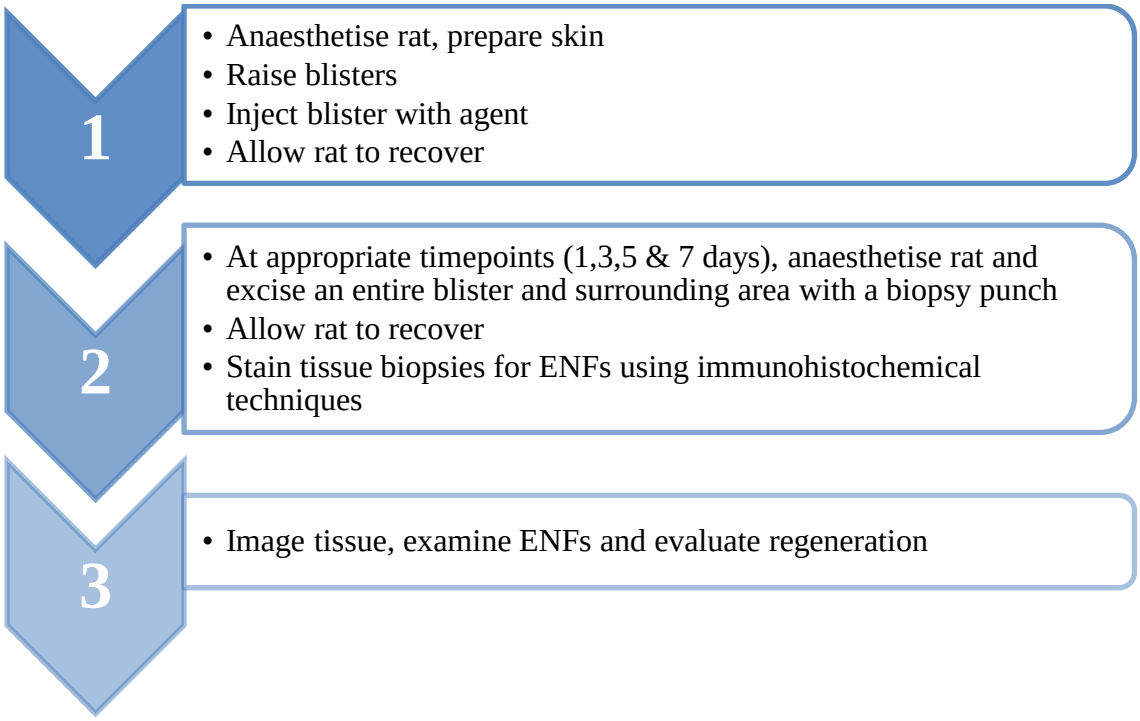

5.3 RESULTS

5.3.1 Capsaicin-induced chemical denervation

Capsaicin-induced denervation was used as a chemical model of denervation. The majority of ENFs are TRPV1+ neurons, which are susceptible to capsaicin (Nolano et al., 1999). However, an anti-TRPV1 antibody was not an appropriate antibody for the evaluation of ENF regeneration in this model, as TRPV1 is present in keratinocytes as well as ENFs and appeared to deliver non-specific high background staining (Fig 5.6 A-B). A pan neuronal marker was used in place of an anti-TRPV1 antibody. In humans, PGP9.5 is the standard pan-neuronal ENF marker to be used for ENF quantification (Lauria et al., 2010), however, PGP9.5 did not robustly stain ENFs in rat tissue (Fig 5.6). However, in healthy and diabetic patients, PGP9.5 and βIII-tubulin are reported to co-localise in ENFs (Lauria et al., 2003, Lauria et al., 2004); therefore βIII-tubulin was used in place of PGP9.5 and resulted in distinct and reliable staining (Fig 5.6). Anti βIII-tubulin was therefore used for the remainder of all *in vivo* experiments.

As the kinetics of capsaicin induced denervation in rats were untested using 8% capsaicin cream approach, firstly, the effect of applying capsaicin for different times (15, 30 and 60 minutes) was assessed. Qualitatively, it was very clear that 1 hour caused marked denervation, with 15 and 30 minutes not having as robust a result (Fig 5.7; E-F compared to A-D). Therefore, 1 hour capsaicin application was used in further experiments.

Weekly biopsies were harvested in order to assess the effect of MTII on ENF regeneration post capsaicin-induced denervation. Although TRPV1+ neurons do not comprise all ENFs,

and capsaicin specifically causes retraction of TRPV1+ ENFs, a robust and significant denervation (62%, $p<0.05$) was still observed using a pan neuronal marker, 7 days after capsaicin treatment (48.4 ± 1.5 ENFs/mm in control tissue compared to 18.4±3.8 ENFs/mm in capsaicin treated tissue, Fig 5.8).

Surprisingly, by 14 days, complete regeneration in saline-treated capsaicin tissue had occurred. Saline-treated capsaicin treated skin had an ENF density of 42.1 ± 4.0 ENFs/mm, compared to saline treated control skin 49.6 ± 1.5 ENFs/mm (Fig 5.9). In contrast, in the presence of an intradermal injection of MTII, caused complete regeneration in just 7 days (Fig 5.8). As this was a pilot study, with no previous data available to perform a power calculation, it was unknown whether this number of animals would be sufficient to generate statistical significance. However, there was a significant difference between capsaicin denervated skin treated with saline vs MTII ($p<0.02$). Capsaicin denervated skin treated with MTII had an average ENF density of 45.0 ± 4.9 ENFs/mm, compared to control skin treated with saline, which had a density 48.4 ± 1.5 ENFs/mm. These results demonstrate the potent effect of MTII in chemical induced denervation. Qualitatively, there appeared to be a modest increase in branching of ENFs in response to MTII in control tissue, however this requires further validation.

Figure 5.6 βIII-Tubulin is a robust marker for ENFs.

Representative images of punch biopsies taken from dorsal rat skin. Dotted lines indicate demarcation of viable epidermis (E) and dermis (D). In some cases, non-viable epidermis (stratum corneum) is visible above the epidermis, which is autofluorescent. **(A-B)** Images demonstrate nonspecific staining by pan neuronal marker, anti-PGP9.5 antibody. **(C-D)** Images demonstrate staining by anti-TRPV1 antibody. **(E-F)** Nerves are stained robustly with pan-neuronal marker βIII-tubulin. **(G)** Omission of primary antibody demonstrates specificity of the secondary antibody **(H)** Mouse IgG1 control indicates non-specific blinding attributed to mouse IgG1 in βIII-tubulin antibody. Background staining is localised to the stratum corneum.

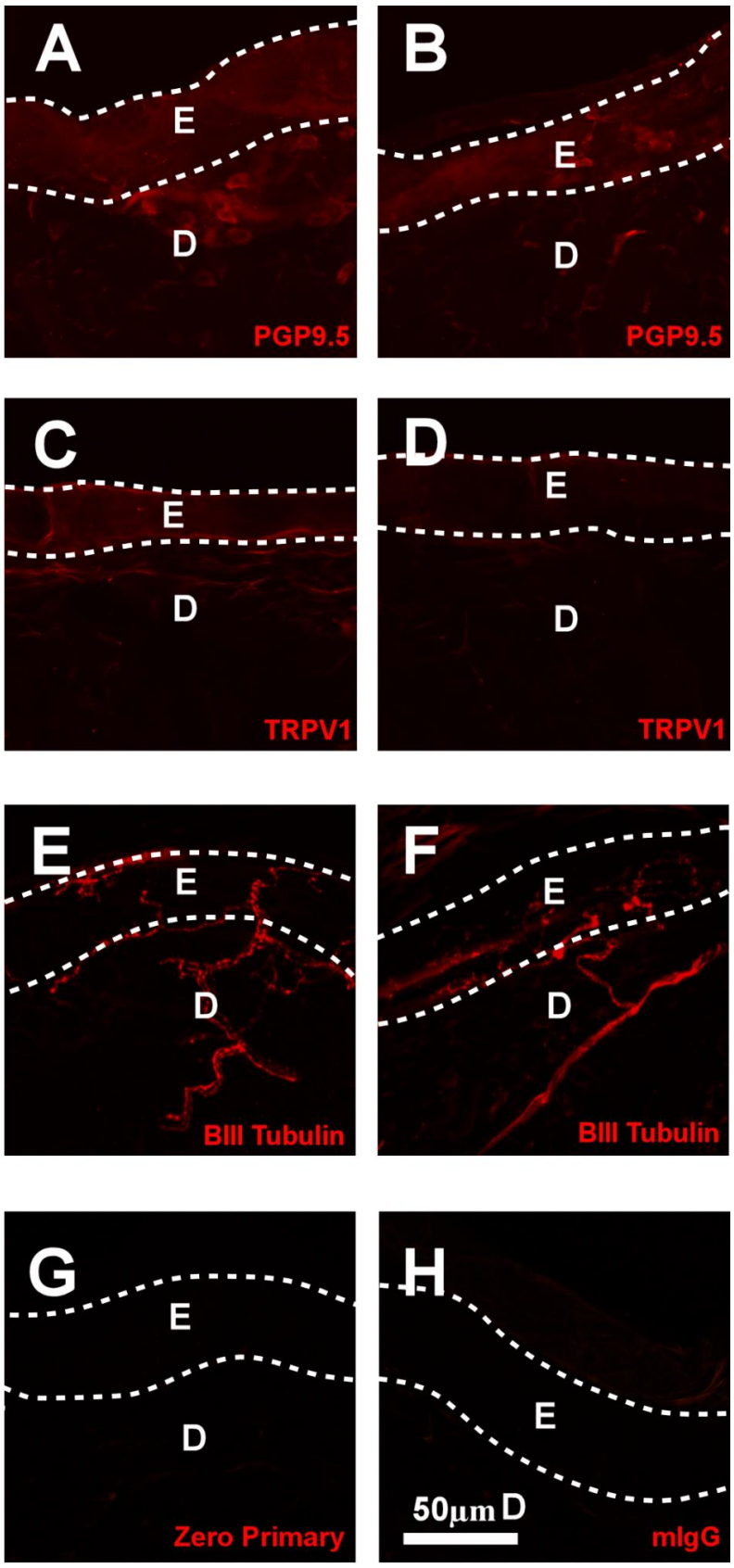
A
E
D
PGP9.5
B
E
D
PGP9.5
C
E
D
TRPV1
D
E
D
TRPV1
E
E
D
BIII Tubulin
F
E
D
BIII Tubulin
G
E
D
Zero Primary
H
E
50μm D
mIgG

Figure 5.7 Denervation observed after 15, 30 and 60 minute applications of 8% capsaicin

Representative images of punch biopsies taken 3 days after capsaicin application. Dotted lines indicate demarcation of viable epidermis (E) and dermis (D). In some cases, non-viable epidermis (stratum corneum) is visible above the epidermis. Nerves are stained with pan-neuronal marker βIII-tubulin (red). **(A-B)** Images of skin treated with capsaicin for 15 minutes. **(C-D)** Images of skin treated with capsaicin for 30 minutes. **(E-F)** Images of skin treated with capsaicin for 60 minutes. Scale bar applies to all figures.

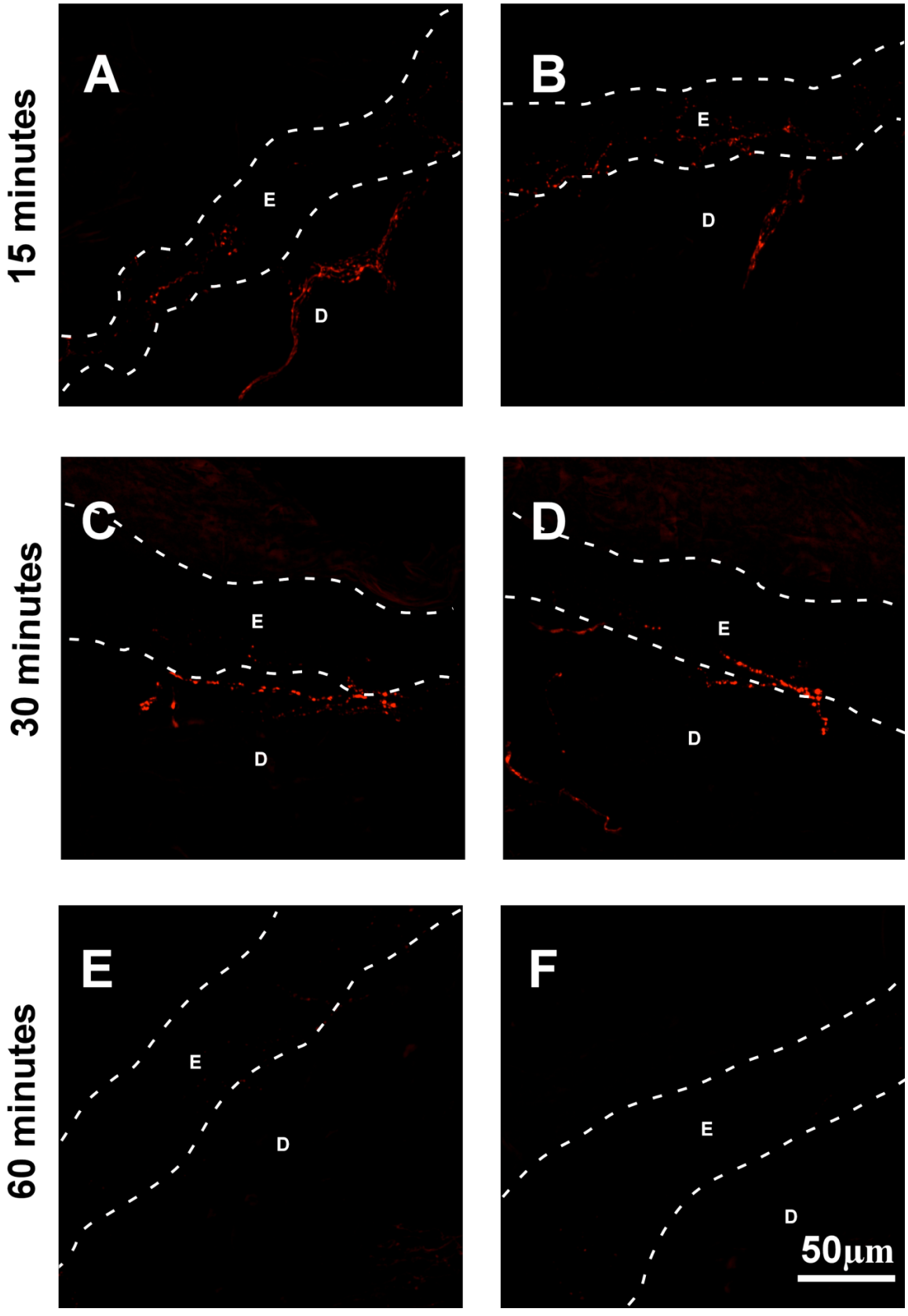
15 minutes
30 minutes
60 minutes
A
B
C
D
E
F
E
D
50µm

Figure 5.8 MTII rescues capsaicin induced denervation within 7 days

Representative images of ENFs in punch biopsies taken 14 days after capsaicin application. Dotted lines indicate demarcation of viable epidermis (E) and dermis (D). In some cases, autofluorescent non-viable epidermis is visible above the epidermis (stratum corneum). Nerves stained with pan-neuronal marker βIII-tubulin (red). **(A)** Image of control skin with saline injections, 7 days after control cream was applied. **(B)** Image of capsaicin denervated skin with saline injections, 7 days after capsaicin cream was applied. **(C)** Image of control skin treated with MTII injections, 7 days after control cream was applied. **(D)** Image of capsaicin denervated skin with MTII injections, 7 days after capsaicin cream was applied. **(E)** Graph showing quantification of nerve density, demonstrated by nerve fibre immunoreactivity per mm of epidermis.*P<0.05, **P<0.02. Scale bar applies to all figures.

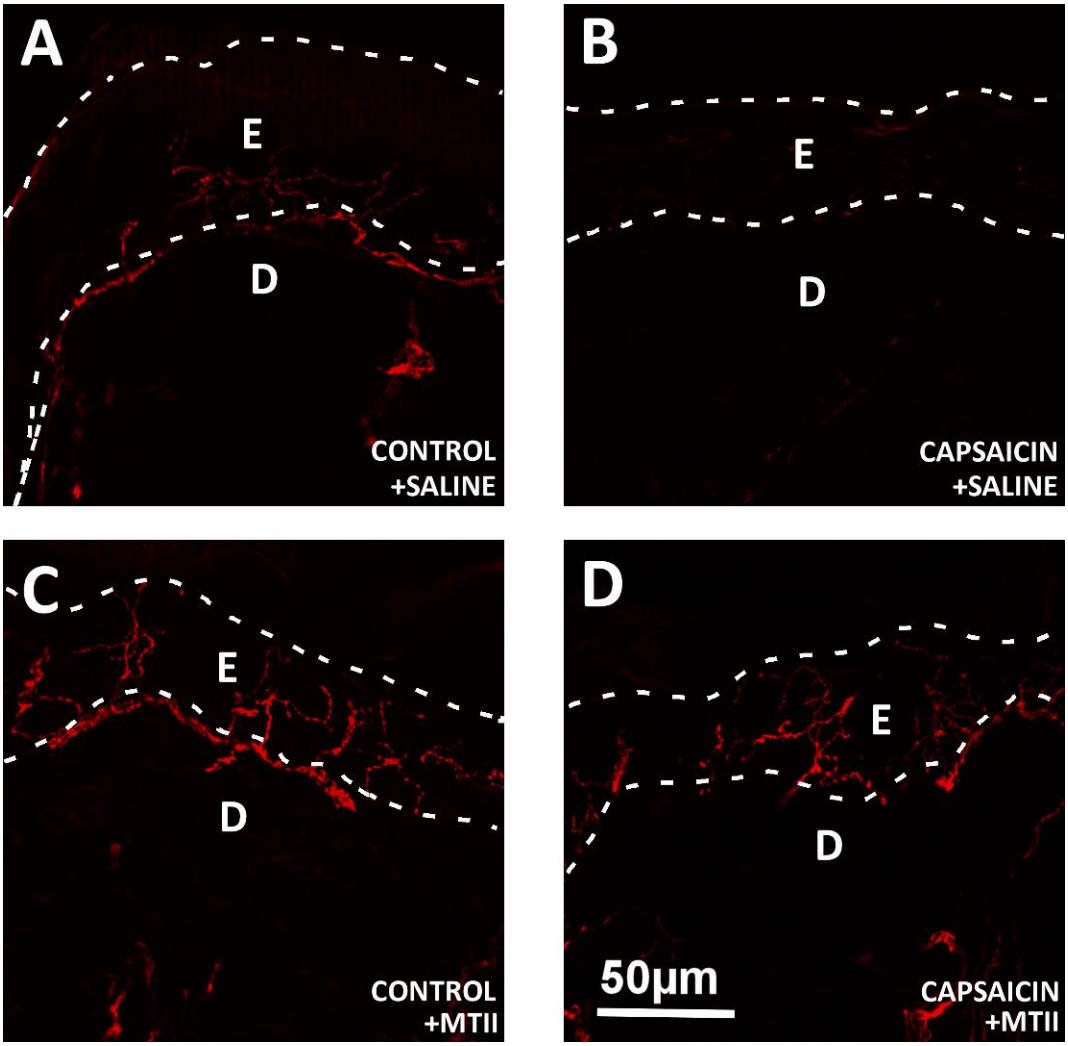
A
E
D
CONTROL
+SALINE
B
E
D
CAPSAICIN
+SALINE
C
E
D
CONTROL
+MTII
D
E
D
50µm
CAPSAICIN
+MTII

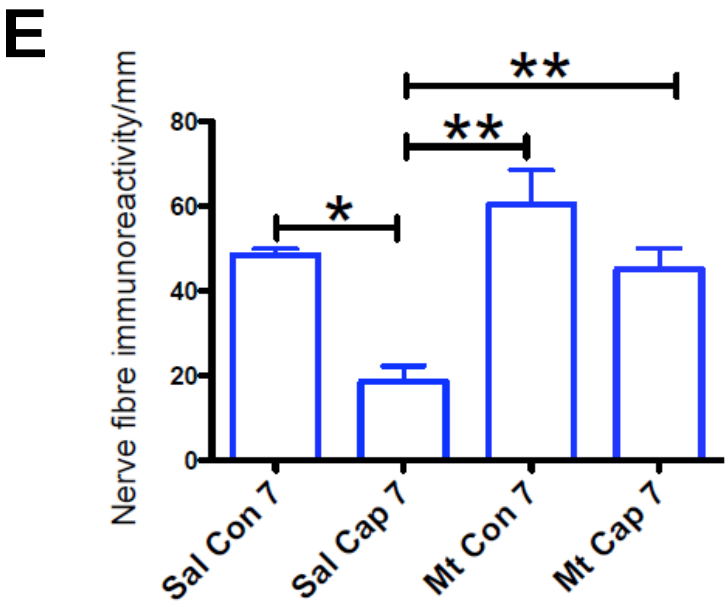
E
Nerve fibre immunoreactivity/mm
80
60
40
20
0
*
**
**
Sal Con 7
Sal Cap 7
Mt Con 7
Mt Cap 7

Figure 5.9 Capsaicin induced denervation regenerates over 14 days.

Representative images of ENFs in punch biopsies taken 14 days after capsaicin application. Dotted lines indicate demarcation of viable epidermis (E) and dermis (D). In some cases, autofluorescent non-viable epidermis is visible above the epidermis (stratum corneum). Nerves stained with pan-neuronal marker βIII-tubulin (red). **(A)** Image of control skin with saline injections, 14 days after control cream was applied. **(B)** Image of capsaicin denervated skin with saline injections, 14 days after capsaicin cream was applied. **(C)** Image of control skin treated with MTII injections, 14 days after control cream was applied. **(D)** Image of capsaicin denervated skin with MTII injections, 14 days after capsaicin cream was applied. **(E)** Graph showing quantification of nerve density, demonstrated by nerve fibre immunoreactivity per mm of epidermis.*P<0.05, **P<0.02. Scale bar applies to all figures.

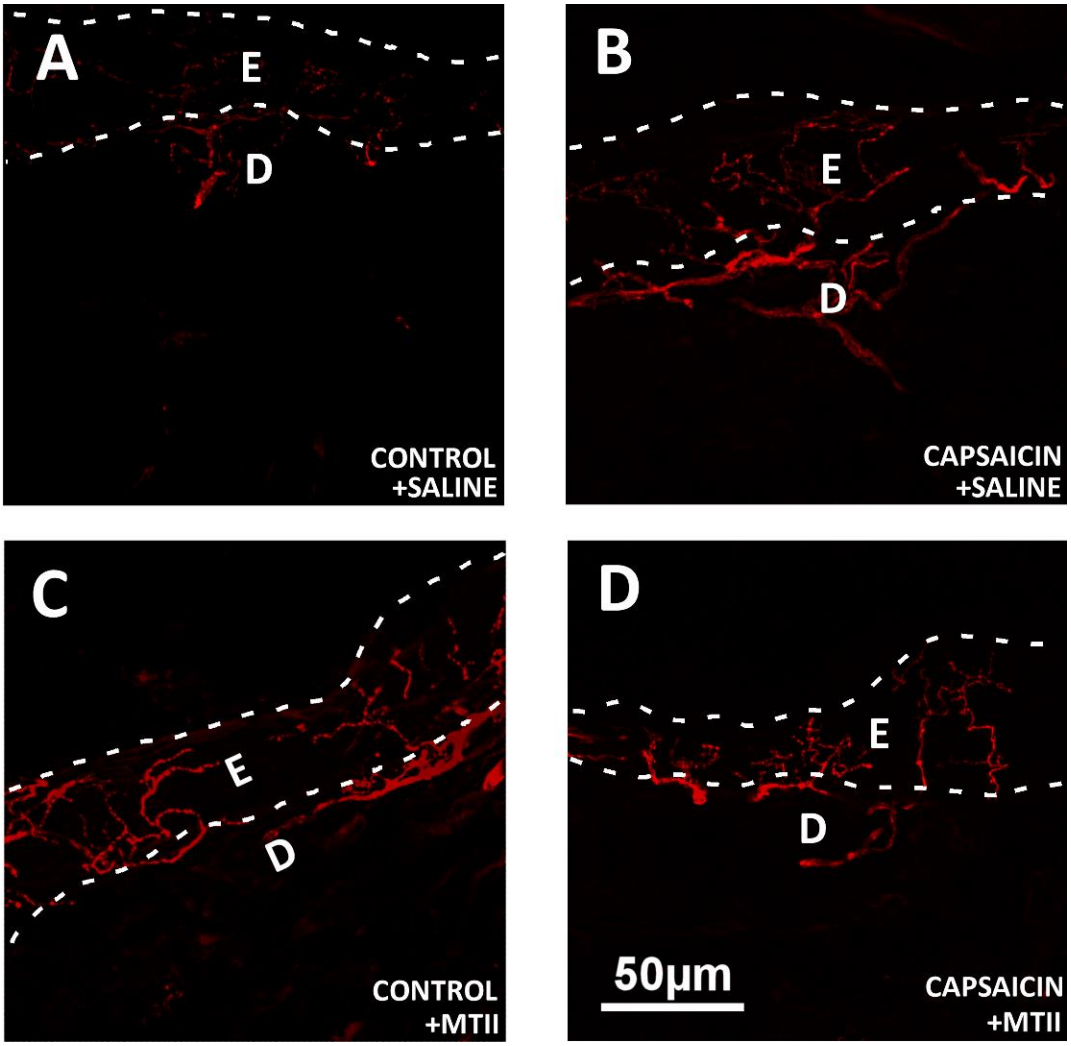
A
E
D
CONTROL
+SALINE
B
E
D
CAPSAICIN
+SALINE
C
E
D
CONTROL
+MTII
D
E
D
50µm
CAPSAICIN
+MTII

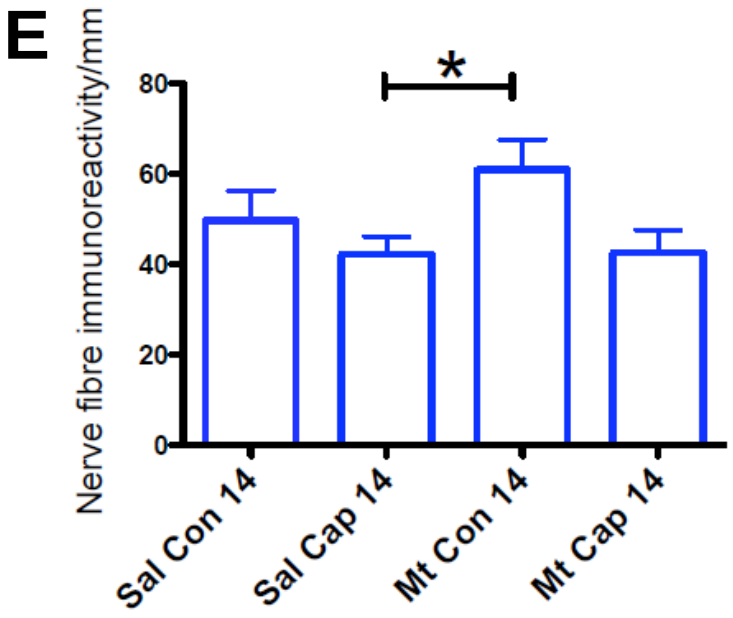
E
Nerve fibre immunoreactivity/mm
80
60
40
20
0
*
Sal Con 14
Sal Cap 14
Mt Con 14
Mt Cap 14

5.3.2 Diabetic neuropathy

In order to evaluate function of MTII in a clinically relevant model of neuropathy, diabetic neuropathy was established in a cohort of rats. Diabetes was established by supplementing rats with a high fat diet, and administering dual injections of STZ to specifically ablate insulin producing β-cells (Like et al., 1978). Diabetic neuropathy with characteristic mechanical allodynia becomes established in these rats (Reed et al., 2000), however the progression of neuropathy over the timecourse of disease has not been thoroughly evaluated.

The course of diabetes was monitored with weekly blood glucose tests. Nerve function was characterised by testing nociception of the hindlimb plantar surface with von Frey monofilaments, and allowed for the development of neuropathy to be detected. Neuropathy was confirmed by biopsy. Examination of punch biopsies from the hindlimbs demonstrated that the model of neuropathy clearly exhibited the typical loss of ENFs and thinning of the epidermis (demonstrated qualitatively in Fig 5.10). Loss of ENFs are associated with the development of mechanical allodynia, but are not indicative of the severity of disease (Lauria et al., 2010). As such, von Frey monofilament testing of mechanical sensitivity was performed to evaluate the development and extent of mechanical allodynia (Weinstein, 1993). Typical nociceptive-like withdrawal of the hindlimb occurs when a pressure of 26 grams is applied with von Frey monofilaments (Fig 5.11). A drop in pressure required to elicit a withdrawal response indicates an increase in mechanical sensitivity and thus development in mechanical allodynia. Characteristic development of mechanical allodynia was observed in diabetic rats, visualised by deviation of mechanical threshold in response to von Frey monofilaments compared to the control group by week 6 (Fig 5.12). Mechanical tolerance occurs when a stimulus is repeated, such that a reduction of the reaction or response

occurs over a period of time. Rats developed tolerance to the repeated stimuli from von Frey monofilaments, such that a greater mass of monofilament was required to elicit a paw withdrawal response over time. Unfortunately, rats developed tolerance to the von Frey testing protocol. In control rats this phenomenon was observed around 6 weeks. In diabetic rats, tolerance was observed to progress much more gradually, and may have been offset by the development of mechanical allodynia (Fig 5.11). Due to the development of tolerance to von Frey monofilaments over time, data from rats commencing treatment after week 14 (as a result of delayed onset of diabetes) was omitted from these graphs. Furthermore, the remaining numbers in this dataset were too small to subject to statistical analysis appropriately. The only conclusions that can be drawn from these von Frey measurements is that the use of Von Frey testing is not suited to longitudinal studies in rats.

Table 5.1 Average blood glucose prior to, and at end of, treatment period.

	CTRL/SAL	**DB/SAL**	**DB/MTII**	**DB/EmB**
Average blood glucose at week 14, prior to treatment with MT, saline or EmtinB (mmol/L)	8.4	>21*	>27*	>26*
Average blood glucose at week 18, at end of treatment with MT, saline or EmtinB (mmol/L)	7.8	>26*	>33*	>29*

*Glucose measurement device has a threshold of 33.3, and as such SEM cannot be calculated.

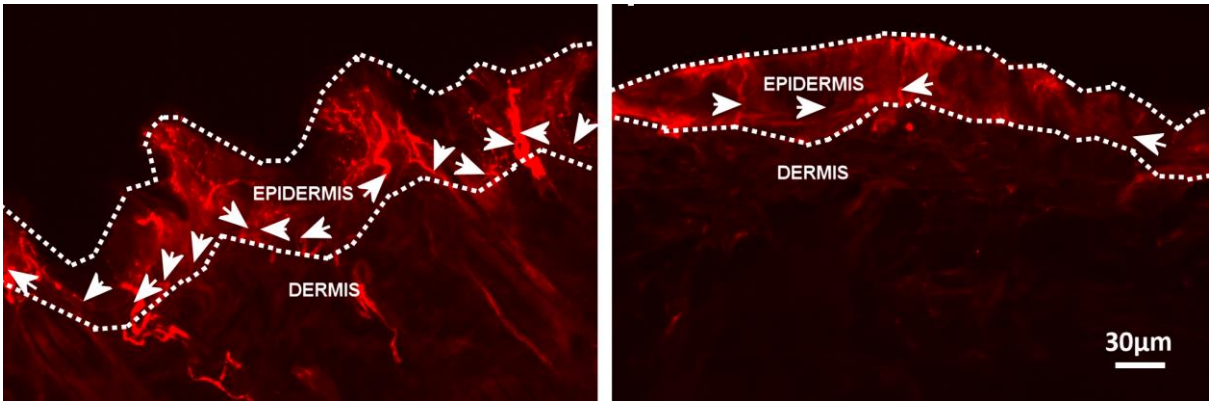

Figure 5.10 Representative punch biopsies of hindlimb skin taken above the gastrocnemius in rats prior to treatment.

Hindlimb biopsy from **(A)** control rat, and **(B)** diabetic rat (6 weeks after confirmation of diabetes). Hindlimb skin is highly elastic and retracts after biopsy increasing the apparent ENF density. Confocal microscope images show ENFs (dentoted by arrows) stained by anti-βIII-tubulin (red). Qualitative analysis suggests that diabetic rats showed a decrease in skin ENF density indicating established neuropathy. Thinning of the epidermis is also noted in diabetic skin.

Figure 5.11 Characterisation of functional changes in sensation in diabetic neuropathy in non-diabetic and STZ/HFD diabetic rats

Average mass of von Frey monofilament required to elicit a paw withdrawal response in rat hindpaws prior to treatment interventions (saline, EmtinB or MTII). **(A)** Control non-diabetic rats began to develop tolerance to the repeated stimuli after 4 weeks of testing. Grey shaded area indicates tolerance development. **(B)** Pooled diabetic rat data responses to von Frey fibres from all diabetic groups prior to introduction treatment. Data normalised for varied onset of diabetes. The development of tolerance in diabetic rats develops gradually.

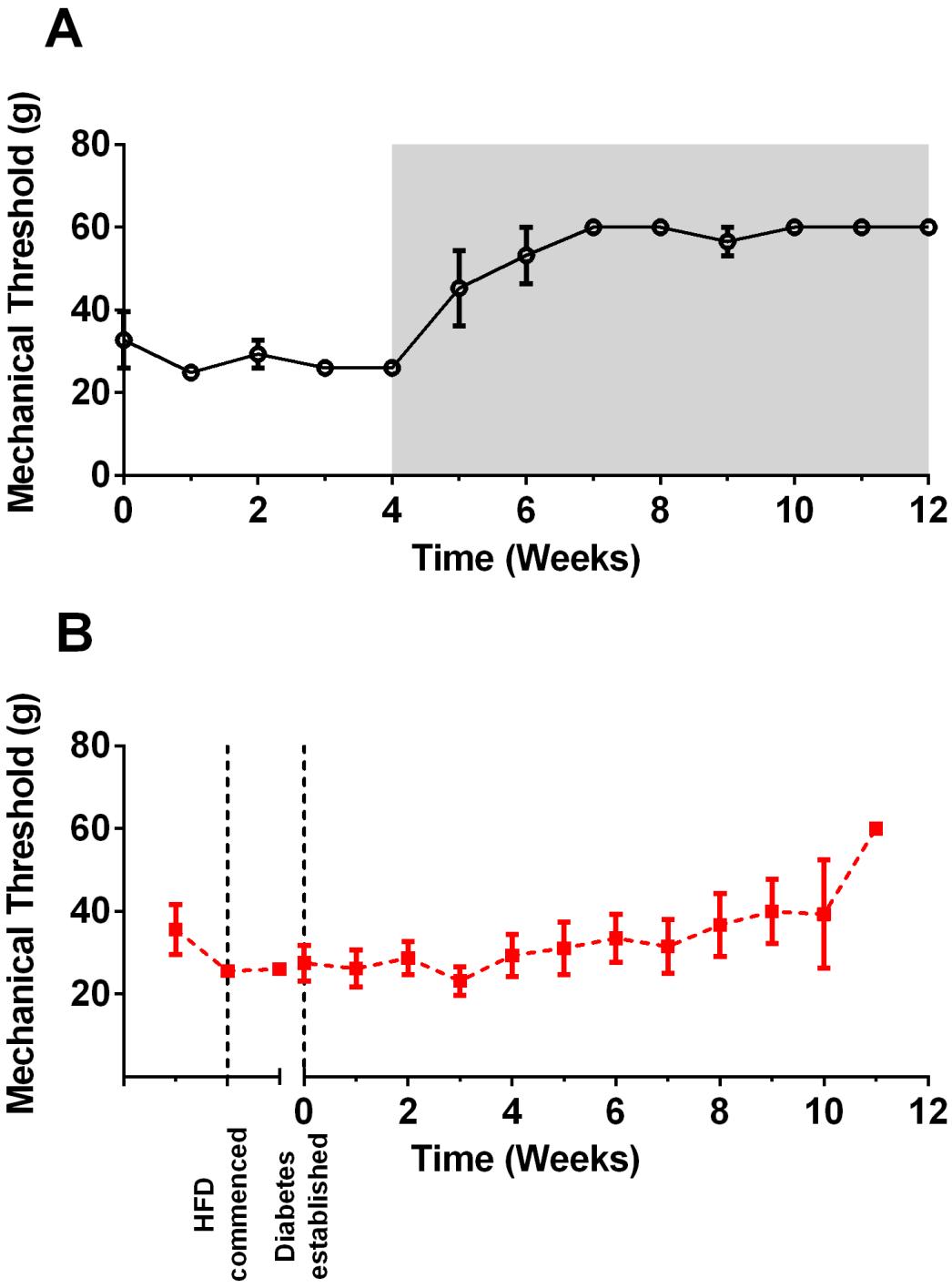
A
Mechanical Threshold (g)
80
60
40
20
0
0
2
4
6
8
10
12
Time (Weeks)
B
Mechanical Threshold (g)
80
60
40
20
0
2
4
6
8
10
12
Time (Weeks)
HFD commenced
Diabetes established

Figure 5.12 Mechanical thresholds before and after treatment with MTII, EmtinB and saline

Average mass of von Frey monofilament required to elicit a paw withdrawal response in control rat hindpaws in control rats and diabetic rats. Grey shaded area indicates treatment period. Divergence in mechanical sensitivities between control and diabetic groups begins from week 6.

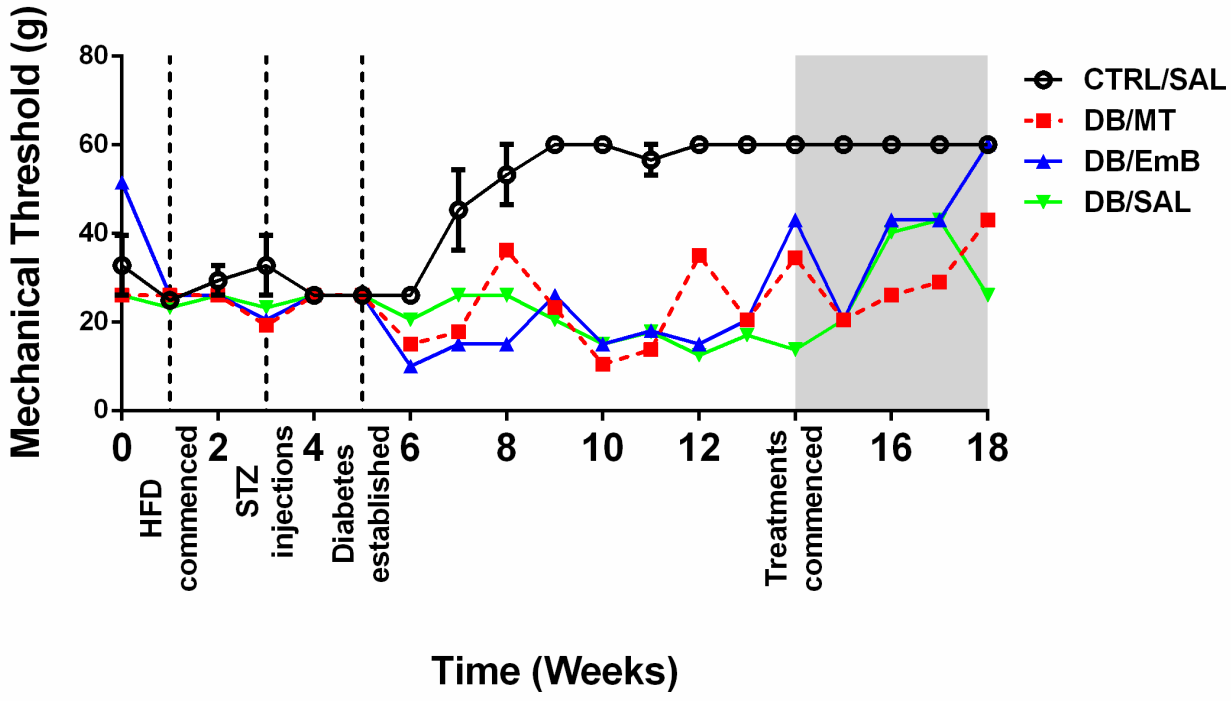
Mechanical Threshold (g)
80
60
40
20
0
0
2
4
6
8
10
12
16
18
HFD commenced
STZ injections
Diabetes established
Treatments commenced
Time (Weeks)
CTRL/SAL
DB/MT
DB/EmB
DB/SAL

5.3.3 Blister-induced focal denervation

The use of blisters as a form of focal denervation is a novel concept, and as such, was established and assessed for reproducibility. Producing blisters on glaborous skin, particularly on skin with a very high density of hair follicles (such as is found on rats), was difficult. Due to hair follicles forming anchor points, many blisters simply erupted when the blister filled with fluid, with the anchor points (Arrows, Figure 5.13) becoming dislodged, leaving a "pore." As a result, the blister instead was raised until only a nominal amount of fluid filled the void between the dermis and epidermis (approximately 40 minutes). However, blisters were not easily injectable as careful insertion of a needle collapsed the delicate epidermis, causing the injected fluid to leak out through the injection point. It was not possible to seal the hole with surgical glue before much of the solution had leaked out, and as such it was not possible to deliver a consistent volume into the blister void. Instead, blisters were injected using an indirect approach, injecting the surrounding intact tissue and delivering the needle into the bottom of the blister (see Fig 5.13). When the void was then filled with solution, as the hair follicle anchors "lifted," they could be sealed with surgical glue. However, due to the strength and density of these anchor points, one could not inject enough fluid to fill the whole blister, and the volume injected was variable depending on each blister. Furthermore, as this tissue was hairy, it was also highly vascularised. Therefore even the relatively gentle suction resulted in petechiae formation, which in itself, adds an additional variable. Although this approach was able to get MTII into the skin in an ideal fashion, it required anaesthetising the rat for extended periods of time. Given that blisters were not consistently reproducible or consistently injectable, this precluded its consideration as a feasible model of denervation and was not investigated further.

Figure 5.13 Images of blister induced focal denervation model

(A) Dorsum of rat with blister device applied **(B)** Image of typical blister raised after blister device has been applied for 40 minutes. Blister generally does not coalesce and hair follicles form anchor points (white arrows) **(C)** Image of injected blister sealed with surgical glue. Scale bar applies both to panel B & C **(D)** Histological section of blister stained with H&E. Hair follicles (HF) anchor the blisters (arrows) and form openings in the epidermis (*). **(E)** Histological section of injected blister stained with H&E, with injected MTII stained with DAB (black arrows). Scale bar applies to panel D & E.

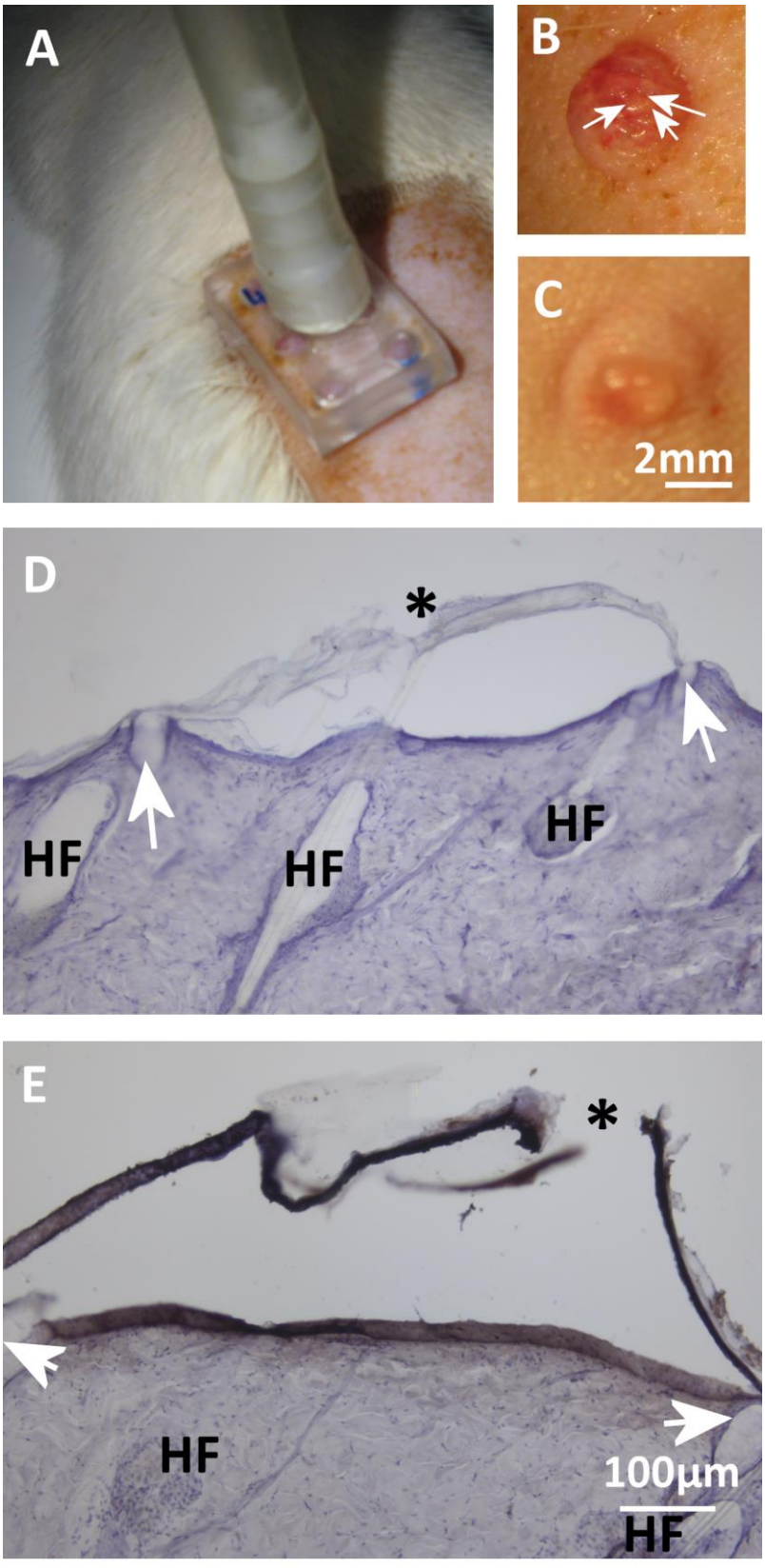
A
B
C
2mm
D
*
HF
HF
HF
E
*
HF
100µm
HF

5.4 DISCUSSION

This chapter demonstrates that intradermal injection of MTII had a potent effect on promoting regeneration of nerves in response to capsaicin-induced denervation. This chapter evaluated a number of experimental models in which to test the ability of MTII to support regeneration of epidermal nerve fibres.

The capsaicin model of denervation proved an excellent model to assess for the regenerative effects of MTII, when delivered by intradermal injection. Although capsaicin is an established means of chemical denervation of the skin, dosages and number of applications vary widely. 8% capsaicin patches are used clinically to treat conditions such as post-herpetic neuralgia in humans, by causing the pain-triggering ENFs to retract deep into the dermis (Maihofner and Heskamp, 2013, Mou et al., 2013). In addition, they only require a single, one hour application (compared to multiple lower-dose applications) and as such were well suited to an experimental paradigm in rats. As 8% capsaicin patches had not been currently approved by the Australian TGA at the time of commencing these experiments and hence were unavailable locally, an 8% capsaicin cream was formulated instead and used in place of the patches. A single one hour application of 8% capsaicin cream resulted in robust loss of ENFs.

Capsaicin application resulted in a robust and predictable denervation and as such was a reliable model for testing MTII. Regeneration of saline treated capsaicin tissue was complete within 14 days. As the time course of ENF regeneration in response to 8% capsaicin in humans is 50-100 days (Polydefkis et al., 2004, Anand and Bley, 2011), the speed with which

regeneration was observed in rats was unexpected. Furthermore, as this was a pilot study, with no previous data available to perform a power calculation, it was unknown whether this data would generate statistical significance. MTII treatment of capsaicin-denervated skin promoted restoration of histological ENF density, resulting in regeneration of ENFs in just 7 days, when compared to saline treatment. Bolus injection of MTII into the dermis would likely result in blanket delivery of MTII to the tissue and not set up a microgradient whereby the concentration of MTII is highest in the epidermis. Therefore, it is not possible to state whether the effects observed were due to a directed guidance of regenerating nerves back into the epidermis, or simply enhanced neurite outgrowth. It is also not possible to state whether the enhanced nerve regeneration in response to MTII was an LRP-mediated response. This question could be addressed with co-administration of pan-LRP inhibitor, RAP, with MTII. Regardless, the enhanced regeneration is a promising result which warrants further investigation. Furthermore, examination of shorter time points would also be intriguing, as it is possible that the observed effect of MTII occurred well within 7 days. In humans, ENF density in the capsaicin model of denervation is quantitated using the accepted formula of Lauria and colleagues (2005). However, this does not take into account changes in branching of ENFs within the epidermis. Qualitative examination of ENFs in punch biopsies would suggest an effect of MTII on promoting branching. Furthermore, the observation that MTII injection into control tissue resulted in a non-significant trend towards an increase in ENF density (60.2 ± 8.2 ENFs/mm) compared to saline treated control tissue (48.4 ± 1.5 ENFs/mm), would appear to support the notion of increased branching in response to MTII. Excessive sprouting may be detrimental and results in aberrant sensation, such as allodynia (Zimmermann, 2001). Excess regrowth of nerves and subsequent development of

neuropathic pain is a complication observed in previous clinical trials for neuropathy involving the use of neurotrophins or other growth factors (Apfel, 2002). An assessment of the efficacy of lower concentrations and fewer injections of MTII would be pertinent, to ensure the maximal regeneration outcomes and least likelihood of excess sprouting.

In the capsaicin model of denervation, the stimulus leading to ENF retraction is absent during the treatment period, however, in the case of diabetic neuropathy, the stimuli affecting ENFs persists as long as the diabetic condition remains. It is important to consider that without correction or resolve of the stimuli that lead to ENF loss in diabetes, any restoration of ENF density in response to MTII treatment may not be prolonged. Although STZ/HFD rats are an established model of type II diabetes, in the literature there is diversity in the dose of STZ, %fat in the high fat diet, age and breed of rats (Islam and Choi, 2007). As such, it was necessary to monitor the course of both diabetes and neuropathy by regular testing of blood glucose and mechanical sensibility, respectively. The diabetic neuropathy model was established and exhibited a characteristic loss of ENFs and thinning of the epidermis. An unforeseen difficulty in functional evaluation arose from the finding that control rats developed tolerance to the repeated stimuli from von Frey monofilaments around 6 weeks, and because a similar effect was observed in the diabetic groups (albeit delayed), it was difficult to ascertain the onset of mechanical allodynia, which would have ordinarily marked the onset of the treatment intervention. It became clear that von Frey testing is not suited to longitudinal studies evaluating mechanical sensitivity thresholds in rats. The tolerance effect made interpretation of the mechanical threshold difficult and likely masked any therapeutic effects one may have observed in response to MTII or EmtinB. Future experiments should not use von Frey testing at such regular intervals, and treatments should be administered

earlier to overcome the likelihood of observing tolerance. As a result of the issues surrounding the development of tolerance, and delayed onset of diabetes in some animals, only a few animals from each cohort who had treatment commenced at precisely the same time could be directly compared. However, these numbers were too small to perform statistical analyses. In the future, other measures of sensory modalities could be investigated, for example, testing of thermal nociception. In order to assess thermal sensory thresholds, the hindpaw withdrawal response can be measured, which is the time elapsed until the hindpaw is withdrawn after placing the plantar surface of the subject on a heated or cooled surface. This is a well-established behaviour measurement protocol used to measure changes in thermal sensation (Hargreaves et al., 1988). Particularly in light of the observed pre-diabetic neuropathy symptoms in humans (Callaghan et al., 2012), an earlier therapeutic intervention in an animal model of diabetic neuropathy is warranted. Due to time constraints, the histological evaluation of this work will form the basis of a future honours project and as such could not be included in this PhD.

Epidermal blisters may provide a unique opportunity for a proof-of-concept study into the effect of MTII in guiding the growth of regenerating nerves *in vivo.* Theoretically, they allow for the controlled transdermal delivery of MTII to the site of severed, regenerating nerves, and establish a local gradient within the epidermis and underlying dermis. Although not a therapeutically viable approach for delivering MTII in humans (producing many small blisters to treat an affected area of skin would not be suitable), blisters provide an opportunity to deliver a small volume of MTII which could diffuse into the surrounding tissue and produce a subtle gradient. A gradient would allow for an investigation into whether MTII could direct the growth of regenerating nerve fibres *in vivo*. Whilst this approach could be

used to create a concentration gradient of MTII, as visualised by immunohistochemistry, it was not consistently reproducible.

Considerations remain for intradermal injection as a viable delivery method of MTII. Intradermal injections mechanically perforate skin, causing pain and localised trauma, potential inflammatory processes and infection, and results in the formation of scar tissue if injected in the same location repeatedly. Scar tissue was particularly evident in 14-day samples and although these regions were avoided in analysis, this is potentially confounding as scar tissue would likely impede regeneration of ENFs. Furthermore, in terms of potential clinical applicability, Hamilton (1995) reports that needle phobia is a condition affecting at least 10% of the population, and as such, an ongoing effort into finding a means by which to deliver MTII topically should be maintained. Overall, the finding that MTII rapidly accelerated nerve regeneration in capsaicin-induced denervation supports the hypothesis, and indicates that MTII shows great promise as a therapeutic candidate in peripheral nerve damage.

CHAPTER 6

Conclusions and future directions

CHAPTER 6

CONCLUSIONS AND FUTURE DIRECTIONS

The work within this thesis sheds new light on the function of LRP1 and LRP2 receptors as chemotactic receptors, and in conjunction with the existing body of knowledge, provides evidence of a putative role for LRPs as neurotrophic factor-like receptors – that is, to promote survival, neurite outgrowth, and chemotactic guidance of neurons (Purves, 1988, Oppenheim et al., 1991, Lindsay, 1996).

To the best of our knowledge, there is no prior evidence of a mechanism by which LRP1 and LRP2 promote axon guidance. Specifically outlined in this thesis is the discovery that LRP1 and LRP2 are able to direct growth cone navigation. Multiple LRP ligands (α2m, tPA, MTII and MTIII) were shown to direct axon guidance. The signalling mechanisms investigated suggest that LRP-MT signalling is Ca^{2+} dependent, and can operate via classical and non-classical mechanisms. Based on evidence within this thesis, MT-LRP signalling likely requires crosstalk between multiple receptors, including the neurotrophin receptor TrkA. This is the first time crosstalk between LRP1 and LRP2 receptors have been proposed. Importantly, I also demonstrated the therapeutic potential of the MT-LRP signalling system which was shown to enhance regeneration of denervated skin *in vivo*.

Consistent with the contrasting effects of MTII and MTIII, which were chemoattraction and chemorepulsion, respectively, this thesis reveals a disparity in their downstream signalling pathways. For the first time, I provide evidence that MTIII requires LRP1 and LRP2 for its

signalling. As both MTII- and MTIII-LRP signalling pathways were Ca^{2+} dependent, further effort should be placed on acertaining which Ca^{2+} channels on the plasma membrane are required for the response, and also whether store-operated calcium entry processes are required to release Ca^{2+} from internal stores. It is known that it is not just the amount of Ca^{2+} that enters the growth cone that is important for the turning response that eventuates, but the local source of Ca^{2+} as well; so from a mechanistic point of view this question is pertinent, as understanding the underlying signalling mechanism would provide scope for the development of novel pharmacological agents. Given the intimate association between Ca^{2+} and cyclic nucleotides in growth cone turning (Song et al., 1998), and the ability of Ca^{2+} signalling proteins to regulate cyclic nucleotide levels (Nishiyama et al., 2003), it would be logical to devote further investigation into the role of cyclic nucleotides in the mechanism of LRP-mediated growth cone turning as this would most likely contribute to the mechanism of action. Preliminary experiments have been performed by myself in this area, and support the notion that cyclic nucleotides are involved in LRP-MTII and LRP-MTIII signalling. Furthermore, based on the ability for LRP1 ligands, such as α2M, to induce Ca^{2+} influx through NMDA channels (Bacskai et al., 2000), it is important to ask whether α2M, tPA, MTII and MTIII function in a similar manner in growth cone turning. NMDA receptors are involved in the directed guidance of *Xenopus* spinal neurons (Zheng et al., 1996), but a similar role has not been investigated in mammalian cells. If so, this would be the first time NMDA receptors are described as receptors involved in growth cone motility in mammalian cells.

Understanding the mechanisms by which MTs elicit this chemotactic response in neuronal growth cones has important implications for future therapeutic developments of MTs in

neuropathies and neuronal injury. During development, neuronal growth cones use a range of guidance cues to navigate the embryonic environment, establishing the early framework of the neuronal circuitry. While the major families of guidance cues such as netrins, ephrins and semaphorins are well established, it is likely that other context-dependent guidance cues exist. For example, the extracellular environment associated with growth cones in the developing nervous system is likely to be very different to that encountered by regenerating neurons after a neuropathy or following physical injury in the mature brain. This raises the question whether other receptor-ligand signalling complexes outside those established in neurodevelopment, such as the MT-LRP signalling system, might be exploited in neuronal regeneration. Indeed, the finding that MTII enhanced regeneration in a model of chemical induced denervation strongly suggests that this may be the case.

In addition to the current body of knowledge, the findings within this thesis implicate MTII as a therapeutic candidate in peripheral nerve axotomy and neuropathy. Neuronal injuries, such as those sustained from cutaneous damage or in neuropathies, are not amenable to gross surgical intervention. This thesis is the first to report the finding that MTII is able to promote regeneration in a model of chemical induced denervation of peripheral nerve fibres, and as such, offers a unique approach to remedy an otherwise untreatable nerve injury. There are many potential indications for MTII as a therapeutic small molecule that warrant further investigation. Sometimes the development of neuropathy is predictable, such as in neuropathies with an underlying genetic basis (for example, a slow progressive peripheral demyelinating neuropathy) or as a side effect of drugs such as chemotherapeutic agents. As such, therapeutics, which may act as a prophylactic or slow disease progression, can be administered. The development of neuropathy in response to some chemotherapeutic agents

is becoming an increasingly frequent problem, and is also a dose-limiting factor (Grisold et al., 2012). Future studies should address whether MTII has a protective effect in chemotherapeutic induced neuropathy.

As a therapeutic, MTII requires an appropriate site-directed delivery approach. In neuropathies affecting ENFs, regeneration would require regulated outgrowth towards the skin's surface. The promise of MTII as a multimodal therapeutic warrants further investigation into developing a carrier to allow MTII to be delivered into the skin topically to guide accurate axon regeneration. There are several approaches to promote transdermal delivery which warrant further investigation. Those approaches include the use of ultrasound techniques, transiently heating the skin, and through the use of nanopatches. In addition, combinations of penetration enhancement techniques may show synergistic effects (Karande et al., 2004). Because iontophoresis provides a transport driving force, it may be especially useful when coupled with another method that increases skin permeability or penetration. For example, combining iontophoresis with microdermabrasion increases flux of 5-aminolaevulinic acid by 15 times (Fang et al., 2004).

A relatively recent development in the field of transdermal drug delivery is the invention of the Nanopatch^{TM}. The Nanopatch is a specialised drug delivery system, which essentially is a refined version of the traditional injection, currently trialled for vaccine delivery (Prow et al., 2010). The nanopatch is constructed with an array of super-fine tapering microneedles that when applied to the skin is painless; it delivers the molecule more accurately and evenly to the area of interest, and may facilitate the use of even lower doses (Fernando et al., 2010). Nanopatches also have the advantage of less scar tissue formation – intradermal injections

cause micro-trauma of the skin, with repeated injections in the same locale resulting in scar tissue formation.

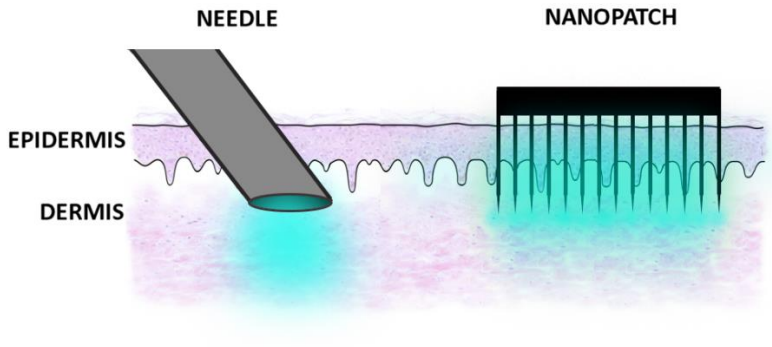

Schematic representation of the distribution of drug from needle delivery versus the nanopatch. (Fernando et al., 2010)

Ultrasound is an additional approach used to enhance delivery of drugs into the skin. The most effective form of ultrasound for drug delivery is cavitational ultrasound, which specifically uses low frequencies, facilitating the formation of cavitational bubbles in the applied solution. As the bubbles collapse at the skin surface, the shearing force that results disrupts the stratum corneum and delivers microjets of liquid into the epidermis. In addition, it may also increase fluidity of the lipid bilayer (Prausnitz and Langer, 2008). It has successfully been used experimentally to deliver large molecules into the skin, and is currently used to accelerate the delivery of topical anaesthetic lidocaine in an FDA-approved system (SonoPrep®). The aforementioned avenues are worth considering for future developments of an MTII topical delivery system.

Diabetic neuropathy is the single most prevalent form of neuropathy worldwide (Callaghan et al., 2012). Although there are a number of types of diabetic neuropathy, the most common is diabetic peripheral neuropathy which exhibits a characteristic loss of epidermal nerve fibres, resulting in a number of poorly tolerated symptoms (Dyck et al., 2011). Although a study was commenced into the ability of MTII to promote regeneration in a model of diabetic neuropathy, due to time constraints, the outcome in terms of ENF regeneration was not evaluated within this thesis. However, in an experimental model of chemical induced denervation I showed MTII could enhance regeneration, and it is possible that a similar effect may be observed in diabetic neuropathy. A caveat to address is that due to varied etiology of diabetes, the underlying pathophysiology may mean that a loss of ENFs are resultant from neuronal death, not just retraction of the outermost ENF, and as such, regeneration may be an unrealistic expectation. MTII may, however, facilitate a pro-survival interaction with existing neurons.

The ability of MTII and MTIII to guide neuronal growth, in addition to their established repertoire of action, is intriguing; these findings suggest a similarity with cytokines and growth factors. Though MTs are constitutively expressed, they are upregulated in a number of host defence mechanisms and downregulated or upregulated in several disease states (Antonelli et al., 2012). Comparing and contrasting the effects of MTII with the function of neurotrophic factors (which are a subset of growth factors specific to neurons) indicates surprising overlaps in function and as such warrants review.

The function of neurotrophic factors in neurons is to promote survival, differentiation, maintenance and chemotactic guidance to neurons (Buchman and Davies, 1993). Different subsets of sensory neurons in the PNS require trophic support and pro-survival signals from

different neurotrophic factors (Buchman and Davies, 1993). For example, the family of neurotrophic factors include the nerve growth factor (NGF), which provides the trophic signals for small unmyelinated nociceptive neurons, brain derived neurotrophic factor (BDNF), which provides the trophic signals for mechanoreceptive (tension and pressure relaying) neurons, and neurotrophic factor-3 (NT-3), which provides the trophic signals for large proprioceptive (touch relaying) neurons (Baudet et al., 2000, Kirstein and Farinas, 2002). The requirement of specific chemotactic factors by neurons can change during development; for example, a subset of non-peptidergic sensory neurons switches from NGF to GDNF dependency postnatally (Molliver and Snider, 1997). Different neurotrophic factors show overlapping, yet distinct patterns of activities and a lack of specificity for neuronal types (Lindsay, 1996). Different neurotrophic factors share receptors and their subunits, indicating redundancy and pleiotropism in chemotactic function (Davies, 1994). Not all neurotrophic factors have roles in directing growth in development. NGF is a chemoattractant of growth cones of sensory neurons (Levi-Montalcini, 1979), although little use is made of this property in establishing initial target contact (Vogel and Davies, 1991). Similarly, the work described in this thesis demonstrates that MTII is also a chemoattractant of sensory neuron growth cones, but given that MTI/II knockout mice do not appear to have major faults in sensory neuron pathfinding in development, the importance of its chemotactic function in development shares intriguing similarity with NGF.

During development, neurons endocytose growth factors or neurotrophins secreted from their target tissue by receptor mediated processes, which are transported in a retrograde fashion to the cell body to induce the expression of genes that are involved in survival (Kirstein and Farinas, 2002). As long as this connection is maintained, this signalling is continuously

stimulating survival (Eade and Allan, 2009). Therefore, neurotrophic factors are important for survival and maintenance of neurons (Purves, 1988, Oppenheim et al., 1991). Similarly, many studies corroborate the fact that MTI/II have important roles in promoting neuronal survival, especially in response to stressors or toxicants (West et al., 2008). MTII is endocytosed via LRP receptors (Ambjorn et al., 2008), and in addition, our lab has visualised retrograde transport of MTII down axons to the cell body (West *et al.*, Unpublished data). MTs are able to translocate to the nucleus, where they are able to indirectly influence gene transcription by delivery of vital zinc to zinc-finger transcription factors within the nucleus (Cherian and Apostolova, 2000).

Some growth factors are transported in an anterograde fashion: one example is bFGF. bFGF is synthesized and released by retinal cells *in vivo* (Hageman et al., 1991) and exogenous bFGF is transported anterogradely in retinal ganglion cell axons toward the superior colliculus (Ferguson and Johnson, 1991), which depends on afferent input for survival of its neurons. Similarly, it is well established that MTI/II and MTIII have endogenous neuroprotective functions in the retina, safeguarding neurons from degenerative processes (Ito et al., 2013b). Our laboratory has previously shown that intravitreal injection of MTII after an optic crush injury promotes neuronal regeneration (Chung et al., 2008), and given that MT is endocytosed it is possible that MTII is transported to the cell body to deliver zinc, in addition to the LRP-mediated transcriptional changes which result in growth promoting and anti-apoptotic effects (Chung et al., 2008).

Not only do some neurons (particularly sensory neurons) produce neurotrophic factors, but they may also express their corresponding receptors and act in an autocrine fashion (Acheson and Lindsay, 1996). For example, some DRG neurons synthesise BDNF, and express its

cognate receptor, TrkB (Klein et al., 1990, Klein et al., 1991). This facilitates a self-sustaining cycle of growth and maintenance prior to forming a connection with its target cell. Although it is not clear whether MT performs in this specific manner, it is able to act in an autocrine fashion: MTs can promote self-upregulation, particularly in response to metal toxicity (Alvarez et al., 2012).

In vivo, neurotrophic factors also behave in a paracrine fashion. Cerebellar granule cells depend on Purkinje cells for survival (Herrup and Sunter, 1987). Secretion of aFGF , BDNF, and NT-3 are likely candidates behind this pro-survival interaction (Hatten et al., 1988, Maisonpierre et al., 1990, Lamballe et al., 1991, Cheng et al., 2001). It has been demonstrated that MTII can be secreted by astrocytes, and elicit pro-survival effects on surrounding neurons, thereby also demonstrating paracrine function (Chung et al., 2008). It is clear that there is convincing evidence that MTII behaves in a similar manner to many neurotrophic factors; in some cases, exhibiting more characteristics of neurotrophic factors than some archetypal neurotrophic factors themselves.

This thesis describes new roles for LRP1 and LRP2 in axon pathfinding, particularly in the context of the developing, injured and diseased nervous system, new functions for LRP ligands, α2M, tPA, MTII and MTIII, and provides compelling evidence that MTII is able to promote regeneration of nerve fibres in chemical induced denervation. This body of work provides the basis for many additional studies into LRP receptor/ligand biology and therapeutic application, and challenges the way we currently view LRP1 and LRP2 receptors.

APPENDIX 1

7.1 SOLUTION PROTOCOLS

7.1.1 DMEM-F12: 1L

Combine 15.6g Dulbecco's Modified Eagle's Medium F-12 medium powder, 16mL 7.5% sodium bicarbonate solution, 800mL dH_20 until powder is just dissolved. Adjust pH to 7.2 with NaOH. Make up to 1L. Filter sterilise into autoclaved schott bottle. Store at 4°C.

7.1.2 Sensory neuron media (SNM): 50mL

Combine 46mL DMEM-F12 (1:1), 500µL Stock solution penicillin G (10,000U/mL) and streptomycin (10,000µg/mL), 25µL Nerve Growth Factor, 2.5mL Fetal calf serum and 500µL N2 neural medium supplement. Keep stored in 37°C and 5% CO_2 supplemented incubator, with lid partially unscrewed. Prepare fresh as required.

7.1.3 Phosphate Buffered Saline (PBS): 1L

Combine 8g NaCl, 1.44g Na_2HPO_4, 0.2g KCl, 0.24g KH_2PO_4, 800mL dH_20. Adjust pH to 7.4. Make up to 1L with dH_2O. Autoclave. Can be stored at room temperature. For PBS-T add 0.1% Tween after solution has been pH adjusted.

7.1.4 TBS 1:1: 1L

Dissolve 3g TRIS, 0.2g KCl and 8g NaCl in 800mL dH_20. pH adjusted to 8.0. Make up to 1L. For TBS-T add 0.1% Tween after solution has been pH adjusted.

7.1.5 Hank's Balanced Salt Solution, Ca^{+2} free media: 30mL

Add 0.285g Hank's Balanced Salt Solution (HBSS), Ca^{+2} and Mg^{+2} free media powder and 140µL 7.5% Sodium bicarbonate solution to dH_20, and mix until dissolved. pH adjusted to 7.2 with HCl. Make up to 30mL. Filter sterilise. Add 300µL Stock solution penicillin G (10,000U/mL) and streptomycin (10,000µg/mL), 15µL Nerve Growth Factor, 300µL N2 neural medium supplement. Keep stored in 37°C and 5% CO_2 supplemented incubator, with lid partially unscrewed. Prepare fresh as required.

7.1.6 0.4% Triton X: 100mL

Combine 99.6mL PBS and 400µL Triton X-114 stock solution. Store at room temperature.

7.1.7 4% Paraformaldehyde (PFA): 500mL

Combine 500mL PBS with 20g paraformaldehyde (PFA) in a fume hood. Stir on a heated stirrer until the temperature reaches 60°C. Ensure temperature is monitored as the flashpoint for PFA is 90°C. Adjust pH to 8 with 5M NaOH and allow PFA to dissolve. Allow to cool then adjust pH to 7.2 with HCl. Store at -20°C or at 4°C if to be used within a week.

7.1.8 Zamboni's Fixative : 5L

Combine 460ml 0.2M Na_2HPO_4+ 1540ml 0.2M NaH_2PO_4. Adjust pH to 7.2-7.4. Add 2L 2% paraformaldehyde and 705ml saturated picric acid (about 5g per 400ml water). Stable at 4°C for 1 year

7.1.9 Nuclear Fast Red solution: 100mL

Combine 0.1 g Nuclear Fast Red with 100 ml 5% Aluminum-sulfate solution ($Al_2(SO_4)3 \cdot 18H_20$ aluminium sulfate octadecahydrate). Boil for 5 min. Add grain of thymol as preservative.

7.1.10 Poly-L-ornithine 1mg/mL solution: To make 5ml

Combine 500µl 10mg/ml stock Poly-L-ornithine solution with 4500µl 50mM TRIS, pH 7.4. use immediately.

7.1.11 50mM TRIS: To make 10mL

Combine 500µL 1M TRIS stock, pH 7.4, 9500µL MilliQ H_2O. Store at room temperature.

7.1.12 50ug/mL Laminin: To make 1mL

Combine 50µL 100µg/ml Laminin stock solution with 950µL 150mM NaCl/50mM TRIS solution. Use immediately.

7.1.13 150mM NaCl/50mM TRIS: To make 10mL

Combine 500µL 1M TRIS pH 7.4, 300µl 5M NaCl, 9.2mL Milli-Q H_2O. Store at room temperature.

Bibliography

BIBLIOGRAPHY

Acheson A, Lindsay RM (1996) Non target-derived roles of the neurotrophins. Philos Trans R Soc Lond B Biol Sci 351:417-422.

Aguayo AJ, David S, Bray GM (1981) Influences of the glial environment on the elongation of axons after injury: transplantation studies in adult rodents. J Exp Biol 95:231-240.

Aivo J, Lindsrom BM, Soilu-Hanninen M (2012) A Randomised, Double-Blind, Placebo-Controlled Trial with Vitamin D3 in MS: Subgroup Analysis of Patients with Baseline Disease Activity Despite Interferon Treatment. Mult Scler Int 2012:802796.

Akiyama H, Matsu-ura T, Mikoshiba K, Kamiguchi H (2009) Control of neuronal growth cone navigation by asymmetric inositol 1,4,5-trisphosphate signals. Sci Signal 2:ra34.

Akkina SK, Patterson CL, Wright DE (2001) GDNF rescues nonpeptidergic unmyelinated primary afferents in streptozotocin-treated diabetic mice. Exp Neurol 167:173-182.

Alto LT, Havton LA, Conner JM, Hollis ER, 2nd, Blesch A, Tuszynski MH (2009) Chemotropic guidance facilitates axonal regeneration and synapse formation after spinal cord injury. Nat Neurosci 12:1106-1113.

Alvarez L, Gonzalez-Iglesias H, Garcia M, Ghosh S, Sanz-Medel A, Coca-Prados M (2012) The stoichiometric transition from Zn6Cu1-metallothionein to Zn7-metallothionein underlies the up-regulation of metallothionein (MT) expression: quantitative analysis of MT-metal load in eye cells. J Biol Chem 287:28456-28469.

Ambjorn M, Asmussen JW, Lindstam M, Gotfryd K, Jacobsen C, Kiselyov VV, Moestrup SK, Penkowa M, Bock E, Berezin V (2008) Metallothionein and a peptide modeled after metallothionein, EmtinB, induce neuronal differentiation and survival through binding to receptors of the low-density lipoprotein receptor family. J Neurochem 104:21-37.

Anand P (2004) Neurotrophic factors and their receptors in human sensory neuropathies. Prog Brain Res 146:477-492.

Anand P, Bley K (2011) Topical capsaicin for pain management: therapeutic potential and mechanisms of action of the new high-concentration capsaicin 8% patch. Br J Anaesth 107:490-502.

Andersen OM, Vorum H, Honore B, Thogersen HC (2003) Ca2+ binding to complement-type repeat domains 5 and 6 from the low-density lipoprotein receptor-related protein. BMC Biochem 4:7.

Andrade N, Komnenovic V, Blake SM, Jossin Y, Howell B, Goffinet A, Schneider WJ, Nimpf J (2007) ApoER2/VLDL receptor and Dab1 in the rostral migratory stream function in postnatal neuronal migration independently of Reelin. Proc Natl Acad Sci U S A 104:8508-8513.

Antonelli MC, Guillemin GJ, Raisman-Vozari R, Del-Bel EA, Aschner M, Collins MA, Tizabi Y, Moratalla R, West AK (2012) New strategies in neuroprotection and neurorepair. Neurotox Res 21:49-56.

Apfel SC (1999) Neurotrophic factors in the therapy of diabetic neuropathy. Am J Med 107:34S-42S.

Apfel SC (2002) Nerve growth factor for the treatment of diabetic neuropathy: what went wrong, what went right, and what does the future hold? Int Rev Neurobiol 50:393-413.

Arie Y, Iketani M, Takamatsu K, Mikoshiba K, Goshima Y, Takei K (2009) Developmental changes in the regulation of calcium-dependent neurite outgrowth. Biochem Biophys Res Commun 379:11-15.

Armstrong PB, Quigley JP (1999) Alpha2-macroglobulin: an evolutionarily conserved arm of the innate immune system. Dev Comp Immunol 23:375-390.

Ashcom JD, Tiller SE, Dickerson K, Cravens JL, Argraves WS, Strickland DK (1990) The human alpha 2-macroglobulin receptor: identification of a 420-kD cell surface glycoprotein specific for the activated conformation of alpha 2-macroglobulin. J Cell Biol 110:1041-1048.

Asmussen JW, Ambjorn M, Bock E, Berezin V (2009a) Peptides modeled after the alpha-domain of metallothionein induce neurite outgrowth and promote survival of cerebellar granule neurons. Eur J Cell Biol 88:433-443.

Asmussen JW, Von Sperling ML, Penkowa M (2009b) Intraneuronal signaling pathways of metallothionein. J Neurosci Res 87:2926-2936.

Bacskai BJ, Xia MQ, Strickland DK, Rebeck GW, Hyman BT (2000) The endocytic receptor protein LRP also mediates neuronal calcium signaling via N-methyl-D-aspartate receptors. Proc Natl Acad Sci U S A 97:11551-11556.

Balordi F, Fishell G (2007) Mosaic removal of hedgehog signaling in the adult SVZ reveals that the residual wild-type stem cells have a limited capacity for self-renewal. J Neurosci 27:14248-14259.

Barcelona PF, Jaldin-Fincati JR, Sanchez MC, Chiabrando GA (2013) Activated alpha2-macroglobulin induces Muller glial cell migration by regulating MT1-MMP activity through LRP1. FASEB J 27:3181-3197.

Barnes H, Larsen B, Tyers M, van Der Geer P (2001) Tyrosine-phosphorylated low density lipoprotein receptor-related protein 1 (Lrp1) associates with the adaptor protein SHC in SRC-transformed cells. J Biol Chem 276:19119-19125.

Baron R (2006) Mechanisms of disease: neuropathic pain--a clinical perspective. Nat Clin Pract Neurol 2:95-106.

Baudet C, Mikaels A, Westphal H, Johansen J, Johansen TE, Ernfors P (2000) Positive and negative interactions of GDNF, NTN and ART in developing sensory neuron subpopulations, and their collaboration with neurotrophins. Development 127:4335-4344.

Beffert U, Stolt PC, Herz J (2004) Functions of lipoprotein receptors in neurons. J Lipid Res 45:403-409.

Beffert U, Weeber EJ, Durudas A, Qiu S, Masiulis I, Sweatt JD, Li WP, Adelmann G, Frotscher M, Hammer RE, Herz J (2005) Modulation of synaptic plasticity and memory by Reelin involves differential splicing of the lipoprotein receptor Apoer2. Neuron 47:567-579.

Benson HA (2005) Transdermal drug delivery: penetration enhancement techniques. Curr Drug Deliv 2:23-33.

Bentley D, O'Connor TP (1994) Cytoskeletal events in growth cone steering. Curr Opin Neurobiol 4:43-48.

Berridge MJ, Lipp P, Bootman MD (2000) The versatility and universality of calcium signalling. Nat Rev Mol Cell Biol 1:11-21.
Bespalov MM, Sidorova YA, Tumova S, Ahonen-Bishopp A, Magalhaes AC, Kulesskiy E, Paveliev M, Rivera C, Rauvala H, Saarma M (2011) Heparan sulfate proteoglycan syndecan-3 is a novel receptor for GDNF, neurturin, and artemin. J Cell Biol 192:153-169.
Bharucha NE, Bharucha AE, Bharucha EP (1991) Prevalence of peripheral neuropathy in the Parsi community of Bombay. Neurology 41:1315-1317.
Bhide PG, Frost DO (1991) Stages of growth of hamster retinofugal axons: implications for developing axonal pathways with multiple targets. J Neurosci 11:485-504.
Bierhaus A, Nawroth PP (2012) Critical evaluation of mouse models used to study pain and loss of pain perception in diabetic neuropathy. Exp Clin Endocrinol Diabetes 120:188-190.
Birder LA, Perl ER (1994) Cutaneous sensory receptors. J Clin Neurophysiol 11:534-552.
Bisby MA (1980) Axonal transport of labeled protein and regeneration rate in nerves of streptozocin-diabetic rats. Exp Neurol 69:74-84.
Bootman MD, Lipp P, Berridge MJ (2001) The organisation and functions of local Ca(2+) signals. J Cell Sci 114:2213-2222.
Boric M, Skopljanac I, Ferhatovic L, Jelicic Kadic A, Banozic A, Puljak L (2013) Reduced epidermal thickness, nerve degeneration and increased pain-related behavior in rats with diabetes type 1 and 2. J Chem Neuroanat 53:33-40.
Boucher P, Liu P, Gotthardt M, Hiesberger T, Anderson RG, Herz J (2002) Platelet-derived growth factor mediates tyrosine phosphorylation of the cytoplasmic domain of the low Density lipoprotein receptor-related protein in caveolae. J Biol Chem 277:15507-15513.
Brannagan TH, 3rd (2012) Current issues in peripheral neuropathy. J Peripher Nerv Syst 17 Suppl 2:1-3.
Bridgman PC, Dailey ME (1989) The organization of myosin and actin in rapid frozen nerve growth cones. J Cell Biol 108:95-109.
Brown J, Bianco JI, McGrath JJ, Eyles DW (2003) 1,25-dihydroxyvitamin D3 induces nerve growth factor, promotes neurite outgrowth and inhibits mitosis in embryonic rat hippocampal neurons. Neurosci Lett 343:139-143.
Brown MS, Herz J, Goldstein JL (1997) LDL-receptor structure. Calcium cages, acid baths and recycling receptors. Nature 388:629-630.
Brown SD, Twells RC, Hey PJ, Cox RD, Levy ER, Soderman AR, Metzker ML, Caskey CT, Todd JA, Hess JF (1998) Isolation and characterization of LRP6, a novel member of the low density lipoprotein receptor gene family. Biochem Biophys Res Commun 248:879-888.
Brunet A, Datta SR, Greenberg ME (2001) Transcription-dependent and -independent control of neuronal survival by the PI3K-Akt signaling pathway. Curr Opin Neurobiol 11:297-305.
Bu G, Geuze HJ, Strous GJ, Schwartz AL (1995) 39 kDa receptor-associated protein is an ER resident protein and molecular chaperone for LDL receptor-related protein. EMBO J 14:2269-2280.

Bu G, Maksymovitch EA, Nerbonne JM, Schwartz AL (1994) Expression and function of the low density lipoprotein receptor-related protein (LRP) in mammalian central neurons. J Biol Chem 269:18521-18528.

Bu G, Maksymovitch EA, Schwartz AL (1993) Receptor-mediated endocytosis of tissue-type plasminogen activator by low density lipoprotein receptor-related protein on human hepatoma HepG2 cells. J Biol Chem 268:13002-13009.

Buchman VL, Davies AM (1993) Different neurotrophins are expressed and act in a developmental sequence to promote the survival of embryonic sensory neurons. Development 118:989-1001.

Buffo A, Rolando C, Ceruti S (2009) Astrocytes in the damaged brain: Molecular and cellular insights into their reactive response and healing potential. Biochem Pharmacol.

Cabanlit M, Wills S, Goines P, Ashwood P, Van de Water J (2007) Brain-specific autoantibodies in the plasma of subjects with autistic spectrum disorder. Ann N Y Acad Sci 1107:92-103.

Cajal RY (1952) Structure and connections of neurons. Bull Los Angel Neuro Soc 17:5-46.

Calcutt NA, Jolivalt CG, Fernyhough P (2008) Growth factors as therapeutics for diabetic neuropathy. Curr Drug Targets 9:47-59.

Callaghan BC, Cheng HT, Stables CL, Smith AL, Feldman EL (2012) Diabetic neuropathy: clinical manifestations and current treatments. Lancet Neurol 11:521-534.

Candrilli SD, Davis KL, Kan HJ, Lucero MA, Rousculp MD (2007) Prevalence and the associated burden of illness of symptoms of diabetic peripheral neuropathy and diabetic retinopathy. J Diabetes Complications 21:306-314.

Cannell JJ, Grant WB (2013) What is the role of vitamin D in autism? Dermatoendocrinol 5:199-204.

Carmeliet P, Bouche A, De Clercq C, Janssen S, Pollefeyt S, Wyns S, Mulligan RC, Collen D (1995) Biological effects of disruption of the tissue-type plasminogen activator, urokinase-type plasminogen activator, and plasminogen activator inhibitor-1 genes in mice. Ann N Y Acad Sci 748:367-381; discussion 381-362.

Carmeliet P, Tessier-Lavigne M (2005) Common mechanisms of nerve and blood vessel wiring. Nature 436:193-200.

Carrasco J, Penkowa M, Giralt M, Camats J, Molinero A, Campbell IL, Palmiter RD, Hidalgo J (2003) Role of metallothionein-III following central nervous system damage. Neurobiol Dis 13:22-36.

Carrasco J, Penkowa M, Hadberg H, Molinero A, Hidalgo J (2000) Enhanced seizures and hippocampal neurodegeneration following kainic acid-induced seizures in metallothionein-I + II-deficient mice. Eur J Neurosci 12:2311-2322.

Caterina MJ, Schumacher MA, Tominaga M, Rosen TA, Levine JD, Julius D (1997) The capsaicin receptor: a heat-activated ion channel in the pain pathway. Nature 389:816-824.

Caudy M, Bentley D (1986) Pioneer growth cone steering along a series of neuronal and non-neuronal cues of different affinities. J Neurosci 6:1781-1795.

Cavus I, Koo PH, Teyler TJ (1996) Inhibition of long-term potentiation development in rat hippocampal slice by alpha 2-macroglobulin, an acute-phase protein in the brain. J Neurosci Res 43:282-288.

Chabas JF, Stephan D, Marqueste T, Garcia S, Lavaut MN, Nguyen C, Legre R, Khrestchatisky M, Decherchi P, Feron F (2013) Cholecalciferol (vitamin D(3)) improves myelination and recovery after nerve injury. PLoS One 8:e65034.

Chang HY, Takei K, Sydor AM, Born T, Rusnak F, Jay DG (1995) Asymmetric retraction of growth cone filopodia following focal inactivation of calcineurin. Nature 376:686-690.

Chang L, Karin M (2001) Mammalian MAP kinase signalling cascades. Nature 410:37-40.

Chatterjee M (2001) Vitamin D and genomic stability. Mutat Res 475:69-87.

Chen SR, Cai YQ, Pan HL (2009) Plasticity and emerging role of BKCa channels in nociceptive control in neuropathic pain. J Neurochem 110:352-362.

Chen Y, Beffert U, Ertunc M, Tang TS, Kavalali ET, Bezprozvanny I, Herz J (2005) Reelin modulates NMDA receptor activity in cortical neurons. J Neurosci 25:8209-8216.

Cheng L, Tian Z, Sun R, Wang Z, Shen J, Shan Z, Jin L, Lei L (2011) ApoER2 and VLDLR in the developing human telencephalon. Eur J Paediatr Neurol 15:361-367.

Cheng Y, Tao Y, Black IB, DiCicco-Bloom E (2001) A single peripheral injection of basic fibroblast growth factor (bFGF) stimulates granule cell production and increases cerebellar growth in newborn rats. J Neurobiol 46:220-229.

Cherian MG, Apostolova MD (2000) Nuclear localization of metallothionein during cell proliferation and differentiation. Cell Mol Biol (Noisy-le-grand) 46:347-356.

Christ A, Christa A, Kur E, Lioubinski O, Bachmann S, Willnow TE, Hammes A (2012) LRP2 is an auxiliary SHH receptor required to condition the forebrain ventral midline for inductive signals. Dev Cell 22:268-278.

Christensen EI, Birn H (2002) Megalin and cubilin: multifunctional endocytic receptors. Nat Rev Mol Cell Biol 3:256-266.

Christianson JA, Ryals JM, Johnson MS, Dobrowsky RT, Wright DE (2007) Neurotrophic modulation of myelinated cutaneous innervation and mechanical sensory loss in diabetic mice. Neuroscience 145:303-313.

Chun JT, Wang L, Pasinetti GM, Finch CE, Zlokovic BV (1999) Glycoprotein 330/megalin (LRP-2) has low prevalence as mRNA and protein in brain microvessels and choroid plexus. Exp Neurol 157:194-201.

Chung RS, Penkowa M, Dittmann J, King CE, Bartlett C, Asmussen JW, Hidalgo J, Carrasco J, Leung YK, Walker AK, Fung SJ, Dunlop SA, Fitzgerald M, Beazley LD, Chuah MI, Vickers JC, West AK (2008) Redefining the role of metallothionein within the injured brain: extracellular metallothioneins play an important role in the astrocyte-neuron response to injury. J Biol Chem 283:15349-15358.

Chung RS, Vickers JC, Chuah MI, West AK (2003) Metallothionein-IIA promotes initial neurite elongation and postinjury reactive neurite growth and facilitates healing after focal cortical brain injury. J Neurosci 23:3336-3342.

Clements RS, Jr. (1986) The polyol pathway. A historical review. Drugs 32 Suppl 2:3-5.

Coggeshall RE, Carlton SM (1998) Ultrastructural analysis of NMDA, AMPA, and kainate receptors on unmyelinated and myelinated axons in the periphery. J Comp Neurol 391:78-86.

Cohen S, Levi-Montalcini R, Hamburger V (1954) A NERVE GROWTH-STIMULATING FACTOR ISOLATED FROM SARCOM AS 37 AND 180. Proc Natl Acad Sci U S A 40:1014-1018.

Conklin MW, Lin MS, Spitzer NC (2005) Local calcium transients contribute to disappearance of pFAK, focal complex removal and deadhesion of neuronal growth cones and fibroblasts. Dev Biol 287:201-212.

Cornet A, Baudet C, Neveu I, Baron-Van Evercooren A, Brachet P, Naveilhan P (1998) 1,25-Dihydroxyvitamin D3 regulates the expression of VDR and NGF gene in Schwann cells in vitro. J Neurosci Res 53:742-746.

Coyle P, Philcox JC, Carey LC, Rofe AM (2002) Metallothionein: the multipurpose protein. Cell Mol Life Sci 59:627-647.

Crookston KP, Webb DJ, Wolf BB, Gonias SL (1994) Classification of alpha 2-macroglobulin-cytokine interactions based on affinity of noncovalent association in solution under apparent equilibrium conditions. J Biol Chem 269:1533-1540.

Cui X, McGrath JJ, Burne TH, Mackay-Sim A, Eyles DW (2007) Maternal vitamin D depletion alters neurogenesis in the developing rat brain. Int J Dev Neurosci 25:227-232.

D'Arcangelo G (2005) Apoer2: a reelin receptor to remember. Neuron 47:471-473.

D'Arcangelo G, Homayouni R, Keshvara L, Rice DS, Sheldon M, Curran T (1999) Reelin is a ligand for lipoprotein receptors. Neuron 24:471-479.

Davies AM (1994) The role of neurotrophins during successive stages of sensory neuron development. Prog Growth Factor Res 5:263-289.

Dean AJ, Bellgrove MA, Hall T, Phan WM, Eyles DW, Kvaskoff D, McGrath JJ (2011) Effects of vitamin D supplementation on cognitive and emotional functioning in young adults--a randomised controlled trial. PLoS One 6:e25966.

Deutsch SI, Burket JA, Katz E (2010) Does subtle disturbance of neuronal migration contribute to schizophrenia and other neurodevelopmental disorders? Potential genetic mechanisms with possible treatment implications. Eur Neuropsychopharmacol 20:281-287.

Dey I, Midha N, Singh G, Forsyth A, Walsh SK, Singh B, Kumar R, Toth C, Midha R (2013) Diabetic Schwann cells suffer from nerve growth factor and neurotrophin-3 underproduction and poor associability with axons. Glia 61:1990-1999.

Dickson BJ (2002) Molecular mechanisms of axon guidance. Science 298:1959-1964.

Dixit N, Bali V, Baboota S, Ahuja A, Ali J (2007) Iontophoresis - an approach for controlled drug delivery: a review. Curr Drug Deliv 4:1-10.

Doherty P, Williams G, Williams EJ (2000) CAMs and axonal growth: a critical evaluation of the role of calcium and the MAPK cascade. Mol Cell Neurosci 16:283-295.

Domanitskaya E, Wacker A, Mauti O, Baeriswyl T, Esteve P, Bovolenta P, Stoeckli ET (2010) Sonic hedgehog guides post-crossing commissural axons both directly and indirectly by regulating Wnt activity. J Neurosci 30:11167-11176.

Dontchev VD, Letourneau PC (2003) Growth cones integrate signaling from multiple guidance cues. J Histochem Cytochem 51:435-444.

Du Y, Bales KR, Dodel RC, Liu X, Glinn MA, Horn JW, Little SP, Paul SM (1998) Alpha2-macroglobulin attenuates beta-amyloid peptide 1-40 fibril formation and associated neurotoxicity of cultured fetal rat cortical neurons. J Neurochem 70:1182-1188.

Dyck PJ, Albers JW, Andersen H, Arezzo JC, Biessels GJ, Bril V, Feldman EL, Litchy WJ, O'Brien PC, Russell JW (2011) Diabetic Polyneuropathies: Update on Research Definition, Diagnostic Criteria and Estimation of Severity. Diabetes Metab Res Rev.

Dyck PJ, Kratz KM, Karnes JL, Litchy WJ, Klein R, Pach JM, Wilson DM, O'Brien PC, Melton LJ, 3rd, Service FJ (1993) The prevalence by staged severity of various types of diabetic neuropathy, retinopathy, and nephropathy in a population-based cohort: the Rochester Diabetic Neuropathy Study. Neurology 43:817-824.

Dyson SE, Harvey AR, Trapp BD, Heath JW (1988) Ultrastructural and immunohistochemical analysis of axonal regrowth and myelination in membranes which form over lesion sites in the rat visual system. J Neurocytol 17:797-808.

Eade KT, Allan DW (2009) Neuronal phenotype in the mature nervous system is maintained by persistent retrograde bone morphogenetic protein signaling. J Neurosci 29:3852-3864.

Ebenezer GJ, O'Donnell R, Hauer P, Cimino NP, McArthur JC, Polydefkis M (2011) Impaired neurovascular repair in subjects with diabetes following experimental intracutaneous axotomy. Brain 134:1853-1863.

Ekstrom AR, Tomlinson DR (1989) Impaired nerve regeneration in streptozotocin-diabetic rats. Effects of treatment with an aldose reductase inhibitor. J Neurol Sci 93:231-237.

Esadeg S, He H, Pijnenborg R, Van Leuven F, Croy BA (2003) Alpha-2 macroglobulin controls trophoblast positioning in mouse implantation sites. Placenta 24:912-921.

Eyles D, Brown J, Mackay-Sim A, McGrath J, Feron F (2003) Vitamin D3 and brain development. Neuroscience 118:641-653.

Eyles DW, Feron F, Cui X, Kesby JP, Harms LH, Ko P, McGrath JJ, Burne TH (2009) Developmental vitamin D deficiency causes abnormal brain development. Psychoneuroendocrinology 34 Suppl 1:S247-257.

Ezeoke A, Mellor A, Buckley P, Miller B (2013) A systematic, quantitative review of blood autoantibodies in schizophrenia. Schizophr Res 150:245-251.

Facer P, Casula MA, Smith GD, Benham CD, Chessell IP, Bountra C, Sinisi M, Birch R, Anand P (2007) Differential expression of the capsaicin receptor TRPV1 and related novel receptors TRPV3, TRPV4 and TRPM8 in normal human tissues and changes in traumatic and diabetic neuropathy. BMC Neurol 7:11.

Fagan AM, Bu G, Sun Y, Daugherty A, Holtzman DM (1996) Apolipoprotein E-containing high density lipoprotein promotes neurite outgrowth and is a ligand for the low density lipoprotein receptor-related protein. J Biol Chem 271:30121-30125.

Fan J, Raper JA (1995) Localized collapsing cues can steer growth cones without inducing their full collapse. Neuron 14:263-274.

Fang JY, Lee WR, Shen SC, Fang YP, Hu CH (2004) Enhancement of topical 5-aminolaevulinic acid delivery by erbium:YAG laser and microdermabrasion: a comparison with iontophoresis and electroporation. Br J Dermatol 151:132-140.

Farmer KL, Li C, Dobrowsky RT (2012) Diabetic peripheral neuropathy: should a chaperone accompany our therapeutic approach? Pharmacol Rev 64:880-900.

Ferguson IA, Johnson EM, Jr. (1991) Fibroblast growth factor receptor-bearing neurons in the CNS: identification by receptor-mediated retrograde transport. J Comp Neurol 313:693-706.

Fernando GJ, Chen X, Prow TW, Crichton ML, Fairmaid EJ, Roberts MS, Frazer IH, Brown LE, Kendall MA (2010) Potent immunity to low doses of influenza vaccine by probabilistic guided micro-targeted skin delivery in a mouse model. PLoS One 5:e10266.

Feron F, Burne TH, Brown J, Smith E, McGrath JJ, Mackay-Sim A, Eyles DW (2005) Developmental Vitamin D3 deficiency alters the adult rat brain. Brain Res Bull 65:141-148.

Figliuzzi M, Bianchi R, Cavagnini C, Lombardi R, Porretta-Serapiglia C, Lauria G, Avezza F, Canta A, Carozzi V, Chiorazzi A, Marmiroli P, Meregalli C, Oggioni N, Sala B, Cavaletti G, Remuzzi A (2013) Islet transplantation and insulin administration relieve long-term complications and rescue the residual endogenous pancreatic beta cells. Am J Pathol 183:1527-1538.

Fitch MT, Silver J (2008) CNS injury, glial scars, and inflammation: Inhibitory extracellular matrices and regeneration failure. Exp Neurol 209:294-301.

Fitzgerald M, Nairn P, Bartlett CA, Chung RS, West AK, Beazley LD (2007) Metallothionein-IIA promotes neurite growth via the megalin receptor. Exp Brain Res 183:171-180.

Fleming CE, Mar FM, Franquinho F, Saraiva MJ, Sousa MM (2009a) Transthyretin internalization by sensory neurons is megalin mediated and necessary for its neuritogenic activity. J Neurosci 29:3220-3232.

Fleming CE, Nunes AF, Sousa MM (2009b) Transthyretin: more than meets the eye. Prog Neurobiol.

Fleming CE, Saraiva MJ, Sousa MM (2007) Transthyretin enhances nerve regeneration. J Neurochem 103:831-839.

Flores AJ, Lavernia CJ, Owens PW (2000) Anatomy and physiology of peripheral nerve injury and repair. Am J Orthop 29:167-173.

Folch J, Pedros I, Patraca I, Sureda F, Junyent F, Beas-Zarate C, Verdaguer E, Pallas M, Auladell C, Camins A (2012) Neuroprotective and anti-ageing role of leptin. J Mol Endocrinol 49:R149-156.

Forbes EM, Thompson AW, Yuan J, Goodhill GJ (2012) Calcium and cAMP levels interact to determine attraction versus repulsion in axon guidance. Neuron 490-503.

Gajera CR, Emich H, Lioubinski O, Christ A, Beckervordersandforth-Bonk R, Yoshikawa K, Bachmann S, Christensen EI, Gotz M, Kempermann G, Peterson AS, Willnow TE, Hammes A (2010) LRP2 in ependymal cells regulates BMP signaling in the adult neurogenic niche. J Cell Sci 123:1922-1930.

Gallagher H, Oleinikov AV, Fenske C, Newman DJ (2004) The adaptor disabled-2 binds to the third psi xNPxY sequence on the cytoplasmic tail of megalin. Biochimie 86:179-182.

Gallo G, Lefcort FB, Letourneau PC (1997) The trkA receptor mediates growth cone turning toward a localized source of nerve growth factor. J Neurosci 17:5445-5454.

Gallo G, Letourneau P (2002) Axon guidance: proteins turnover in turning growth cones. Curr Biol 12:R560-562.

Gallo G, Yee HF, Jr., Letourneau PC (2002) Actin turnover is required to prevent axon retraction driven by endogenous actomyosin contractility. J Cell Biol 158:1219-1228.

Garcion E, Wion-Barbot N, Montero-Menei CN, Berger F, Wion D (2002) New clues about vitamin D functions in the nervous system. Trends Endocrinol Metab 13:100-105.

Gasperini R, Choi-Lundberg D, Thompson MJ, Mitchell CB, Foa L (2009) Homer regulates calcium signalling in growth cone turning. Neural Dev 4:29.

Gasperini RJ, Hou X, Parkington H, Coleman H, Klaver DW, Vincent AJ, Foa LC, Small DH (2011) TRPM8 and Nav1.8 sodium channels are required for transthyretin-induced

calcium influx in growth cones of small-diameter TrkA-positive sensory neurons. Mol Neurodegener 6:19.
Gasteiger E, Hoogland C, Gattiker A, Duvaud S, Wilkins MR, Appel RD, Bairoch A (2005) Protein Identification and Analysis Tools on the ExPASy Server;. In: The Proteomics Protocols Handbook, Humana Press vol. pp. 571-607 (Walker, J., ed).
Gaultier A, Arandjelovic S, Li X, Janes J, Dragojlovic N, Zhou GP, Dolkas J, Myers RR, Gonias SL, Campana WM (2008) A shed form of LDL receptor-related protein-1 regulates peripheral nerve injury and neuropathic pain in rodents. J Clin Invest 118:161-172.
Geng Z, Xu FY, Huang SH, Chen ZY (2011) Sorting protein-related receptor SorLA controls regulated secretion of glial cell line-derived neurotrophic factor. J Biol Chem 286:41871-41882.
Ghasemlou N, Von Hehn CA, Yekkikrala A, Chiu IM, Cobos EJ, Cronin SJ, Brenneis C, Ma ECH, Hwang S, Woolf CJ (2012) Activation of TRPA by the protein Metallothionein 2. In: Society for Neurosciences, vol. 784.08/NN12 New Orleans, LA.
Giralt M, Penkowa M, Hernandez J, Molinero A, Carrasco J, Lago N, Camats J, Campbell IL, Hidalgo J (2002a) Metallothionein-1+2 deficiency increases brain pathology in transgenic mice with astrocyte-targeted expression of interleukin 6. Neurobiol Dis 9:319-338.
Giralt M, Penkowa M, Lago N, Molinero A, Hidalgo J (2002b) Metallothionein-1+2 protect the CNS after a focal brain injury. Exp Neurol 173:114-128.
Glerup S, Lume M, Olsen D, Nyengaard JR, Vaegter CB, Gustafsen C, Christensen EI, Kjolby M, Hay-Schmidt A, Bender D, Madsen P, Saarma M, Nykjaer A, Petersen CM (2013) SorLA controls neurotrophic activity by sorting of GDNF and its receptors GFRalpha1 and RET. Cell Rep 3:186-199.
Gliemann J, Hermey G, Nykjaer A, Petersen CM, Jacobsen C, Andreasen PA (2004) The mosaic receptor sorLA/LR11 binds components of the plasminogen-activating system and platelet-derived growth factor-BB similarly to LRP1 (low-density lipoprotein receptor-related protein), but mediates slow internalization of bound ligand. Biochem J 381:203-212.
Gomez TM, Zheng JQ (2006) The molecular basis for calcium-dependent axon pathfinding. Nat Rev Neurosci 7:115-125.
Gonias SL, LaMarre J, Crookston KP, Webb DJ, Wolf BB, Lopes MB, Moses HL, Hayes MA (1994) Alpha 2-macroglobulin and the alpha 2-macroglobulin receptor/LRP. A growth regulatory axis. Ann N Y Acad Sci 737:273-290.
Gordon I, Grauer E, Genis I, Sehayek E, Michaelson DM (1995) Memory deficits and cholinergic impairments in apolipoprotein E-deficient mice. Neurosci Lett 199:1-4.
Gordon T (2009) The role of neurotrophic factors in nerve regeneration. Neurosurg Focus 26:E3.
Gotthardt M, Trommsdorff M, Nevitt MF, Shelton J, Richardson JA, Stockinger W, Nimpf J, Herz J (2000) Interactions of the low density lipoprotein receptor gene family with cytosolic adaptor and scaffold proteins suggest diverse biological functions in cellular communication and signal transduction. J Biol Chem 275:25616-25624.
Greene DA, Lattimer SA (1985) The polyol pathway in dysfunction of diabetic peripheral nerve. Diabet Med 2:206-210.

Grisold W, Cavaletti G, Windebank AJ (2012) Peripheral neuropathies from chemotherapeutics and targeted agents: diagnosis, treatment, and prevention. Neuro Oncol 14 Suppl 4:iv45-54.
Grobmyer SR, Kuo A, Orishimo M, Okada SS, Cines DB, Barnathan ES (1993) Determinants of binding and internalization of tissue-type plasminogen activator by human vascular smooth muscle and endothelial cells. J Biol Chem 268:13291-13300.
Grover LM, Teyler TJ (1990) Two components of long-term potentiation induced by different patterns of afferent activation. Nature 347:477-479.
Guirland C, Suzuki S, Kojima M, Lu B, Zheng JQ (2004) Lipid rafts mediate chemotropic guidance of nerve growth cones. Neuron 42:51-62.
Gundersen RW, Barrett JN (1980) Characterization of the turning response of dorsal root neurites toward nerve growth factor. J Cell Biol 87:546-554.
Guttman M, Prieto JH, Croy JE, Komives EA (2010) Decoding of lipoprotein-receptor interactions: properties of ligand binding modules governing interactions with apolipoprotein E. Biochemistry 49:1207-1216.
Hageman GS, Kirchoff-Rempe MA, Lewis GP, Fisher SK, Anderson DH (1991) Sequestration of basic fibroblast growth factor in the primate retinal interphotoreceptor matrix. Proc Natl Acad Sci U S A 88:6706-6710.
Hakansson L, Venge P (1983) Partial characterization and identification of chemokinetic factors in serum. Scand J Immunol 18:531-537.
Hampe W, Urny J, Franke I, Hoffmeister-Ullerich SA, Herrmann D, Petersen CM, Lohmann J, Schaller HC (1999) A head-activator binding protein is present in hydra in a soluble and a membrane-anchored form. Development 126:4077-4086.
Handelmann GE, Boyles JK, Weisgraber KH, Mahley RW, Pitas RE (1992) Effects of apolipoprotein E, beta-very low density lipoproteins, and cholesterol on the extension of neurites by rabbit dorsal root ganglion neurons in vitro. J Lipid Res 33:1677-1688.
Hanover JA, Willingham MC, Pastan I (1983) Receptor-mediated endocytosis of alpha 2-macroglobulin: solubilization and partial purification of the fibroblast alpha 2-macroglobulin receptor. Ann N Y Acad Sci 421:410-423.
Hargreaves K, Dubner R, Brown F, Flores C, Joris J (1988) A new and sensitive method for measuring thermal nociception in cutaneous hyperalgesia. Pain 32:77-88.
Harms LR, Burne TH, Eyles DW, McGrath JJ (2011) Vitamin D and the brain. Best Pract Res Clin Endocrinol Metab 25:657-669.
Hatten ME, Lynch M, Rydel RE, Sanchez J, Joseph-Silverstein J, Moscatelli D, Rifkin DB (1988) In vitro neurite extension by granule neurons is dependent upon astroglial-derived fibroblast growth factor. Dev Biol 125:280-289.
Haussler MR, Whitfield GK, Kaneko I, Haussler CA, Hsieh D, Hsieh JC, Jurutka PW (2013) Molecular mechanisms of vitamin D action. Calcif Tissue Int 92:77-98.
Hayashi H, Campenot RB, Vance DE, Vance JE (2007) Apolipoprotein E-containing lipoproteins protect neurons from apoptosis via a signaling pathway involving low-density lipoprotein receptor-related protein-1. J Neurosci 27:1933-1941.
He X, Semenov M, Tamai K, Zeng X (2004) LDL receptor-related proteins 5 and 6 in Wnt/beta-catenin signaling: arrows point the way. Development 131:1663-1677.
Henley JR, Huang KH, Wang D, Poo MM (2004) Calcium mediates bidirectional growth cone turning induced by myelin-associated glycoprotein. Neuron 44:909-916.

Herrup K, Sunter K (1987) Numerical matching during cerebellar development: quantitative analysis of granule cell death in staggerer mouse chimeras. J Neurosci 7:829-836.
Herz J (2009) Apolipoprotein E receptors in the nervous system. Curr Opin Lipidol 20:190-196.
Herz J, Bock HH (2002) Lipoprotein receptors in the nervous system. Annu Rev Biochem 71:405-434.
Herz J, Clouthier DE, Hammer RE (1992) LDL receptor-related protein internalizes and degrades uPA-PAI-1 complexes and is essential for embryo implantation. Cell 71:411-421.
Herz J, Goldstein JL, Strickland DK, Ho YK, Brown MS (1991) 39-kDa protein modulates binding of ligands to low density lipoprotein receptor-related protein/alpha 2-macroglobulin receptor. J Biol Chem 266:21232-21238.
Herz J, Gotthardt M, Willnow TE (2000) Cellular signalling by lipoprotein receptors. Curr Opin Lipidol 11:161-166.
Herz J, Hamann U, Rogne S, Myklebost O, Gausepohl H, Stanley KK (1988) Surface location and high affinity for calcium of a 500-kd liver membrane protein closely related to the LDL-receptor suggest a physiological role as lipoprotein receptor. EMBO J 7:4119-4127.
Hewer S, Lucas R, van der Mei I, Taylor BV (2013) Vitamin D and multiple sclerosis. J Clin Neurosci 20:634-641.
Hey PJ, Twells RC, Phillips MS, Yusuke N, Brown SD, Kawaguchi Y, Cox R, Guochun X, Dugan V, Hammond H, Metzker ML, Todd JA, Hess JF (1998) Cloning of a novel member of the low-density lipoprotein receptor family. Gene 216:103-111.
Hidalgo J, Aschner M, Zatta P, Vasak M (2001) Roles of the metallothionein family of proteins in the central nervous system. Brain Res Bull 55:133-145.
Hiesberger T, Trommsdorff M, Howell BW, Goffinet A, Mumby MC, Cooper JA, Herz J (1999) Direct binding of Reelin to VLDL receptor and ApoE receptor 2 induces tyrosine phosphorylation of disabled-1 and modulates tau phosphorylation. Neuron 24:481-489.
Higuchi M, Ito T, Imai Y, Iwaki T, Hattori M, Kohsaka S, Niho Y, Sakaki Y (1994) Expression of the alpha 2-macroglobulin-encoding gene in rat brain and cultured astrocytes. Gene 141:155-162.
Hines JH, Abu-Rub M, Henley JR (2010) Asymmetric endocytosis and remodeling of beta1-integrin adhesions during growth cone chemorepulsion by MAG. Nat Neurosci 13:829-837.
Hjalm G, Murray E, Crumley G, Harazim W, Lundgren S, Onyango I, Ek B, Larsson M, Juhlin C, Hellman P, Davis H, Akerstrom G, Rask L, Morse B (1996) Cloning and sequencing of human gp330, a Ca(2+)-binding receptor with potential intracellular signaling properties. Eur J Biochem 239:132-137.
Hocevar BA, Mou F, Rennolds JL, Morris SM, Cooper JA, Howe PH (2003) Regulation of the Wnt signaling pathway by disabled-2 (Dab2). EMBO J 22:3084-3094.
Hoe HS, Rebeck GW (2005) Regulation of ApoE receptor proteolysis by ligand binding. Brain Res Mol Brain Res 137:31-39.
Hoffman PN, Cleveland DW (1988) Neurofilament and tubulin expression recapitulates the developmental program during axonal regeneration: induction of a specific beta-tubulin isotype. Proc Natl Acad Sci U S A 85:4530-4533.

Hoglund K, Salter H (2013) Molecular biomarkers of neurodegeneration. Expert Rev Mol Diagn 13:845-861.
Hollo A, Clemens Z, Kamondi A, Lakatos P, Szucs A (2012) Correction of vitamin D deficiency improves seizure control in epilepsy: a pilot study. Epilepsy Behav 24:131-133.
Hollyday M, Morgan-Carr M (1995) Chick wing innervation. II. Morphology of motor and sensory axons and their growth cones during early development. J Comp Neurol 357:254-271.
Holtzman DM, Pitas RE, Kilbridge J, Nathan B, Mahley RW, Bu G, Schwartz AL (1995) Low density lipoprotein receptor-related protein mediates apolipoprotein E-dependent neurite outgrowth in a central nervous system-derived neuronal cell line. Proc Natl Acad Sci U S A 92:9480-9484.
Hong S, Wiley JW (2005) Early painful diabetic neuropathy is associated with differential changes in the expression and function of vanilloid receptor 1. J Biol Chem 280:618-627.
Hosaka K, Takeda T, Iino N, Hosojima M, Sato H, Kaseda R, Yamamoto K, Kobayashi A, Gejyo F, Saito A (2009) Megalin and nonmuscle myosin heavy chain IIA interact with the adaptor protein Disabled-2 in proximal tubule cells. Kidney Int 75:1308-1315.
Hou YW, Chan MH, Hsu HR, Liu BR, Chen CP, Chen HH, Lee HJ (2007) Transdermal delivery of proteins mediated by non-covalently associated arginine-rich intracellular delivery peptides. Exp Dermatol 16:999-1006.
Houston DW, Wylie C (2002) Cloning and expression of Xenopus Lrp5 and Lrp6 genes. Mech Dev 117:337-342.
Hu K, Yang J, Tanaka S, Gonias SL, Mars WM, Liu Y (2006) Tissue-type plasminogen activator acts as a cytokine that triggers intracellular signal transduction and induces matrix metalloproteinase-9 gene expression. J Biol Chem 281:2120-2127.
Hu YM, Chen SR, Chen H, Pan HL (2014) CK2 Inhibition Reverses Pain Hypersensitivity and Potentiated Spinal NMDA Receptor Activity Caused by Calcineurin Inhibitor. J Pharmacol Exp Ther.
Hu YQ, Dluzen DE, Koo PH (1994) Intracranial infusion of monoamine-activated alpha 2-macroglobulin decreases dopamine concentrations within the rat caudate putamen. J Neurosci Res 38:531-537.
Huang CH, Cheng JC, Chen JC, Tseng CP (2007) Evaluation of the role of Disabled-2 in nerve growth factor-mediated neurite outgrowth and cellular signalling. Cell Signal 19:1339-1347.
Huang SS, Ling TY, Tseng WF, Huang YH, Tang FM, Leal SM, Huang JS (2003) Cellular growth inhibition by IGFBP-3 and TGF-beta1 requires LRP-1. FASEB J 17:2068-2081.
Huang YZ, Pan E, Xiong ZQ, McNamara JO (2008) Zinc-mediated transactivation of TrkB potentiates the hippocampal mossy fiber-CA3 pyramid synapse. Neuron 57:546-558.
Huebner EA, Strittmatter SM (2009) Axon regeneration in the peripheral and central nervous systems. Results Probl Cell Differ 48:339-351.
Ibanez CF (2010) Beyond the cell surface: new mechanisms of receptor function. Biochem Biophys Res Commun 396:24-27.

Islam MS (2013) Animal models of diabetic neuropathy: progress since 1960s. J Diabetes Res 2013:149452.
Islam MS, Choi H (2007) Nongenetic model of type 2 diabetes: a comparative study. Pharmacology 79:243-249.
Ito H, Morishita R, Iwamoto I, Mizuno M, Nagata K (2013a) MAGI-1 acts as a scaffolding molecule for NGF receptor-mediated signaling pathway. Biochim Biophys Acta 1833:2302-2310.
Ito H, Morishita R, Sudo K, Nishimura YV, Inaguma Y, Iwamoto I, Nagata K (2012) Biochemical and morphological characterization of MAGI-1 in neuronal tissue. J Neurosci Res 90:1776-1781.
Ito Y, Tanaka H, Hara H (2013b) The potential roles of metallothionein as a therapeutic target for cerebral ischemia and retinal diseases. Curr Pharm Biotechnol 14:400-407.
Jacobsen L, Madsen P, Jacobsen C, Nielsen MS, Gliemann J, Petersen CM (2001) Activation and functional characterization of the mosaic receptor SorLA/LR11. J Biol Chem 276:22788-22796.
Ji Y, Gong Y, Gan W, Beach T, Holtzman DM, Wisniewski T (2003) Apolipoprotein E isoform-specific regulation of dendritic spine morphology in apolipoprotein E transgenic mice and Alzheimer's disease patients. Neuroscience 122:305-315.
Julius D, Basbaum AI (2001) Molecular mechanisms of nociception. Nature 413:203-210.
Kantarci S, Al-Gazali L, Hill RS, Donnai D, Black GC, Bieth E, Chassaing N, Lacombe D, Devriendt K, Teebi A, Loscertales M, Robson C, Liu T, MacLaughlin DT, Noonan KM, Russell MK, Walsh CA, Donahoe PK, Pober BR (2007) Mutations in LRP2, which encodes the multiligand receptor megalin, cause Donnai-Barrow and facio-oculo-acoustico-renal syndromes. Nat Genet 39:957-959.
Karande P, Jain A, Mitragotri S (2004) Discovery of transdermal penetration enhancers by high-throughput screening. Nat Biotechnol 22:192-197.
Kato M, Patel MS, Levasseur R, Lobov I, Chang BH, Glass DA, 2nd, Hartmann C, Li L, Hwang TH, Brayton CF, Lang RA, Karsenty G, Chan L (2002) Cbfa1-independent decrease in osteoblast proliferation, osteopenia, and persistent embryonic eye vascularization in mice deficient in Lrp5, a Wnt coreceptor. J Cell Biol 157:303-314.
Kelly OG, Pinson KI, Skarnes WC (2004) The Wnt co-receptors Lrp5 and Lrp6 are essential for gastrulation in mice. Development 131:2803-2815.
Kennedy JM, Zochodne DW (2005) Impaired peripheral nerve regeneration in diabetes mellitus. J Peripher Nerv Syst 10:144-157.
Kennedy WR, Nolano M, Wendelschafer-Crabb G, Johnson TL, Tamura E (1999) A skin blister method to study epidermal nerves in peripheral nerve disease. Muscle Nerve 22:360-371.
Kennedy WR, Wendelschafer-Crabb G (1993) The innervation of human epidermis. J Neurol Sci 115:184-190.
Kim DH, Iijima H, Goto K, Sakai J, Ishii H, Kim HJ, Suzuki H, Kondo H, Saeki S, Yamamoto T (1996) Human apolipoprotein E receptor 2. A novel lipoprotein receptor of the low density lipoprotein receptor family predominantly expressed in brain. J Biol Chem 271:8373-8380.
Kim HG, Hwang YP, Han EH, Choi CY, Yeo CY, Kim JY, Lee KY, Jeong HG (2009) Metallothionein-III provides neuronal protection through activation of nuclear factor-

kappaB via the TrkA/phosphatidylinositol-3 kinase/Akt signaling pathway. Toxicol Sci 112:435-449.
Kirstein M, Farinas I (2002) Sensing life: regulation of sensory neuron survival by neurotrophins. Cell Mol Life Sci 59:1787-1802.
Kiselyov K, Xu X, Mozhayeva G, Kuo T, Pessah I, Mignery G, Zhu X, Birnbaumer L, Muallem S (1998) Functional interaction between InsP3 receptors and store-operated Htrp3 channels. Nature 396:478-482.
Klassen RB, Crenshaw K, Kozyraki R, Verroust PJ, Tio L, Atrian S, Allen PL, Hammond TG (2004) Megalin mediates renal uptake of heavy metal metallothionein complexes. Am J Physiol Renal Physiol 287:F393-403.
Klein R, Martin-Zanca D, Barbacid M, Parada LF (1990) Expression of the tyrosine kinase receptor gene trkB is confined to the murine embryonic and adult nervous system. Development 109:845-850.
Klein R, Nanduri V, Jing SA, Lamballe F, Tapley P, Bryant S, Cordon-Cardo C, Jones KR, Reichardt LF, Barbacid M (1991) The trkB tyrosine protein kinase is a receptor for brain-derived neurotrophic factor and neurotrophin-3. Cell 66:395-403.
Knauer MF, Orlando RA, Glabe CG (1996) Cell surface APP751 forms complexes with protease nexin 2 ligands and is internalized via the low density lipoprotein receptor-related protein (LRP). Brain Res 740:6-14.
Kobayashi H, Uchida Y, Ihara Y, Nakajima K, Kohsaka S, Miyatake T, Tsuji S (1993) Molecular cloning of rat growth inhibitory factor cDNA and the expression in the central nervous system. Brain Res Mol Brain Res 19:188-194.
Koch KW, Stryer L (1988) Highly cooperative feedback control of retinal rod guanylate cyclase by calcium ions. Nature 334:64-66.
Kodelja V, Heisig M, Northemann W, Heinrich PC, Zimmermann W (1986) Alpha 2-macroglobulin gene expression during rat development studied by in situ hybridization. EMBO J 5:3151-3156.
Kolodkin AL (1996) Growth cones and the cues that repel them. Trends Neurosci 19:507-513.
Korey CA, Van Vactor D (2000) From the growth cone surface to the cytoskeleton: one journey, many paths. J Neurobiol 44:184-193.
Korwek KM, Trotter JH, Ladu MJ, Sullivan PM, Weeber EJ (2009) ApoE isoform-dependent changes in hippocampal synaptic function. Mol Neurodegener 4:21.
Krieger M, Herz J (1994) Structures and functions of multiligand lipoprotein receptors: macrophage scavenger receptors and LDL receptor-related protein (LRP). Annu Rev Biochem 63:601-637.
Krystosek A, Seeds NW (1981) Plasminogen activator release at the neuronal growth cone. Science 213:1532-1534.
Krystosek A, Seeds NW (1984) Peripheral neurons and Schwann cells secrete plasminogen activator. J Cell Biol 98:773-776.
Krystosek A, Seeds NW (1986) Normal and malignant cells, including neurons, deposit plasminogen activator on the growth substrata. Exp Cell Res 166:31-46.
Kung LH, Gong K, Adedoyin M, Ng J, Bhargava A, Ohara PT, Jasmin L (2013) Evidence for glutamate as a neuroglial transmitter within sensory ganglia. PLoS One 8:e68312.
Kur E, Christa A, Veth KN, Gajera CR, Andrade-Navarro MA, Zhang J, Willer JR, Gregg RG, Abdelilah-Seyfried S, Bachmann S, Link BA, Hammes A, Willnow TE (2011)

Loss of Lrp2 in zebrafish disrupts pronephric tubular clearance but not forebrain development. Dev Dyn 240:1567-1577.
Kyriakis JM, Banerjee P, Nikolakaki E, Dai T, Rubie EA, Ahmad MF, Avruch J, Woodgett JR (1994) The stress-activated protein kinase subfamily of c-Jun kinases. Nature 369:156-160.
Lamballe F, Klein R, Barbacid M (1991) trkC, a new member of the trk family of tyrosine protein kinases, is a receptor for neurotrophin-3. Cell 66:967-979.
Landmesser L (1986) Axonal guidance and the formation of neuronal circuits. Trends in Neurosciences.
Larin SS, Gorlina NK, Kozlov IG, Cheredeev AN, Zorin NA, Zorina RM (2002) Binding of alpha2-macroglobulin to collagen type I: modification of collagen matrix by alpha2-macroglobulin induces the enhancement of macrophage migration. Russ J Immunol 7:34-40.
Larsson M, Hjalm G, Sakwe AM, Engstrom A, Hoglund AS, Larsson E, Robinson RC, Sundberg C, Rask L (2003) Selective interaction of megalin with postsynaptic density-95 (PSD-95)-like membrane-associated guanylate kinase (MAGUK) proteins. Biochem J 373:381-391.
Lauren J, Gimbel DA, Nygaard HB, Gilbert JW, Strittmatter SM (2009) Cellular prion protein mediates impairment of synaptic plasticity by amyloid-beta oligomers. Nature 457:1128-1132.
Lauria G (2007) Recent developments in the management of peripheral neuropathy using skin biopsy. Rev Neurol (Paris) 163:1266-1270.
Lauria G, Borgna M, Morbin M, Lombardi R, Mazzoleni G, Sghirlanzoni A, Pareyson D (2004) Tubule and neurofilament immunoreactivity in human hairy skin: markers for intraepidermal nerve fibers. Muscle Nerve 30:310-316.
Lauria G, Cornblath DR, Johansson O, McArthur JC, Mellgren SI, Nolano M, Rosenberg N, Sommer C (2005) EFNS guidelines on the use of skin biopsy in the diagnosis of peripheral neuropathy. Eur J Neurol 12:747-758.
Lauria G, Hsieh ST, Johansson O, Kennedy WR, Leger JM, Mellgren SI, Nolano M, Merkies IS, Polydefkis M, Smith AG, Sommer C, Valls-Sole J (2010) European Federation of Neurological Societies/Peripheral Nerve Society Guideline on the use of skin biopsy in the diagnosis of small fiber neuropathy. Report of a joint task force of the European Federation of Neurological Societies and the Peripheral Nerve Society. Eur J Neurol 17:903-912, e944-909.
Lauria G, Morbin M, Lombardi R, Borgna M, Mazzoleni G, Sghirlanzoni A, Pareyson D (2003) Axonal swellings predict the degeneration of epidermal nerve fibers in painful neuropathies. Neurology 61:631-636.
Lazo JS, Kondo Y, Dellapiazza D, Michalska AE, Choo KH, Pitt BR (1995) Enhanced sensitivity to oxidative stress in cultured embryonic cells from transgenic mice deficient in metallothionein I and II genes. J Biol Chem 270:5506-5510.
Lee TC, Barshes NR, O'Mahony CA, Nguyen L, Brunicardi FC, Ricordi C, Alejandro R, Schock AP, Mote A, Goss JA (2005) The effect of pancreatic islet transplantation on progression of diabetic retinopathy and neuropathy. Transplant Proc 37:2263-2265.
Leinninger GM, Vincent AM, Feldman EL (2004) The role of growth factors in diabetic peripheral neuropathy. J Peripher Nerv Syst 9:26-53.

Leung J, Bennett W, Herbert R, West A, Lee P, Wake H, Fields R, Chuah M, Chung R (2012) Metallothionein promotes regenerative axonal sprouting of dorsal root ganglion neurons after physical axotomy. Cell Mol Life Sci 69:809-817.

Leung JY, Bennett WR, Herbert RP, West AK, Lee PR, Wake H, Fields RD, Chuah MI, Chung RS (2012) Metallothionein promotes regenerative axonal sprouting of dorsal root ganglion neurons after physical axotomy. Cell Mol Life Sci 69:809-817.

Levi-Montalcini R (1979) Trophic, tropic and transforming effects of the nerve growth factor on its target cells. Bull Mem Acad R Med Belg 134:217-228.

Levi-Montalcini R, Angeletti PU (1963) Essential role of the nerve growth factor in the survival and maintenance of dissociated sensory and sympathetic embryonic nerve cells in vitro. Dev Biol 7:653-659.

Levin ED, Perraut C, Pollard N, Freedman JH (2006) Metallothionein expression and neurocognitive function in mice. Physiol Behav 87:513-518.

Lewis AK, Bridgman PC (1992) Nerve growth cone lamellipodia contain two populations of actin filaments that differ in organization and polarity. J Cell Biol 119:1219-1243.

Li Y, Cam J, Bu G (2001a) Low-density lipoprotein receptor family: endocytosis and signal transduction. Mol Neurobiol 23:53-67.

Li Y, Cong R, Biemesderfer D (2008) The COOH terminus of megalin regulates gene expression in opossum kidney proximal tubule cells. Am J Physiol Cell Physiol 295:C529-537.

Li Y, Jia YC, Cui K, Li N, Zheng ZY, Wang YZ, Yuan XB (2005) Essential role of TRPC channels in the guidance of nerve growth cones by brain-derived neurotrophic factor. Nature 434:894-898.

Li Y, van Kerkhof P, Marzolo MP, Strous GJ, Bu G (2001b) Identification of a major cyclic AMP-dependent protein kinase A phosphorylation site within the cytoplasmic tail of the low-density lipoprotein receptor-related protein: implication for receptor-mediated endocytosis. Mol Cell Biol 21:1185-1195.

Light AR, Trevino DL, Perl ER (1979) Morphological features of functionally defined neurons in the marginal zone and substantia gelatinosa of the spinal dorsal horn. J Comp Neurol 186:151-171.

Like AA, Appel MC, Williams RM, Rossini AA (1978) Streptozotocin-induced pancreatic insulitis in mice. Morphologic and physiologic studies. Lab Invest 38:470-486.

Lillis AP, Mikhailenko I, Strickland DK (2005) Beyond endocytosis: LRP function in cell migration, proliferation and vascular permeability. J Thromb Haemost 3:1884-1893.

Lillis AP, Van Duyn LB, Murphy-Ullrich JE, Strickland DK (2008) LDL receptor-related protein 1: unique tissue-specific functions revealed by selective gene knockout studies. Physiol Rev 88:887-918.

Lim HH, Park CS (2005) Identification and functional characterization of ankyrin-repeat family protein ANKRA as a protein interacting with BKCa channel. Mol Biol Cell 16:1013-1025.

Lim KS, Won YW, Park YS, Kim YH (2010) Preparation and functional analysis of recombinant protein transduction domain-metallothionein fusion proteins. Biochimie 92:964-970.

Lim M, Park L, Shin G, Hong H, Kang I, Park Y (2008) Induction of apoptosis of Beta cells of the pancreas by advanced glycation end-products, important mediators of chronic complications of diabetes mellitus. Ann N Y Acad Sci 1150:311-315.

Lindsay RM (1996) Role of neurotrophins and trk receptors in the development and maintenance of sensory neurons: an overview. Philos Trans R Soc Lond B Biol Sci 351:365-373.

Liu BR, Huang YW, Winiarz JG, Chiang HJ, Lee HJ (2011) Intracellular delivery of quantum dots mediated by a histidine- and arginine-rich HR9 cell-penetrating peptide through the direct membrane translocation mechanism. Biomaterials 32:3520-3537.

Liu BR, Lin MD, Chiang HJ, Lee HJ (2012) Arginine-rich cell-penetrating peptides deliver gene into living human cells. Gene 505:37-45.

Liu CX, Musco S, Lisitsina NM, Yaklichkin SY, Lisitsyn NA (2000a) Genomic organization of a new candidate tumor suppressor gene, LRP1B. Genomics 69:271-274.

Liu F, Ma F, Kong G, Wu K, Deng Z, Wang H (2014) Zinc Supplementation Alleviates Diabetic Peripheral Neuropathy by Inhibiting Oxidative Stress and Upregulating Metallothionein in Peripheral Nerves of Diabetic Rats. Biol Trace Elem Res.

Liu H, Mantyh PW, Basbaum AI (1997) NMDA-receptor regulation of substance P release from primary afferent nociceptors. Nature 386:721-724.

Liu Q, Trotter J, Zhang J, Peters MM, Cheng H, Bao J, Han X, Weeber EJ, Bu G (2010) Neuronal LRP1 knockout in adult mice leads to impaired brain lipid metabolism and progressive, age-dependent synapse loss and neurodegeneration. J Neurosci 30:17068-17078.

Liu Q, Zhang J, Tran H, Verbeek MM, Reiss K, Estus S, Bu G (2009) LRP1 shedding in human brain: roles of ADAM10 and ADAM17. Mol Neurodegener 4:17.

Liu Y, Jones M, Hingtgen CM, Bu G, Laribee N, Tanzi RE, Moir RD, Nath A, He JJ (2000b) Uptake of HIV-1 tat protein mediated by low-density lipoprotein receptor-related protein disrupts the neuronal metabolic balance of the receptor ligands. Nat Med 6:1380-1387.

Lochner JE, Honigman LS, Grant WF, Gessford SK, Hansen AB, Silverman MA, Scalettar BA (2006) Activity-dependent release of tissue plasminogen activator from the dendritic spines of hippocampal neurons revealed by live-cell imaging. J Neurobiol 66:564-577.

Lohof AM, Quillan M, Dan Y, Poo MM (1992) Asymmetric modulation of cytosolic cAMP activity induces growth cone turning. J Neurosci 12:1253-1261.

Lolley RN, Racz E (1982) Calcium modulation of cyclic GMP synthesis in rat visual cells. Vision Res 22:1481-1486.

Loseth S, Stalberg E, Jorde R, Mellgren SI (2008) Early diabetic neuropathy: thermal thresholds and intraepidermal nerve fibre density in patients with normal nerve conduction studies. J Neurol 255:1197-1202.

Loukinova E, Ranganathan S, Kuznetsov S, Gorlatova N, Migliorini MM, Loukinov D, Ulery PG, Mikhailenko I, Lawrence DA, Strickland DK (2002) Platelet-derived growth factor (PDGF)-induced tyrosine phosphorylation of the low density lipoprotein receptor-related protein (LRP). Evidence for integrated co-receptor function betwenn LRP and the PDGF. J Biol Chem 277:15499-15506.

Lyuksyutova AI, Lu CC, Milanesio N, King LA, Guo N, Wang Y, Nathans J, Tessier-Lavigne M, Zou Y (2003) Anterior-posterior guidance of commissural axons by Wnt-frizzled signaling. Science 302:1984-1988.

Maier W, Bednorz M, Meister S, Roebroek A, Weggen S, Schmitt U, Pietrzik CU (2013) LRP1 is critical for the surface distribution and internalization of the NR2B NMDA receptor subtype. Mol Neurodegener 8:25.

Maihofner C, Heskamp ML (2013) Prospective, non-interventional study on the tolerability and analgesic effectiveness over 12 weeks after a single application of capsaicin 8% cutaneous patch in 1044 patients with peripheral neuropathic pain: first results of the QUEPP study. Curr Med Res Opin 29:673-683.

Maisonpierre PC, Belluscio L, Friedman B, Alderson RF, Wiegand SJ, Furth ME, Lindsay RM, Yancopoulos GD (1990) NT-3, BDNF, and NGF in the developing rat nervous system: parallel as well as reciprocal patterns of expression. Neuron 5:501-509.

Malmberg AB, Mizisin AP, Calcutt NA, von Stein T, Robbins WR, Bley KR (2004) Reduced heat sensitivity and epidermal nerve fiber immunostaining following single applications of a high-concentration capsaicin patch. Pain 111:360-367.

Mantuano E, Jo M, Gonias SL, Campana WM (2010) Low density lipoprotein receptor-related protein (LRP1) regulates Rac1 and RhoA reciprocally to control Schwann cell adhesion and migration. J Biol Chem 285:14259-14266.

Mantuano E, Lam MS, Gonias SL (2013) LRP1 assembles unique co-receptor systems to initiate cell signaling in response to tissue-type plasminogen activator and myelin-associated glycoprotein. J Biol Chem 288:34009-34018.

Mar FM, Bonni A, Sousa MM (2014) Cell intrinsic control of axon regeneration. EMBO Rep 15:254-263.

Marco P, Sola RG, Ramon y Cajal S, DeFelipe J (1997) Loss of inhibitory synapses on the soma and axon initial segment of pyramidal cells in human epileptic peritumoural neocortex: implications for epilepsy. Brain Res Bull 44:47-66.

Martin AM, Kuhlmann C, Trossbach S, Jaeger S, Waldron E, Roebroek A, Luhmann HJ, Laatsch A, Weggen S, Lessmann V, Pietrzik CU (2008) The functional role of the second NPXY motif of the LRP1 beta-chain in tissue-type plasminogen activator-mediated activation of N-methyl-D-aspartate receptors. J Biol Chem 283:12004-12013.

Martyn CN, Hughes RA (1997) Epidemiology of peripheral neuropathy. J Neurol Neurosurg Psychiatry 62:310-318.

Marynen P, Van Leuven F, Cassiman JJ, Van den Berghe H (1984) Solubilization and affinity purification of the alpha 2-macroglobulin receptor from human fibroblasts. J Biol Chem 259:7075-7079.

Marzolo MP, Farfan P (2011) New insights into the roles of megalin/LRP2 and the regulation of its functional expression. Biol Res 44:89-105.

Masliah E, Mallory M, Ge N, Alford M, Veinbergs I, Roses AD (1995) Neurodegeneration in the central nervous system of apoE-deficient mice. Exp Neurol 136:107-122.

Mason HA, Ito S, Corfas G (2001) Extracellular signals that regulate the tangential migration of olfactory bulb neuronal precursors: inducers, inhibitors, and repellents. J Neurosci 21:7654-7663.

Mauch DH, Nagler K, Schumacher S, Goritz C, Muller EC, Otto A, Pfrieger FW (2001) CNS synaptogenesis promoted by glia-derived cholesterol. Science 294:1354-1357.

May P, Herz J, Bock HH (2005) Molecular mechanisms of lipoprotein receptor signalling. Cell Mol Life Sci 62:2325-2338.

May P, Rohlmann A, Bock HH, Zurhove K, Marth JD, Schomburg ED, Noebels JL, Beffert U, Sweatt JD, Weeber EJ, Herz J (2004) Neuronal LRP1 functionally associates with postsynaptic proteins and is required for normal motor function in mice. Mol Cell Biol 24:8872-8883.

McCarthy RA, Barth JL, Chintalapudi MR, Knaak C, Argraves WS (2002) Megalin functions as an endocytic sonic hedgehog receptor. J Biol Chem 277:25660-25667.

McGrath JJ, Eyles DW, Pedersen CB, Anderson C, Ko P, Burne TH, Norgaard-Pedersen B, Hougaard DM, Mortensen PB (2010) Neonatal vitamin D status and risk of schizophrenia: a population-based case-control study. Arch Gen Psychiatry 67:889-894.

Medcalf RL (2007) Fibrinolysis, inflammation, and regulation of the plasminogen activating system. J Thromb Haemost 5 Suppl 1:132-142.

Medved LV, Migliorini M, Mikhailenko I, Barrientos LG, Llinas M, Strickland DK (1999) Domain organization of the 39-kDa receptor-associated protein. J Biol Chem 274:717-727.

Merritt JE, Armstrong WP, Benham CD, Hallam TJ, Jacob R, Jaxa-Chamiec A, Leigh BK, McCarthy SA, Moores KE, Rink TJ (1990) SK&F 96365, a novel inhibitor of receptor-mediated calcium entry. Biochem J 271:515-522.

Miao X, Sun W, Fu Y, Miao L, Cai L (2013) Zinc homeostasis in the metabolic syndrome and diabetes. Front Med 7:31-52.

Min D, Kim H, Park L, Kim TH, Hwang S, Kim MJ, Jang S, Park Y (2012) Amelioration of diabetic neuropathy by TAT-mediated enhanced delivery of metallothionein and SOD. Endocrinology 153:81-91.

Ming G, Song H, Berninger B, Inagaki N, Tessier-Lavigne M, Poo M (1999) Phospholipase C-gamma and phosphoinositide 3-kinase mediate cytoplasmic signaling in nerve growth cone guidance. Neuron 23:139-148.

Moestrup SK, Gliemann J, Pallesen G (1992) Distribution of the alpha 2-macroglobulin receptor/low density lipoprotein receptor-related protein in human tissues. Cell Tissue Res 269:375-382.

Molliver DC, Snider WD (1997) Nerve growth factor receptor TrkA is down-regulated during postnatal development by a subset of dorsal root ganglion neurons. J Comp Neurol 381:428-438.

Morellini NM, Giles NL, Rea S, Adcroft KF, Falder S, King CE, Dunlop SA, Beazley LD, West AK, Wood FM, Fear MW (2008) Exogenous metallothionein-IIA promotes accelerated healing after a burn wound. Wound Repair Regen 16:682-690.

Mori T, Iijima N, Kitabatake K, Kohsaka S (1990) Alpha 2-macroglobulin is an astroglia-derived neurite-promoting factor for cultured neurons from rat central nervous system. Brain Res 527:55-61.

Mostafa GA, Al-Ayadhi LY (2011) Increased serum levels of anti-ganglioside M1 auto-antibodies in autistic children: relation to the disease severity. J Neuroinflammation 8:39.

Mou J, Paillard F, Turnbull B, Trudeau J, Stoker M, Katz NP (2013) Efficacy of Qutenza(R) (capsaicin) 8% patch for neuropathic pain: a meta-analysis of the Qutenza Clinical Trials Database. Pain 154:1632-1639.

Mulder M, Jansen PJ, Janssen BJ, van de Berg WD, van der Boom H, Havekes LM, de Kloet RE, Ramaekers FC, Blokland A (2004) Low-density lipoprotein receptor-knockout

mice display impaired spatial memory associated with a decreased synaptic density in the hippocampus. Neurobiol Dis 16:212-219.
Nagai T, Yamada K, Yoshimura M, Ishikawa K, Miyamoto Y, Hashimoto K, Noda Y, Nitta A, Nabeshima T (2004) The tissue plasminogen activator-plasmin system participates in the rewarding effect of morphine by regulating dopamine release. Proc Natl Acad Sci U S A 101:3650-3655.
Nakajima C, Kulik A, Frotscher M, Herz J, Schafer M, Bock HH, May P (2013) Low density lipoprotein receptor-related protein 1 (LRP1) modulates N-methyl-D-aspartate (NMDA) receptor-dependent intracellular signaling and NMDA-induced regulation of postsynaptic protein complexes. J Biol Chem 288:21909-21923.
Nanchahal J, Riches DJ (1982) The healing of suction blisters in pig skin. J Cutan Pathol 9:303-315.
Narita M, Bu G, Holtzman DM, Schwartz AL (1997) The low-density lipoprotein receptor-related protein, a multifunctional apolipoprotein E receptor, modulates hippocampal neurite development. J Neurochem 68:587-595.
Navarro AI, Rico B (2014) Focal adhesion kinase function in neuronal development. Curr Opin Neurobiol 27C:89-95.
Naveilhan P, Neveu I, Wion D, Brachet P (1996) 1,25-Dihydroxyvitamin D3, an inducer of glial cell line-derived neurotrophic factor. Neuroreport 7:2171-2175.
Naziroglu M, Dikici DM, Dursun S (2012) Role of oxidative stress and Ca(2)(+) signaling on molecular pathways of neuropathic pain in diabetes: focus on TRP channels. Neurochem Res 37:2065-2075.
Neveu I, Naveilhan P, Jehan F, Baudet C, Wion D, De Luca HF, Brachet P (1994) 1,25-dihydroxyvitamin D3 regulates the synthesis of nerve growth factor in primary cultures of glial cells. Brain Res Mol Brain Res 24:70-76.
Nichols AJ, Olson EC (2010) Reelin promotes neuronal orientation and dendritogenesis during preplate splitting. Cereb Cortex 20:2213-2223.
Nicole O, Docagne F, Ali C, Margaill I, Carmeliet P, MacKenzie ET, Vivien D, Buisson A (2001) The proteolytic activity of tissue-plasminogen activator enhances NMDA receptor-mediated signaling. Nat Med 7:59-64.
Nimpf J, Stifani S, Bilous PT, Schneider WJ (1994) The somatic cell-specific low density lipoprotein receptor-related protein of the chicken. Close kinship to mammalian low density lipoprotein receptor gene family members. J Biol Chem 269:212-219.
Nishiyama M, Hoshino A, Tsai L, Henley JR, Goshima Y, Tessier-Lavigne M, Poo MM, Hong K (2003) Cyclic AMP/GMP-dependent modulation of Ca2+ channels sets the polarity of nerve growth-cone turning. Nature 423:990-995.
Niu S, Renfro A, Quattrocchi CC, Sheldon M, D'Arcangelo G (2004) Reelin promotes hippocampal dendrite development through the VLDLR/ApoER2-Dab1 pathway. Neuron 41:71-84.
Niu S, Yabut O, D'Arcangelo G (2008) The Reelin signaling pathway promotes dendritic spine development in hippocampal neurons. J Neurosci 28:10339-10348.
Nolano M, Simone DA, Wendelschafer-Crabb G, Johnson T, Hazen E, Kennedy WR (1999) Topical capsaicin in humans: parallel loss of epidermal nerve fibers and pain sensation. Pain 81:135-145.
Norris CM, Halpain S, Foster TC (1998) Reversal of age-related alterations in synaptic plasticity by blockade of L-type Ca2+ channels. J Neurosci 18:3171-3179.

Norris CM, Korol DL, Foster TC (1996) Increased susceptibility to induction of long-term depression and long-term potentiation reversal during aging. J Neurosci 16:5382-5392.

Novella SP, Inzucchi SE, Goldstein JM (2001) The frequency of undiagnosed diabetes and impaired glucose tolerance in patients with idiopathic sensory neuropathy. Muscle Nerve 24:1229-1231.

Nusetti S, Obregon F, Quintal M, Benzo Z, Lima L (2005) Taurine and zinc modulate outgrowth from goldfish retinal explants. Neurochem Res 30:1483-1492.

Nykjaer A, Dragun D, Walther D, Vorum H, Jacobsen C, Herz J, Melsen F, Christensen EI, Willnow TE (1999) An endocytic pathway essential for renal uptake and activation of the steroid 25-(OH) vitamin D3. Cell 96:507-515.

Oleinikov AV, Zhao J, Makker SP (2000) Cytosolic adaptor protein Dab2 is an intracellular ligand of endocytic receptor gp600/megalin. Biochem J 347 Pt 3:613-621.

Ooashi N, Futatsugi A, Yoshihara F, Mikoshiba K, Kamiguchi H (2005) Cell adhesion molecules regulate Ca2+-mediated steering of growth cones via cyclic AMP and ryanodine receptor type 3. J Cell Biol 170:1159-1167.

Oppenheim RW, Prevette D, Yin QW, Collins F, MacDonald J (1991) Control of embryonic motoneuron survival in vivo by ciliary neurotrophic factor. Science 251:1616-1618.

Orr AW, Pedraza CE, Pallero MA, Elzie CA, Goicoechea S, Strickland DK, Murphy-Ullrich JE (2003) Low density lipoprotein receptor-related protein is a calreticulin coreceptor that signals focal adhesion disassembly. J Cell Biol 161:1179-1189.

Panoutsopoulou IG, Wendelschafer-Crabb G, Hodges JS, Kennedy WR (2009) Skin blister and skin biopsy to quantify epidermal nerves: a comparative study. Neurology 72:1205-1210.

Park L, Min D, Kim H, Chung HY, Lee CH, Park IS, Kim Y, Park Y (2011) Tat-enhanced delivery of metallothionein can partially prevent the development of diabetes. Free Radic Biol Med 51:1666-1674.

Patrie KM, Drescher AJ, Goyal M, Wiggins RC, Margolis B (2001) The membrane-associated guanylate kinase protein MAGI-1 binds megalin and is present in glomerular podocytes. J Am Soc Nephrol 12:667-677.

Pavez M (2013) Deciphering how Metallothionein-III and Alpha-2-Macroglobulin induce cell motility via LRP receptors. In: School of Medicine, vol. Bachelor of Medical Research Hobart: University of Tasmania.

Pawlak R, Magarinos AM, Melchor J, McEwen B, Strickland S (2003) Tissue plasminogen activator in the amygdala is critical for stress-induced anxiety-like behavior. Nat Neurosci 6:168-174.

Pedarzani P, Kulik A, Muller M, Ballanyi K, Stocker M (2000) Molecular determinants of Ca2+-dependent K+ channel function in rat dorsal vagal neurones. J Physiol 527 Pt 2:283-290.

Pfrieger FW (2003a) Cholesterol homeostasis and function in neurons of the central nervous system. Cell Mol Life Sci 60:1158-1171.

Pfrieger FW (2003b) Role of cholesterol in synapse formation and function. Biochim Biophys Acta 1610:271-280.

Philip-Ephraim EE, Eyong KI, Chinenye S, William UE, Ephraim RP (2013) The burden of inpatient neurologic disease in a tropical African hospital. Can J Neurol Sci 40:576-579.

Pinson KI, Brennan J, Monkley S, Avery BJ, Skarnes WC (2000) An LDL-receptor-related protein mediates Wnt signalling in mice. Nature 407:535-538.
Polydefkis M, Griffin JW, McArthur J (2003) New insights into diabetic polyneuropathy. JAMA 290:1371-1376.
Polydefkis M, Hauer P, Griffin JW, McArthur JC (2001) Skin biopsy as a tool to assess distal small fiber innervation in diabetic neuropathy. Diabetes Technol Ther 3:23-28.
Polydefkis M, Hauer P, Sheth S, Sirdofsky M, Griffin JW, McArthur JC (2004) The time course of epidermal nerve fibre regeneration: studies in normal controls and in people with diabetes, with and without neuropathy. Brain 127:1606-1615.
Postuma RB, Martins RN, Cappai R, Beyreuther K, Masters CL, Strickland DK, Mok SS, Small DH (1998) Effects of the amyloid protein precursor of Alzheimer's disease and other ligands of the LDL receptor-related protein on neurite outgrowth from sympathetic neurons in culture. FEBS Lett 428:13-16.
Pradat PF, Kennel P, Naimi-Sadaoui S, Finiels F, Orsini C, Revah F, Delaere P, Mallet J (2001) Continuous delivery of neurotrophin 3 by gene therapy has a neuroprotective effect in experimental models of diabetic and acrylamide neuropathies. Hum Gene Ther 12:2237-2249.
Prausnitz MR, Langer R (2008) Transdermal drug delivery. Nat Biotechnol 26:1261-1268.
Prow TW, Chen X, Prow NA, Fernando GJ, Tan CS, Raphael AP, Chang D, Ruutu MP, Jenkins DW, Pyke A, Crichton ML, Raphaelli K, Goh LY, Frazer IH, Roberts MS, Gardner J, Khromykh AA, Suhrbier A, Hall RA, Kendall MA (2010) Nanopatch-targeted skin vaccination against West Nile Virus and Chikungunya virus in mice. Small 6:1776-1784.
Przybelski RJ, Binkley NC (2007) Is vitamin D important for preserving cognition? A positive correlation of serum 25-hydroxyvitamin D concentration with cognitive function. Arch Biochem Biophys 460:202-205.
Purves D (ed.) (1988) A Trophic Theory of Neural Connections: Harvard University Press, Cambridge, MA.
Puttaparthi K, Gitomer WL, Krishnan U, Son M, Rajendran B, Elliott JL (2002) Disease progression in a transgenic model of familial amyotrophic lateral sclerosis is dependent on both neuronal and non-neuronal zinc binding proteins. J Neurosci 22:8790-8796.
Qian Z, Gilbert ME, Colicos MA, Kandel ER, Kuhl D (1993) Tissue-plasminogen activator is induced as an immediate-early gene during seizure, kindling and long-term potentiation. Nature 361:453-457.
Qiu S, Zhao LF, Korwek KM, Weeber EJ (2006) Differential reelin-induced enhancement of NMDA and AMPA receptor activity in the adult hippocampus. J Neurosci 26:12943-12955.
Qiu Z, Strickland DK, Hyman BT, Rebeck GW (2002a) alpha 2-Macroglobulin exposure reduces calcium responses to N-methyl-D-aspartate via low density lipoprotein receptor-related protein in cultured hippocampal neurons. J Biol Chem 277:14458-14466.
Qiu Z, Strickland DK, Hyman BT, Rebeck GW (2002b) alpha 2-Macroglobulin exposure reduces calcium responses to N-methyl-D-aspartate via low density lipoprotein receptor-related protein in cultured hippocampal neurons. J Biol Chem 277:14458-14466.

Quaife CJ, Findley SD, Erickson JC, Froelick GJ, Kelly EJ, Zambrowicz BP, Palmiter RD (1994) Induction of a new metallothionein isoform (MT-IV) occurs during differentiation of stratified squamous epithelia. Biochemistry 33:7250-7259.

Quinn KA, Pye VJ, Dai YP, Chesterman CN, Owensby DA (1999) Characterization of the soluble form of the low density lipoprotein receptor-related protein (LRP). Exp Cell Res 251:433-441.

Rajan B, Polydefkis M, Hauer P, Griffin JW, McArthur JC (2003) Epidermal reinnervation after intracutaneous axotomy in man. J Comp Neurol 457:24-36.

Raychowdhury R, Niles JL, McCluskey RT, Smith JA (1989) Autoimmune target in Heymann nephritis is a glycoprotein with homology to the LDL receptor. Science 244:1163-1165.

Rebeck GW (2009) Nontraditional signaling mechanisms of lipoprotein receptors. Sci Signal 2:pe28.

Reed MJ, Meszaros K, Entes LJ, Claypool MD, Pinkett JG, Gadbois TM, Reaven GM (2000) A new rat model of type 2 diabetes: the fat-fed, streptozotocin-treated rat. Metabolism 49:1390-1394.

Remiche G, Kadhim H, Maris C, Mavroudakis N (2013) [Peripheral neuropathies, from diagnosis to treatment, review of the literature and lessons from the local experience]. Rev Med Brux 34:211-220.

Remuzzi A, Cornolti R, Bianchi R, Figliuzzi M, Porretta-Serapiglia C, Oggioni N, Carozzi V, Crippa L, Avezza F, Fiordaliso F, Salio M, Lauria G, Lombardi R, Cavaletti G (2009) Regression of diabetic complications by islet transplantation in the rat. Diabetologia 52:2653-2661.

Revuelta-Lopez E, Castellano J, Roura S, Galvez-Monton C, Nasarre L, Benitez S, Bayes-Genis A, Badimon L, Llorente-Cortes V (2013) Hypoxia induces metalloproteinase-9 activation and human vascular smooth muscle cell migration through low-density lipoprotein receptor-related protein 1-mediated Pyk2 phosphorylation. Arterioscler Thromb Vasc Biol 33:2877-2887.

Rogers JT, Weeber EJ (2008) Reelin and apoE actions on signal transduction, synaptic function and memory formation. Neuron Glia Biol 4:259-270.

Roustit M, Blaise S, Cracowski JL (2009) Sodium nitroprusside iontophoresis on the finger pad does not consistently increase skin blood flow in healthy controls and patients with systemic sclerosis. Microvasc Res 77:260-264.

Saarma M, Sariola H (1999) Other neurotrophic factors: glial cell line-derived neurotrophic factor (GDNF). Microsc Res Tech 45:292-302.

Salles FJ, Strickland S (2002) Localization and regulation of the tissue plasminogen activator-plasmin system in the hippocampus. J Neurosci 22:2125-2134.

Salonen EM, Zitting A, Vaheri A (1984) Laminin interacts with plasminogen and its tissue-type activator. FEBS Lett 172:29-32.

Samonte IE, Sato A, Mayer WE, Shintani S, Klein J (2002) Linkage relationships of genes coding for alpha2-macroglobulin, C3 and C4 in the zebrafish: implications for the evolution of the complement and Mhc systems. Scand J Immunol 56:344-352.

Samson AL, Nevin ST, Croucher D, Niego B, Daniel PB, Weiss TW, Moreno E, Monard D, Lawrence DA, Medcalf RL (2008) Tissue-type plasminogen activator requires a co-receptor to enhance NMDA receptor function. J Neurochem 107:1091-1101.

Sanders SJ, Murtha MT, Gupta AR, Murdoch JD, Raubeson MJ, Willsey AJ, Ercan-Sencicek AG, DiLullo NM, Parikshak NN, Stein JL, Walker MF, Ober GT, Teran NA, Song Y, El-Fishawy P, Murtha RC, Choi M, Overton JD, Bjornson RD, Carriero NJ, Meyer KA, Bilguvar K, Mane SM, Sestan N, Lifton RP, Gunel M, Roeder K, Geschwind DH, Devlin B, State MW (2012) De novo mutations revealed by whole-exome sequencing are strongly associated with autism. Nature 485:237-241.

Saraiva MJ (2003) Cellular consequences of transthyretin deposition. Amyloid 10 Suppl 1:13-16.

Sato M, Lopez-Mascaraque L, Heffner CD, O'Leary DD (1994) Action of a diffusible target-derived chemoattractant on cortical axon branch induction and directed growth. Neuron 13:791-803.

Schmidt RE, Dorsey DA, Beaudet LN, Parvin CA, Escandon E (2001) Effect of NGF and neurotrophin-3 treatment on experimental diabetic autonomic neuropathy. J Neuropathol Exp Neurol 60:263-273.

Seeds NW, Basham ME, Ferguson JE (2003) Absence of tissue plasminogen activator gene or activity impairs mouse cerebellar motor learning. J Neurosci 23:7368-7375.

Seeds NW, Basham ME, Haffke SP (1999) Neuronal migration is retarded in mice lacking the tissue plasminogen activator gene. Proc Natl Acad Sci U S A 96:14118-14123.

Seeds NW, Williams BL, Bickford PC (1995) Tissue plasminogen activator induction in Purkinje neurons after cerebellar motor learning. Science 270:1992-1994.

Sekine K, Kawauchi T, Kubo K, Honda T, Herz J, Hattori M, Kinashi T, Nakajima K (2012) Reelin controls neuronal positioning by promoting cell-matrix adhesion via inside-out activation of integrin alpha5beta1. Neuron 76:353-369.

Sellers JR (2000) Myosins: a diverse superfamily. Biochim Biophys Acta 1496:3-22.

Selvais C, D'Auria L, Tyteca D, Perrot G, Lemoine P, Troeberg L, Dedieu S, Noel A, Nagase H, Henriet P, Courtoy PJ, Marbaix E, Emonard H (2011) Cell cholesterol modulates metalloproteinase-dependent shedding of low-density lipoprotein receptor-related protein-1 (LRP-1) and clearance function. FASEB J 25:2770-2781.

Shaffer JA, Edmondson D, Wasson LT, Falzon L, Homma K, Ezeokoli N, Li P, Davidson KW (2014) Vitamin D Supplementation for Depressive Symptoms: A Systematic Review and Meta-Analysis of Randomized Controlled Trials. Psychosom Med.

Shelly M, Lim BK, Cancedda L, Heilshorn SC, Gao H, Poo MM (2010) Local and long-range reciprocal regulation of cAMP and cGMP in axon/dendrite formation. Science 327:547-552.

Shi Y, Mantuano E, Inoue G, Campana WM, Gonias SL (2009) Ligand binding to LRP1 transactivates Trk receptors by a Src family kinase-dependent pathway. Sci Signal 2:ra18.

Shi YB, Fang JL, Liu XY, Du L, Tang WX (2002) Fourier transform IR and Fourier transform Raman spectroscopy studies of metallothionein-III: amide I band assignments and secondary structural comparison with metallothioneins-I and -II. Biopolymers 65:81-88.

Shirasaki R, Katsumata R, Murakami F (1998) Change in chemoattractant responsiveness of developing axons at an intermediate target. Science 279:105-107.

Shun CT, Chang YC, Wu HP, Hsieh SC, Lin WM, Lin YH, Tai TY, Hsieh ST (2004) Skin denervation in type 2 diabetes: correlations with diabetic duration and functional impairments. Brain 127:1593-1605.

Siddoju S, Sachdeva V, Friden PM, Yu YY, Banga AK (2011) Acyclovir skin depot characterization following in vivo iontophoretic delivery. Skin Res Technol 17:234-244.
Siegel GJ, Chauhan NB (2000) Neurotrophic factors in Alzheimer's and Parkinson's disease brain. Brain Res Brain Res Rev 33:199-227.
Simonovic M, Dolmer K, Huang W, Strickland DK, Volz K, Gettins PG (2001) Calcium coordination and pH dependence of the calcium affinity of ligand-binding repeat CR7 from the LRP. Comparison with related domains from the LRP and the LDL receptor. Biochemistry 40:15127-15134.
Singer W (1986) The brain as a self-organizing system. Eur Arch Psychiatry Neurol Sci 236:4-9.
Singh A, Hildebrand ME, Garcia E, Snutch TP (2010) The transient receptor potential channel antagonist SKF96365 is a potent blocker of low-voltage-activated T-type calcium channels. Br J Pharmacol 160:1464-1475.
Singleton JR, Smith AG, Bromberg MB (2001) Painful sensory polyneuropathy associated with impaired glucose tolerance. Muscle Nerve 24:1225-1228.
Sinnreich M, Taylor BV, Dyck PJ (2005) Diabetic neuropathies. Classification, clinical features, and pathophysiological basis. Neurologist 11:63-79.
Skornicka EL, Shi X, Koo PH (2002) Comparative binding of biotinylated neurotrophins to alpha(2)-macroglobulin family of proteins: relationship between cytokine-binding and neuro-modulatory activities of the macroglobulins. J Neurosci Res 67:346-353.
Song H, Ming G, He Z, Lehmann M, McKerracher L, Tessier-Lavigne M, Poo M (1998) Conversion of neuronal growth cone responses from repulsion to attraction by cyclic nucleotides. Science 281:1515-1518.
Song HJ, Poo MM (1999) Signal transduction underlying growth cone guidance by diffusible factors. Curr Opin Neurobiol 9:355-363.
Sorensen L, Molyneaux L, Yue DK (2006a) The level of small nerve fiber dysfunction does not predict pain in diabetic Neuropathy: a study using quantitative sensory testing. Clin J Pain 22:261-265.
Sorensen L, Molyneaux L, Yue DK (2006b) The relationship among pain, sensory loss, and small nerve fibers in diabetes. Diabetes Care 29:883-887.
Sottrup-Jensen L (1989) Alpha-macroglobulins: structure, shape, and mechanism of proteinase complex formation. J Biol Chem 264:11539-11542.
Sottrup-Jensen L, Stepanik TM, Kristensen T, Lonblad PB, Jones CM, Wierzbicki DM, Magnusson S, Domdey H, Wetsel RA, Lundwall A, et al. (1985) Common evolutionary origin of alpha 2-macroglobulin and complement components C3 and C4. Proc Natl Acad Sci U S A 82:9-13.
Sousa JC, Grandela C, Fernandez-Ruiz J, de Miguel R, de Sousa L, Magalhaes AI, Saraiva MJ, Sousa N, Palha JA (2004) Transthyretin is involved in depression-like behaviour and exploratory activity. J Neurochem 88:1052-1058.
Sousa JC, Marques F, Dias-Ferreira E, Cerqueira JJ, Sousa N, Palha JA (2007) Transthyretin influences spatial reference memory. Neurobiol Learn Mem 88:381-385.
Sousa MM, Norden AG, Jacobsen C, Willnow TE, Christensen EI, Thakker RV, Verroust PJ, Moestrup SK, Saraiva MJ (2000) Evidence for the role of megalin in renal uptake of transthyretin. J Biol Chem 275:38176-38181.

Sperry RW (1963) Chemoaffinity in the orderly growth of nerve fiber patterns and connections Proc Natl Acad Sci U S A 50:703-710.

Spoelgen R, Adams KW, Koker M, Thomas AV, Andersen OM, Hallett PJ, Bercury KK, Joyner DF, Deng M, Stoothoff WH, Strickland DK, Willnow TE, Hyman BT (2009) Interaction of the apolipoprotein E receptors low density lipoprotein receptor-related protein and sorLA/LR11. Neuroscience 158:1460-1468.

Spoelgen R, Hammes A, Anzenberger U, Zechner D, Andersen OM, Jerchow B, Willnow TE (2005) LRP2/megalin is required for patterning of the ventral telencephalon. Development 132:405-414.

Spuch C, Ortolano S, Navarro C (2012) LRP-1 and LRP-2 receptors function in the membrane neuron. Trafficking mechanisms and proteolytic processing in Alzheimer's disease. Front Physiol 3:269.

Srinivasan K, Viswanad B, Asrat L, Kaul CL, Ramarao P (2005) Combination of high-fat diet-fed and low-dose streptozotocin-treated rat: a model for type 2 diabetes and pharmacological screening. Pharmacol Res 52:313-320.

Stewart N, Simpson S, Jr., van der Mei I, Ponsonby AL, Blizzard L, Dwyer T, Pittas F, Eyles D, Ko P, Taylor BV (2012) Interferon-beta and serum 25-hydroxyvitamin D interact to modulate relapse risk in MS. Neurology 79:254-260.

Stiles TL, Dickendesher TL, Gaultier A, Fernandez-Castaneda A, Mantuano E, Giger RJ, Gonias SL (2013) LDL receptor-related protein-1 is a sialic-acid-independent receptor for myelin-associated glycoprotein that functions in neurite outgrowth inhibition by MAG and CNS myelin. J Cell Sci 126:209-220.

Stockinger W, Hengstschlager-Ottnad E, Novak S, Matus A, Huttinger M, Bauer J, Lassmann H, Schneider WJ, Nimpf J (1998) The low density lipoprotein receptor gene family. Differential expression of two alpha2-macroglobulin receptors in the brain. J Biol Chem 273:32213-32221.

Strickland DK, Ashcom JD, Williams S, Burgess WH, Migliorini M, Argraves WS (1990) Sequence identity between the alpha 2-macroglobulin receptor and low density lipoprotein receptor-related protein suggests that this molecule is a multifunctional receptor. J Biol Chem 265:17401-17404.

Strutt D (2003) Frizzled signalling and cell polarisation in Drosophila and vertebrates. Development 130:4501-4513.

Stumpf WE, Privette TH (1989) Light, vitamin D and psychiatry. Role of 1,25 dihydroxyvitamin D3 (soltriol) in etiology and therapy of seasonal affective disorder and other mental processes. Psychopharmacology (Berl) 97:285-294.

Su J, Klemm MA, Josephson AM, Fox MA (2013) Contributions of VLDLR and LRP8 in the establishment of retinogeniculate projections. Neural Dev 8:11.

Sumner CJ, Sheth S, Griffin JW, Cornblath DR, Polydefkis M (2003) The spectrum of neuropathy in diabetes and impaired glucose tolerance. Neurology 60:108-111.

Suter DM, Forscher P (2000) Substrate-cytoskeletal coupling as a mechanism for the regulation of growth cone motility and guidance. J Neurobiol 44:97-113.

Takahashi S, Kawarabayasi Y, Nakai T, Sakai J, Yamamoto T (1992) Rabbit very low density lipoprotein receptor: a low density lipoprotein receptor-like protein with distinct ligand specificity. Proc Natl Acad Sci U S A 89:9252-9256.

Tamai K, Semenov M, Kato Y, Spokony R, Liu C, Katsuyama Y, Hess F, Saint-Jeannet JP, He X (2000) LDL-receptor-related proteins in Wnt signal transduction. Nature 407:530-535.

Tamai K, Zeng X, Liu C, Zhang X, Harada Y, Chang Z, He X (2004) A mechanism for Wnt coreceptor activation. Mol Cell 13:149-156.

Tavee J, Zhou L (2009) Small fiber neuropathy: A burning problem. Cleve Clin J Med 76:297-305.

Taylor AM, Ribeiro-da-Silva A (2011) GDNF levels in the lower lip skin in a rat model of trigeminal neuropathic pain: implications for nonpeptidergic fiber reinnervation and parasympathetic sprouting. Pain 152:1502-1510.

Teesalu T, Kulla A, Simisker A, Siren V, Lawrence DA, Asser T, Vaheri A (2004) Tissue plasminogen activator and neuroserpin are widely expressed in the human central nervous system. Thromb Haemost 92:358-368.

Terenghi G (1999) Peripheral nerve regeneration and neurotrophic factors. J Anat 194 (Pt 1):1-14.

Tessier-Lavigne M, Goodman CS (1996) The molecular biology of axon guidance. Science 274:1123-1133.

Tessier-Lavigne M, Placzek M, Lumsden AG, Dodd J, Jessell TM (1988) Chemotropic guidance of developing axons in the mammalian central nervous system. Nature 336:775-778.

Thornalley PJ, Vasak M (1985) Possible role for metallothionein in protection against radiation-induced oxidative stress. Kinetics and mechanism of its reaction with superoxide and hydroxyl radicals. Biochim Biophys Acta 827:36-44.

Togashi K, von Schimmelmann MJ, Nishiyama M, Lim CS, Yoshida N, Yun B, Molday RS, Goshima Y, Hong K (2008) Cyclic GMP-gated CNG channels function in Sema3A-induced growth cone repulsion. Neuron 58:694-707.

Tojima T (2012) Intracellular signaling and membrane trafficking control bidirectional growth cone guidance. Neurosci Res 73:269-274.

Tojima T, Hines JH, Henley JR, Kamiguchi H (2011) Second messengers and membrane trafficking direct and organize growth cone steering. Nat Rev Neurosci 12:191-203.

Tojima T, Itofusa R, Kamiguchi H (2009) The nitric oxide-cGMP pathway controls the directional polarity of growth cone guidance via modulating cytosolic Ca2+ signals. J Neurosci 29:7886-7897.

Trendelenburg G, Prass K, Priller J, Kapinya K, Polley A, Muselmann C, Ruscher K, Kannbley U, Schmitt AO, Castell S, Wiegand F, Meisel A, Rosenthal A, Dirnagl U (2002) Serial analysis of gene expression identifies metallothionein-II as major neuroprotective gene in mouse focal cerebral ischemia. J Neurosci 22:5879-5888.

Trommsdorff M, Borg JP, Margolis B, Herz J (1998) Interaction of cytosolic adaptor proteins with neuronal apolipoprotein E receptors and the amyloid precursor protein. J Biol Chem 273:33556-33560.

Trommsdorff M, Gotthardt M, Hiesberger T, Shelton J, Stockinger W, Nimpf J, Hammer RE, Richardson JA, Herz J (1999) Reeler/Disabled-like disruption of neuronal migration in knockout mice lacking the VLDL receptor and ApoE receptor 2. Cell 97:689-701.

Vaillant C, Michos O, Orolicki S, Brellier F, Taieb S, Moreno E, Te H, Zeller R, Monard D (2007) Protease nexin 1 and its receptor LRP modulate SHH signalling during cerebellar development. Development 134:1745-1754.

van der Mei IA, Ponsonby AL, Dwyer T, Blizzard L, Taylor BV, Kilpatrick T, Butzkueven H, McMichael AJ (2007) Vitamin D levels in people with multiple sclerosis and community controls in Tasmania, Australia. J Neurol 254:581-590.
van Hecke O, Austin SK, Khan RA, Smith BH, Torrance N (2014) Neuropathic pain in the general population: A systematic review of epidemiological studies. Pain 155:654-662.
Van Uden E, Veinbergs I, Mallory M, Orlando R, Masliah E (1999) A novel role for receptor-associated protein in somatostatin modulation: implications for Alzheimer's disease. Neuroscience 88:687-700.
Varon S, Manthorpe M, Adler R (1979) Cholinergic neuronotrophic factors: I. Survival, neurite outgrowth and choline acetyltransferase activity in monolayer cultures from chick embryo ciliary ganglia. Brain Res 173:29-45.
Vasconcelos L, Parn K, Langel U (2013) Therapeutic potential of cell-penetrating peptides. Ther Deliv 4:573-591.
Vincent AM, Callaghan BC, Smith AL, Feldman EL (2011) Diabetic neuropathy: cellular mechanisms as therapeutic targets. Nat Rev Neurol 7:573-583.
Vogel KS, Davies AM (1991) The duration of neurotrophic factor independence in early sensory neurons is matched to the time course of target field innervation. Neuron 7:819-830.
von Arnim CA, Kinoshita A, Peltan ID, Tangredi MM, Herl L, Lee BM, Spoelgen R, Hshieh TT, Ranganathan S, Battey FD, Liu CX, Bacskai BJ, Sever S, Irizarry MC, Strickland DK, Hyman BT (2005) The low density lipoprotein receptor-related protein (LRP) is a novel beta-secretase (BACE1) substrate. J Biol Chem 280:17777-17785.
Wallace M, Pappagallo M (2011) Qutenza(R): a capsaicin 8% patch for the management of postherpetic neuralgia. Expert Rev Neurother 11:15-27.
Wang PY, Petralia RS, Wang YX, Wenthold RJ, Brenowitz SD (2011) Functional NMDA receptors at axonal growth cones of young hippocampal neurons. J Neurosci 31:9289-9297.
Wang Y, Chiang YH, Su TP, Hayashi T, Morales M, Hoffer BJ, Lin SZ (2000) Vitamin D(3) attenuates cortical infarction induced by middle cerebral arterial ligation in rats. Neuropharmacology 39:873-880.
Weatherbee SD, Anderson KV, Niswander LA (2006) LDL-receptor-related protein 4 is crucial for formation of the neuromuscular junction. Development 133:4993-5000.
Weeber EJ, Beffert U, Jones C, Christian JM, Forster E, Sweatt JD, Herz J (2002) Reelin and ApoE receptors cooperate to enhance hippocampal synaptic plasticity and learning. J Biol Chem 277:39944-39952.
Wehrli M, Dougan ST, Caldwell K, O'Keefe L, Schwartz S, Vaizel-Ohayon D, Schejter E, Tomlinson A, DiNardo S (2000) arrow encodes an LDL-receptor-related protein essential for Wingless signalling. Nature 407:527-530.
Weinstein S (1993) Fifty years of somatosensory research: from the Semmes-Weinstein monofilaments to the Weinstein Enhanced Sensory Test. J Hand Ther 6:11-22; discussion 50.
Wen Z, Guirland C, Ming GL, Zheng JQ (2004) A CaMKII/calcineurin switch controls the direction of Ca(2+)-dependent growth cone guidance. Neuron 43:835-846.

West AK, Hidalgo J, Eddins D, Levin ED, Aschner M (2008) Metallothionein in the central nervous system: Roles in protection, regeneration and cognition. Neurotoxicology 29:489-503.

Wicher G, Larsson M, Rask L, Aldskogius H (2005) Low-density lipoprotein receptor-related protein (LRP)-2/megalin is transiently expressed in a subpopulation of neural progenitors in the embryonic mouse spinal cord. J Comp Neurol 492:123-131.

Wilkins CH, Sheline YI, Roe CM, Birge SJ, Morris JC (2006) Vitamin D deficiency is associated with low mood and worse cognitive performance in older adults. Am J Geriatr Psychiatry 14:1032-1040.

Williams SE, Ashcom JD, Argraves WS, Strickland DK (1992) A novel mechanism for controlling the activity of alpha 2-macroglobulin receptor/low density lipoprotein receptor-related protein. Multiple regulatory sites for 39-kDa receptor-associated protein. J Biol Chem 267:9035-9040.

Willnow TE, Goldstein JL, Orth K, Brown MS, Herz J (1992) Low density lipoprotein receptor-related protein and gp330 bind similar ligands, including plasminogen activator-inhibitor complexes and lactoferrin, an inhibitor of chylomicron remnant clearance. J Biol Chem 267:26172-26180.

Willnow TE, Hilpert J, Armstrong SA, Rohlmann A, Hammer RE, Burns DK, Herz J (1996a) Defective forebrain development in mice lacking gp330/megalin. Proc Natl Acad Sci U S A 93:8460-8464.

Willnow TE, Moehring JM, Inocencio NM, Moehring TJ, Herz J (1996b) The low-density-lipoprotein receptor-related protein (LRP) is processed by furin in vivo and in vitro. Biochem J 313 (Pt 1):71-76.

Wodarz A, Nusse R (1998) Mechanisms of Wnt signaling in development. Annu Rev Cell Dev Biol 14:59-88.

Woldt E, Matz RL, Terrand J, Mlih M, Gracia C, Foppolo S, Martin S, Bruban V, Ji J, Velot E, Herz J, Boucher P (2011) Differential signaling by adaptor molecules LRP1 and ShcA regulates adipogenesis by the insulin-like growth factor-1 receptor. J Biol Chem 286:16775-16782.

Wolf BB, Lopes MB, VandenBerg SR, Gonias SL (1992) Characterization and immunohistochemical localization of alpha 2-macroglobulin receptor (low-density lipoprotein receptor-related protein) in human brain. Am J Pathol 141:37-42.

Won JC, Kim SS, Ko KS, Cha BY (2014) Current Status of Diabetic Peripheral Neuropathy in Korea: Report of a Hospital-Based Study of Type 2 Diabetic Patients in Korea by the Diabetic Neuropathy Study Group of the Korean Diabetes Association. Diabetes Metab J 38:25-31.

Woolf CJ, Salter MW (2000) Neuronal plasticity: increasing the gain in pain. Science 288:1765-1769.

Wu KY, Hengst U, Cox LJ, Macosko EZ, Jeromin A, Urquhart ER, Jaffrey SR (2005) Local translation of RhoA regulates growth cone collapse. Nature 436:1020-1024.

Wu Y, Liu Y, Hou P, Yan Z, Kong W, Liu B, Li X, Yao J, Zhang Y, Qin F, Ding J (2013) TRPV1 channels are functionally coupled with BK(mSlo1) channels in rat dorsal root ganglion (DRG) neurons. PLoS One 8:e78203.

Xia Z, Storm DR (1997) Calmodulin-regulated adenylyl cyclases and neuromodulation. Curr Opin Neurobiol 7:391-396.

Xu B, Roos JL, Dexheimer P, Boone B, Plummer B, Levy S, Gogos JA, Karayiorgou M (2011) Exome sequencing supports a de novo mutational paradigm for schizophrenia. Nat Genet 43:864-868.

Xu W (2011) PSD-95-like membrane associated guanylate kinases (PSD-MAGUKs) and synaptic plasticity. Curr Opin Neurobiol 21:306-312.

Yamamoto M, Ikeda K, Ohshima K, Tsugu H, Kimura H, Tomonaga M (1998) Expression and cellular localization of low-density lipoprotein receptor-related protein/alpha 2-macroglobulin receptor in human glioblastoma in vivo. Brain Tumor Pathol 15:23-30.

Yamauchi K, Yamauchi T, Mantuano E, Murakami K, Henry K, Takahashi K, Campana WM (2013) Low-density lipoprotein receptor related protein-1 (LRP1)-dependent cell signaling promotes neurotrophic activity in embryonic sensory neurons. PLoS One 8:e75497.

Yamazaki H, Bujo H, Kusunoki J, Seimiya K, Kanaki T, Morisaki N, Schneider WJ, Saito Y (1996) Elements of neural adhesion molecules and a yeast vacuolar protein sorting receptor are present in a novel mammalian low density lipoprotein receptor family member. J Biol Chem 271:24761-24768.

Yang-Snyder J, Miller JR, Brown JD, Lai CJ, Moon RT (1996) A frizzled homolog functions in a vertebrate Wnt signaling pathway. Curr Biol 6:1302-1306.

Yang F, Moss LG, Phillips GN, Jr. (1996) The molecular structure of green fluorescent protein. Nat Biotechnol 14:1246-1251.

Yin X, Knecht DA, Lynes MA (2005) Metallothionein mediates leukocyte chemotaxis. BMC Immunol 6:21.

Yoon C, Van Niekerk EA, Henry K, Ishikawa T, Orita S, Tuszynski MH, Campana WM (2013) Low-density lipoprotein receptor-related protein 1 (LRP1)-dependent cell signaling promotes axonal regeneration. J Biol Chem 288:26557-26568.

Yoshida M, Watanabe C, Horie K, Satoh M, Sawada M, Shimada A (2005) Neurobehavioral changes in metallothionein-null mice prenatally exposed to mercury vapor. Toxicol Lett 155:361-368.

Yuseff MI, Farfan P, Bu G, Marzolo MP (2007) A cytoplasmic PPPSP motif determines megalin's phosphorylation and regulates receptor's recycling and surface expression. Traffic 8:1215-1230.

Zhang M, Lv XY, Li J, Xu ZG, Chen L (2008) The characterization of high-fat diet and multiple low-dose streptozotocin induced type 2 diabetes rat model. Exp Diabetes Res 2008:704045.

Zheng JQ (2000) Turning of nerve growth cones induced by localized increases in intracellular calcium ions. Nature 403:89-93.

Zheng JQ, Wan JJ, Poo MM (1996) Essential role of filopodia in chemotropic turning of nerve growth cone induced by a glutamate gradient. J Neurosci 16:1140-1149.

Ziegler D, Gries FA, Spuler M, Lessmann F (1992) The epidemiology of diabetic neuropathy. Diabetic Cardiovascular Autonomic Neuropathy Multicenter Study Group. J Diabetes Complications 6:49-57.

Ziegler D, Luft D (2002) Clinical trials for drugs against diabetic neuropathy: can we combine scientific needs with clinical practicalities? Int Rev Neurobiol 50:431-463.

Zimmermann M (2001) Pathobiology of neuropathic pain. Eur J Pharmacol 429:23-37.

Zimmet P, Alberti KG, Shaw J (2001) Global and societal implications of the diabetes epidemic. Nature 414:782-787.

Zlokovic BV (2011) Neurovascular pathways to neurodegeneration in Alzheimer's disease and other disorders. Nat Rev Neurosci 12:723-738.
Zochodne DW, Guo GF, Magnowski B, Bangash M (2007) Regenerative failure of diabetic nerves bridging transection injuries. Diabetes Metab Res Rev 23:490-496.
Zochodne DW, Sun HS, Cheng C, Eyer J (2004) Accelerated diabetic neuropathy in axons without neurofilaments. Brain 127:2193-2200.
Zong ZP, Fujikawa-Yamamoto K, Teraoka K, Yamagishi H, Tanino M, Odashima S (1994) Potentiation of K252a, a protein kinase inhibitor-induced polyploidization by cAMP in cultured fibrosarcoma cell line. Biochem Biophys Res Commun 205:746-750.
Zou Z, Chung B, Nguyen T, Mentone S, Thomson B, Biemesderfer D (2004) Linking receptor-mediated endocytosis and cell signaling: evidence for regulated intramembrane proteolysis of megalin in proximal tubule. J Biol Chem 279:34302-34310.
Zurhove K, Nakajima C, Herz J, Bock HH, May P (2008) Gamma-secretase limits the inflammatory response through the processing of LRP1. Sci Signal 1:ra15.